A quantitative approach to diversity, preservation, and taphonomic bias in fossil spider assemblages in lacustrine deposits

By

Matthew R Downen
M.S., University of Kansas, 2014
B.Sc., Western Kentucky University, 2012

Submitted to the graduate degree program in Geology and the Graduate Faculty of the University of Kansas in partial fulfillment of the requirements for the degree of Doctor of Philosophy.

_____

Chair: Paul A. Selden

_____

Deborah R. Smith

_____

Alison N. Olcott

_____

Jennifer A. Roberts

_____

Eugene Rankey

Date Defended: 10 July 2020

The dissertation committee for Matthew R Downen certifies that this is the approved version of the following dissertation:

A quantitative approach to diversity, preservation, and taponomic bias in fossil spider assemblages in lacustrine deposits

Chair: Paul A. Selden

Date Approved: 8 June 2020

Abstract

Spiders (Araneae) are an incredibly diverse and abundant group that has colonized nearly every terrestrial habitat and existed for about 300 million years. These attributes make spiders an excellent group for investigating large scale paleobiological questions throughout geologic time. Fossil spiders are relatively rare, but are found in the geologic record as inclusions in amber and lacustrine deposits. Whereas over 1200 fossil spiders have been described, a disparity exists between amber and lacustrine fossil spiders. Compared to amber, fossil spider assemblages in lacustrine deposits are understudied with respect to taxonomy and diversity, the pathways responsible for preservation, and the biases that influence their composition. This dissertation explores fossil spider assemblages preserved in lacustrine environments to quantify the biases that influence our perception of biodiversity in the fossil record and understand the nature of taphonomic pathways in paleoenvironments of Fossil-Lagerstätten. Biases are shown here to be inconsistent across lacustrine deposits, with repsect to diversity, size, life mode, and sex supporting the idea that fossil assemblages are not completely accurate representations of ancient ecosystems. In addition, microbes are interpreted to play a significant role in the unusual preservation of fossil spiders from the Oligocene Aix-en-Provence Formation of France suggesting microbial mats can be important components of the taphonomic pathway in Fossil-Lagerstätten. This dissertation expands on the evolutionary history of spiders and their preservation in lacustrine deposits, and provides a more complete view of the fossil record of spiders.

Acknowledgements

I would like to thank and acknowledge a number of people, who without, this dissertation would not be possible. Firstly, I would like to thank my parents. My mother, Pam Shearer, has always been supportive and encouraged me to pursue my dreams, all the way back to when she made me a paleontologist outfit for career day in the second grade. I would also like to thank my Mema, Cynthia Rowe, who passed away near the end of my graduate career—she was always a champion in my corner and always told me how proud she was of me. I would also like to thank my Kentucky friends, Rachel, Amy, and Cassie, for being great friends throughout our undergrad in geology, and continuing to support me throughout my graduate career. Upon moving to Kansas, I made some wonderful additional friends — to Jack and Nick and the rest of the Kansas City crew, and Chris and Quinn, you made Kansas a much homier place to me and I'm so thankful for all of your support while I've been a graduate student at KU. Some of my most loyal companions have been Ichi, my cat, and my pet arachnids including Bianca the tarantula, Persephone the vinegaroon, and Artemis the scorpion.

I learned how challenging pursuing a Ph.D. is, and I could not have done it without the support of my friends and family.

At KU, I would like to thank my advisor, Paul Selden, who took me on first as a master's student, after asking me, "Do you like spiders? Would you be interested in working on fossil spiders?" and then later asking me, "Do you want to keep working on fossil spiders? I'll take you on for a Ph.D." I am grateful for being able to work with him and thankful for the opportunities he has provided and the research he has encouraged me to pursue. Paul has also supported all of

my outreach endeavors like showing off spiders at the KU Natural History Museum events. I would also like to thank my committee members—Alison Olcott for her help with the Aix-en-Provence taphonomy project and teaching me a variety of analytical instrumentation, as well as her collaboration on various teaching and LGBTQ+ related avenues; Deb Smith for her help with modern spiders and letting me teach arachnid paleontology for her classes; and Gene Rankey and Jen Roberts for their invaluable help with editing, methodology, and direction. Others at KU I would like to thank include Diane Kamola and Leigh Stearns for their support and mentorship as a Graduate Teaching Assistant throughout my Ph.D.

My advisor, committee members, and other faculty have helped immensely with my growth as a scientist and professional development, and for that I am grateful.

I also want to acknowledge my previous lab mates, James Lamsdell and Erin Saupe, and Michelle Casey, another KU alum, for their support at the beginning of my academic career and Ph.D.

I would like to acknowledge Patrick Getty for his support in paleontology, geoscience education, and collaboration on LGBTQ+ topics in geology, Kriss Leftwich for always being my Geological Society of America meeting buddy, and Tabs and NDD for being a constant source of support while I've been a graduate student.

Finally, I would like to thank all of those who were coauthors, collaborators, provided specimens, as well as funding agencies that all helped make this research and dissertation possible.

Table of Contents

Introduction

The fossil record documents life through time, but is relatively incomplete. For example, a bias exists in the fossil record toward the preservation of hard parts, which are more likely to be preserved than soft tissues of soft-bodied organisms that typically decay rapidly. Taphonomy, the study of the processes and factors that control how remains become fossilized, can be used to infer what information is lost about ancient ecological communities and help elucidate the nature of taphonomic pathways in paleoenvironments that lead to exceptional preservation. Instances of exceptional preservation in the geologic record are known as Fossil-Lagerstätten, and are primarily defined by the preservation of soft tissues. Fossil-Lagerstätten represent snapshots of ancient ecological communities and can provide a wealth of information about biodiversity through time. Many Fossil-Lagerstätten form in lacustrine depositional settings, a result of the conditions necessary for soft tissue preservation such as anoxia, rapid burial, rapid mineralization, and microbial activity.

Spiders lack mineralized hard parts, and are thus considered soft-bodied organisms. As a result, spiders are rare in the fossil record, except in lacustrine deposits and amber, which favor the preservation of soft tissues. Amber spiders are relatively well studied compared to spiders preserved in lacustrine deposits due to the high level of morphological detail and 3D preservation in amber, while fossil spiders from lacustrine deposits are less studied, or are in need of revision. These differing modes of preservation also have very different taphonomic pathways, with likely more variability within lacustrine deposits. Hitherto, no studies have examined the taphonomic biases of fossil spider assemblages in lacustrine deposits, and thus for some deposits that taphonomic pathway is poorly understood.

This dissertation explores the fossil record of spiders by investigating the biases influencing fossil spider assemblages preserved in lacustrine deposits and the mechanisms and pathways responsible for preservation in Fossil-Lagerstätten. The first part of this dissertation (Chapters 1–4) focuses on fossil spider taxonomy and includes spiders from the Cretaceous Crato Formation of Brazil, the Eocene Kishenehn Formation of Montana, and the Eocene Florissant Formation of Colorado. Revised and newly described spiders preserved as three-dimensional replacements are from the Crato Formation and include the earliest found palpimanid spider (Palpimanidae) and several webweaving spiders. These spiders are imaged with micro-computed tomography (micro-CT) to produce 3D models that reveal details of the spiders otherwise lost in the rock matrix. The first fossil spiders are described from the Kishenehn Formation and include new species of webweaving spiders and a ground-dwelling spider that could only be identified to family. From the Florissant Formation, a large Nephiline spider is redescribed and compared to extant Nephiline with electron microscopy. The second part of the dissertation (Chapter 5) focuses on the preservation of fossil spiders from the Oligocene Aix-en-Provence Formation from France. This study uses a multitechnique approach that includes fluorescence microscopy, scanning electron microscopy, and energy dispersive spectroscopy to reveal a taphonomic pathway that is influenced heavily by microbial activity resulting in the preservation of organic compounds from spider cuticle. The final part of the dissertation (Chapter 6) focuses on the biases related to taxonomy, size, life mode, and sex that influence fossil spider assemblages in lacustrine deposits. Biases are found to vary across lacustrine deposits and, instead, are variable with respect to the composition of the fossil spider assemblage. These results differ from amber, but together do provide a clearer picture of the fossil record of spiders.

Chapter 1

The earliest palpimanid spider (Araneae: Palpimanidae), from the Crato Fossil-Lagerstätte (Cretaceous, Brazil)

(Formatted for submission to *Journal of Arachnology*)

Matthew R. Downen: Department of Geology, University of Kansas, Ritchie Hall, Earth, Energy, and Environment Center, 1414 Naismith Dr Room 254, Lawrence, KS 66045, USA. E-mail: mattdownen@ku.edu

Paul A. Selden: Department of Geology, University of Kansas, Lindley Hall Room 121, 1475 Jayhawk Boulevard, Lawrence, Kansas 66045, USA, and Natural History Museum, Cromwell Road, London SW7 5BD, UK. E-mail: selden@ku.edu

Abstract. The Crato Formation (Lower Cretaceous) of Brazil is well known for an exceptionally preserved terrestrial arthropod fossil assemblage. Spiders are relatively abundant, but few have been formally described. A fossil spider belonging to the family Palpimanidae, araneophageous ground-dwelling spiders with distinctly robust front legs, is preserved with the dorsal side hidden within the rock matrix. For the first time, micro-computed tomography (micro-CT) was used to image a fossil spider preserved in rock matrix, to reveal the dorsal side of this specimen, revealing the eye arrangement, a useful taxonomic character in most spiders, and a deflated abdomen, likely the result of taphonomic processes. The specimen possesses other distinguishing characteristics of Palpimanidae, including an inflated first leg femur, a heavily sclerotized scutum, and a reduced number of spinnerets (2) surrounded by a sclerotized ring. The spider has eight eyes with the lateral pairs extremely close together, a trait suggestive of the subfamily Chediminae. The specimen also possesses an unusual first leg patella with a retrolateral excavation and a thorn-like projection. A new genus is erected, and the spider is named *Cretapalpus vittari* n. gen., n. sp. A phylogenetic analysis including extant species from each of the subfamilies within Palpimanidae places the fossil at the base of Chediminae. This report is the earliest fossil palpimanid and first chedimine from South America. A fossil chedimine in South America is not surprising because the South American and African plates were still relatively close during the Early Cretaceous.

Keywords: Mesozoic, paleobiogeography, Palpimanoidea, South America, systematics

INTRODUCTION

Palpimanidae is a small family (18 genera, 150 species) of nocturnal, ground-dwelling spiders whose members occur mainly in tropical and subtropical regions of the world, except Australia (Jocqué & Dippenaar-Schoeman 2006; World Spider Catalog 2020). They are characterized by an extremely thick cuticle on all parts of the body except the opisthosoma (even here, there are commonly sclerotized scuta) and enlarged front legs. By this means, they stalk and capture other spiders as prey, yet are armored against retaliatory bites (Cerveira & Jackson 2005; Pekár et al. 2011). Palpimanidae is historically a poorly studied group but, recently, several genera have been revisited or newly described.

Spiders from the Cretaceous Fossil-Lagerstätte (locality of exceptional fossil preservation) of Crato, Brazil, are relatively numerous but, hitherto, few have been described (Mesquita 1996; Selden et al. 2006; Raven et al. 2015). Here, we present a single specimen of a palpimanid from this locality. It is the oldest member of the family and the first Mesozoic record; the previously known oldest, and only known fossil occurrence of Palpimanidae, are three juvenile specimens of the extant genus *Otiothops* MacLeay, 1839 from the Neogene Dominican amber (Wunderlich 1988); a possible palpimanid has also been reported from mid-Cretaceous Burmese amber (Wunderlich 2017). Nevertheless, the superfamily Palpimanoidea has representatives dating back to the Jurassic period (Penney 2004; Selden et al. 2008; Selden & Dunlop, 2014; Wunderlich 2015; Selden et al. 2019; and references therein), so the existence of the nominate family in the early Cretaceous is not unexpected. Palpimanoidea, especially the family Archaeidae, has received much more attention in phylogenetic studies. Little work has been done on phylogenetic relationships specifically within Palpimanidae (Wood et al. 2012).

Palpimanidae is divided into three subfamilies: Chediminae, Otiothopinae, and Palpimaninae (Platnick 1975, 1985). The specimen described here is referred to the subfamily Chediminae, a clade known today only from Africa across to south Asia (Zonstein & Marusik 2013). The fossil possesses closely spaced lateral eyes, a characteristic commonly used for placement in Chediminae. No extant specimens of Chediminae have been discovered from South America; however, the presence of a fossil specimen in Brazilian sediments is not unexpected, given that the South American and African continents were still in close proximity in the early Cretaceous, and other fauna from the Crato beds show similar affinities to present-day African clades; e.g., Solifugae, Scorpiones (Selden & Shear 1996; Menon 2007).

STRATIGRAPHY AND PALEOECOLOGY

The specimen comes from one of the quarries in the Nova Olinda Member of the Crato Formation around the town of Nova Olinda, Ceará Province, northeastern Brazil. The Nova Olinda member is at the base of the Crato Formation and is composed of alternating laminated limestones and mixed carbonate and siliciclastic beds (Martill & Heimhofer 2007). The accepted age of late Aptian (115–120 Ma) for the Crato Formation is based on palynological data (Heimhofer & Hochuli 2010). The depositional environment is interpreted as a stratified lake with hypersaline bottom waters in a semi-arid to arid environment (Heimhofer et al. 2010). The lake basin was the result of extensional tectonics when active rifting was separating the South American and African continents during the early Cretaceous (Martill 2007).

Notable fauna from this deposit include fish and pterosaurs, but terrestrial invertebrates like insects dominate the fossil assemblage (Martill et al. 2007). Spiders are relatively abundant, although rarer than insects. The preserved arachnofauna provides interesting insight into the

paleoenvironment. The presence of solifuges supports the semi-arid climate interpretation; however, other fossilized arachnids like scorpions and amblypygids suggest possibly more humid conditions (Selden & Shear 1996; Dunlop & Martill 2001; Menon 2007). There were likely a variety of environments relatively close to the Crato paleolake from which organisms could be transported. Most of the arachnids in the deposit are spiders, with many resembling aerial web-weaving spiders.

MATERIAL AND METHODS

Materials.—The specimen consists of a part only, in ventral view, with some legs extended, others partly (e.g., left leg III, right leg IV) or fully (e.g., right leg II) flexed (Fig. 1). The distal podomeres of some legs are absent, presumably lost with the counterpart; these are: metatarsus and tarsus of leg I, tibia to tarsus of leg II, left (on the right, the tarsus of leg II is present, folded back alongside the proximal part of the leg, Fig. 1), and most of the tarsi of legs III (right) and IV; left leg III is complete to the tip of the tarsus. The cuticle of the fossil is preserved in a buff-colored, finely laminated limestone (Plattenkalk) by replacement with goethite (hydrated iron oxide); a finely tuberculate surface sculpture can be seen on external surfaces (e.g., on the ventral scutum, Fig. 1), and the sternum has a coarsely tuberculate sculpture. Within the matrix, spines and setae can be seen at the margins of podomeres (e.g., right tibia and metatarsus IV, Fig. 1). Within the specimen, cavities are filled partly with calcite crystals, though some pale tan, fibrous material (e.g., in right femur II, Fig. 1) likely represents replaced muscle. The exceptional preservation of the insects in the Nova Olinda Member has recently been described recently by (Barling et al. 2015). These authors showed that the goethite seen in specimens in weathered matrix actually replaces other iron minerals, that are present in the unweathered samples. Nevertheless, the mineralization has replaced the original organic material in remarkably fine

detail. Palpimanids have a distinctively thick cuticle (Pekár 2011, table 3), and so this specimen is preserved three-dimensions, except for the soft parts of the opisthosoma, which are deflated and folded, especially when viewed in 3D (Fig. 2). The deflated abdomen is likely the result of taphonomic processes related to osmosis and the hypersaline bottom waters of the Crato paleolake (Downen et al. 2016).

Methods.—The specimen was studied using a Leica M205C stereomicroscope, photographed with a Canon EOS 5D MkII digital camera attached to the microscope and captured with DSLR Assistant software (www.kaasoft.com) on an Apple MacBook Pro computer. Drawings were made using a drawing tube attached to the microscope. Photographs were manipulated using Adobe Photoshop software, and final drawings were made using Graphic (www.graphic.com). All measurements are in millimeters and were made from the drawings using Graphic. Measurements of paired organs are means of left and right. Note that, because of the three-dimensional preservation, it is not possible to get accurate measurements for some podomeres, posterior femora and patellae in particular, and the distorted opisthosoma defies accurate measurement.

The sample was cut with a Dremel saw into a rectangular prism to minimize the amount of matrix. The dorsal side of the specimen was imaged using an FEI HeliScan micro-CT scanner in the Earth, Energy and Environment Center (EEEC) at the University of Kansas, Lawrence KS. The specimen was mounted upright on a stub with double-sided sticky tape and rotated through the x-ray beam for approximately eight hours (Appendix 1). The data was reconstructed using qmango software (Thermo Fisher Scientific). Segmentation and 3D visualization was conducted in PerGeos Software for Digital Rock Analysis at the University of Kansas. Measurements of 3D images were made using PerGeos Software and Adobe Photoshop.

Cladistic analysis and character matrices.—Two analyses were conducted. The fossil and four other palpimanid genera were scored into the matrix used in Selden et al. (2019, Appendix 1), which is based on the matrix used in Wood et al. (2012). The analysis also used the same methods in Selden et al. (2012). The analysis employed MrBayes v3.2.6 and generated a majority rule consensus tree. The tree was imported into FigTree v1.4.4 and manipulated for visuals. The matrix and associated code for the analysis is included as a NEXUS file in supplementary material. A second analysis was run using PAUP* v4.0a (build 167)(Swofford 2003). In this analysis, only palpimanid genera and one outgroup were included to examine relationships within Palpimanidae. This simple phylogenetic analysis based on morphological characters was conducted to determine to which subfamily the fossil spider belongs. The fossil specimen, although exceptionally preserved, lacks many useful visible characters that are observed in extant specimens such as genitalia, the fovea, and details of the chelicerae. Morphological characters were chosen primarily based on what is visible in the fossil and by characters used to distinguish the three subfamilies. Characters of extant palpimanids were taken from descriptions and figures from previous literature. A simple heuristic search (Optimality criterion = parsimony) returned five trees (supplemental material) and a 50% Majority-rule consensus tree. The trees were manipulated in FigTree v1.4.4 for visuals.

Taxon sampling.—The Crato specimen was compared with palpimanids described in the recent literature. The phylogenetic analysis based on the Selden et al. (2019) matrix included the fossil specimen and four additional palpimanid genera: *Chedimanops sp*. Zonstein & Marusik, 2017, *Levymanus sp.* Zonstein & Marusik, 2013, *Steriphopus sp.* Simon, 1887, and *Otiothops sp*. The smaller analysis focusing explicitly on Palpimanidae was based on seven taxa. Species from each of the three subfamilies were included in descriptive comparisons and the simple

phylogenetic analysis. Chediminae is the most diverse subfamily with regard to number of genera (11), but only three species, each from a separate genus, were included here. From Chediminae: *Levymanus gershomi* Zonstein & Marusik, 2013; *Steriphopus macleayi* Simon, 1887. *Palpimanus* Dufour, 1820 (Palpimaninae) and *Otiothops* (Otiothopinae) are the most species-rich genera. From Otiothopinae: *Otiothops chiaque* Cala-Riquelme, Quijano-Cuervo & Agnarsson in Cala-Riquelme et al., 2018; *Otiothops atalaia* Castro, Baptista, Grismado & Ramírez, 2015. Palpimaninae only contains three genera: *Palpimanus*, *Ikuma* Lawrence, 1938, and *Badia* Roewer, 1961. *Palpimanus sp.* was already included in the Selden et al (2019) and Wood et al. (2012) matrix. No taxonomic work exists for *Ikuma* and *Badia* beyond the 1960s, so *Palpimanus processigor* Strand, 1913 was used. The outgroup was represented by *Huttonia palpimanoides* Pickard-Cambridge, 1880 (Huttoniidae). Huttoniidae has been included in previous molecular and morphological phylogenetic analyses, and commonly is placed as the sister group to Palpimanidae (Wood et al. 2012)

Morphological Characters.—The 10 morphological characters used in this analysis are listed below. Each character state is coded as (0) or (1), with (?) representing an unknown. All characters are coded as (0) for their state in *Huttonia*.

1. Leg I: (0) not inflated, (1) inflated.

2. Size of Leg I patella: (0) fe/pa > 1.25, (1) fe/pa ≤ 1.25

3. Distance between lateral eyes (ALE-PLE): (0) > 0.01, (1) < 0.01.

4. The distance between posterior median eyes (PME): (0) > 0.01, (1) < 0.01.

5. PME size: (0) subequal to other eyes, (1) larger than other eyes.

6. Anterior eye row shape: (0) straight or recurved, (1) procurved.

7. Tegular sclerites: (0) present, (1) absent.

8. Labium shape: (0) labium longer than wide, (1) labium as long as wide.

9. Maxillae shape: (0) rotated so distal edge is convergent, (1) not rotated so project forward.

Conductor of male pedipalp: (0) present, (1) absent.Abbreviations: AME anterior median eye(s), car carapace, ch chelicera, cp clypeus, cx coxa, fe femur, L length, lb labium, LE lateral eye(s), mt metatarsus, mx maxilla, op opisthosoma, pa patella, Pd pedipalp, PME posterior median eye(s), sp spinnerets, st sternum, ta tarsus, ti tibia, W width. Repository abbreviation: KUMIP University of Kansas Natural History Museum, Department of Invertebrate Paleontology.

SYSTEMATIC PALEONTOLOGY

Order Araneae Clerck, 1757

Suborder Opisthothelae Pocock, 1892

Infraorder Araneomorphae Smith, 1902

Superfamily Palpimanoidea *sensu* Wood, 2012

Family Palpimanidae Thorell, 1870

Remarks.—The characters of the family which place the fossil in the Palpimanidae are: inflated first leg (all podomeres from coxa to at least tibia are swollen in comparison with other legs); free labium; single pair of spinnerets (presumably anterior), surrounded by a sclerotized

ring; sternum scutiform, coarsely tuberculate, with extensions between coxae (Platnick 1975; Jocqué & Dippenaar-Schoeman 2006).

Genus ***Cretapalpus*** new genus

Diagnosis.—Distinguished from all other palpimanids by the patella of the first leg which is short, excavated retrolaterally, and bears a distal prolateral apophysis.

Etymology.—After the Latin *creta* for chalk and *palpus* for the palp-footed spiders.

Type species.—*Cretapalpus vittari* n. sp. (monotypic).

Cretapalpus vittari new species

Figures 1–3.

Palpimanid spider: Selden & Penney 2017: fig. 16.

Etymology.—Named for the Brazilian singer, songwriter, and drag queen Pabllo Vittar.

Type.—Holotype subadult male, only known specimen, part only, KUMIP 374705, from Nova Olinda Member of the Crato Formation; Early Cretaceous (late Aptian) age; quarry at Nova Olinda, Ceará Province, Brazil; deposited in the University of Kansas Natural History Museum, Department of Invertebrate Paleontology.

Diagnosis.—As for the genus.

Description.—Carapace suboval in outline, narrowing slightly anteriorly, anteriorly truncated in dorsal and lateral view, steeply sloping posteriorly. Labium triangular, as long as wide, and notched distally. Maxillae stout, almost as long as wide, tapering distally. Sternum

scutiform, heavily tuberculated, extensions around coxae and pedicle attachment. Eye region slightly projected forward. Eight eyes in two rows; AE row slightly recurved, PE row slightly recurved. AME largest (diameter = 0.19, 2× diameter of other eyes), other eyes subequal (average = 0.82). Distance between AME 0.11. Distance between AME and ALE 0.12. Distance between lateral eyes < 0.01. Clypeus height 0.39 (2× diameter of AME). Chelicerae 2× long as clypeus height. Patellae short, with excavation >½ their length. Distal prolateral apophysis on patellae 0.29 long. Opisthosoma rounded in outline, about as long as wide. Ventral scutum nearly ½ length of opisthosoma and nearly equal to length of sternum, lacking extensions, with heavily sclerotized ring around pedicle.

Measurements: body L 4.71; car L 1.81, W 1.80 (L/W 1.01); op L 2.27, W 2.23 (L/W 1.01); st L 1.33, W 1.01 (L/W 1.32); lb L 0.42, W 0.32 (L/W 1.32); mx L 0.40, W 0.34 (L/W 1.18). Podomere lengths: Pd ta 0.49; leg I cx 0.89, tr 0.89, fe 2.11 (W 0.86, L/W 2.45), pa 1.05, ti ≥1.14; leg II cx 0.64, tr 0.22, fe 1.65 (W 0.42, L/W 3.92), pa 0.67, ta 0.71; leg III cx 0.61, tr 0.31, fe 1.21 (W 0.36, L/W 3.35), pa 0.37, ti 1.19, mt 0.95, ta 0.56; leg IV cx 0.57, fe 2.03 (W 0.41, L/W 4.99), pa 0.62, ti 1.52, mt 1.53. Ventral scutum L 1.18, W 1.49, L/W 0.79.

DISCUSSION

The classification of spiders, especially at the generic and specific level, typically relies on genitalic characteristics of the male and female. This is also true for palpimanid spiders, with recent papers also including the internal structure of the copulatory organs of females (Castro et al. 2015; Zonstein et al. 2016; Zonstein & Marusik 2017a). The specimen described here is a subadult male, indicated by the thorn-like modifications on the front legs and unmodified palps (Fig. 3). Some male palpimanines, like *Palpimanus armatus* Pocock, 1898, possess a thorn-like

extension of the cuticle on the femur and patella of the first leg. These features suggest the specimen is a male, and was initially suggestive that the fossil was a palpimanine but, based on characteristics of the eyes and mouthparts, *Cretapalpus* is unlikely to belong to Palpimaninae. Characteristics of the eyes, including size and arrangement, are helpful in understanding the subfamily and phylogenetic placement of *Cretapalpus*. The closely spaced lateral eyes of the Crato specimen are suggestive of Chediminae. Closely spaced or touching lateral eyes distinguish Chediminae from Palpimaninae, which have widely spaced lateral eyes (Platnick 1981; Zonstein & Marusik 2019). The palpimanines also have an AME/PME ratio of approximately 1.6–1.9, whereas the chedimines possess larger AME to PME. The chedimines *L. germoshi* and *S. macleayi* have an AME/PME ratio of 5 and 2.5, respectively, in *D. biplagiatus* the PME are slightly larger (AME/PME = 0.86), and species of *Chedimanops* Zonstein & Marusik, 2017 lack PME (Zonstein & Marusik 2013; Zonstein et al 2016; Zonstein & Marusik 2017b). The AE row of the Crato specimen and other chedimines appear to be straight or slightly recurved in contrast to the four palpimanines included here, which have an AE row that is procurved. *Palpimanus* has a slightly longer labium and maxillae that fan out distally (Zonstein & Marusik 2019). The mouthparts, labium and maxillae of the Crato specimen closely resemble those of *Levymanus*, a chedimine from Israel (Zonstein & Marusik 2013; Zonstein et al. 2017).

Distinguishing *Cretapalpus* from otiothopine genera is more difficult. Otiothopines lack the tegular sclerites characteristic of chedimines. This feature is not visible in the Crato specimen, but other characteristics visible in the specimen can be compared to genera within the Otiothopinae. Some otiothopines also possess closely spaced or touching lateral eyes, but many also possess closely spaced posterior median eyes, unlike Cretapalpus and other chedimines, except for *Diaphorocellus biplagiatius* Simon, 1893 (Brescovit & Bonaldo 1993; Zonstein et al.

2016; Cala-Riquelme et al. 2018). The only preserved tarsi are on leg 3 of the left side and leg 2 of the right side (ventral up) and appear to lack dense claw tufts. This is different from *Otiothops*, which possess dense claw tufts on legs 2–4, but it could be possible that the claw tufts are simply not preserved in the fossil specimen. The AE row of *Cretapalpus* and extant chedimines and otiothopines is mostly straight, with the exception of *Fernandezina* Birabén, 1951, which is recurved. *Fernandezina* also lack the greatly inflated femur of the first leg that *Cretapalpus* and other chedimines possess (Ramírez & Grismado 1996; Platnick, et al. 1999).

In a recent molecular phylogenetic analysis Chediminae was recovered as the most derived group within Palpimanidae and sister to *Palpimanus*, while Otiothopinae, represented by *Otiothops* and *Anisaedus* Simon, 1893 was the most basal (Wood et al. 2018). The phylogeny presented here places *Cretapalpus* with certainty within Palpimanidae (Fig. 4). In contrast to the molecular phylogeny, palpimanines are presented here as the most basal in the tree, and *Otiothops* as sister to the chedimine group. A thorough and comprehensive phylogenetic analysis of Palpimanidae combining molecular and more robust morphological characters is needed to confidently hypothesize evolutionary relationships at the subfamily level.

Cretapalpus is the first reported Mesozoic occurrence of Palpimanidae and the first chedimine palpimanid reported from South America. Today, chedimines are found throughout Africa, the Middle East, and Southern Asia. Otiothopinae has been reported from almost every country in South America, several islands in the Caribbean, as well as a few countries in Africa and Asia (Brescovit & Bonaldo 1993). Palpimaninae has been reported mostly in Africa, the Middle East, and the Mediterranean. During the early Cretaceous, the South American and African continents were still relatively close or partially connected. All subfamilies of Palpimanidae were likely dispersed throughout Gondwana before the breakup of the

supercontinent. The reason for the absence of Chediminae in South America today is unknown. It is possible chedimines are present in South America, but are rare and have not yet been observed. Other spider-bearing lacustrine deposits in China and Korea, as well as Burmese amber, have shown the superfamily Palpimanoidea was quite diverse during the Mesozoic (Wunderlich 2008; Park et al. 2019; Selden et al. 2019). As the oldest fossil representative of Palpimanidae thus far, *Cretapalpus vittari* extends the age of the family back 10–13 million years within the Cretaceous.

ACKNOWLEDGEMENTS

We thank Sergei Zonstein for comments on palpimanids; Arsalan Zolfaghari and Sherifa Cudjoe for micro-CT scanning and PerGeos software assistance at the University of Kansas; PAS thanks Dave Martill and Bob Loveridge for help in the field in Brazil.

LITERATURE CITED

Barling, N., D.M. Martill, S.W. Heads & F. Gallien. 2015. High fidelity preservation of fossil insects from the Crato Formation (Lower Cretaceous) of Brazil. Cretaceous Research 52:605–622.

Birabén, M. 1951. *Fernandezina*, nuevo género de Palpimanidae (Araneae). Acta Zoologica Lilloana 12:545–549.

Brescovit, A.D. & A.B. Bonaldo. 1993. On the genus *Otiothops* in Brazil (Araneae, Palpimanidae). Bulletin de l'Institut Royal des Sciences Naturelles de Belgique. Entomologie 63:47–50.

Cala-Riquelme, F., L. Quijano-Cuervo, A. Sabogal-González & I. Agnarsson. 2018. New species of Otiothopinae (Araneae: Palpimanidae) from Colombia. Zootaxa 4442:413–426.

Castro, D., Baptista, R., Grismado, C. & M.J. Ramírez, 2015. New species and records of Otiothopinae from the Southern Atlantic Rainforest, with notes on the claw tufts in *Fernandezina* Birabén (Araneae: Palpimanidae). Zootaxa 4012:465–478.

Cerveira, A.M. & R.R. Jackson. 2005. Specialised predation by *Palpimanus* sp. (Araneae: Palpimanidae) on jumping spiders (Araneae: Salticidae). Journal of East African Natural History 94:303–318.

Downen, M.R., P.A. Selden & S.T. Hasiotis. 2016. Spider leg flexure as an indicator for estimating salinity in lacustrine paleoenvironments. Palaeogeography, Palaeoclimatology, Palaeoecology 445:115–123.

Dunlop, J.A. & D.M. Martill. 2001. The first whipspider (Arachnida: Amblypygi) and three new whipscorpions (Arachnida: Thelyphonida) from the Lower Cretaceous Crato Formation of Brazil. Transactions of the Royal Society of Edinburgh: Earth Science 92:325–334.

Heimhofer, U. & P.A. Hochuli. 2010. Early Cretaceous angiosperm pollen from a low-latitude succession (Araripe Basin, NE Brazil). Review of Palaeobotany and Palynology 161:105–126.

Heimhofer, U., D. Ariztegui, M. Lenniger, S.P. Hesselbo, D.M. Martill & A.M. Rios-Netto. 2010. Deciphering the depositional environment of the laminated Crato fossil beds (Early Cretaceous, Araripe Basin, North-eastern Brazil). Sedimentology 57:677–694.

Jocqué, R. & A.S. Dippenaar-Schoeman. 2006. Spider families of the world. Royal Museum for Central Africa. Tervuren, Belgium.

Martill, D. 2007. The Geology of the Crato Formation. Pp. 8–24. *In* The Crato Fossil Beds of Brazil: Window into an Ancient World. Cambridge University Press.

Martill, D. & U. Heimhofer. 2007. Stratigraphy of the Crato formation. Pp. 15–30. *In* The Crato fossil beds of Brazil: window into an ancient world. Cambridge University Press.

Menon, F. 2007. Higher systematics of scorpions from the Crato Formation, Lower Cretaceous of Brazil. Palaeontology 50:185–195.

Mesquita, M.V. 1996. *Cretaraneus martinsnetoi* n. sp.(Araneoidea) da Formação Santana, Cretáceo Inferior da Bacia do Araripe. Revista Geociências-UNG-Ser 1:24–31.

Park, T-Y. S., K-S. Nam & P.A. Selden. 2019. A diverse new spider (Araneae) fauna from the Jinju Formation, Cretaceous (Albian) of Korea. Journal of Systematic Palaeontology 15:1051–1077.

Pekár, S., J. Šobotník & Y. Lubin. 2011. Armoured spiderman: morphological and behavioural adaptations of a specialised araneophagous predator (Araneae: Palpimanidae) Naturwissenschaften 98:593–603.

Penney, D. 2004. Cretaceous Canadian amber spider and the palpimanoidean nature of lagonomegopids. Acta Palaeontologica Polonica 49:579–584.

Platnick, N.I. 1975. A revision of the palpimanid spiders of the new subfamily Otiothopinae (Araneae, Palpimanidae). American Museum Novitates 2562:1–32.

Platnick, N.I. 1981. A review of the spider subfamily Palpimaninae (Araneae, Palpimanidae), I. Bulletin of the British Arachnological Society 5:169–173.

Platnick, N.I. 1985. On the Chilean spiders of the family Palpimanidae (Arachnida, Araneae). Journal of Arachnology 13:399–400.

Platnick, N.I., C.J. Grismado & M.J. Ramírez. 1999. On the genera of the spider subfamily Otiothopinae (Araneae, Palpimanidae). American Museum Novitates 3257.

Ramírez, M.J. & C.J. Grismado. 1996. A new *Fernandezina* from Brazil (Araneae, Palpimanidae). Iheringia, Série Zoologia 80:117–119.

Raven R.J., P.A. Jell, & R.A. Knezour. 2015. *Edwa maryae* gen. et sp. nov. in the Norian Blackstone Formation of the Ipswich Basin—the first Triassic spider (Mygalomorphae) from Australia. Alcheringa: An Australasian Journal of Palaeontology 39:259–263.

Selden, P.A. & W.A. Shear. 1996. The first Mesozoic Solifugae (Arachnida), from the Cretaceous of Brazil, and a redescription of the Palaeozoic solifuge. Palaeontology **39**:583–604.

Selden, P.A., F. da C. Casado & M.V. Mesquita. 2006. Mygalomorph spiders (Araneae: Dipluridae) from the Lower Cretaceous Crato Lagerstätte, Araripe Basin, north-east Brazil. Palaeontology 49:817–826.

Selden, P.A., H. Diying & R. Dong. 2008. Palpimanoid spiders from the Jurassic of China. The Journal of Arachnology 36:306–322.

Selden, P. A. & J.A. Dunlop. 2014. The first fossil spider (Araneae: Palpimanoidea) from the Lower Jurassic (Grimmen, Germany). Zootaxa 3894:161–168.

Selden, P.A., D. Huang & R.J. Garwood. 2019. New spiders (Araneae: Palpimanoidea) from the Jurassic Yanliao Biota of China. Journal of Systematic Palaeontology 18:137–185.

Selden, P.A. & D. Penney. 2014. Imaging techniques in the study of fossil spiders. Earth-Science Reviews 166:111–113.

Strand, E. 1913. Arachnida. I. *In*: Schubotz, H. (ed.) Wissenschaftliche Ergebnisse der Deutschen Zentral-Afrika-Expedition 1907-1908, unter Führung Adolf Friedrichs, Herzogs zu Mecklenburg. Klinkhardt & Biermann, Leipzig. 4(Zool. 2)325–474.

Wood, H.M., V.L. González, M. Lloyd, J. Coddington & N, Scharff. 2018. Next-generation museum genomics: Phylogenetic relationships among palpimanoid spiders using sequence capture techniques (Araneae: Palpimanoidea). Molecular phylogenetics and evolution 127:907–918.

Wood, H.M., C.E. Griswold, & R.G. Gillespie. 2012. Phylogenetic placement of pelican spiders (Archaeidae, Araneae), with insight into evolution of the "neck" and predatory behaviours of the superfamily Palpimanoidea. Cladistics 28:598–626.

World Spider Catalog. 2020. World Spider Catalog. version 21.0. Natural History Museum Bern, online at http://wsc.nmbe.ch

Wunderlich, J. 1988. Die fossilen Spinnen im dominikanischen Bernstein. Beiträge zur Araneologie 2:1–378.

Wunderlich, J. 2008. The dominance of ancient spider families of the Araneae: Haplogyne in the Cretaceous, and the late diversification of advanced ecribellate spiders of the Entelegynae

after the Cretaceous– Tertiary boundary extinction events, with descriptions of new families. Beiträge zur Araneologie, 5:524–675.

Wunderlich, J. 2015. On the evolution and the classification of spiders, the Mesozoic spider faunas, and descriptions of new Cretaceous taxa mainly in amber from Myanmar (Burma) (Arachnida: Araneae). Beiträge zur Araneologie 9:21–408.

Wunderlich, J. 2017. New and rare fossil spiders (Araneae) in mid Cretaceous amber from Myanmar (Burma), including the description of new extinct families of the suborders Mesothelae and Opisthothelae as well as notes on the taxonomy, the evolution and the biogeography of the Mesothelae. Beiträge zur Araneologie 10:72–279.

Zonstein, S.L. & Y.M Marusik. 2013. On *Levymanus*, a remarkable new spider genus from Israel, with notes on the Chediminae (Araneae, Palpimanidae). ZooKeys 326:27–45.

Zonstein, S.L. & Y.M Marusik. 2017a. A redescription of *Chedima purpurea* Simon, 1873, with notes on the unique copulative stopper mechanism in females (Aranei: Palpimanidae). Arthropoda Selecta 26:225–232.

Zonstein, S.L. & Y.M. Marusik. 2017b. Descriptions of the two-eyed African spider genera *Chedimanops* gen. n. and *Hybosidella* gen. n. (Araneae, Palpimanidae, Chediminae). African Invertebrates 58:23–47.

Zonstein, S.L. & Y.M Marusik. 2019. On the revisited types of four poorly known African species of *Palpimanus* (Araneae, Palpimanidae). African Invertebrates 60:83–95.

Zonstein, S.L., Y.M Marusik & M.M. Kovblyuk. 2017. New data on the spider genus *Levymanus* (Araneae: Palpimanidae). Oriental Insects 51:221–226.

Zonstein, S.L., Y.M Marusik & M.M. Omelko. 2016. Redescription of the type species of *Diaphorocellus* Simon, 1893 (Araneae, Palpimanidae, Chediminae). African Invertebrates 57:93–103.

EXPLANATION OF FIGURES

Figure 1.—*Cretapalpus vittari* n. gen. & sp. Photograph and interpretative drawing of ventral side. Gray areas represent missing cuticle. Scale bar = 1 mm.

Figure 2.—*Cretapalpus vittari* n. gen. & sp. 3D rendered volume of the fossil. A) In dorsal view, the carapace, eye pattern, pedipalps, patella excavation, and deflated abdomen are visible. B) Lateral view. Scale bar = 1 mm.

Figure 3.—*Cretapalpus vittari* n. gen. & sp. 3D rendered volume of the fossil. A) Oblique view of anterior and ventral showing clypeus, chelicerae, eyes, and palps that with unmodified tarsi. B) Head on view of anterior showing excavations on patella of the first leg. Scale bar = 1 mm.

Figure 4.—Phylogeny of extant genera and *Cretapalpus vittari* n. gen. & sp.A) Phylogenetic reconstruction based on Selden et al. (2019) matrix. All palpimanid genera except *Palpimanus* are unresolved as a polytomy. B) 50% Majority-rule consensus phylogeny of palpimanid genera with subfamilies indicated.

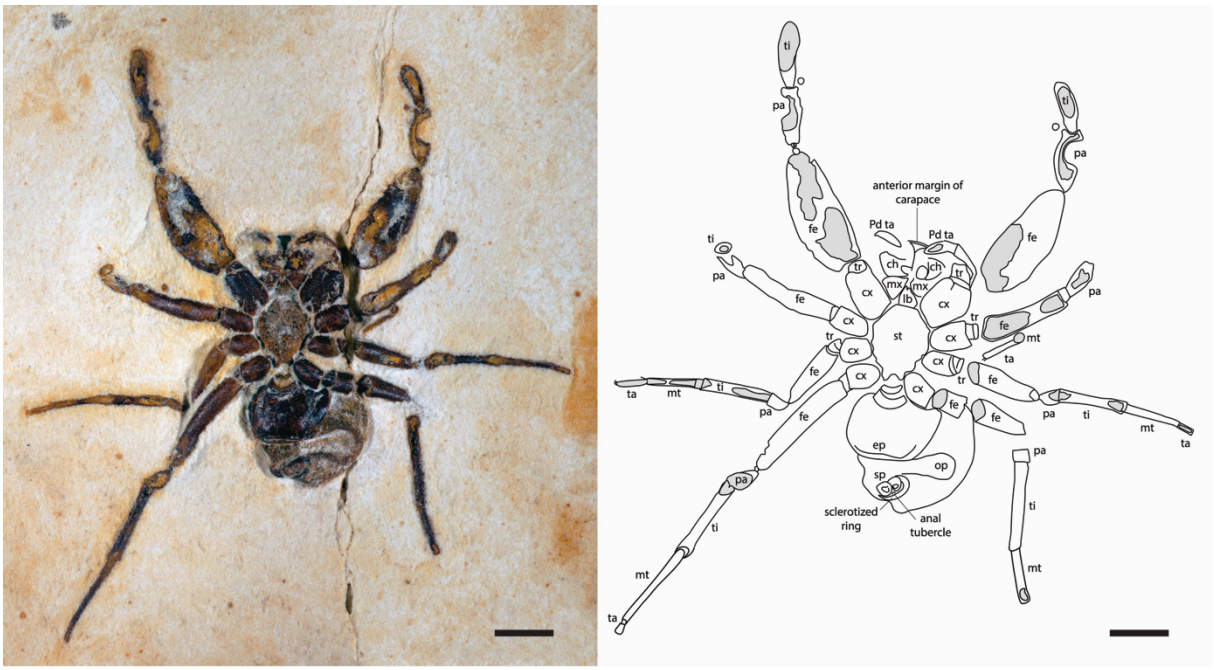
ti
pa
fe
Pd ta
anterior margin of carapace
ch
mx
lb
tr
cx
st
mt
ta
ep
op
sp
sclerotized ring
anal tubercle

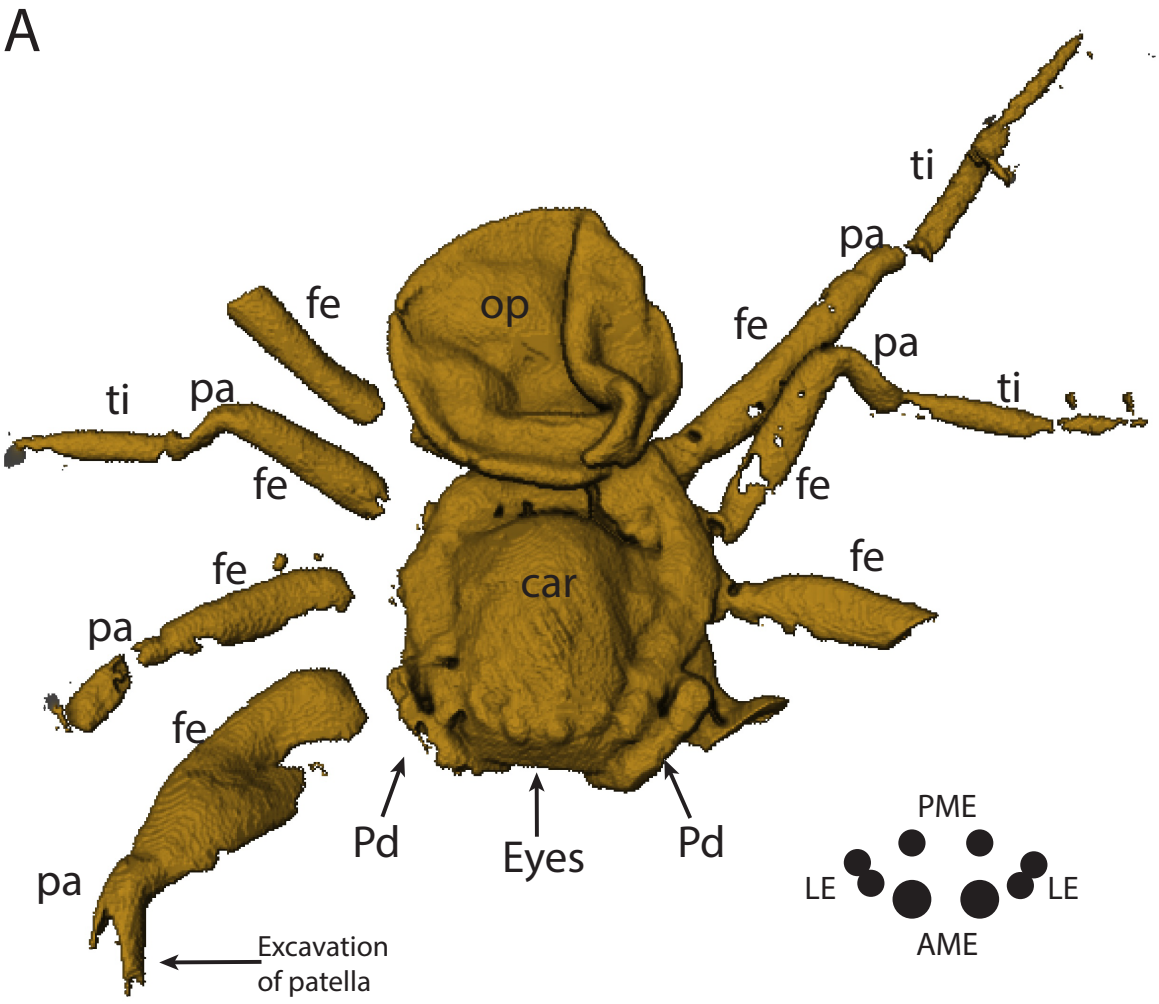
A
ti
pa
fe
op
fe
pa
ti
ti
pa
fe
fe
fe
car
fe
pa
fe
pa
Pd
Eyes
Pd
PME
LE
LE
AME
Excavation
of patella

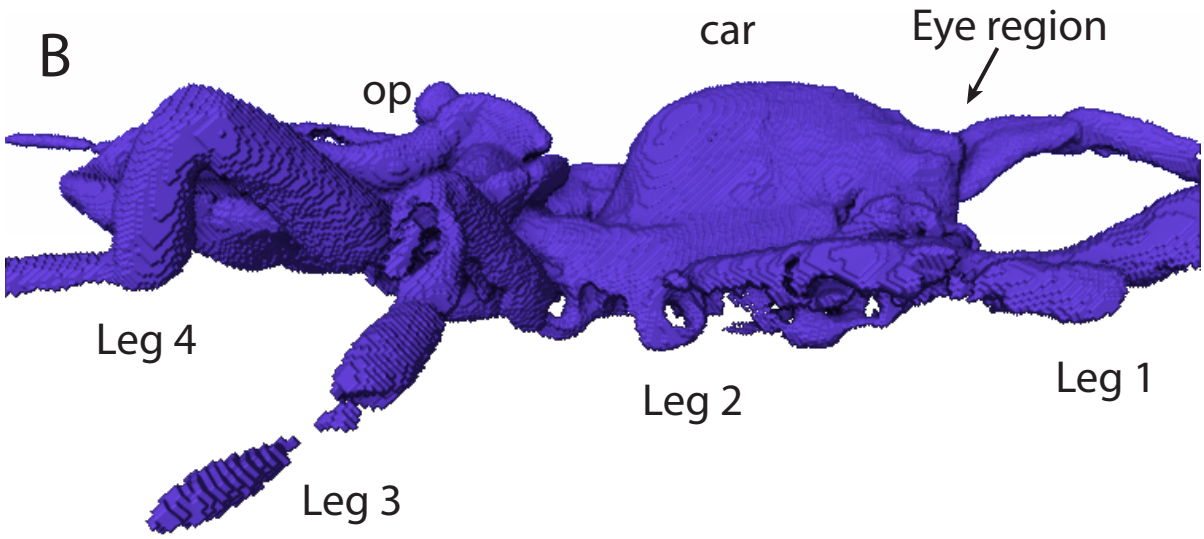
B
car
Eye region
op
Leg 4
Leg 2
Leg 1
Leg 3

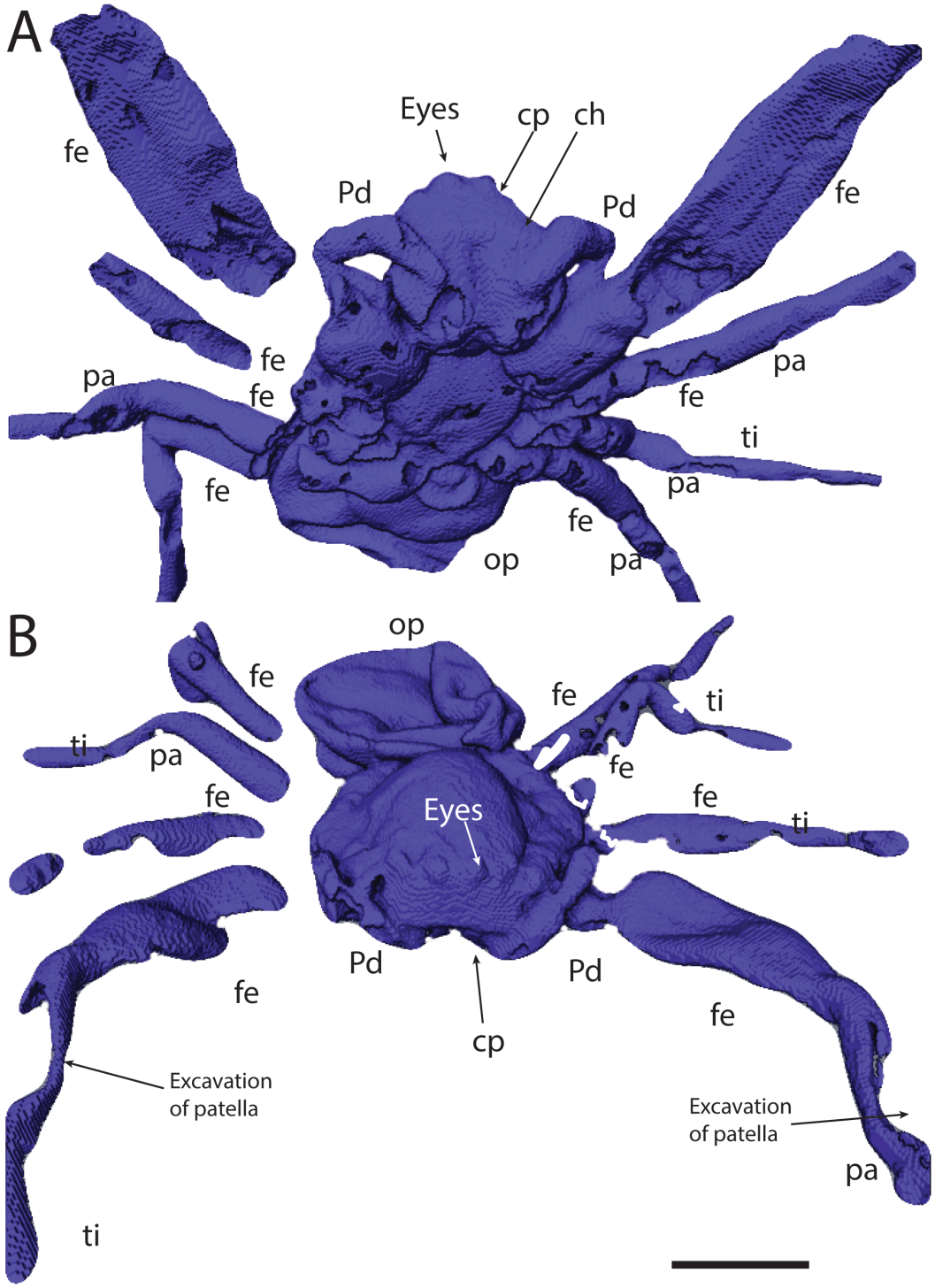
A
Eyes
cp
ch
Pd
Pd
fe
fe
fe
fe
pa
pa
fe
fe
ti
fe
pa
fe
op
pa
B
op
fe
fe
ti
ti
pa
fe
fe
fe
Eyes
ti
Pd
Pd
fe
fe
cp
Excavation
of patella
Excavation
of patella
pa
ti

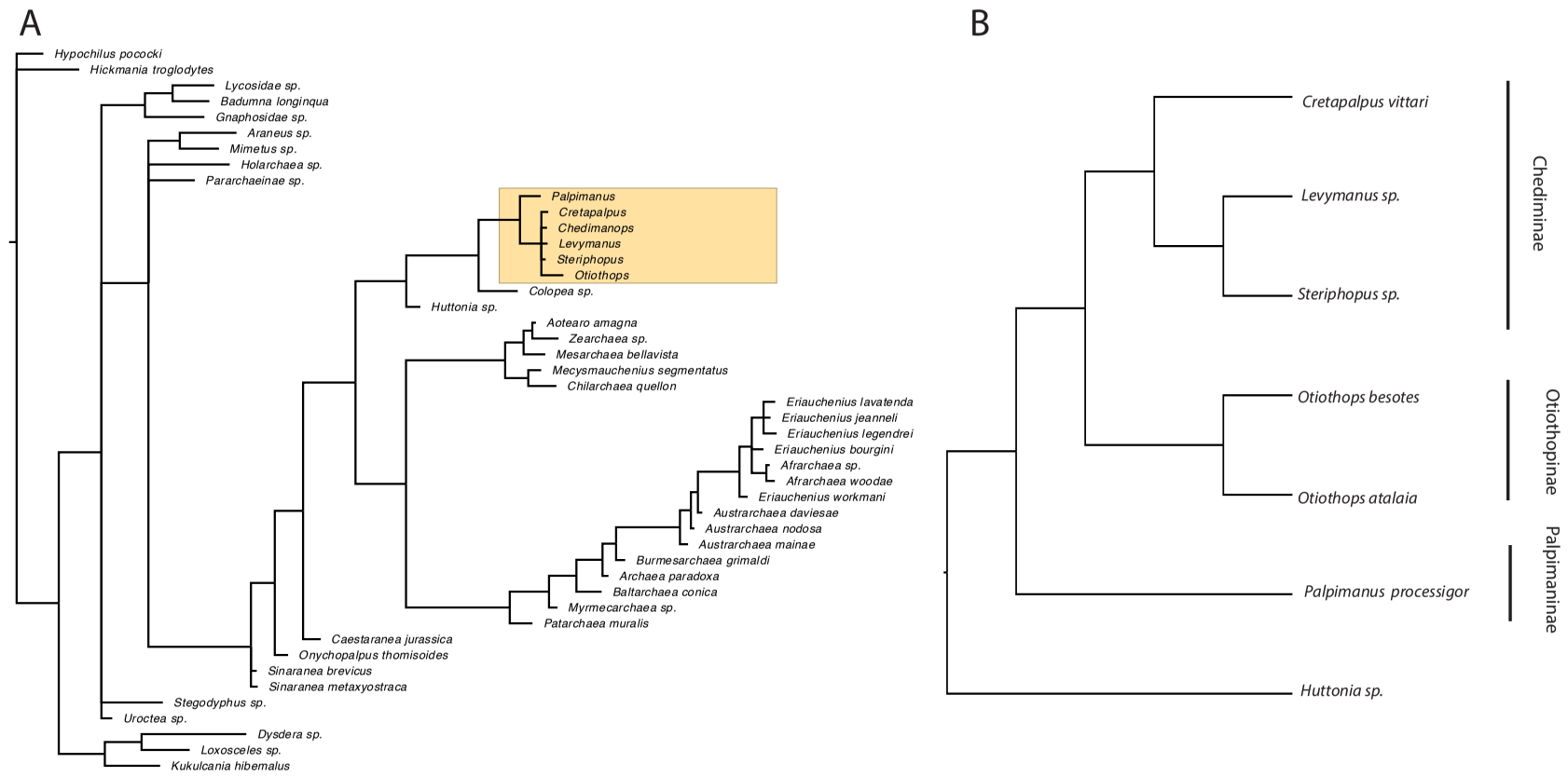
A
Hypochilus pococki
Hickmania troglodytes
Lycosidae sp.
Badumna longinqua
Gnaphosidae sp.
Araneus sp.
Mimetus sp.
Holarchaea sp.
Pararchaeinae sp.
Palpimanus
Cretapalpus
Chedimanops
Levymanus
Steriphopus
Otiothops
Colopea sp.
Huttonia sp.
Aotearo amagna
Zearchaea sp.
Mesarchaea bellavista
Mecysmauchenius segmentatus
Chilarchaea quellon
Eriauchenius lavatenda
Eriauchenius jeanneli
Eriauchenius legendrei
Eriauchenius bourgini
Afrarchaea sp.
Afrarchaea woodae
Eriauchenius workmani
Austrarchaea daviesae
Austrarchaea nodosa
Austrarchaea mainae
Burmesarchaea grimaldi
Archaea paradoxa
Baltarchaea conica
Myrmecarchaea sp.
Patarchaea muralis
Caestaranea jurassica
Onychopalpus thomisoides
Sinaranea brevicus
Sinaranea metaxyostraca
Stegodyphus sp.
Uroctea sp.
Dysdera sp.
Loxosceles sp.
Kukulcania hibernalus
B
Cretapalpus vittari
Levymanus sp.
Steriphopus sp.
Otiothops besotes
Otiothops atalaia
Palpimanus processigor
Huttonia sp.
Chediminae
Otiothopinae
Palpimaninae

Chapter 2

The diversity of spiders (Araneae) from the Crato Formation (Early Cretaceous, Brazil)

(Formatted for submission to *Cretaceous Research*)

Matthew R. Downen[1], **Sherifa Cudjoe**[2] and **Paul A. Selden**[1,3]: [1]Department of Geology, University of Kansas, 1414 Naismith Dr. Lawrence, KS 66045. E-mail: mattdownen@ku.edu; [2]Chemical and Petroleum Engineering, University of Kansas, 1530 W. 15th, Lawrence, KS 66045. E-mail: scudjoe@ku.edu; [3]The Natural History Museum, London, UK. E-mail: selden@ku.edu

Abstract

Spiders are relatively rare as fossils, but are most often preserved in amber or lacustrine deposits. The Crato Formation is an Early Cretaceous Fossil-Lagerstätte of lacustrine origin from northeastern Brazil with a relative abundance of fossil spiders preserved as three-dimensional replacements with goethite (iron hydroxide). Many of these spiders belong to Araneoidea, a superfamily of spiders known to weave aerial webs for prey capture. The first spider described from the Crato Formation was an araneid: *Cretaraneus martinsnetoi* Mesquita, 1996, but reexamination of the holotype and other specimens suggests these spiders are not representative of *Cretaraneus* Selden, 1990, so a new genus, *Olindarachne* gen. nov., is erected. The assemblage described here also includes two indeterminate araneoids, two large spiders representative of Nephilinae (Araneidae), and two spiders possibly belonging to the family

Tetragnathidae. The composition of the Crato fossil spider assemblage reflects a spider community dominated by orbweaving spiders. The Crato Formation is the only source of fossil spiders from South America reported thus far, and differs from other Cretaceous spider-bearing lacustrine and amber deposits.

Keywords: Araneidae, Orbweaver, Mesozoic, Aptian, Lagerstätten, Lacustrine

Highlights:

- New fossil spiders are described from the Cretaceous Crato Formation of Brazil
- Fossil spiders are recontructed in 3D with micro-CT imaging
- Large orbweaving spiders dominate the Crato fossil assemblage

1. Introduction

Fossil spiders are relatively rare, but most commonly are found preserved in amber or lacustrine deposits and reflect snapshots of diversity through time. Many of the fossil spiders that have been described formally come from Cenozoic ambers but, in recent years, the Mesozoic record has been expanded. Some of the earliest Mesozoic fossil spiders are from the Triassic of South Africa (225 Ma), Virginia (225 Ma), and Australia (225 Ma), and are represented by relatively few fossil specimens (Raven et al., 2015; Selden et al., 2009, 1999). The Jurassic record includes the earliest fossil spider assemblages in which spiders are relatively abundant, with specimens numbering in the hundreds. A lacustrine deposit from China, the Haifanggou Formation (also known as the Jiulongshan Formation; 162 Ma) has produced an impressive diversity of fossil spiders that includes a variety of palpimanoid (Palpimanoidea) and cribellate stem-deinopoid

(Deinopoidea) spiders. Significant Cretaceous spider-bearing deposits include the Burmese amber (99 Ma) of Myanmar, the Jinju Formation of Korea (112 Ma), the Yixian Formation of China (125 Ma), and others (Park et al., 2019; Penney and Selden, 2011; Selden et al., 2016; Selden and Ren, 2017). The Cretaceous marks the appearance of many extant spider families in the fossil record, and many of these families are relatively diverse today. The fossil spiders in this paper come from the Crato Formation of northeastern Brazil, an Early Cretaceous (late Aptian) Fossil-Lagerstätte.

Hitherto, few spiders have been formally described from the Crato deposit, and include three spiders from the family Dipluridae, a recently described palpimanid, and an araneid spider (Mesquita, 1996; Selden et al., 2006; Downen and Selden, 2020). The previously described spiders were assigned to genus and species. Here, we present a summary of previously described, revised, and new Araneae from the Crato Formation that includes the families Dipluridae, Palpimanidae, Araneidae, Nephilidae, and possibly Tetragnathidae.

The first fossil spiders described from the Crato Formation belong to the family Dipluridae (Infraorder: Mygalomorphae) (Selden et al., 2006). Diplurids are easily recognizable by their strong porrect chelicerae and long posterior lateral spinnerets. These small to medium-sized (5–15 mm) spiders construct sheet webs with a funnel-shaped retreat (Coyle and Ketner, 1990). The fossil record of Dipluridae extends back to the Triassic (226 Ma), yet Triassic spiders are rare and only a few mygalomorph spiders have been described from this time period (Raven et al., 2015). Two species of mygalomorphs spiders from the Crato Formation are placed in Dipluridae based on their elongated posterior spinnerets. A male and female of each species were assigned to *Cretadiplura caera* and *Dinodiplura ambulacra* by Selden et al. (2006). Both species

were reviewed with emended diagnoses, and the female of *D. ambulacra* was determined a male and assigned to *Seldischnoplura seldeni* (Raven et al., 2015).

Palpimanids (Palpimanidae) are ground-dwelling spiders with a distinctly enlarged first pair of legs and a relatively sparse fossil record. A palpimanid spider, *Cretapalpus vittari* Downen, 2020 from the Crato Formation is preserved exceptionally well in 3D. The only other fossil palpimanids come from the Dominican amber (25 Ma), and a possible palpimanid from Burmese amber (Wunderlich, 1988, 2017). These spiders are relatively rare today, but can be found in subtropical to tropical regions of South America, Africa, the Middle East, and Southeast Asia (Jocqué and Dippenaar-Schoeman, 2007). Palpimanids are araneophagous, preying on other spiders, and likely use a retreat invading approach (Cerveira and Jackson, 2005; Jocqué and Dippenaar-Schoeman, 2007; Pekár et al., 2011).

Superfamily Araneoidea includes several families of aerial web-spinning spiders, some of which are recognized in the Crato Formation. Araneids (Araneidae), commonly known as the true orbweavers, are one of the most diverse groups of spiders today (3,078 species: World Spider Catalog). The earliest fossil araneid spider is *Mesozygiella dunlopi* Penney & Ortuño, 2006 preserved in Cretaceous (121–115 Ma) amber from Álava, Spain (Penney and Ortuño, 2006). Araneidae have also been described from Burmese amber (Cretaceous: 99 Ma), New Jersey amber (Cretaceous: 93.9–89 Ma), and a multitude of other amber and lacustrine deposits from the Cenozoic (Penney, 2004; Poinar and Buckley, 2012; Scudder, 1890; Wunderlich, 1988, 2004). The fossil spider *Cretaraneus martinsnetoi* Mesquita, 1996 from the Crato Formation is redescribed from the holotype and additional material and is transferred from *Cretaraneus* into a newly erected genus, *Olindarachne* gen. nov. within Araneidae (Mesquita, 2012). One specimen

is distinct from the majority of the other fossils, but the preservation is comparatively poor to the other spiders so it is left as Araneoidea *incerte sedis* and not placed in a family.

Nephilinae is a subfamily within Araneidae, with a complicated taxonomic history. Nephilines have previously existed as a family (Nephilidae) or incorporated into other existing families. A close relationship between nephilines and araneids is well supported, and recently Nephilidae was again proposed as a separate family (Scharff et al., 2019). The earliest nephiline spider is *Cretaraneus vilalte* Selden, 1990 from a Cretaceous (145–139 Ma) lacustrine deposit in Sierra de Montsech, Spain (Selden, 1990). The fossil spiders described here represent the earliest record of the nephiline genus *Trichonephila* Dahl, 1912 (previously reported, but not formally described in Dunlop & Penney (2012)). Other fossil nephilines include the Cretaceous *Gerantonephila burmanica* Poinar, 2012 from Burmese amber and two Eocene spiders from lacustrine deposits: *Trichonephila pennatipes* from the Florissant Formation (34 Ma) of Colorado and a recently described juvenile *Nephila* from the Palana Formation (57–54 Ma) in India (Patel et al., 2019). Nephilines are some of the largest spiders today, and create large orbwebs with gold-tinted silk. They are distributed throughout the subtropics and tropics.

Tetragnathids (Tetragnathidae), the long-jawed orbweavers, are similar to araneids, but differ in their mouthparts and genitalia (Jocqué and Dippenaar-Schoeman, 2007). The fossil record of Tetragnathidae also extends back to the Early Cretaceous. The earliest tetragnathid spider (145–139 Ma) is *Macryphantes cowdeni* Selden, 1990 from the Cretaceous of Sierra de Montsech, Spain, although *Macryphantes* may represent a stem-deinopoid (Selden, 1990; Selden et al., 2016). *M. cowdeni* has also been described from the Cretaceous (131–126 Ma) of Las Hoyas, Spain with an additional tetragnathid *Huergina diazromerall* Selden and Penney, 2003 *(Selden and Penney, 2003)*. Tetragnathids are also present in Cenozoic deposits, such as the

Florissant Formation and Baltic and Dominican ambers (Scudder, 1890; Wunderlich, 1988, 2004). Two specimens described here represent possible tetragnathids based on their habitus.

2. Geological setting and paleoecology

The Crato Formation is a series of alternating heterolithic beds and laminated carbonates from the Araripe Basin of Brazil (Heimhofer and Martill, 2007; Martill, 1993). At the base of the Crato Formation is the Nova Olinda Member, from which the fossils are found (Fig. 1). The Nova Olinda Member is a Plattenkalk, laminated limestones, with two types of laminated carbonate facies: clay-carbonate rhythmites and laminated limestones (Neumann et al., 2003). The source of the carbonate is likely the result of authigenic precipitation and stromatolitic microbialites (Heimhofer et al., 2010; Warren et al., 2016). The basin was formed as the result of the rifting of the South American and African continents. The age of the formation has been interpreted as late Aptian, based on ostracodes and palynomorphs (Batten, 2007; Carlos Coimbra et al., 2002).

The thin laminations suggest a low-energy environment during deposition of the Nova Olinda Member. Bioturbation, traces, and fossils of benthic organisms are absent in this member, suggesting anoxic bottom conditions (Martill and Wilby 1993). Salinity of the lake in which the Crato Formation was deposited has been debated, and interpretations range from fresh water to hypersaline (Heimhofer et al., 2010; Maisey, 1990; Martill et al., 2007b; Neumann et al., 2003). Recently, the paleosalinity was reinvestigated using spider taphonomy experiments that support the presence of hypersalinity in the ancient paleolake (Downen et al., 2016). This interpretation is in congruence with evidence of hypersalinity suggested by the presence of pseudomorphs after halite (Martill et al., 2007b).

GROUP	FORMATION	MEMBER	LITHOLOGY
ARARIPE	IPUBI		Mainly gypsum
	CRATO	CASA DE PEDRA	Heterolithic - including black shales and muddy sandstones
		JAMACARU	Laminated limestones
		CALDAS	Heterolithic - inlcuing silty mudstones, silts and fine to medium sandstones. Some thin laminated limestones
		NOVA OLINDA	Laminated limestones
		Transition beds	
	CASA DE PEDRA		

Figure 1. Generalized map and stratigraphy of Crato Formation. Crato Formation outcrops are near the town of Crato, Brazil in the Araripe basin (modified from Martill et al., 2007).

During the Early Cretaceous, the Araripe Basin was positioned ~10° south of the paleoequator, and thus located within the tropics (Chumakov et al., 1995; Föllmi, 2012; Hallam, 1985, 1984). In addition, the fossil flora within the Crato Formation possess characteristics of extant plants that live in areas of limited rainfall and dry conditions, suggesting a semi-arid to arid climate (Alvin, 1982; Martill et al., 2007a). A fossil solifugid from the Crato Formation supports this interpretation, as extant camel spiders (Solifugae) live in semi-arid to arid environments (Dunlop and Martill, 2004; Selden and Shear, 1996). In contrast, some fauna, including other fossil arachnids like scorpions (Scorpiones) and whip spiders (Amblypgyi), suggest more humid conditions (Dunlop and Barov, 2005; Menon, 2007). The most accepted paleoenvironmental interpretation for the Crato Formation is a stratified lake with hypersaline

bottom waters (Heimhofer et al., 2010). The surrounding paleoenvironment was like semi-arid to arid, with nearby tropical habitats. Organisms likely were washed into the paleolake during storms or flash flooding events, as evidenced by the presence of entire plants fossils with leaves, stems, and roots preserved (Martill, 1993; Lima et al., 2014).

3. Materials and methods

3.1 Material

All specimens come from the Lower Cretaceous (Aptian) Nova Olinda Member of the Crato Formation, northeast Brazil from quarries at Nova Olinda, Ceará Province, Brazil. Holotype UnG/1T-50, female specimen is in the paleontological collections at the Department of Geosciences, Universidade Guarilhos, São Paulo, Brazil, and was studied by PAS in 2002. Photographic slides of the holotype were scanned with an Epson scanner at 24-bit color and 4800 dpi resolution for study at the University of Kansas. Other materials: F1887/SAN/ARICJW (male) in the private arachnid collection of Joerg Wunderlich, Oberer Häuselbergweg 25 69493 Hirschberg, Germany; Wun 002, DM 005, KUMIP 374690, KUMIP 374677 in the Department of Invertebrate Paleontology, University of Kansas Natural History Museum, Lawrence, Kansas; MB.A.976, MB.A.984, MB.A.981 in the Natural History Museum, Berlin (Museum für Naturkunde Berlin).

The unusual preservation of fossils from the Crato Formation is exceptional, yet problematic with regard to identifying the spiders. The Crato fossil spiders are preserved as three-dimensional mineralized replacements in contrast to the compression fossils of China and most other lacustrine deposits. As a result, this type of preservation mostly reflects the actual morphology of the spiders when they were alive. Unfortunately, many specimens are heavily weathered, having been altered from their original replaced mineralogy to goethite or hematite

(Barling et al., 2015). Most of the spiders are also preserved ventral side up, with the dorsal side hidden in the matrix. Some specimens preserved dorsal side up appear to have fractured, removing most of the carapace.This weathering and resting position results in many of the diagnostic characteristics used in assigning specimens to family or genus being obscured or not visible. Another challenge to classification is the somewhat shriveled abdomens and flexed (curled) legs (Fig. 2A). These features are likely due to hypersaline conditions in the paleolake where the spiders were deposited (Downen et al., 2016). The curled appendages often disappear into the matrix, making obtaining podomere lengths challenging, or the obscure structures in ventral view, such as the mouthparts. The shriveled abdomens may appear somewhat distorted, but some specimens appear to have internal organs and tissues preserved (Fig. 2B). Fine setae are often not visible, except where the cuticle has flaked away. Macrosetae are preserved in many specimens, but in relatively low abundance suggesting the macrosetae were likely broken off when laminae were split. There are a number of challenges to classification that are mostly related to taphonomy, so many of the spiders here are identified using the general habitus and measurements.

3.2 Methods

Specimens were photographed with a Canon EOS 5D Mark II digital camera attached to a Leica M650C microscope. Specimens were wetted with 70% ethanol to enhance details not easily seen when dry. Nephilids were described from a single specimen at the University of Kansas and photographs of specimens from the museum in Berlin. Measurements were made from the photographs using the measurement tool in Adobe Photoshop, and drawings were made from the photographs using Adobe Illustrator CS6.

Specimens were cut with a Dremel saw to minimize the amount of matrix and optimize resolution for micro-computed tomography (micro-CT). The fossils were imaged using an FEI HeliScan micro-CT scanner in the Earth, Energy and Environment Center (EEEC) at the University of Kansas, Lawrence KS. Each specimen was mounted upright on a stub with double-sided sticky tape and rotated through the x-ray beam (Supplemental Material). Raw x-ray data was reconstructed using qmango software (Thermo Fisher Scientific). Segmentation and 3D visualization was conducted in PerGeos Software for Digital Rock Analysis at the University of Kansas. Image renderings were manipulated in Adobe Photoshop.

Abbreviations are as follows: at = anal tubercle, BL = book lung, ch = chelicerae, cl = claw, co = conductor, cx = coxa, cy = cymbium, dh = distal haematodocha, ef = epigastric furrow, en = endite, fe = femur, fg = fang, lb = labium, pa = patella, mA = median apophysis, mt = metatarsus, op = opisthosoma, pr = prosoma, pd = pedipalps, sp = spinnerets, st = sternum, strA = subterminal apophysis, ta = tarsus, ti = tibia, trA = terminal apophysis. All measurements are in millimeters. A "+" following a measurement indicates a body part that is not fully visible or disappears into the matrix.

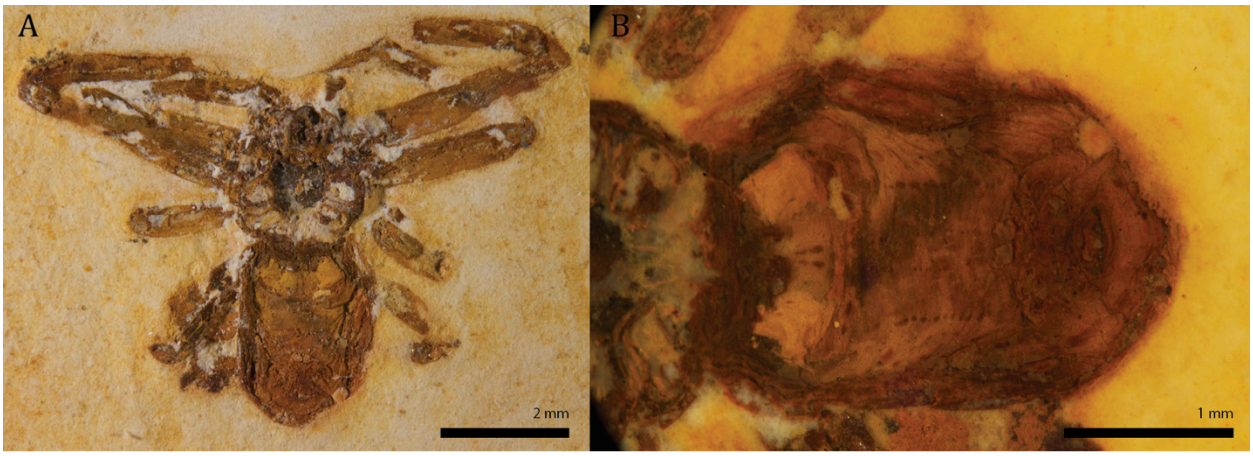

Figure 2. Preservation and appearance of fossil spiders from the Crato Formation of Brazil. A) Typical flexed (curled) leg position of most Crato spiders. B) Soft tissue preservation of the abdomen.

4. Systematic Paleontology

Order Araneae Clerck, 1757

Suborder Opisthothelae Pocock, 1892

Infraorder Araneomorphae Smith, 1902

Araneaomorphae *incerte sedis*

(Fig. 3)

Remarks. The specimen described here lacks visible booklungs and spinnerets, but is placed in Araneomorphae based on the chelicerae which are relatively small, not porrect, and are not of an orthognath orientation. The specimen also has long and slender legs which is more characteristic of araneomorph spiders.

Description of KUMIP 374690. Female. Carapace outlined rounded in dorsal view. Abdomen longer than wide, but deformed due to preservation. Dense setae covering pedipalps. Leg 1 fe

4.15, pa 0.76, ti 4.51, mt 2.18+; Leg 2 fe 4.00, pa 0.54, ti 4.20, mt 3.27+; Leg 3 fe 3.00, pa 0.54, ti 3.29, mt 1.21, ta 0.86; Leg 4 fe 3.93, pa 0.56, ti 2.67+.

Remarks. The specimen possesses long and slender legs with elongated podomeres, which are seen in several different spider families. Femora I, II, and IV are subequal in length and the third femur is the shortest, but not by much (3/4 as long as other femora). In orbweaving spiders, the third leg is distinctly short, so it is unlikely the specimen represents Araneidae, Tetragnathidae, or Uloboridae. In deinopids (Deinopidae), the front two pairs of legs are long with legs III and IV relatively subequal and the body is usually elongated. The specimen here has a considerably long femur IV and tibia IV that are definitely longer than on leg III and has a shorter abdomen and rounded carapace. The tibia and metatarsus of each leg are also very long and roughly subequal to eachother. Other spider families that include thin- and long-legged webweavers are Pholcidae and Nesticidae, but spiders in these families have pseudosegmented tarsi, which this specimen lacks. Several haplogyne spiders also exhibit similar leg forms, and include the families Hypochilidae, Scytodidae, and Sicariidae. Female hypochilids possess a pectinate palpal claw, which the specimen lacks (the palps are preserved as impressions with abundant setae, but no claw). In scytodids, the female also posses a claw and has the posterior of the sternum blunt, in contrast to the fossil. Sicariids do not have a palpal claw, but the sternum is wider than long and, in the fossil specimen, the outline of the sternum can be seen to be longer than wide. A long-legged lagonomegopid, *Jinjumegops* Selden, 2019 (Lagaonomegopidae) was recovered from the Cretaceous of Korea with legs that resembles the legs of the fossil here, but *Jinjumegops* has a carapace with a protruding cephalic region and porrect chelicerae (Selden et al., 2019). Because the spider lacks any significant characteristics with any major family of spiders, it is left as Araneomorphae *incertae sedis*.

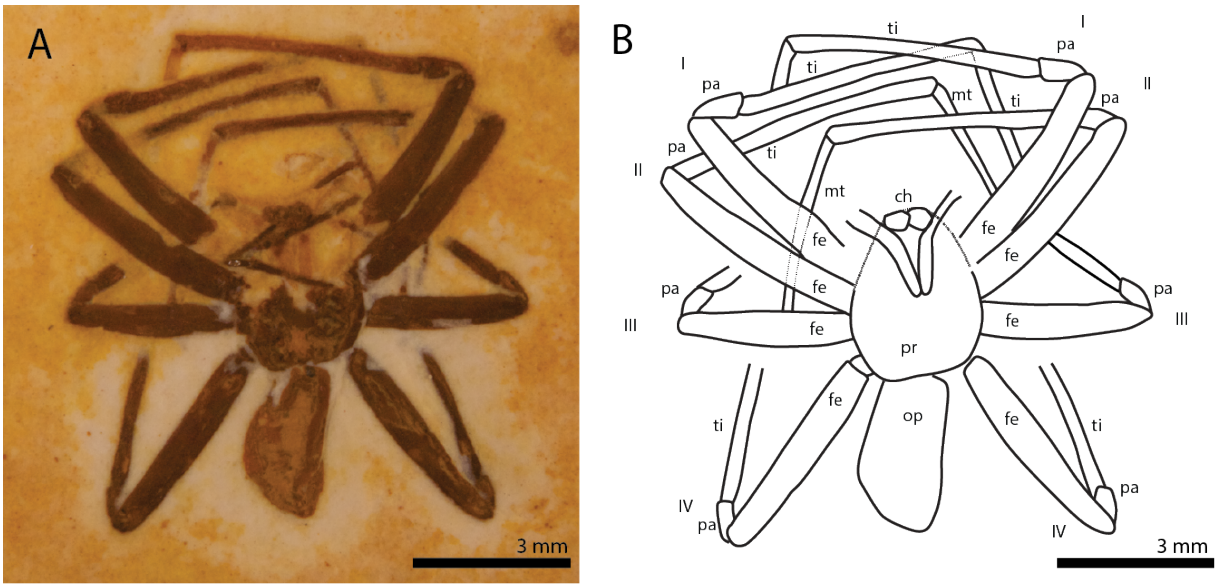

Figure 3. Araneomorphae *incretae sedis* photograph and interpretative drawing. A–B) Araneoid specimen KUMIP 374690 in dorsal view.

Superfamily Araneoidea Latreille, 1806

Fam., gen. et sp. Indet.

(Fig. 4)

Description of Crato 14. Female. Oval carapace, length 2.80, height 1.98. Height of cephalic area about as long as chelicerae. Relatively small, thin palp, length 1.28. Globose abdomen, length 2.85. Legs extremely long and slender (Leg 1 3x length of body). Longer tibiae and metatarsi on most legs. Macrosetae on metatarsi, Leg 1 and Leg 4 femora, Leg 1 patella. Podomere lengths: Leg 1 fe 6.05, pa 1.00, ti 6.40, mt 5.29, ta 1.62; Leg II fe 4.88, pa 0.86, ti 5.33, mt 6.16; Leg IV fe 6.11, pa 1.10, ti 5.12, mt 6.16, ta 1.68.

Remarks. The identity of this spider is enigmatic. The poor preservation makes taxonomic classification difficult, as it lacks many features that could be used to diagnose a family. The extremely long slender legs are suggestive of Pholcidae, Nesticidae, and araneoid families. The

tibia and metatarsus of some pholcids and nesticids are much longer than the femur, like the fossils; however pholcids typically have pseudosegmented tarsi, which this specimen lacks. Nesticids and theridiids possess a comb of either curved or serrated bristles, respectively, on the fourth tarsus. No distinct curved or serrated bristles are observed on the fourth tarsus of this specimen, although other setae and macrosetae are visible. Theridiids also typically lack femoral macrosetae, which the fossil possesses. This leaves araneoids in Araneidae, Tetragnathidae, and Linyphiidae as a possible placement.

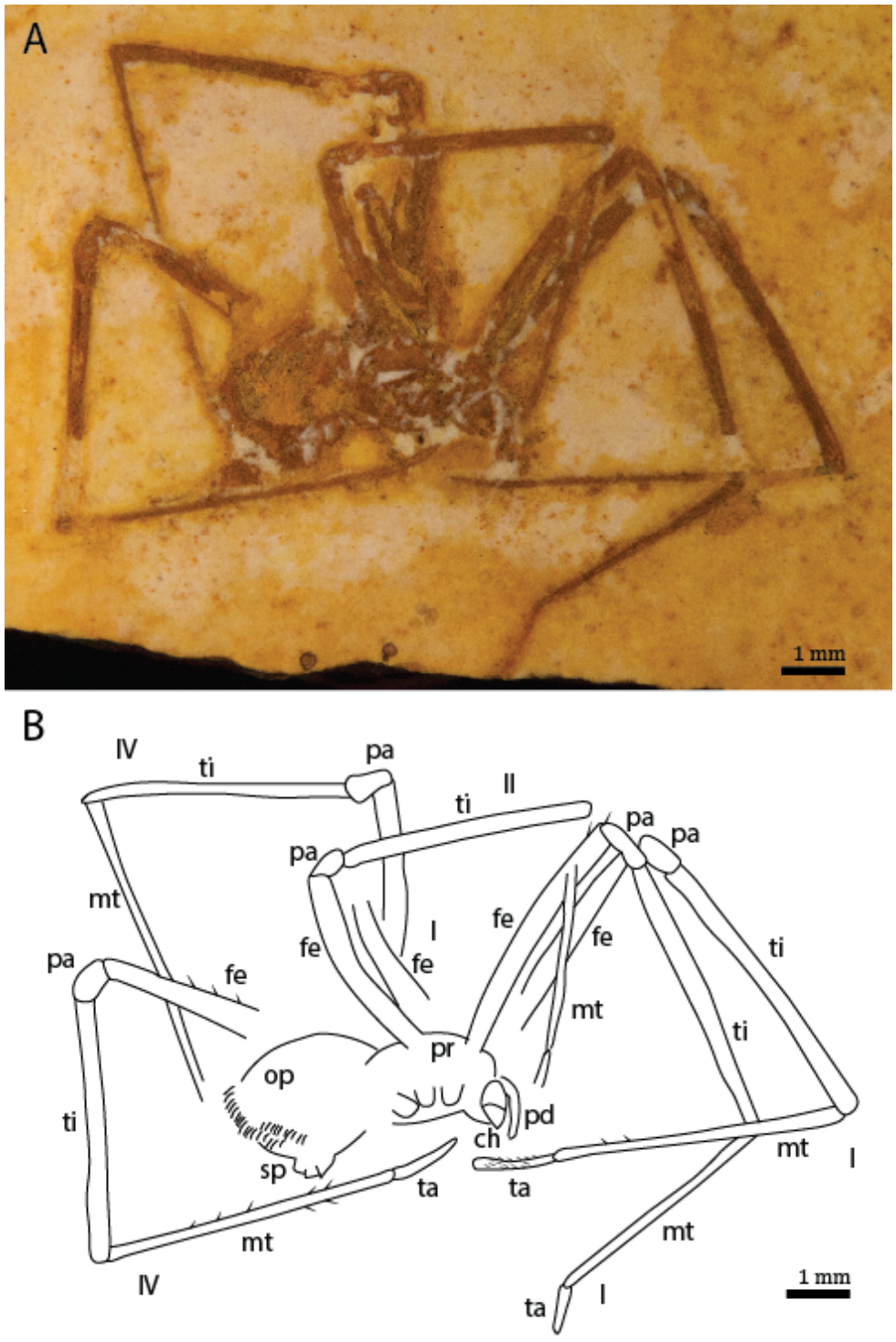

Figure 4. Araneoidea *incertae sedis* photograph and interpretative drawing. A–B) Araneoid specimen KUMIP 374677 in lateral view.

Family Araneidae Clerck, 1757

Remarks. The spiders are placed in family Araneidae based on the following characteristics: ecribellate, a carapace longer than wide with a narrowed and raised cephalic region, labium wider than long, squarish endites, a triangular sternum longer than wide, a longest first pair of legs and shortest the third pair of legs, legs covered in abundant setae and macrosetae, an abdomen that is longer than wide and overhangs the carapace, and a median apophysis.

Genus ***Olindarachne*** gen. nov.

(Figs. 5–7)

Olindarachne martinsnetoi (Mesquita, 1996)

Olindarachne martinsnetoi new combination

Emended diagnosis. Araneid spider with long first two pairs of legs (twice the length of the body); robust femur I and II, femur I length to body length ratio of ~1.54; spines present on patella. Male palp with narrowed subterminal apophysis and a sigmoid terminal apophysis widened at the base.

Type species. *Cretaraneus martinsnetoi* (Mesquita, 1996).

Derivation of name. After the Nova Olinda Member of the Crato Formation, the stratum in which this abundant spider is found.

Description of holotype UnG/1T-50. Female. Carapace longer than wide, L 1.82, W 1.56 (L/W 1.16), narrows anteriorly. Raised eye region. Chelicerae stout. Opisthosoma subelliptical, longer than wide, L 2.83, W 2.13 (L/W 1.33). Walking leg formula 1243. First two pairs of legs robust. Leg _ twice as long as body length. Third pair of legs noticeably shorter than others. Metatarsi distinctly thinner than tibiae. Macrosetae present on femora, patellae, tibiae. Podomere lengths:

Leg I fe 2.88, pa 1.04, ti 2.42, mt 1.92, ta 0.81, Leg II fe 2.74, pa 0.85, ti 1.87, mt 1.97, ta 0.87, Leg III fe 1.61, pa 0.41, ti 1.16, mt 0.97, ta 0.41, Leg IV fe 1.42, pa 0.56, ti 1.49, mt 1.36, ta 0.57.

Description of MB.A.984. Female. Carapace longer than wide, L 3.09, W 2.51 (L/W 1.23), slightly narrowed cephalic region. Right palp L 2.18, left palp L 2.33, patellae shortest, other palpal podomeres subequal. Opisthosoma oval and longer than wide, L 4.31, W 3.5, (L/W 1.23), overhangs carapace. Walking leg formula 1243. Legs I and II longer and more robust than legs III and IV. Macrosetae on Leg I femora and metatarsi, Leg III patellae. Metatarsi distinctly thinner than tibiae. Podomere lengths: Leg I fe 4.65, pa 1.22, ti 3.95, mt 4.49, ta 0.96; Leg II fe 3.47, pa 1.09, ti 2.73, mt 3.30, ta 0.69; Leg III fe 2.17, pa 0.56, ti 1.63, mt 1.66, ta 0.37; Leg IV fe 2.57, pa 0.95, ti 2.33, mt 2.56, ta 1.00.

Description of Wun 002. Female. Carapace longer than wide, L 1.62, W 1.42 (L/W 1.14). Labium wider than long, rhombus-like shape with rounded edges. Sternum subtriangular, longer than wide, concave toward chelicerae, tapering toward abdomen. Setae and macrosetae present on fe, pa, ti, mt. Opisthosoma oval, longer than wide, L 1,87, W 1.56 (L/W 1.19). Walking leg formula 1243. Leg I nearly twice as long as body. Podomere lengths: Leg I fe 2.70, pa 0.52, ti 2.16, mt 0.97+, Leg II fe 1.94, pa 0.34, ti 1.56, mt 0.86, ta 0.44, Leg III fe 1.18, pa 0.39, ti 0.49+, Leg IV fe 1.25.

Description of F1887/SAN/ARICJW. Adult male. Subrounded carapace bulging laterally, narrows anteriorly, L 2.48, W 2.88 (L/W 0.86). Palp with relatively small cymbium and complex bulb. Median apophysis a single horn-shaped protrusion without teeth or spurs. Subterminal apophysis(?) peg-shaped and narrow. Terminal apophysis sigmoid shaped, widened

at base and tapering distally to a point. Opisthosoma oval, slightly tapering toward posterior, L 3.03, W 2.33 (L/W 1.30). Walking leg formula 1243. Legs I and II robust. Femur length to carapace length ratio 1.50. Podomere lengths: Leg I fe 3.72, pa 1.05, ti 2.67, Leg II fe 3.11, pa 0.89, ti 2.20, mt 1.36+, Leg III fe 1.58, Leg IV fe 2.19, pa 0.73, ti 2.27, mt 0.88+.

Description of DM 005. Adult female. Rounded carapace, bulging laterally, longer than wide, narrows anteriorly, L 4.00, W 3.79 (L/W 1.05). Raised eye region. Chelicerae project downward. Pedipalps L 1.54, palpal tarsi relatively long. Opisthosoma oval, L 4.64, W 3.03 (L/W 1.53). Walking leg formula 1243. First pair of legs over twice as long as Leg 3 (18.17+/9.13). Legs I and II more robust than Legs III and IV. Two tarsal claws visible on right leg III and right leg IV. Femur I length to carapace length ratio 1.52. Setae and macrosetae present on all visible podomeres. Ventral row of four macrosetae on tibiae I. Metatarsi distinctly thinner than tibiae. Podomere lengths: Leg I fe 6.08, pa 1.95, ti 0.73+, Leg II fe 4.66, pa 1.54, ti 3.7, mt 4.01, ta 1.65, Leg III fe 2.81, pa 1.05, ti 1.93, mt 2.21, ta 1.13, Leg IV fe 3.38, pa 1.34, ti 3.55, mt 2.89, ta 1.21.

Remarks. The previous interpretation of these abundant spiders in the Crato Formation was by Mesquita (1996), who placed them in the genus *Cretaraneus*. Selden (1990) described *Cretaraneus vilaltae* from an Early Cretaceous locality at Sierra de Montsech, Spain. The diagnosis of *Cretaraneus* is as follows: “Araneoid spider with subelliptical carapace bearing raised cephalic area and no fovea; subtriangular sternum; small, subtriangular labium; serrate setae covering all parts of body. Chelicerae relatively large (0·4 × length of carapace), forwardly directed (at least in adult male), with inner and outer row of denticles (not peg-teeth), and mesal ridge; male palp with long embolus, and small, proximal ?paracymbium; legs relatively equal in length, about three times the length of carapace; femora, tibiae and metatarsi with spines; tarsi

with pectinate paired claws, small median claw, and associated serrate bristles; no true trichobothria globose abdomen." (Selden 1990, p. 270).

The definition of *Cretaraneus martinsnetoi* Mesquita 1996 (p. 25) is as follows "afora os caracteres listados para o gênero, esta espécie apresenta diferenciação das quelíceras, com formato arredondado e presença de espinhos na patela"; i.e., apart from the characters listed for the genus, this species is differentiated by the chelicerae with rounded shape and the presence of spines on the patella." In addition, Mesquita (1996 p. 26) mentioned further differences, in that the chelicerae being of rounded shape in *C. martinsnetoi*, they are turned back over the carapace and lack a claw ("O espécime em discussão difere na posição das queliceras, que se encontram voltadas sobre o abdome, possuem o formato arredondado e sem garras"). The Crato fossil spiders do share traits in common with *C. vilaltae* Selden 1990, including a raised cephalic area and abundant setae. Several differences exist, however, that suggest the Crato spiders do not represent *Cretaraneus*. The carapace is rounded and narrows anteriorly, unlike *Cretaraneus*. The legs of *Cretaraneus* are relatively equal in length, but in *Olindarachne*, the first two pairs of legs are quite long and Leg III is very short. The femur/carapace length ratio of *Olindarachne* is approximately 1.54 (average of holotype and paratype) whereas the femur/carapace length ratio of *C. vilaltae* is 1:1. The holotype has a Leg I length to carapace ratio of 4.98, and paratype Crato 88 has a Leg I length to carapace ratio of 4.94, whereas *C. vialtae* has a ratio of 3.54, indicating much longer legs in the specimens described here. Spines are present on the first patella of the Crato spiders, unlike *C. vilaltae*, a difference also noted by Mesquita (1996). The chelicerae of *Cretaraneus* are forwardly directed and relatively large, but the chelicerae of *Olindaranche* appear to be directed downward and comparatively smaller.

At the time of the original description of *C. martinsnetoi*, *Cretaraneus* was not placed in a family, but the genus was later recognized as belonging to Nephilidae based on morphology of the male pedipalp (Selden & Penney 2003). Nephilidae has since been transferred to Araneidae as subfamily Nephilinae. Nephilines possess a wider than long sternum and endites that widen anteriorly, suggesting the holotype and the others do not belong to Nephilinae. The presence of a median aphysis excludes *O. martinsetoi* from other araneoids: Tetragnathidae, Theridiidae, and Linyphiidae (Coddington 1986; Levi 2002). Tetragnathids also typically possess longer, forward-projecting chelicerae, endites that widen distally, a labium longer than wide, and more slender legs. Many of the *O. martinsnetoi* have setae visible on the fourth tarsus, but lack a tarsal comb, which is characteristic of Theridiidae. No calamistrum or cribellum is present, thus, excluding Uloboridae or Deinopidae.

Figure 5. *Olindarachne martinsnetoi* new combination photographs and interpretative drawings. A–B) Holotype O. martinsnetoi UnG/1T-50 in dorsal view. C–D) Paratype *O. martinsnetoi* MB.A.984 in dorsal view. E–F) Paratype *O. martinsnetoi* Wun002 in ventral view. Stippled areas represent fine setae impressions where replaced cuticle has flaked away.

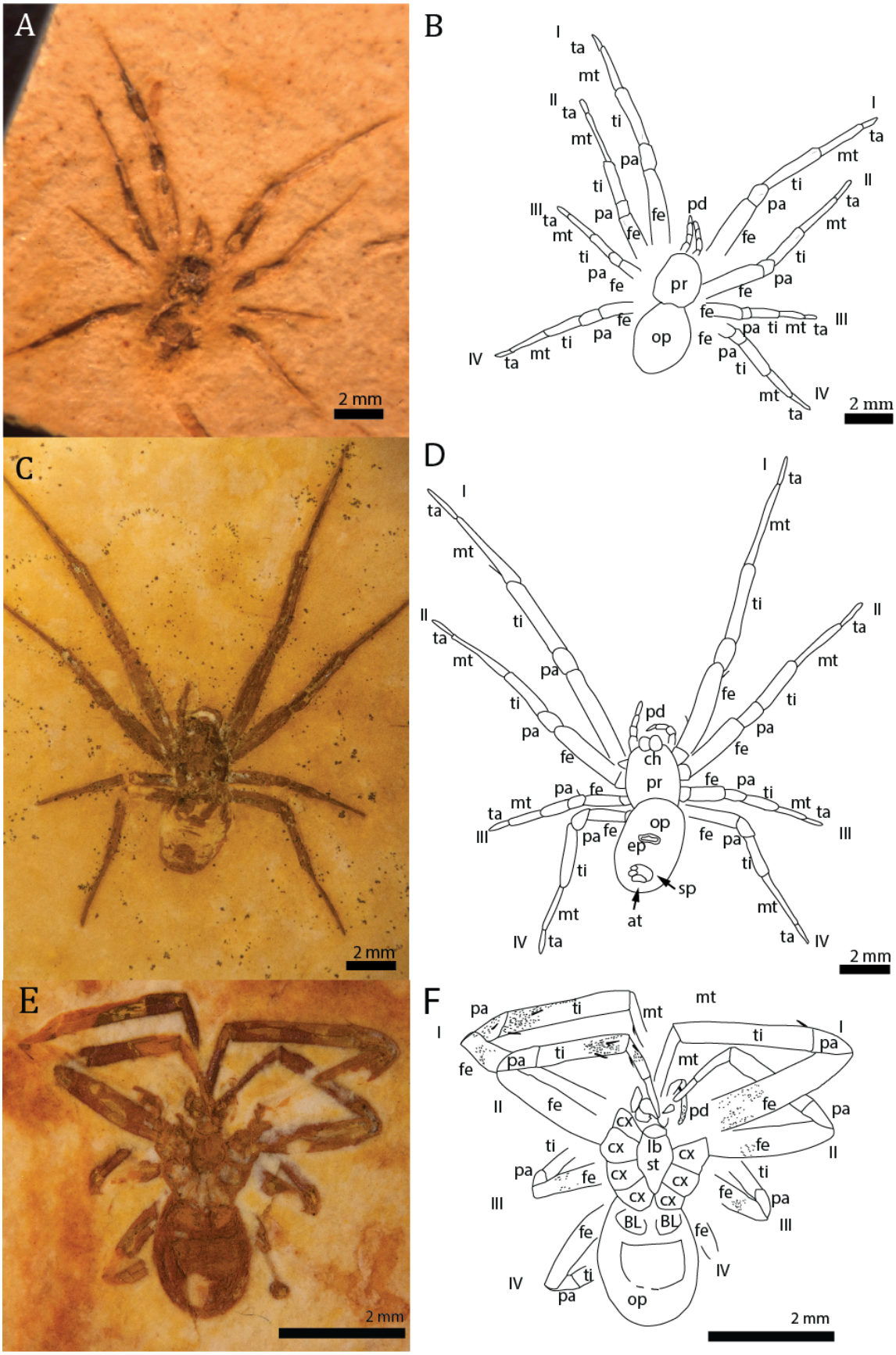
A
2 mm
B
I
ta
mt
II
ti
pa
fe
pd
III
pr
op
IV
2 mm
C
2 mm
D
ch
ep
sp
at
2 mm
E
2 mm
F
cx
lb
st
BL
2 mm

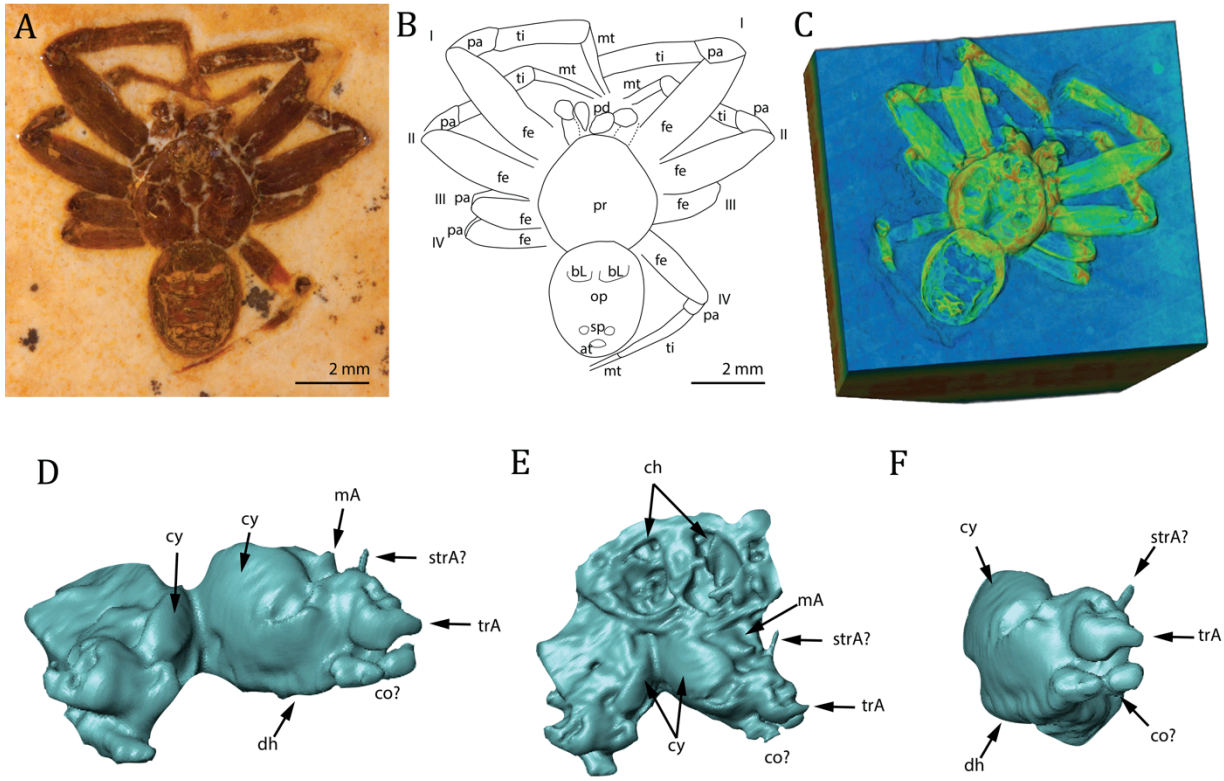

Figure 6. *Olindarachne martinsnetoi* new combination photographs, interpretative drawings, and micro-CT volume renderins. A–B) Paratype male *O. martinsnetoi* F1887/SAN/ARICJW in dorsal view. C) 3D reconstruction from micro-CT imaging. Red represents areas of higher relief of the fossil. D) Rendering of palps in anterior view. E) Rendering of palps in dorsal view with chelicerae in cross section. F) Rendering of right palp in oblique view.

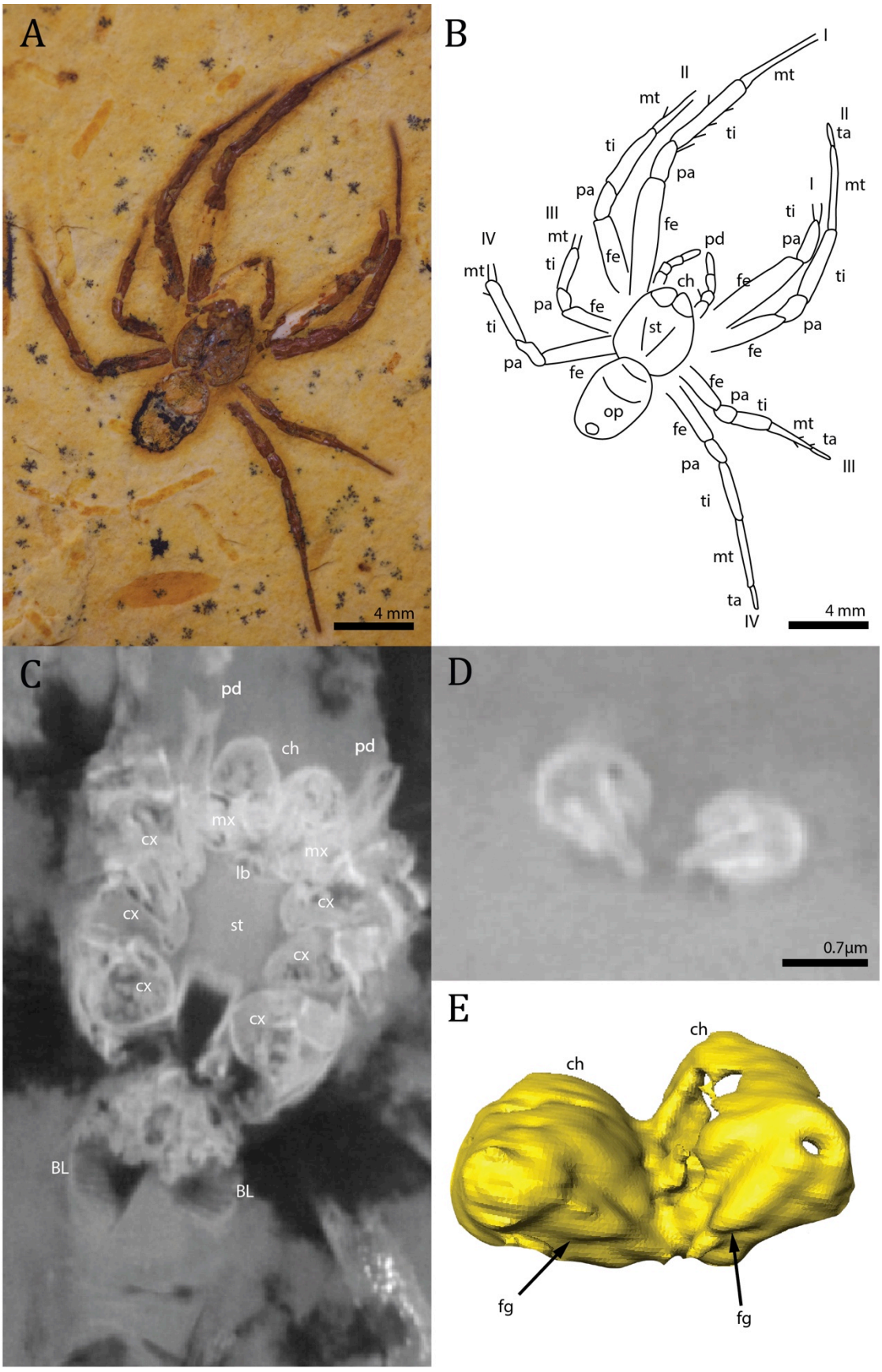
A
4 mm
B
I
II
mt
ti
pa
fe
pd
ch
st
III
IV
ta
op
4 mm
C
pd
ch
mx
cx
lb
st
BL
D
0.7µm
E
ch
fg

Figure 7. *Olindarachne martinsnetoi* Paratype DM005 photographs and interpretative drawings. A–B) Dorsal view. C) X-ray slice from micro–CT showing ventral features of the spider. D) X-ray slice of fangs. F) Rendering of chelicerae and fangs.

Subfamily Nephilinae Simon, 1894

Nephilinae *incerte sedis*

(Fig. 8)

Remarks. The spiders are placed in the subfamily Nephilinae based on their extremely large size and elongate tapered abdomen. *Mongolarachne* Selden, 2013 from the Jurassic of China is also a large spider, and was previously mistaken for a *Nephila* Leach, 1815 (Selden et al., 2011; Selden et al., 2013). *Mongolachne* is cribellate and possesses setal brushes on the tibia of all legs and is cribellate. While there is no cribellum observed in any of the specimens, the spinneret area in all of the specimens have been heavily weathered and aren't visible in any detail. No calamistrum is visible on any of the specimens where the fourth tarsus is visible, but this may be a taphonomic artifact. Brushes of macrosetae on the tibia or femur are characteristic of many nephiline species, but are not observed in either of the fossils; however, most adult *Nephila* and *Trichonephila* lose these brushes as adults. In addition to the two female specimens described here, other nephiline spiders in the collection also lack the setal brushes, but do have other macrosetae and setae preserved along the legs. Dense brushes of macrosetae are relatively conspicuous, and there is no evidence of these brushes in any of the fossil examined.

Description of MB.A.976. Adult female. Carapace pyriform length 9.55, width 4.87; narrowed cephalic region. Opisthosoma elongate tapered toward posterior, length 12.56, width 6.99. First pair of legs very long. Three tarsal claws. Walking leg formula 1243. Podomere lengths: Left

Leg I fe 17.80, pa 4.74, ti 16.51, mt 17.91, ta 4.35; Left Leg II fe 14.31, pa 2.82, ti 12.32, mt 12.00, ta 3.40; Left Leg IV fe 7.76, pa 2.81, ti 11.30, mt 7.63, ta 3.71.

Description of KarlsruheNephilid. Adult female. Carapace longer than wide, length 7.77, width 3.67. Chelicerae large, round in cross section, diameter 1.23. Sternum longer than wide, doesn't extend far between coxae IV. Labium subtriangular, longer than wide. Opisthosoma ovoid, longer than wide, length 9.33, width 4.83, tapering posteriorly. Walking leg formula 1243. Leg I very long. Metatarsus I and II longer than femur I and IV. Ventral row of spine-like macrosetae on proximal half of tibia I and II. Ventral row of spine-like macrosetae along full length of metatarsus I and II. Podomere lengths: Right Leg I fe 11.77, pa 2.82, ti 11.62, mt 12.13, ta 1.35+; Right Leg II fe 8.38, pa 2.40, ti 6.34, mt 11.13; Right Leg III fe 5.52, pa 1.46, ti 3.11+; Right Leg IV fe 7.53, pa 1.95, ti 5.66, mt 7.11, ta 1.95. Left Leg I fe 11.59, pa 2.27, ti 10.89, mt 12.89, ta 3.08; Left Leg II fe 8.83, pa 1.78, ti 7.12, mt 9.23, ta 1.58; Left Leg III fe 5.63, pa 1.39, ti 4.49, mt 1.61+; Left Leg IV fe 7.46, pa 1.98, ti 5.27, mt 6.78, ta 2.01.

Remarks. Both specimens are unable to be assigned to a genus. They general habitus most closely resembles *Nephila* and *Trichonephila* Dahl, 1912. MB.A.976 is relatively poorly preserved in a lateral/dorsal view. KarlsruheNephilid is preserved ventral side up. A previously reported difference from *Nephila* (before the separation of *Nephila* and *Trichonephila*) and other araneids is a metatarsus longer than the combined length of the tibia and patella. In the Crato fossils, the metatarsus is longer than the femur, but not longer than the tibia + patella. The age of the origination of *Trichonephila* is estimated to be about 60 Ma, and nephilines in general are present in the Cretaceous (Kuntner et al., 2019). The fossils are certainly nephilines, but may represent an earlier genus distinct from *Nephila* and *Trichonephila*.

Nephilinae? *incertae sedis*

(Fig. 9)

Remarks. This small spider is relatively poorly preserved, but is clearly a male based on the swollen palps. The long legs of this specimen and shorter third leg suggest it is an orbweaver, and the elongated podomeres resemble nephilines. Male nephilines are significantly smaller than females, and the sexual size dimorphism index (SSD = body length of female / body length of male) of this male specimen is 5.70, and well within the range of SSD indices for other nephilines like *Trichonephila* and *Nephila* (Kuntner et al., 2019; Table S1).

Description of MB.A.981. Male. Rounded carapace (1.93). Chelicerae small. Labium triangular, slightly wider than long. Oval abdomen slightly longer than wide (1.87/1.60). Walking leg formula 1243; Legs long and slender and covered in short dense setae. Cluster of macrosetae on Leg 3 femur. Podomere lengths: Leg 1 fe 4.96, pa 0.76, ti 5.35, mt 4.97, ta 1.73; Leg 2 fe 3.76, pa 0.51, ti 3.8, mt 3.30, ta 0.5+; Leg 3 fe 2.70, pa 0.54, ti 2.11, mt 1.87+; Leg 4 fe 2.97, pa 0.68, ti 2.7, mt 3.52, ta 1.24.

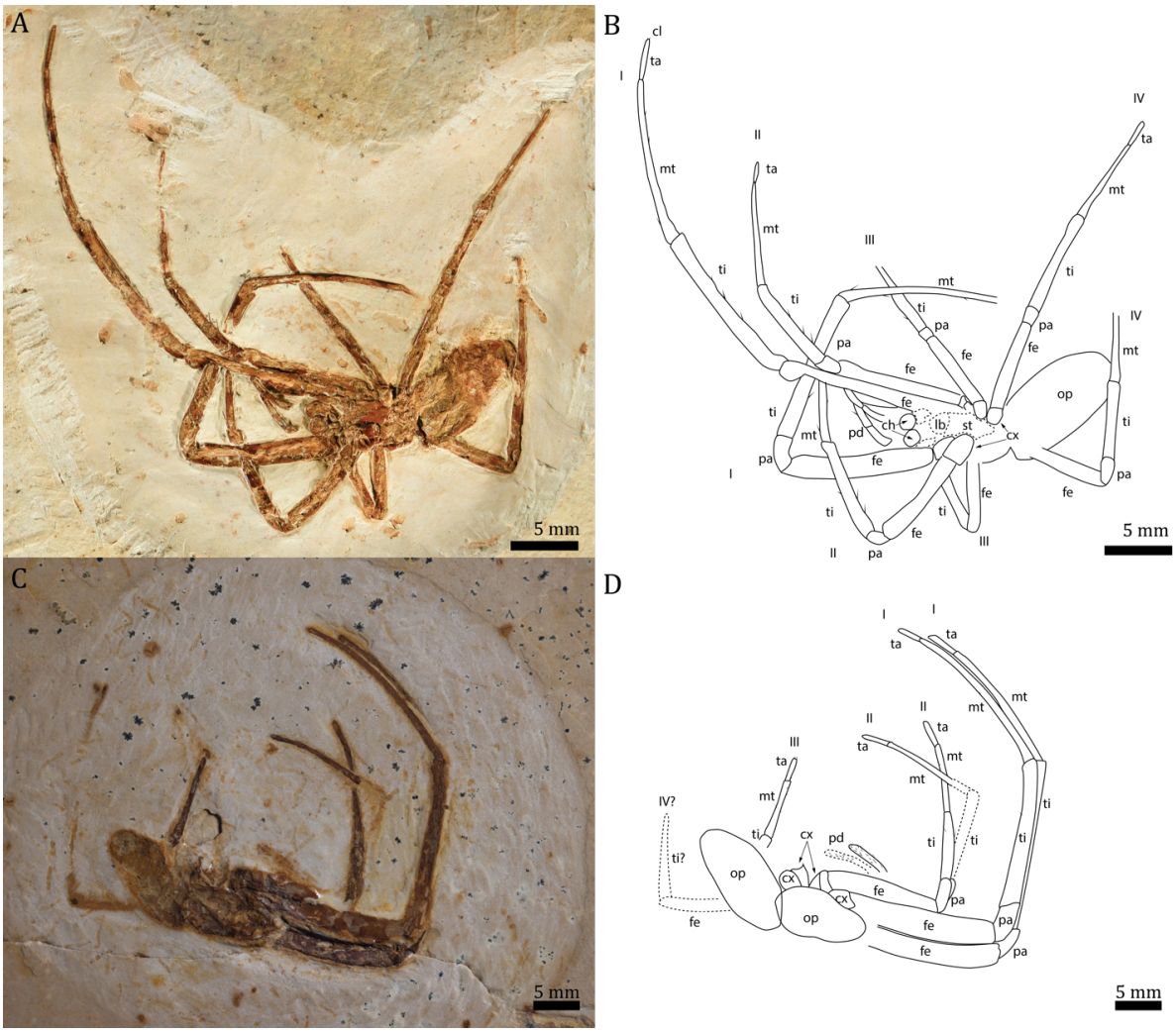

Figure 8. Nephilinae *incertae sedis* photographs and interpretative drawings; A–B) Female MB.A.976 in lateral view. C–D) Female KarlsruheNephilid in ventral view.

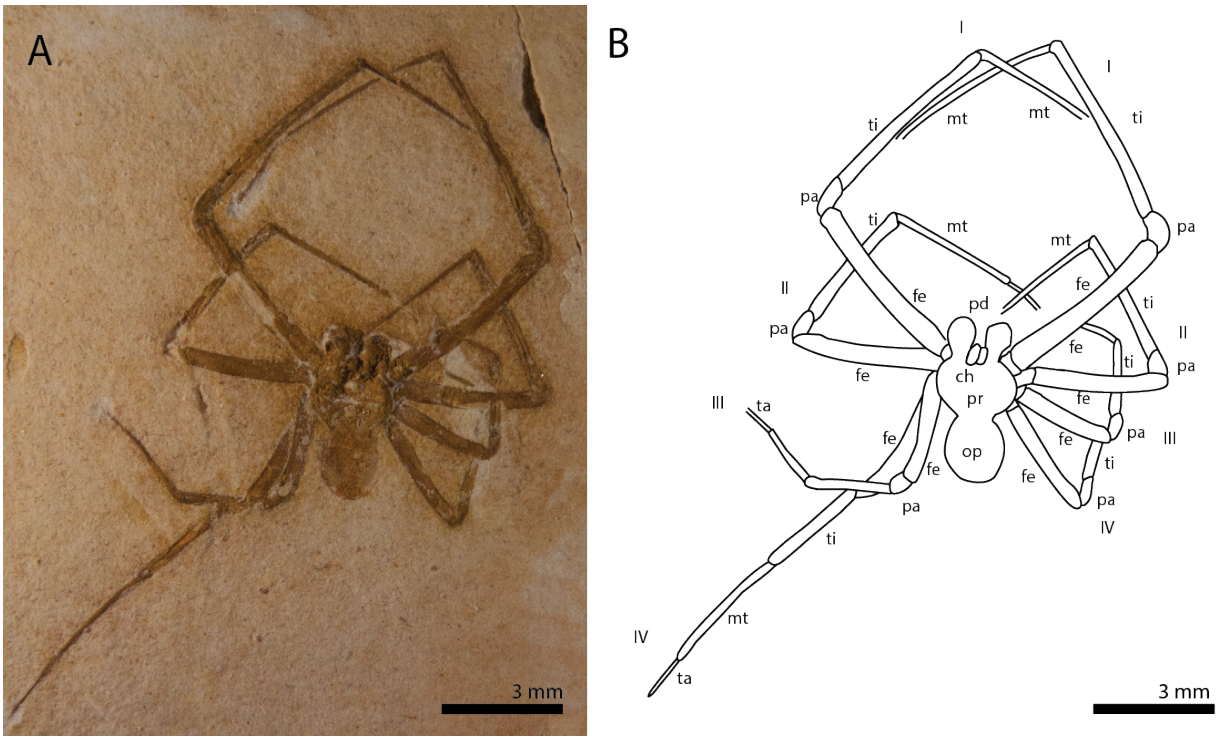

Figure 9. Nephilinae? *increte sedis* photographs and interpretative drawings; A–B) Male MB.A.981 in dorsal view.

5. Discussion

The spiders described here do not extend the age ranges of family Araneidae. After the transfer of Nephilidae into Araneidae, the previously named *Cretaraneus martinsnetoi* represented Araneidae from South America, and the new assignment to *Olindarachne* does not change that. *Nephila* was previously mentioned by Dunlop and Penney (2012), but not formally described. This outcome does indicate that araneids and other aerial web-spinning spiders were distributed across Pangaea before the extensive continental rifting that separated Gondwana from the other landmasses.

The Crato Formation is currently the only lacustrine deposit in South America with a relatively high abundance of formally described fossil spiders, and the spider fossil assemblage differs in composition from other Mesozoic lacustrine deposits. From the material examined here, most of the spiders appear to be orbweavers with only one ground-dwelling spider (Palpimanidae). In contrast, other Mesozoic lacustrine deposits appear to have greater representation of ground-dwelling spiders. The Jurassic Haifanggou Formation has a diverse assemblage of palpimanoids and stem-deinopoids. These groups were likely relatively diverse during the Jurassic, but today deinopoids are represented only by two families (Deinopidae and Uloboridae) with 353 species, and palpimanoids are represented by five families (Archaeidae, Huttoniidae, Mecysmaucheniidae, Palpimanidae, and Stenochilidae) and 281 species, and thus relatively less diverse than other modern families (World Spider Catalog 2020). The spider assemblage from the Cretaceous Jinju Formation of Korea is also includes palpimanoids. Lagonomegopids (Lagonomegopidae) have been reported from Cretaceous Burmese, Spanish, and North American ambers as well as the Jinju Formation, but are noticeably absent from the Crato Formation (Guo et al., 2020; Park et al., 2019; Penney, 2005). This disparity in the types of spiders preserved from these different fossil assemblages is likely connected to differences in the depositional settings and paleoenvironments.

The vast majority of the specimens in the Crato collection at the University of Kansas appear to be araneoids, and conspecific to *Olindarachne martinsnetoi*, and represent varous stages of life from small juveniles to large adults. These spiders likely would have constructed orbwebs in vegetation surrounding the Crato paleolake or near streams that ran into the lake. Some tetragnathids are known to preferentially select habitats over bodies of water as web-building sites (Gillespie, 1987). The relatively large body size of many of these orbweaving

spiders suggests the presence of nearby habitats with complex vegetation (Halaj et al., 2000). Mayflies (Ephemeroptera), grasshoppers (Orthoptera), true bugs (Hemiptera), and dragonflies (Odonata) dominate the insect portion of the fossil assemblage, and these insects were likely common prey for the orbweaving spiders (Maisey, 1991; Martill, 1993; Martill et al., 2007a). Extant *Nephila* and *Trichonephila* weave the largest webs of any orbweaver, typically up to 1.5 m in diameter and would have been capable of capturing large insect prey (Kuntner et al., 2019; Moore, 1977; Robinson and Mirick, 1971). Spiders like the sheet-weaving diplurids likely would have preyed upon orthopterans, hemipterans, and other ground-dwelling insect prey (Coyle and Ketner, 1990). Modern palpimanids prey upon a variety of other spiders including orbweavers (Araneidae and Tetragnathidae) and cursorial spiders (Pekár et al., 2011). Cursorial spiders do not spin webs for prey capture, and instead, are mostly ground dwelling. Modern spiders like wolf spiders (Lycosidae) and crab spiders (Thomisidae) are prey for extant palpimanids, but the fossil record of these families do not extend back to the Cretaceous. Palpimanids have also shown to favor a retreat-invading predatory lifestyle, suggesting diplurids may have been potential prey for palpimanids (Cerveira and Jackson, 2005).

6. Concluding Remarks

The Crato Formation of Brazil contains a diverse assemblage of terrestrial arthropods, with an abundance of fossil spiders. Previously, only a few fossil spiders had been formally described formally including representatives from the families Dipluridae, Palpimanidae, and Araneidae. The spider *Cretaraneus martinsnetoi*, the first formally described fossil spider from the Crato Formation, has been determined not to be congeneric with *Cretaraneus*, and instead, is placed into its own genus: *Olindarachne* gen. nov. Many of the spiders appear to be conspecific with *O. martinsnetoi*, but other fossils represent additional araneomorph and araneoid spiders including

the large nephiline spiders. At present, this fossil assemblage is the only record of fossil spiders described from South America, and reveals a prolific arachnid community of aerial orbweaving spiders.

7. Acknowledgements

We thank Arsalan Zolfaghari (University of Kansas) for micro-CT imaging; Joerg Wunderlich (Beiträge zur Araneologie), Dave Martill (Universty of Portsmouth), Jason Dunlop (Museum für Naturkunde), and the American Museum of Natural History for specimen loans.

Funding: This work was supported by the University of Kansas Doctoral Student Research Fund and the American Arachnological Society.

8. Literature Cited

Alvin, K.L., 1982. Cheirolepidiaceae: Biology, structure and paleoecology. Rev. Palaeobot. Palynol. 37, 71–98.

Barling, N., Martill, D.M., Heads, S.W., Gallien, F., 2015. High fidelity preservation of fossil insects from the Crato Formation (Lower Cretaceous) of Brazil. Cretaceous Res. 52, 605–622.

Batten, D.J., 2007. Spores and pollen from the Crato Formation: biostratigraphic and palaeoenvironmental implications. *In* Martill, D.M. The Crato fossil beds of Brazil: window into an ancient world. Cambridge University Press, Cambridge 566–573.

Carlos Coimbra, J., Arai, M., Luisa Carreño, A., 2002. Biostratigraphy of Lower Cretaceous microfossils from the Araripe Basin, northeastern Brazil. Geobios Mem. Spec. 35, 687–698.

Cerveira, A.M., Jackson, R.R., 2005. Specialised predation by *Palpimanus sp.* (Araneae: Palpimanidae) on jumping spiders (Araneae: Salticidae). J. East Afr. Nat. Hist. 94, 303–317.

Chumakov, N.M., Zharkov, M.A., Herman, A.B., Doludenko, M.P., Kalandadze, N.M., Lebedev, E.L., Ponomarenko, A.G., Rautian, A.S., 1995. Climatic belts of the mid-Cretaceous time. Stratigr. Geol. Correl. 3, 241–260.

Coddington, J. 1986. The monophyletic origin of the orb-web. In. Shear, W.A. ed. Spiders: Webs, Behavior and Evolution. Stanford University Press, California 319–363.

Coyle, F.A., Ketner, N.D., 1990. Observations on the prey and prey capture behaviour of the funnelweb mygalomorph spider genus Ischnothele (Araneae, Dipluridae). Bulletin of the British Arachnological Society 8, 97–104.

Downen, M.R., Selden, P.A., Hasiotis, S.T., 2016. Spider leg flexure as an indicator for estimating salinity in lacustrine paleoenvironments. Palaeogeogr. Palaeoclimatol. Palaeoecol. 445, 115–123.

Dunlop, J.A., Barov, V., 2005. A new fossil whip spider (Arachnida: Amblypygi) from the Crato Formation of Brazil. Revista Ibérica de Aracnología 12, 53–62.

Dunlop, J.A., Martill, D.M., 2004. Four additional specimens of the fossil camel spider Cratosolpuga wunderlichi Selden 1996 (Arachnida: Solifugae) from the Lower Cretaceous Crato Formation of Brazil. Revista ibérica de aracnología 143–156.

Föllmi, K.B., 2012. Early Cretaceous life, climate and anoxia. Cretaceous Res. 35, 230–257.

Gillespie, R.G., 1987. The Mechanism of Habitat Selection in the Long-Jawed Orb-Weaving Spider Tetragnatha elongata (Araneae, Tetragnathidae). J. Arachnol. 15, 81–90.

Guo, X., Selden, P.A., Shih, C., Ren, D., 2020. Two new lagonomegopid spiders (Arachnida: Araneae) from the mid-Cretaceous of Northern Myanmar, with comments on the superfamilial placement of Lagonomegopidae. Cretaceous Res. 106, 104257.

Halaj, J., Ross, D.W., Moldenke, A.R., 2000. Importance of habitat structure to the arthropod

food-web in Douglas-fir canopies. Oikos 90, 139–152.

Hallam, A., 1985. A review of Mesozoic climates. J. Geol. Soc. London 142, 433–445.

Hallam, A., 1984. Pre-Quaternary Sea-Level Changes. Annu. Rev. Earth Planet. Sci. 12, 205–243.

Heimhofer, R., Martill, D., 2007. The sedimentology and depositional environment of the Crato Formation, In Martill D., The Crato Fossil Beds of Brazil: Window into an Ancient World. Cambridge University Press, pp. 44–63.

Heimhofer, U., Ariztegui, D., Lenniger, M., Hesselbo, S.P., Martill, D.M., Rios-Netto, A.M., 2010. Deciphering the depositional environment of the laminated Crato fossil beds (Early Cretaceous, Araripe Basin, North-eastern Brazil). Sedimentology 57, 677–694.

Jocqué, R., Dippenaar-Schoeman, A.S., 2007. Spider Families of the World. Royal Museum for Central Africa, Tervuren.

Kuntner, M., Hamilton, C.A., Cheng, R.-C., Gregorič, M., Lupše, N., Lokovšek, T., Lemmon, E.M., Lemmon, A.R., Agnarsson, I., Coddington, J.A., Bond, J.E., 2019. Golden Orbweavers Ignore Biological Rules: Phylogenomic and Comparative Analyses Unravel a Complex Evolution of Sexual Size Dimorphism. Syst. Biol. 68, 555–572.

Levi, H.W., 2002. Keys To The Genera Of Araneid Orbweavers (Araneae, Araneidae) Of The Americas. The Journal of Arachnology, 30(3): 527–562.

Lima, F.J.D.E., Saraiva, A.A.F., Silva, M.A.P.D.A., Bantim, R.A.M., Sayão, J.M., 2014. A new angiosperm from the Crato Formation (Araripe Basin, Brazil) and comments on the Early Cretaceous Monocotyledons. An. Acad. Bras. Cienc. 86, 1657–1672.

Maisey, J.G., 1991. Santana fossils: an illustrated atlas. TFH Publications Incorporated.

Maisey, J.G., Others, 1990. Stratigraphy and depositional environment of the Crato member

(Santana Formation, Lower Cretaceous of NE Brazil). Insects from the Santana Formation, Lower Cretaceous, of Brazil. Bulletin of the American Museum of Natural History 195, 15–19.

Martill, D.M., 1993. Fossils of the Santana and Crato formations, Brazil. Palaeontological Association.

Martill, D.M., Bechly, G., Loveridge, R.F., 2007a. The Crato Fossil Beds of Brazil: Window into an Ancient World. Cambridge University Press.

Martill, D.M., Loveridge, R., Heimhofer, U., 2007b. Halite pseudomorphs in the Crato Formation (Early Cretaceous, Late Aptian–Early Albian), Araripe Basin, northeast Brazil: further evidence for hypersalinity. Cretaceous Res. 28, 613–620.

Menon, F., 2007. Higher systematics of scorpions from the Crato Formation, lower Cretaceous of Brazil. Palaeontology 50, 185–195.

Mesquita, M.V., 1996. *Cretaraneus martinsnetoi* n.sp. (Araneoidea) da Formação Santana, Cretáceo inferior da Bacia do Araripe. Revista Geociências - UNG-Ser 1, 24–31.

Moore, C.W., 1977. The life cycle, habitat and variation in selected web parameters in the spider, *Nephila clavipes* Koch (Araneidae). Am. Midl. Nat. 98, 95–108.

Neumann, V.H., Borrego, A.G., Cabrera, L., Dino, R., 2003. Organic matter composition and distribution through the Aptian–Albian lacustrine sequences of the Araripe Basin, northeastern Brazil. Int. J. Coal Geol. 54, 21–40.

Park, T.-Y.S., Nam, K.-S., Selden, P.A., 2019. A diverse new spider (Araneae) fauna from the Jinju Formation, Cretaceous (Albian) of Korea. J. Syst. Palaeontol. 17, 1271–1297.

Patel, R., Rana, R.S., Selden, P.A., 2019. An orb-weaver spider (Araneae, Araneidae) from the early Eocene of India. J. Paleontol. 93, 98–104.

Pekár, S., Sobotník, J., Lubin, Y., 2011. Armoured spiderman: morphological and behavioural adaptations of a specialised araneophagous predator (Araneae: Palpimanidae). Naturwissenschaften 98, 593–603.

Penney, D., 2005. The fossil spider family Lagonomegopidae in Cretaceous ambers with descriptions of a new genus and species from Myanmar. J. Arachnol. 33, 439–444.

Penney, D., 2004. Cretaceous Canadian amber spider and the palpimanoidean nature of lagonomegopids. Acta Palaeontol. Pol. 49.

Penney, D., Ortuño, V.M., 2006. Oldest true orb-weaving spider (Araneae: Araneidae). Biol. Lett. 2, 447–450.

Penney, D., Selden, P., 2011. Fossil Spiders: The Evolutionary History of a Mega-diverse Order. Siri Scientific Press.

Poinar, G., Jr, Buckley, R., 2012. Predatory behaviour of the social orb-weaver spider, *Geratonephila burmanica* n. gen., n. sp.(Araneae: Nephilidae) with its wasp prey, *Cascoscelio incassus* n. gen., n. sp.(Hymenoptera: Platygastridae) in Early Cretaceous Burmese amber. Hist. Biol. 24, 519–525.

Raven, R.J., Jell, P.A., Knezour, R.A., 2015. *Edwa maryae* gen. et sp. nov. in the Norian Blackstone Formation of the Ipswich Basin—the first Triassic spider (Mygalomorphae) from Australia. Alcheringa. An Austral. J. of Palaeo. 39, 259–263.

Robinson, M.H., Mirick, H., 1971. The predatory behavior of the golden-web spider *Nephila clavipes* (Araneae: Araneidae). Psyche 78, 123–139.

Scudder, S.H., 1890. The Tertiary Insects of North America. U.S. Government Printing Office.

Selden, P.A., 1990. Lower Cretaceous spiders from the Sierra de Montsech, north-east Spain.

Selden, P.A., Anderson, H.M., Anderson, J.M., 2009. A review of the fossil record of spiders

(Araneae) with special reference to Africa, and description of a new specimen from the Triassic Molteno Formation of South Africa. Afr. Invertebr. 50, 105–116.

Selden, P.A., Anderson, J.M., Anderson, H.M., Fraser, N.C., 1999. Fossil araneomorph spiders from the Triassic of South Africa and Virginia. J. Arachnol. 27, 401–414.

Selden, P.A., da Costa Casado, F., Vianna Mesquita, M., 2006. Mygalomorph spiders (Araneae: Dipluridae) from the Lower Cretaceous Crato lagerstätte, Araripe Basin, north-east Brazil: Cretaceous spiders from Crato, Brazil. Palaeontology 49, 817–826.

Selden, P.A., Penney, D., 2003. Lower Cretaceous spiders (Arthropoda: Arachnida: Araneae) from Spain. Neues Jahrbuch für Geologie und Paläontologie. Monatshefte 2003, 175–192.

Selden, P.A., Ren, D., 2017. A review of Burmese amber arachnids. J. Arachnol. 45, 324–343.

Selden, P.A., Ren, D., Shih, C., 2016. Mesozoic cribellate spiders (Araneae: Deinopoidea) from China. J. Syst. Palaeontol. 14, 49–74.

Selden, P.A., Shear, W.A., 1996. The first Mesozoic Solifugae (Arachnida) from the Cretaceous of Brazil, and a redescription of Palaeozoic solifuge. Palaeontology 39, 583–604.

Selden, P.A., Shih, C., Ren, D., 2013. A giant spider from the Jurassic of China reveals greater diversity of the orbicularian stem group. Naturwissenschaften 100, 1171–1181.

Selden, P.A., Shih, C., Ren, D., 2011. A golden orb-weaver spider (Araneae: Nephilidae: Nephila) from the Middle Jurassic of China. Biol. Lett. 7, 775–778.

Warren, L.V., Varejão, F.G., Quaglio, F., Simões, M.G., Fürsich, F.T., Poiré, D.G., Catto, B., Assine, M.L., 2016. Stromatolites from the Aptian Crato Formation, a hypersaline lake system in the Araripe Basin, northeastern Brazil. Facies 63, 3.

Wunderlich, J., 2017. New and rare fossil spiders (Araneae) in mid Cretaceous amber from Myanmar (Burma), including the description of new extinct families of the suborders

Mesothelae and Opisthothelae as well as notes on the taxonomy, the evolution and the biogeography of the Mesothelae. Beiträge zur Araneologie 10, e279.

Wunderlich, J., 2004. Fossil spiders in amber and copal: conclusions, revisions, new taxa and family diagnoses of fossil and extant taxa. Wunderlich.

Wunderlich, J, 1988. Die Fossilen Spinnen im Dominikanischen Bernstein. Beit. Araneol. 2, 1–378.

Chapter 3

Fossil spiders (Araneae) from the Eocene Kishenehn Formation of Montana

(Formatted for submission to *Paleontologia Electronica*)

Matthew R. Downen[1] and Paul A. Selden[1,2]:

[1]Department of Geology, University of Kansas, 1414 Naismith Dr., Lawrence, Kansas 66045, USA. E-mail: mattdownen@ku.edu

[2]Natural History Museum, Cromwell Road, London, SW7 5BD, UK E-mail: selden@ku.edu

Keywords: Fossil-Lagerstätte; lacustrine; new genus; new species; taxonomy

ABSTRACT

The Kishenehn Formation consists of oil shales and other clastic sediments of lacustrine origin. A diverse assemblage of terrestrial arthropod fossils has been recovered, representing a tropical ecosystem in North America during the Eocene (46 Ma). Most of the fossils are small insects, but about 20 spiders have also been recovered and recently made available for study. Here, the fossil spiders are described for the first time and include new species of orbweaving spiders from the family Araneidae and ground-dwelling spiders from the family Gnaphosidae. Most of the spiders in the assemblage are conspecific: *Pantherarachne greenwalti* gen. & sp. nov., and similar to extant spiders in the genus *Neoscona*. A single gnaphosid is likely a juvenile. A single male spider belonging to Araneomorphae is too poorly preserved to discern family level. The low diversity of this deposit likely is influenced strongly by sample size, but similar deposits like the Green River Formation of Colorado (Eocene) also have low diversity preserved in the lacustrine sediments.

INTRODUCTION

The Kishenehn Formation of Montana (Eocene: 46 Ma) is one of several Cenozoic lacustrine deposits of North America. A diverse assemblage of fossils is represented and includes terrestrial arthropods, plants, aquatic molluscs, and mammals (Pierce and Constenius, 2014). Small insects including flies (Diptera), true bugs (Hemiptera), and extremely minute fairy wasps (Hymenoptera: Mymaridae) are the most abundant fossils, while vertebrates are rare (Greenwalt and Labandeira, 2013; Greenwalt and Engel, 2014; Greenwalt et al., 2014; Lapolla and Greenwalt, 2015). The exceptional preservation has yielded even a blood-engorged mosquito with preserved biomolecules derived from hemoglobin preserved (Greenwalt et al., 2013).

Relatively few fossil spiders have been recovered this deposit and, hitherto, none have been described formally. This paper is a taxonomic survey of the fossil spider assemblage from the Kishenehn Formation.

The assemblage consists of new species of orbweaving spiders (Araneidae), a ground dwelling spider from the family Gnaphosidae, and an indeterminate araneomorph. Most of the spiders in the assemblage are conspecific and similar to extant spiders in the araneid spider genus *Neoscona* Simon, 1864. A single very small spider is likely a juvenile gnaphosid (Gnaphosidae) based on cylindrical spinnerets. A single male spider likely is preserved too poorly preserved to discern family level, and is left as an indeterminate araneomorph. Whereas none of the spiders described here extend the age range of any families, they do present a starting point for comparing spider assemblages preserved in Eocene lacustrine deposits across North America during the Eocene.

The fossil record of Araneidae extends back to the Cretaceous with the earliest araneid, *Mesozygiella dunlopi* Ortuño, 2006 preserved in amber from Álava, Spain (Penney and Ortuño, 2006). Araneids are one of the most diverse groups of spiders today (3100 species; World Spider Catalog, 2020), with many fossils described from amber (91 species). The Cenozoic record of Araneidae in North America currently includes araneids from the Dominican and Chiapas ambers and one lacustrine deposit, the Florissant Formation of Colorado (Scudder, 1890; Petrunkevyc, 1922; Petrunkevitch, 1971; Wunderlich, 1982, 1986, 1988). The Florissant Formation (Eocene: 34 Ma) is a well-known lacustrine deposit with many exceptionally preserved insects and spiders, currently including 14 species of araneids in two genera: *Araneus* Clerck, 1757 and *Tethneus* Scudder, 1885, although many of these fossil spiders from the Florissant Formation are in need of revision (World Spider Catalog 2020).

Gnaphosids are ground-dwelling spiders that do not weave webs to capture prey; instead, they actively hunt on the ground (Jocqué and Dippenaar-Schoeman, 2007). Gnaphosids and their relatives are distinguished from the aerial web-spinning spiders by possessing only two tarsal claws, instead of three, and differing leg lengths. Gnaphosids themselves are distinguished easily from other similar spiders by their widely separated cylindrical spinnerets and claw tufts at the end of each leg (Platnick, 1990). There are currently 2522 species within Gnaphosidae, which also makes them one of the most diverse spider families. The fossil record of Gnaphosidae comes mostly from Baltic amber with 13 species (Menge, 1854; Wunderlich, 2011). Five species are from the Florissant Formation (34 Ma), but many of these need revision (Petrunkevyc, 1922).

GEOLOGIC SETTING AND FOSSIL PRESERVATION

The Kishenehn Formation is located in northwestern Montana, and is composed of two members: the Coal Creek Member and the overlying Pinchot Conglomerate Member. The Coal Creek Member is represented by an 1150 m thick succession of sandstone, siltstone, and oil shale (Constenius et al., 1989). Fossil insects and spiders are found in the middle of the Coal Creek Member in the oil shale. The fossils are preserved as compressions in extremely thin and delicate laminations representing varves. A thin layer of surface silicates obscures many of the fossils (Greenwalt et al., 2014).

The depositional setting and paleoenvironment is interpreted as a freshwater lacustrine system in a subtropical to tropical environment. Fishes, including bowfins (Amiidae) and suckers (Catostomidae), are indicative of freshwater habitats (Wilson, 1988). Sycamores are the most abundant plant fossils and represent humid and warm conditions, whereas other plants like

cattails and waterferns are suggestive of paludal environments (Constenius et al., 1989). Relatively few mammal fossils have been recovered, but include flying lemurs which also support a tropical paleoenvironment (McKenna, 1990).

MATERIALS AND METHODS

Materials

The specimens consist of part only and are preserved in oil shale from the Coal Creek Member of the Kishenehn Shale in northwestern Montana. Greenwalt et al. (2013) lists specific sites of collection. The specimens are deposited in the Department of Paleobiology, National Museum of Natural History, Washington, D.C.

Methods

Due to the coating of silicates on the surface of the fossils, specimens were submerged in 95% ethanol. The specimens were studied using a Leica M205C stereomicroscope, photographed with a Canon EOS 5D MkII digital camera attached to the microscope and captured with DSLR Assistant software (www.kaasoft.com) on an Apple MacBook Pro computer. Drawings were made using a drawing tube attached to the microscope. Photographs were manipulated using Adobe Photoshop software. Fossils were also imaged using an Olympus BX51 Petrographic Scope with a mercury vapor-arc-discharge lamp, and two exciter filters designed to transmit in the UV (330–385 nm wavelength) and violet-blue (400–440 nm wavelength) region. This causes the matrix surrounding the fossils to fluoresce, and thus, increasing the contrast between matrix and cuticle/fossil material.

Abbreviations: AME anterior median eye(s), car carapace, ch chelicera, cx coxa, fe femur, L length, lb labium, LE lateral eye(s), mt metatarsus, mx maxilla, op opisthosoma, pa patella, Pd pedipalp, PME posterior median eye(s), sp spinnerets, st sternum, ta tarsus, ti tibia, W width.

SYSTEMATIC PALEONTOLOGY

Order ARANEAE Clerck, 1757

Suborder OPISTHOTHELAE Pocock, 1892

Infraorder ARANEOMORPHAE Smith, 1902

Araneomorphae *incertae sedis*

(Fig. 1).

Remarks. Parts of this fossil spider are preserved with high fidelity (the legs), whereas other portions are poor in detail (the palps and carapace). The palps, carapace, and some of the leg joints have been replaced with pyrite which contributes to a loss of detail. Mygalomorph spiders typically have large porrect chelicerae and robust legs. The fossil here has relatively small chelicerae that are not porrect, and legs that are relatively slender with heavy spination. The pedipalps are modified, indicating the specimen is an adult male. A large cymbium is observable on each palp, as well as a median apophysis and other structures of the palpal bulb, suggesting it is relatively complex like most araneomorph spiders. Most of the femora are distorted (likely due to compression) and are likely longer than they appear. The third leg of the spider is the shortest, but it is not quite as short as most orbweaving spiders. Tarsus IV possesses fine setae, but no tarsal comb is visible, as is in the family Theridiidae. Two tarsal claws can be made out on some legs, and there do not appear to be any dense claw tufts or scopulae, so the specimen is unlikely to belong to Clubionidae or Corinnidae.

Description of 583.1. Male Carapace rounded, longer than wide (L 0.62, W 0.48). Abdomen about as long as wide (L 0.76, W 0.78), with circular darkened area at anterior extending to almost full length of abdomen. Spinnerets small and conical, at posterior most tip of abdomen

(abdomen does not overhang spinnerets). Cymbium oval, almost half the length of the carapace, covered in fine setae. Hook-shaped median apophysis. Walking leg formula I>II>IV>III.. Legs spinose and covered in fine setae and erect long and thick spine-like macrosetae. Single spine-like macrosetae on each patella, two on proximal tibia of all legs. Shorter macrosetae on metatarsus.

Superfamily ARANEOIDEA

Family ARANEIDAE

Remarks. The following fossils are placed in family Araneidae based on the following characteristics: 3 clawed, entelegyne, ecribellate, long slender legs, and a shortest third pair of legs. The spiders lack a tarsal comb on the fourth tarsus and possesses spine-like macrosetae on some ti and mt, excluding them from Theridiidae. The spiders also lacks a calamistrum and femoral trichobothria excluding them from Uloboridae. The spiders are excluded from Linyphiidae by lacking a single mt trichobothrium on Legs I–IV (although this just may not be visible), and by possessing sternum that does not extend beyond coxa IV and tarsi that are tapering rather than cylindrical.

Araneidae *incertae sedis*

(Fig. 2)

Description of 20412.1. Male. Carapace longer than wide (L 1.3, W 0.91). Posterior half of sternum pointed, with sparse fine setae. Abdomen rounded, about as long as wide (L 1.2, W 1.37); dark patch running through the abdomen midline. Walking leg formula I>II>IV>III.; legs long and slender, clothed in dense fine setae; Leg III distinctly short (2.5x shorter than Leg 1); Metatarsi of Legs I and II noticeably curved; relatively few erect spine-like macrosetae on all

legs: one on proximal mt of Legs I, II, III, none on Leg IV mt; two on proximal ti of Leg III; one proximal and one distal on Leg IV ti.

Podomere lengths: Leg I fe 1.57, pa 0.24, ti 1.59, mt 1.91, ta 0.56, Leg II fe 1.31, pa 0.28, ti 1.10, mt 1.36, ta 0.49, Leg III fe 0.68, pa 0.18, ti 0.55, mt 0.59, ta 0.44, Leg IV fe 1.04, pa 0.15, ti 0.75, mt 0.93, ta 0.36.

Remarks. The position of the legs of this spider is similar to fossil uloborids from Montsech, Spain (Cretaceous) and the Daohugoue Beds of China (Jurassic), however no plumose or feathery setae, which are present in uloborids. The seta of this spider appear smooth. The spider also lacks a cribellum and calamistrum, but these features are lost in adult male uloborids.

Genus *Constenius leonai* gen. nov.

Diagnosis. Distinguished from all other araneids by the combination of a subtriangular abdomen and a cluster of four long thin setae on the palpal patella.

Etymology. The fossil genus is named for Kurt Constenius who collected the fossil.

Type species. *Constenius leonai* n. sp. (monotypic).

Constenius leonai sp. nov.

(Fig. 3)

Etymology. The fossil, nicknamed “Leona’s Spider”, is named for ther mother of Kurt Constenius, Leona, who graciously donated the specimen.

Type. Holotype adult female, only known specimen, part only, Special Spider (not yet accessioned into NMNH), from Coal Creek Member of the Kishenehn Formation; Eocene age;

northwestern Montana; deposited in the Smithsonian Institution National Museum of Natural History, Paleobiology Department.

Diagnosis. As for the genus.

Description of Special Spider. Sternum triangular, longer than wide, with setae that lengthen anteriorly. Labium triangular, wider than long. Maxillae short and stout, widest anteriorly. Chelicerae robust and stout. Palps with abundant setae and macrosetae. Abdomen subtriangular, wider than long (L 0.0.87, W 0.95), distinctly sclerotized portion round and half the length of abdomen. Colulus present. Walking leg formula I>II>IV>III. Legs covered in abundant spine-like macrosetae. Single trichbothrium on proximal tibia of legs III and IV just after pa-ti joint. Length of mt + ta > ti + pa.

Podomere lengths: Pd 0.42 (visible); leg I fe 1.01, pa 0.26, ti 0.99 mt 1.18, ta 0.47; leg II fe 0.94, pa 0.21, ti 0.71, mt 0.83, ta 0.0.36; leg III fe 0.56 , pa 0.16, ti 0.41, mt 0.4, ta 0.25; leg IV fe 0.82, pa 0.2, ti 0.52, mt 0.62, ta 0.24..

Remarks. The fossil is similar to *Metepeira* in that the combined length of metatarsus I and tarsus I is greater than the combined length of tibia I and patella I (Piel, 1998). The subtriangular abdomen is similar to *Neoscona* in ventral view, although the abdomen is more rounded in *Neoscona (Berman and Levi, 1971)*. The fossil also has a distinct patch of color on the anterior ventral portion of the abdomen. Many species in the subfamily Araneinae are distinguished by ventral patches of color, but any patterns useful for classification are not visible here.

Genus *Pantherarachne* gen. nov.

Diagnosis. Distinguished from all other araneids by the combination of characters: an abdomen widely overhanging spinnerets, annulated legs with two dark bands on metatarsus IV, the single trichobothrium at the distal most edge of the metatarsus just before the mt-ta joint.

Etymology. The fossil genus is named for the genus *Panthera* for the tiger-stripe appearance and *arachne* for spider.

Type species. *Pantherarachne greenwalti* n. sp. (monotypic).

Pantherarachne greenwalti sp. nov.

(Fig. 4)

Etymology. The fossil species is named for Dale Greenewalt who collected the fossil and pushed for the spiders to be studied.

Type. Holotype adult female, four specimens, part only, from Coal Creek Member of the Kishenehn Formation; Eocene age; northwestern Montana; deposited in the Smithsonian Institution National Museum of Natural History, Paleobiology Department.

Diagnosis. As for the genus.

Description of 32280. Carapace oval in outline, longer than wide (L 1.49 , W 0.87); sternum heart shaped, longer than wide, attenuated posteriorly, not extending past coxae IV; Labium rebordered (thickened anteriorly), wider than long. Abdomen rounded, longer than wide (L 1.59, W 1.38), clothed in setae, projecting beyond spinnerets. Walking leg formula I>II>IV>III.; stout, but tapering legs, Leg III noticeably short; legs covered in dense fine setae, large macrosetae on most podomeres; trichobothrium on distal Leg IV mt; Legs striped with colored (darkened) bands; Leg IV fe with only distal darkening.

Podomere lengths: Pd 0.77 (visible); leg I fe 1.22, pa 0.34, ti 0.85 mt 0.74, ta 0.38; leg II fe 0.9, pa 0.31, ti 0.8, mt 0.59, ta 0.33; leg III fe 0.49, pa 0.2, ti 0.34, mt 0.35, ta 0.24; leg IV fe 0.73, pa 0.29, ti 0.64, mt 0.54, ta 0.30.

Remarks. The banded legs and podomere lengths resemble those of other araneid genera like Larinioides, Neoscona, and Zygiella (Baba and Tanikawa, 2015; Tanikawa, 2017; Framenau, 2019). Neoscona has fewer bands on Leg IV, and specifically, only one band on metatarsus IV. Some Larinioides have two bands on metatarsus IV, but the distal half of tibia IV is a solid band, in contrast to the fossil. Zygiella also has banded legs, although lighter in color and an abdomen that does not overhang the spinnerets as much as what is observed in the fossil.

Clade DIONYCHA

Family Gnaphosidae Pocock, 1898

Remarks. The fossil is placed in the family Gnaphosidae based on the stout legs (Walking leg formula 4123) and widely separated lateral spinnerets.

Gnaphosidae *incertae sedis*

(Fig. 5).

Description of 20480. Carapace outline suboval, longer than wide (L 0.77, W 0.46). Chelicerae relatively large, projecting forward. Abdomen longer than wide (L 1.24, W 0.73). Labium triangular, as long as wide, and notched distally. Maxillae slightly narrowed at center. Sternum ovoid. Body and legs clothed in dense short setae. Relatively few macrosetae on legs. Claw tufts present.

Podomere lengths: Leg I fe 0.60, pa 0.27, ti 0.56, mt 0.57, ta 0.29; Leg II fe 0.59, pa 0.29, ti 0.46, mt 0.43, ta 0.26; Leg III fe 1.21 pa 0.23, ti 0.29, mt 0.35, ta 0.25; Leg IV fe 0.65 pa 0.30, ti 0.67, mt 0.48, ta 0.30.

Remarks. The small size of the specimen suggests it is a juvenile. There are also no clear reproductive structures visible and the palps are not inflated. The fossil also resembles spiders from Clubionidae and Corinnidae. Both corinnids and clubionids usually have more well developed spines on the legs. Corinnids have shorter spinnerets that are closer together. Clubionids can have elongated cylindrical spinnerets like gnaphosids, but the anterior lateral spinnerets are not as widely separated in clubionids.

DISCUSSION

Although relatively few fossil spiders have been recovered from the Kishenehn Formation thus far, they are still the first formally described spiders from the Eocene of Montana. Fossil spiders have been reported from the Oligocene Canyon Ferry Fossil-Lagerstätte of Montana, but remain undescribed (CoBabe et al., 2002). Other Eocene lacustrine deposits from which fossil spiders have been recovered include the Green River and Florissant formations of Colorado, and Horsefly, British Columbia, Canada.

The Kishenehn fossil assemblage consists mostly of aerial web weaving spiders, which are found in the other Cenozoic lacustrine deposits. The orbweaving spider *P. greenwalti* is easily recognizable from the striped pattern on its legs, and four other spiders from this deposit appear to be the same species. Orbweaving spiders are also found in the Green River Formation (Selden and Wang, 2014), although not of the same family (Tetragnathidae), and none of the spiders appear to resemble *P. greenwalti*. Another similarity between the Kishenehn and Green River spider assemblages is their relatively small size, which is likely the result of taphonomic

bias. The only fossil spider formally described from Horsefly is a pisaurid (Pisauridae), ground-dwelling spiders often referred to as fishing spiders or more commonly known as nursery web spiders (Selden et al., 2009). No such spiders have been found in the Kishenehn Formation thus far, but pisaurids are present in the Florissant Formation. The Florissant Formation contains a much more diverse assemblage of spiders in a variety of families including Araneidae and Gnaphosidae (Scudder, 1890; Petrunkevitch, 1922). The gnaphosid described here does not extend the age range of Gnaphosidae, as several gnaphosids have been described from Baltic amber, but it is the oldest representative of the family found so far in North America.

ACKNOWLEDGEMENTS

We thank Dale Greenwalt reaching out about the spiders for study, Conrad Labandeira and Mark Florence (NMNH) for loan of the specimens in collections at the Smithsonian, and Kurt Constenius (University of Arizona) and family for donation of the special spider; and Alison Olcott (University of Kansas) for use of the fluorescence microscope.

LITERATURE CITED

Baba, Y., and Tanikawa, A., 2015, The handbook of spiders: Bun-Ichi Sogo Shuppan, Tokyo,.

Berman, J.D., and Levi, H.W., 1971, The orb weaver genus Neoscona in North America (Araneae: Araneidae). El género de tejedoras de esferas del género Neoscona en Norteamérica (Araneae: Araneidae): Bulletin of the Museum of Comparative Zoology at Harvard College, v. 141, p. 465–500.

CoBabe, E.A., Chamberlain, K.R., Ivie, M.A., and Giersch, J.J., 2002, A new insect and plant Lagerstatte from a Tertiary lake deposit along the Canyon Ferry Reservoir, southwestern

Montana: Rocky Mountain Geology, v. 37, p. 13–30.

Constenius, K.N., Dawson, M.R., Pierce, H.G., Walter, R.C., and Wilson, M.V.H., 1989, Reconnaissance paleontologic study of the Kishenehn Formation, northwestern Montana and southeastern British Columbia.

Framenau, V.W., 2019, Generic and family transfers, and numina dubia for orb-weaving spiders (Araneae, Araneidae) in the Australasian, Oriental and Pacific regions: Evolutionary Systematics, v. 3, p. 1–27.

Greenwalt, D., and Labandeira, C., 2013, The amazing fossil insects of the Eocene Kishenehn Formation in Northwestern Montana: Rocks & Minerals, v. 88, p. 434–441.

Greenwalt, D., and Engel, M.S., 2014, A diminutive pelecinid wasp from the Eocene Kishenehn Formation of northwestern Montana (Hymenoptera: Pelecinidae): Novitates Paleoentomologicae, p. 1–9.

Greenwalt, D.E., Goreva, Y.S., Siljeström, S.M., Rose, T., and Harbach, R.E., 2013, Hemoglobin-derived porphyrins preserved in a Middle Eocene blood-engorged mosquito: Proceedings of the National Academy of Sciences of the United States of America, v. 110, p. 18496–18500.

Greenwalt, D.E., Rose, T.R., Siljestrom, S.M., Goreva, Y.S., Constenius, K.N., and Wingerath, J.G., 2014, Taphonomy of the fossil insects of the middle Eocene Kishenehn Formation: Acta Palaeontologica Polonica, v. 60, p. 931–948.

Jocqué, R., and Dippenaar-Schoeman, A.S., 2007, Spider Families of the World. Royal Museum for Central Africa, Tervuren.

Lapolla, J.S., and Greenwalt, D.E., 2015, Fossil ants (Hymenoptera: Formicidae) of the Middle Eocene Kishenehn Formation: Sociobiology, v. 62, p. 163–174.

McKenna, M.C., 1990, Plagiomenids (Mammalia:? Dermoptera) from the Oligocene of Oregon, Montana and South Dakota, and Middle Eocene of northwestern Wyoming: dawn of the age of mammals in the northern part of the Rocky Mountain Interior, North America. Geological Society of America, Special Paper, v. 243, p. 211–234.

Menge, A., 1854, Die im Bernstein befindlichen Myriapoden, Arachniden und Apteren der Vorwelt: Die Im Bernstein Befindlichen Organischen Reste Der Vorwelt Gesammelt in Verbindung Mit Mehreren Bearbeitetet Und Herausgegeben 1., p. 124.

Penney, D., and Ortuño, V.M., 2006, Oldest true orb-weaving spider (Araneae: Araneidae): Biology Letters, v. 2, p. 447–450.

Petrunkevitch, A., 1971, Chiapas amber spiders. II: Calif Univ Publ Entomol, v. 1971, 63.

Petrunkevitchc, A., 1922, Tertiary spiders and opilionids of North America: Transactions of the Connecticut Academy of Sciences, v. 25, p. 211–279.

Piel, W.H., 1998, The systematics of neotropical orb-weaving spiders in the genus Metepeira (Araneae, Araneidae): .

Pierce, H.G., and Constenius, K.N., 2014, Terrestrial and Aquatic Mollusks of the Eocene Kishenehn Formation, Middle Fork Flathead River, Montana: Annals of the Carnegie Museum, v. 82, p. 305.

Platnick, N. I. (American Museum of Natural History, New York, NY), 7aug1990, Spinneret

morphology and the phylogeny of ground spiders (Araneae, Gnaphosoidea): American Museum Novitates,.

Scudder, S.H., 1890, The Tertiary Insects of North America: U.S. Government Printing Office, 734 p.

Selden, P.A., and Wang, Y., 2014, Fossil spiders (Araneae) from the Eocene Green River Formation of Colorado: Arthropoda Selecta, v. 23, p. 207–219.

Selden, P.A., Penney, D., Kropf, C., and Horak, P., 2009, A fossil spider (Araneae: Pisauridae) of Eocene age from Horsefly, British Columbia, Canada: Contributions to Natural History, v. 12, p. 1269–1282.

Tanikawa, A., 2017, A new species of Zygiella from Amami-ôshima Island, Japan (Araneae: Araneidae): Acta Arachnologica, v. 66, p. 1–4.

Wilson, M.V.H., 1988, Reconstruction of ancient lake environments using both autochthonous and allochthonous fossils: Palaeogeography, Palaeoclimatology, Palaeoecology, v. 62, p. 609–623.

Wunderlich, and J, 1988, Die Fossilen Spinnen im Dominikanischen Bernstein: Beiträge zur Araneologie., v. 2, p. 1–378.

Wunderlich, J., 1982, Die häufigsten Spinnen (Araneae) des Dominikanischen Bernsteins: Neue Entomologische Nachrichten, v. 1, p. 26–45.

Wunderlich, J., 1986, Fossile Spinnen in Bernstein Und Ihre Heute Lebenden Verwandten: Bauer bei Quelle & Meyer, p.

Wunderlich, J. 2011b. Taxonomy of extant and fossil (Eocene) European ground spiders of the family Gnaphosidae (Araneae), with a key to the genera, and descriptions of new taxa. Beiträge zur Araneologie, v. 6: 19–97.

FIGURES

Figure 1. Specimen 583.1 Araneomorphae *incertae sedis* photograph and interpretive drawing.

Figure 2. Specimen 20412.1 Araneidae *incertae sedis* photograph and interpretive drawing.

Figure 3. Special Spider *Constenius leonai* gen. et sp. nov. A) photograph and interpretive drawing. B) Prosoma region and palps with cluster of long macrosetae (arrow) in UV light. C) Opisthosomal region in UV light showing subtriangular abdomen in UV light. D) Tarsus of Leg IV showing claws and setae in UV light. E) Leg III pa-ti joint with macrosetae and trichobothrium (arrow).

Figure 4. Specimen 32280 *Pantherarachne greenwalti* gen. et sp. nov. photograph and interpretive drawing.

Figure 5. Specimen 20480 Gnaphosidae *incertae sedis* photograph and interpretive drawing.


1 mm

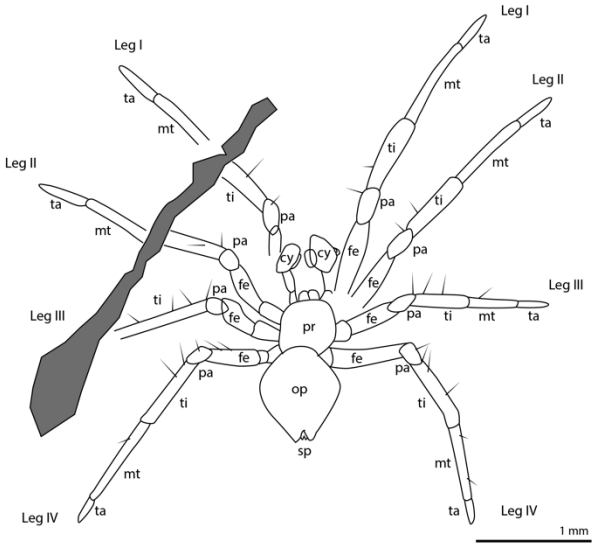
Leg I
ta
mt
ti
pa
fe
cy
pr
op
sp
Leg II
Leg III
Leg IV
1 mm


1 mm

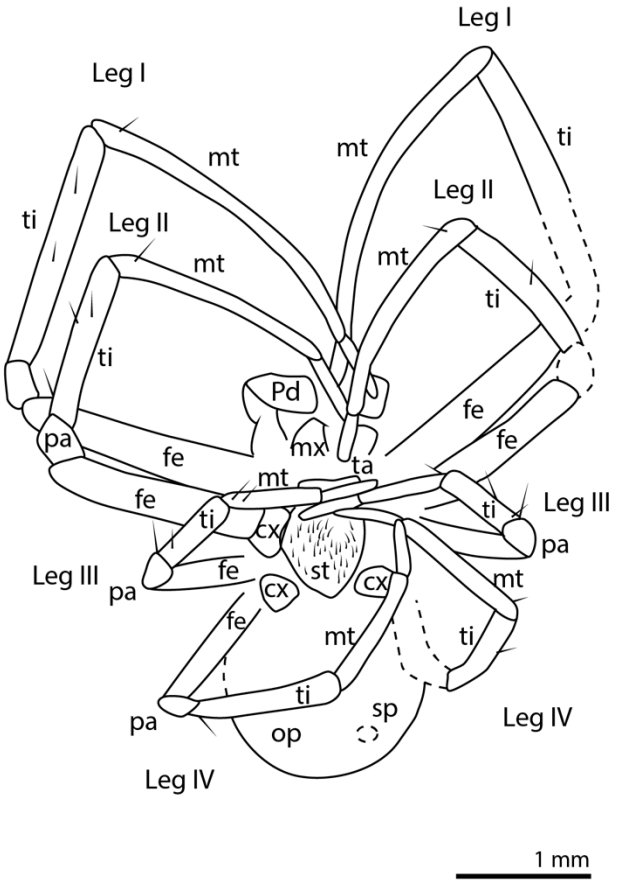
Leg I
Leg I
mt
mt
ti
ti
Leg II
Leg II
mt
mt
ti
ti
Pd
fe
pa
mx
ta
fe
fe
mt
fe
ti
ti
Leg III
cx
pa
st
Leg III
pa
fe
cx
cx
mt
fe
mt
ti
ti
sp
pa
op
Leg IV
Leg IV
1 mm

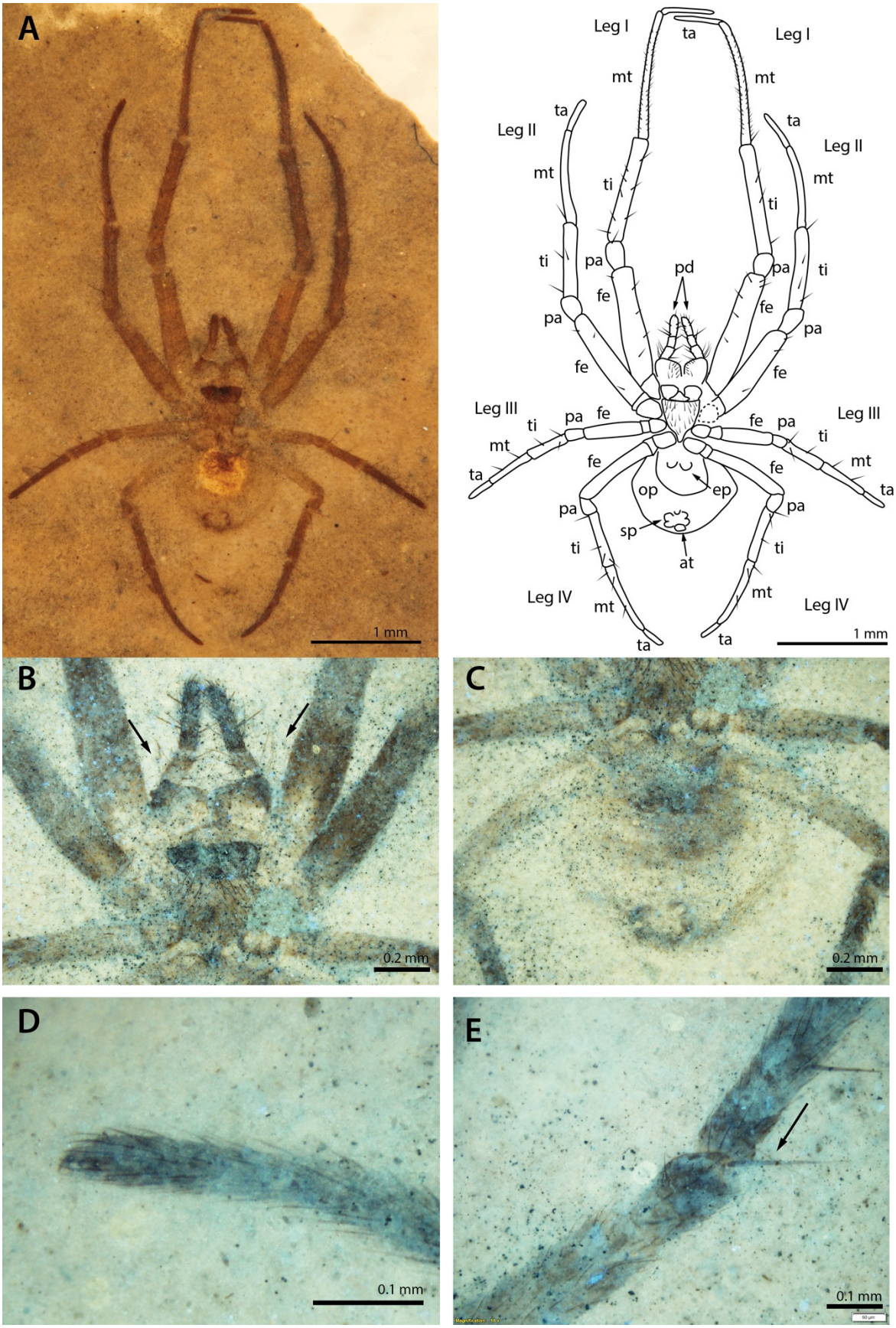
A
1 mm
Leg I
ta
mt
Leg II
ti
pa
pd
fe
Leg III
op
ep
sp
at
Leg IV
1 mm
B
0.2 mm
C
0.2 mm
D
0.1 mm
E
0.1 mm


1 mm

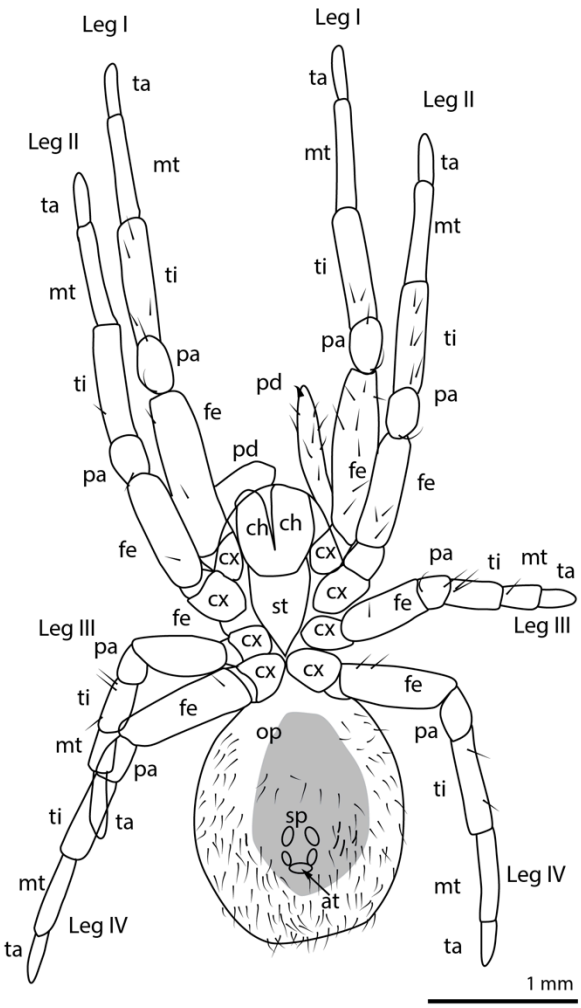
Leg I
Leg I
ta
ta
Leg II
Leg II
mt
mt
ta
ta
mt
ti
ti
mt
ti
pa
pa
ti
pd
pa
fe
fe
pd
pa
fe
fe
ch
ch
fe
cx
cx
pa
ti
mt
ta
cx
cx
st
cx
fe
fe
Leg III
Leg III
cx
pa
cx
cx
fe
ti
fe
op
pa
mt
pa
ti
ti
ta
sp
mt
Leg IV
at
mt
Leg IV
ta
ta
1 mm


1 mm

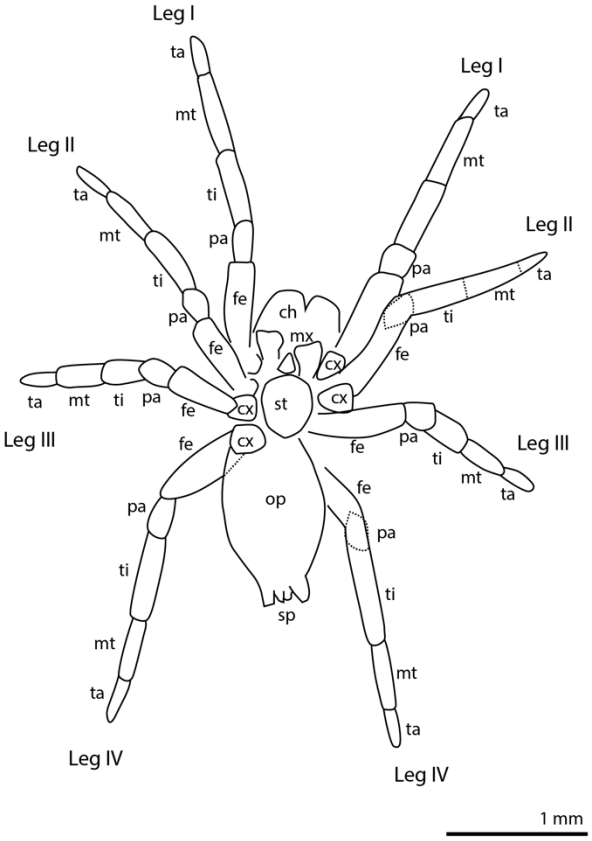
Leg I
ta
mt
ti
pa
fe
Leg II
ta
mt
ti
pa
fe
Leg III
ta
mt
ti
pa
fe
Leg IV
ta
mt
ti
pa
fe
ch
mx
cx
st
cx
cx
op
sp
Leg I
ta
mt
ti
pa
fe
Leg II
ta
mt
ti
pa
fe
Leg III
ta
mt
ti
pa
fe
Leg IV
ta
mt
ti
pa
fe
1 mm

Chapter 4

Revisiting a large fossil spider (Araneidae) from the Florissant Formation (Eocene) of Colorado

(Formatted for submission to *Journal of Arachnology*)

Matt R. Downen[1] and **Paul A. Selden**[1,2.] Department of Geology, University of Kansas, Ritchie Hall Earth, Energy & Environment Center 1414 Naismith Drive, Room 254 Lawrence, KS 66045, USA. E-mail: mattdownen@ku.edu; [2]Natural History Museum, Cromwell Road, London SW7 5BD, UK. E-mail: selden@ku.edu

Abstract. The Florissant Formation of Colorado is an Eocene (34 Ma) Fossil-Lagerstätte from which many fossil spiders have been recovered. The Florissant fossil spider assemblage was first described by Scudder (1890), and later revisited by Petrunkevitch (1922). Many of the 46 species of spiders described have been assigned to modern genera, although the diagnostic characters for the respective genera are not visible in most specimens. The largest fossil spider from Florissant is *Nephila pennatipes* Scudder, 1890. The original interpretations contain errors related to morphology and preservation. Here, the specimen is redescribed and the original interpretation is evaluated and revised. *Trichonephila pennatipes* n. comb. is a large spider with an oval abdomen slightly overhanging the spinnerets, strong setal brushes on the tibiae of Legs I, II, and IV, and a single row of macrosetae on the ventral femur Leg III. The macrosetae of the fossil have been imaged for the first time, revealing an ultrastructure composed of lineations running along the shaft similar to modern *Nephila*, *Trichonephila*, and other araneids. Fluorescence microscopy is used to image *T. pennatipes* and scanning electron microscopy is used to image modern nephilines for comparison.

Keywords: Araneidae, lacustrine, *Nephila*, nephiline, *Trichonephila*

The Florissant Formation is a well-known Eocene (34 Ma) lacustrine deposit in Colorado (Evanoff et al. 2001; Henning et al. 2008) with an abundance of fossil insects and spiders are preserved as compression fossils in thin and delicate shale (Meyer 2003). Although spiders are relatively rare compared to insects in the fossil record, many spiders have been recovered from Florissant and are preserved in exceptional detail. Most of the fossil spiders were described by Scudder (1890), and later revisited by Petrunkevitch (1922) in large taxonomic surveys. The Florissant fossil spiders received attention again later by Ed Licht (1986; 1994) who investigated the paleoecology and taphonomy of Florissant spiders and Kinchloe Roberts et al (2008) by testing a morphometric approach to identifying fossil spiders. Forty-six spider species are currently named from Florissant, with seven modern genera represented (Dunlop et al. 2017). Although the preservation is considered exceptional, it is unlikely that all of the spiders described belong in modern genera. In many of the fossils, diagnostic characteristics like eyes, reproductive structures, spinnerets, and trichobothria are not visible. This challenge is common when describing spiders preserved in lacustrine deposits. The lack of diagnostic characters can make it difficult to assign fossil spiders to genera, and in some cases even a family (Penney & Selden 2011).

The focus of this paper is the fossil spider described by Scudder (1890) as *Nephila pennatipes* Scudder, 1890. *Nephila* Leach, 1815 (Araneidae) are large, pantropical spiders that weave orb webs with silk that has a golden tint, giving them the name the golden orbweavers (Robinson & Robinson 1973; Kuntner et al. 2008; Yong-Chao et al. 2011). Webs can reach 1.5 m in diameter and capture a variety of large insects, and have even been observed to catch flying vertebrates (Robinson & Mirick 1971; Moore 1977). Nephiline spiders have been studied heavily, but have a somewhat complicated taxonomic history. Nephilines originally belonged in

the family Araneidae, but were later transferred to Tetragnathidae (Coddington 1990). At one point, Nephilidae was erected as a separate family for the spiders, but recent studies have reassigned them to Araneidae as subfamily Nephilinae (Kuntner 2005; Dimitrov et al. 2016). Even more recently, several species of *Nephila* were reassigned to *Trichonephila* Dahl, 1911 based on a molecular phylogeny, and Nephilidae was once again established as a family (Kuntner et al. 2019).

The fossil record of nephilines extends back to the Cretaceous, and most of the formally described fossil nephilines are adult males. The oldest described fossil *Nephila* is *Nephila burmanica* Poinar, 2012 preserved in Cretaceous (99 Ma) Burmese amber with wasp prey (Poinar & Buckley 2012). Fossil *Nephila* have also been reported from the Cretaceous Crato Formation (115 Ma) of Brazil, the Eocene Palana Formation (55 Ma) of India, and several species have been described from Baltic amber (44 Ma) and Dominican amber (25 Ma) (Wunderlich 1982, 1986; Penney & Selden 2011; Dunlop & Penney 2012; Patel et al. 2019). The Florissant fossil is assigned to *T. pennatipes* and is redescribed here to improve upon the original interpretations. The fossil is compared with several extant *Nephila* and *Trichonephila*, with particular emphasis on macrosetal patterns. In addition, the setal ultrastructure of *Trichonephila clavipes* Linnaeus, 1767 and *Argiope aurantia* Lucas, 1833 (Araneidae) are investigated and characterized using scanning electron microscopy for comparison to *T. pennatipes*.

MATERIAL AND METHODS

The fossil comes from the Eocene Florissant Formation of Colorado. The holotype and only specimen (No. 61 Origi. 11651) was collected at Florissant, Colorado in 1885, and is held in the Museum of Comparative Zoology, Harvard University, Cambridge, Massachusetts. The

specimen is preserved as a compression fossil, in part only, in a light brown mudstone. The surface of the fossil is irregular and covered in bumps approximately 1 mm across making imaging in low angle light challenging. The specimen is preserved ventral side up and, as a result, features of the carapace are unknown. Other important characteristics for nephilines that are not visible in the fossil due to its preservation include the cheliceral boss, book lung covers, sternal tubercles, and the epigynum.

The fossil specimen was photographed with a Canon EOS 5D Mk II digital camera attached to a Leica M650C microscope. Seventy percent ethanol was used to wet the surface of the fossil and enhance details not evident when dry. Measurements were made from the photographs using the measurement tool in Adobe Photoshop, and drawings were made from the photographs using Adobe Illustrator CS5. Setae and other extremely fine details of the fossil were imaged using an Olympus BX51 Petrographic Scope with a mercury vapor-arc-discharge lamp, and two exciter filters designed to transmit in the UV (330–385 nm wavelength) and violet-blue (400–440 nm wavelength) region.

The femora of two modern nephilines were examined to characterize the pattern of macrosetae on the ventral side: *Trichonephila clavipes* (Linnaeus, 1767) and *N. pilipes* (Fabricius, 1793). The setae of adult females of *T. clavipes* and *Argiope aurantia* Lucas, 1833 were also imaged using a Versa 3D Dual Beam scanning electron microscope (SEM) at the University of Kansas Microscopy and Analytical Imaging Laboratory. The *T. clavipes* specimen was collected in Tampa Bay, Florida in October 2011. The *N. pilipes* specimen was ordered through BioQuip Products Inc. and was collected in Malaysia. The *A. aurantia* was collected in Lawrence, Kansas in 2002. Several types of setae were imaged from the legs and palps of the spiders. The first and second legs were removed from the spider body and immersed into 0.1%

Tween 20 (Sigma Aldrich, Cat. #P1379, Lot. #SLBN1152V) diluted in deionized water. Samples were sonicated for 5 minutes, then the solution was changed to deionized water and sonicated again for 5 minutes. Legs were rinsed with 100% acetone twice (5 min each) and then fixed and stained with 2% Osmium tetroxide (EMS, Cat. #19112, Lot. #170711-03) diluted in 100% acetone overnight (16 hour approximately) at room temperature (RT) inside a fume hood. The following day, samples were washed with 100% acetone twice (5 min each) and immersed into a solution of 1% *p*-Phenylenediamine (Sigma Aldrich, Cat. #P6001, Lot. #WXBB8077N) diluted in 100% acetone for 1 hour at RT. Then, samples were immersed in a mixture of 100% acetone and Hexamethyldisilazane (HMDS [Sigma Aldrich, Cat. #440191, Lot. #SHBH2406V]; 3:1, 1:1, 1:3) for 1 hour per ratio at RT. To complete the chemical drying process, spider legs were immersed in 100% HMDS for 1 hour, then the excess solution was removed, and samples were placed inside a desiccator under vacuum overnight.

Each spider leg was mounted on individual aluminum stubs with carbon tape for image acquisition. Images were acquired on a Cold Field Emission Scanning Electron Microscope, Hitachi High Technologies, SU8230 series, with a secondary electron detectors (SE), at accelerating voltages ranging from 1.0 to 3.0 kV, and aperture 2 (80 μm diameter). Lower (L) and upper (U) detectors, which are located below and above the objective lens respectively to collect SE, were used for both low (LM) and high magnification imaging.

Abbreviations: ALS = anterior lateral spinnerets, at = anal tubercle, BL = book lung, car = carapace, ch = chelicera, cl = claw, co = colulus, cx = coxa, cy = cymbium, EF = epigastric furrow, en = endite, fe = femur, L = length, lb = labium, mt = metatarsus, op = opisthosoma, pa = patella, pd = pedipalp, PLS = posterior lateral spinnerets, sp = spinnerets, st = sternum, ta =

tarsus, ti = tibia, W = width. WBV = blue-violet fluorescence micrograph, WUV = ultraviolet fluorescence micrograph. All measurements are in mm unless otherwise specified.

SYSTEMATICS

Family Araneidae Clerck, 1757

Subfamily Nephilinae Simon, 1894

Genus *Trichonephila* Leach, 1815

Remarks.— This fossil spider is reassigned to *Trichonephila* based on its large size and brushes of setae on the tibiae, the sternum length, and a metatarsus longer than the femur. The setal brushes distinguish this specimen from other nephiline genera such as *Nephilengys* Koch, 1872 and *Herennia* Thorell, 1877. Uloboridae and *Mongolarachne* Selden 2013 (Mongolarachnidae), an extinct genus, also possesses setal brushes, but are cribellate (Selden et al. 2013). The sternum does not extend far between coxae IV like other *Trichonephila*. *Herennia* also has a wider than long sternum in contrast to *T. pennatipes*. The metatarsus is longer than the femur in other *Trichonephila*, but shorter in *N. pilipes*.

Trichonephila pennatipes (Scudder, 1885) new combination

Figures 1–2.

Diagnosis (emended).— Ventral double row of short stout macrosetae equally spaced on legs I, II, IV, positioned near the midline; ventral single row of short macrosetae closely spaced on Leg III positioned near the midline.

Description.— Female. Carapace longer than wide (L = 5.04, W = 3.97). Sternum longer than wide, not extending past coxae IV. Labium subtriangular. Endites longer than wide. Pedipalps stout with abundant setae and several textured macrosetae. Palpal claw with three teeth visible. Opisthosoma ovate slightly overhanging spinnerets (L = 9.87, W = 6.72). Dark median patch of opisthosoma extending from epigastric furrow to spinnerets. Epigastric furrow ⅓ length of opisthosoma from anterior. Leg formula 1243, third leg distinctly shorter. Legs covered in dense short setae (mean L = 83.88 μm, W = 2–3 μm) with rows of short stout macrosetae (L = 143.47 μm, W = 19.09 μm) on each femur, with macrosetae increasing in length distally along leg. Two distinct medial rows of femoral macrosetae on Legs I, II, IV; one distinct medial row on Leg III, extending entire length of femur. Brushes of long setae (mean L = 428.14 μm) at distal 2/3 of tibiae I, II, IV. Cluster of four macrosetae at metatarsus–tarsus joint of Leg IV. large stout spine-like macrosetae with lineations that run along and whorl around the present on all legs and palps. Single trichobothrium on proximal tibia of Leg III. Podomere lengths: Right Leg I fe 8.10, pa 1.27, ti 6.60, mt 8.91, ta 2.27+; Right Leg II fe 6.80, pa 1.29, ti 5.61, mt 8.42, ta 0.78+; Right Leg III fe 4.31, pa 0.92, ti 3.17, mt 4.94+; Right Leg IV fe 6.93, pa 1.09, ti 5.48; Left Leg I fe + pa 9.62, ti 7.09, mt 9.31, ta 1.77+; Left Leg II fe 7.71, pa 1.72, ti .47, mt 7.42, ta 2.34; Left Leg III fe 4.03, pa 1.08, ti 2.80, mt 4.42, ta 1.60; Left Leg IV fe 8.34, pa 1.18, ti 6.59, mt 5.96, ta 2.11+; Right palp 4.19; Left palp 4.01.

Remarks.—The initial description by Scudder (1885) contained a few erroneous interpretations, despite being described by Petrunkevitch (1922: 261) as “entirely correct in every detail.” Scudder described the shape of the cephalic region of the cephalothorax (corselet) as square with two eyes near the anterior center, however, the specimen is preserved ventral side up, and only ventral characteristics are visible. The exact shape of the carapace is obscured by the coxae. No

eyes are visible. The excision of the front margin of the carapace is simply the boundary between the chelicerae. The sternum, labium, endites, and chelicerae were not included in the original description. The abdomen of the spider was originally interpreted as being much longer than wide based on the dark patch of fossil material. At the posterior of the abdomen, a faint outline with setae is visible that extends beyond the dark patch. The dark patch likely represents a more heavily sclerotized part of the opisthosoma, while the whole abdomen is rounder and wider. The spinnerets and epigastric furrow were also absent from Scudder's description. The most diagnostic feature of the spider, the setal brushes, were noted by Scudder (1890: 90) as, "a brush of coarse divergent hairs," and correctly placed them on the distal portion of the tibiae of legs I, II, and IV. Other setae and macrosetae were not mentioned. Scudder (1890: 90) reported the tarsi as, "scarcely less than two-fifths of the whole leg," but only the tarsus of a fourth leg is fully visible.

Electron Microscopy Results.—Several distinct types of setae were recognized from the legs of the modern spiders such as fine setae (short and thin), spine-like macrosetae (long and stout), and trichobothria. In *T. clavipes*, clusters of long thin macrosetae are found in the setal brushes (gaiters). All of the setae and macrosetae on the legs of *T. clavipes* appear to exhibit a similar ultrastructure characterized by a pattern of lineations that whorl around the shaft or run roughly parallel to the long axis of the shaft of the setae; however, the ultrastructure varies slightly with each type of setae (Fig. 3). Spine-like macrosetae on the legs and palps have a pattern of lineations and, in some, a short thorn-like projection. The spine-like macrosetae exhibit a complex pattern of lineations and ridges with each individual lineation having a feather-like appearance, but lacking actual projections as in plumose setae. On the palps, fine setae exhibit a scaly appearance with overlapping blade-like structures. The long and thin macrosetae found in

the setal brushes also have lineations that whorl around the shaft of the hair and lack projections. The ultrastructure of trichobothria is also characterized by lineations that whorl around the shaft, but less complex than the spine-like macrosetae or the macrosetae in the setal brushes. In *Argiope*, the ultrastructure of the finer setae and large spine-like macrosetae are nearly identical to *T. clavipes*.

Macrosetal Patterns.—The pattern of femoral macrosetae differs between the fossil specimen and each of the modern specimens examined (Fig. 4). The majority of the ventral femoral macrosetae of *T. clavipes* are long and stout. The femur of Leg I posses a few short proximal spines that appear to be scattered randomly, within the two rows. Macrosetae within the rows are roughly spaced evenly apart. Legs I, II, and IV have a setal brush covering the distal 2/3 of the femur. Leg III has two rows of long stout macrosetae on the ventral femora, with only 5–6 macrosetae in each row. The macrosetae are spaced evenly apart along the femur. The setal brushes on the tibia cover the distal half of the podomere.

The ventral femoral macrosetae of *N. pilipes* are short and stout. On Leg I, two rows of macrosetae are positioned laterally, and the midline is bare of macrosetae. The spacing of the macrosetae changes along the length of the femora from close together (proximal half with approx. eight macrosetae) to spaced farther apart (distal half with approx. four macrosetae). Legs II and IV have a similar pattern of macrosetae. Leg III has two rows of short stout macrosetae on the ventral side, and are positioned laterally similar to the macrosetae on Leg I. There are fewer macrosetae on Leg III (4–5), and are only present on the proximal 2/3 of the femur. Only 1–2 macrosetae exists at the tibia-metatarsus joint of Leg IV.

DISCUSSION

Scudder (1890) noted the resemblance of the fossil to *Trichonephila plumipes*. The fossil *T. pennatipes* appears to share a mixture of general characteristics with other nephiline species (Levi & Eickstedt 1989; Harvey et al. 2007). The strong setal brushes on tibia I, II, and IV are similar to *T. clavipes* and *T. plumipes*, whereas in species like *N. sexpunctata* and *N. pilipes*, the brushes are reduced or absent. The fossil also lacks the femoral setal brushes present in *T. clavipes*. Setal brushes are present in juvenile *Nephila* and *Trichonephila*, and in adults, are sometimes lost. In *T. clavipes*, *T. plumipes*, *T. antipodiana*, *T. komaci*, *T. edulis*, the metatarsus is longer than the femur, which is also true for the fossil. The metatarsus in *N. pilipes* is shorter than the femur and, in addition, tibia IV is significantly longer than the carapace, a trait unlike most of the *Trichonephila* and the fossil (Harvey et al. 2007). *N. pilipes* also has a sternum that extends between coxae IV, while most of the *Trichonephila* and the fossil have a sternum that does not extend far between coxae IV. While some parts of the abdomen are not visible in *T. pennatipes*, there is a clear epigastric furrow. The ovate abdomen is most similar to *N. plumipes* and *T. sexpunctata*, in contrast to the narrowed or cylindrical abdomens of *T. clavipes* and *N. pilipes*; however, the abdomen only slightly overhangs the spinnerets like *T. clavipes* in contrast to *N. pilipes*, in which the abdomen overhangs the spinnerets more significantly (Harvey et al. 2007). The femoral macrosetae patterns in *N. pennatipes* are also different from the two genera examined in this study. The two rows of short stout macrosetae on the fossil appear to be closer to the midline of the femur than in the other nephilines. The equal spacing of the macrosetae within each row resembles the pattern in *T. clavipes*. This mix of characters makes *T. pennatipes* distinct from other species, but it is suggested here that the fossil least resembles *N. pilipes*.

T. pennatipes is relatively small compared to many extant adult *Nephila* and *Trichonephila*. The specimen is only slightly larger in size than another Eocene (55 Ma) fossil

Nephila from India (Patel et al. 2019). The Indian Nephila lacks enough characters to be given a species name, but was placed with reservation in *Nephila* based on the shape of the abdomen and leg characteristics. *T. pennatipes* differs from the Indian Nephila in the shape of the abdomen (oval vs piriform), the shape of the labium, and the presence of setal brushes. Another small reported nephiline, *Nephila pakistaniensis* Ghafoor & Beg, 2002, is a similar size, but differs from *T. pennatipes* by possessing spatulate setae and reduced setal brushes (Ghafoor & Beg 2002). However, Patel et al. (2019) advised a reevaluation of *N. pakistaniensis*, because the specimen figures are illustrations of a *N. clavata* (Koch, 1878) juvenile (Tikader 1982).

The fossil *T. pennatipes* also shares characteristics with other fossil genera including *Mongolarachne*, a large stem-orbicularian from the Jurassic of China, and *Jurararaneus rasnitsyni* Eskov, 1984 (Jurararaneidae) from the Jurassic of Russia (Selden 2012; Selden et al. 2013). *T. pennatipes* possesses strong brushes of long setae on the tibiae similar to *Mongolarachne*; however *T. pennatipes* lack brushes on the third leg, while *Mongolarachne* possess brushes on all legs. Additionally, both *Mongolarachne* and *Jurararaneus* are cribellate. The metatarsi of leg IV of *T. pennatipes* was examined at 40x magnitude, but no calamistrum was found. A colulus is clearly visible, instead of a cribellum, confirming the fossil spider is ecribellate. *T. pennatipes* also appears to exhibit a similar setal ultrastructure to the plumose macrosetae observed in fossils of *Mongolarachne* and *Jurararaneus*. The plumose macrosetae in these fossils are defined by an ultrastructure resembling lineations and tiny projections that whorl around the shaft of the setae. Although the lineations are observed in the macrosetae of *T. pennatipes*, tiny projections are not. The lineations on the macrosetae in *T. pennatipes* appear similar to modern *Trichonephila*, *Nephila*, and *Argiope*. Green (1970) reported two images from *Nephila* that show macrosetae with faint lineations, although they are not described in the paper (Green 1970). Here, *T. clavipes*

suggests that the lineations on the macrosetae of *N. pennatipes* is not a taphonomic artifact, and lacks tiny projections. In *T. pennatipes*, all types of setae appear smooth, with the exception of the spine-like macrosetae. For the first time, scaly setae are reported in *Trichonephila* on the palps of *T. clavipes*. These scaly setae were not visible in *T. pennatipes*, but this may be due to the magnification of the fluorescence microscope compared to electron microscopy.

The nephiline spiders are, at present, represented by several genera, with the most recent change in taxonomy separating *Trichonephila* from *Nephila*. The origin of nephilines is estimated to be during the Cretaceous (approx. 133 Ma), and this is supported by the *Geratonephila burmanica* from the Burmese amber and nephiline spiders not yet formally described from the Cretaceous (112 Ma) Crato Formation of Brazil (Dunlop & Penney 2012, Fig. 93). *Trichonephila* is estimated to have originated around 60 Ma and *Nephila* around 25 Ma (Kuntner et al. 2019). *T. pennatipes* fits well within the estimates for the origin of the genus. *Trichonephila* is dispersed worldwide throughout the subtropics and tropics but, at present, the only extant nephiline in the United States is *T. clavipes*.

Today, nephilines can be found in the southern-most parts of the United States. The presence of *Trichonephila* in the Florissant Formation indicates a relatively warmer climate in Colorado during the end of Eocene compared to now. The ancient lake in which the Florissant Formation was deposited is interpreted as a quiet freshwater lake created by volcanic damming of the drainage basin (Meyer 2003). The flora in the environments surrounding the Florissant paleolake would have offered plenty of suitable habitats for *T. pennatipes* to spin large webs several meters from the ground (Moore 1977; Meyer 2003). A diverse assemblage of insects has been found from Florissant including beetles, flies, and flying ants, all of which would have been potential prey for *T. pennatipes*.

CONCLUSION

Early authors examined several suites of fossil spiders from lacustrine deposits, and many fossils were left with incomplete descriptions or incorrect interpretations. Fossil spiders preserved in lacustrine deposits can be challenging to describe due to the lack of visible general and diagnostic characteristics. This problem can make taxonomic placement difficult, even at the family level. The diagnostic characters commonly used in nephiline taxonomy are not visible in the fossil such as reproductive organs and colors. Other traits such as macrosetal patterns and spinneret position were used to compare *T. pennatipes* to modern species, and suggest that the fossil belongs in *Trichonephila*.

The descriptions and interpretations of the fossil spider *T. pennatipes* by Scudder (1890) and Petrunkevitch (1922) have been revised using more powerful analytical techniques. For the first time, fluorescence microscopy has been used to examine minute details including the setal ultrastructure of fossil spiders. Although not as powerful as electron microscopy, for delicate fossils like those from the Florissant Formation, this technique is completely nondestructive and simulates wetting by alcohol. Although the general structure of nephiline macrosetae has been observed previously, scanning electron microscopy has revealed a complex and detailed ultrastructure of macrosetae and, for the first time, scaly macrosetae on the legs and palps of *Trichonephila* is reported.

ACKNOWLEDGEMENTS

We thank Laura Leibensperger (Museum of Comparative Zoology, Harvard University) for the loan of the holotype of *Trichonephila pennatipes*; We thank Dr. Deborah Smith (University of Kansas) for providing the specimens of *T. clavipes*, *N. pilipes*, and *A. aurantia*, and for her

support with the electron microscopy investigation; the Microscopy and Analytical Imaging Laboratory at the University of Kansas including Dr. Eduardo Rosa-Molinar, Dr. Noraida Martínez-Rivera, and Judith Fuhrman Harris for exceptional sample preparation, imaging, and interest in the project; and Dr. Alison Olcott (University of Kansas) for help with fluorescence microscopy.

LITERATURE CITED

Bartoleti, L.F. de M., E.A. Peres, T. Sobral-Souza, F. von H.M. Fontes, M.J. da Silva, & V.N. Solferini. 2017. Phylogeography of the dry vegetation endemic species *Nephila sexpunctata* (Araneae: Araneidae) suggests recent expansion of the Neotropical Dry Diagonal: Journal of Biogeography 44:2007–2020.

Coddington, J.A. 1990. Ontogeny and homology in the male palpus of orb weaving spiders and their relatives, with comments on phylogeny (Araneoclada: Araneoidea, Deinopoidea). Smithsonian Contributions to Zoology 496.

Dimitrov, D., L.R. Benavides, M.A. Arnedo, G. Giribet, C.E. Griswold, N. Scharff et al. 2017. Rounding up the usual suspects: a standard target-gene approach for resolving the interfamilial phylogenetic relationships of ecribellate orb-weaving spiders with a new family-rank classification (Araneae, Araneoidea). Cladistics 33:221–250.

Dunlop, J.A. & D. Penney. 2012. Fossil arachnids. Siri Scientific Press.

Dunlop, J.A., D. Penney & D. Jekel. 2018. A summary list of fossil spiders and their relatives. *In* World Spider Catalog. Natural History Museum Bern, online at http://wsc.nmbe.ch, version 19.0.

Evanoff, E., W.C. McIntosh & P. Murphey. 2001. Stratigraphic summary and 40Ar/39Ar geochronology of the Florissant Formation, Colorado Pp. 1–16. *In* Fossil flora and stratigraphy of the Florissant Formation, Colorado. (K.R. Johnson, E. Evanoff & K.M. Gregory-Wodzicki, eds.). Denver Museum of Nature and Science, Denver, CO.

Fabricius, J.C. 1793. Entomologiae systematica emendata et aucta, secundum classes, ordines, genera, species adjectis synonimis, locis, observationibus, descriptionibus. Hafniae 2:407–428.

Ghafoor, A. & M.A. Beg. 2002. Description of two new species of araneid spiders from Pakistan. International Journal of Agriculture and Biology 4:525–527.

Green L.A. 1970. Setal structure and spider phylogeny. Eastern Michigan University, Dissertation

Harvey, M.S., A.D. Austin & M. Adams. 2007. The systematics and biology of the spider genus *Nephila* (Araneae: Nephilidae) in the Australasian region. Invertebrate Systematics 21:407–451.

Henning, J., D.M. Smith, C.R. Nufio, & H.W. Meyer. 2012. Depositional setting and fossil insect preservation: A study of the Late Eocene Florissant Formation, Colorado. Palaios 27:481–488.

Roberts, A. K., D.M. Smith, R.P. Guralnick, P.E. Cushing & J. Krieger. 2008. An outline morphometric approach to identifying fossil spiders: A preliminary examination from the Florissant Formation. Special Papers-Geological Society of America 435:105–116.

Kuntner, M. 2006. Phylogenetic systematics of the Gondwanan nephilid spider lineage Clitaetrinae (Araneae, Nephilidae). Zoologica Scripta 35:19–62.

Kuntner, M., J.A. Coddington, & G. Hormiga. 2008. Phylogeny of extant nephilid orb-weaving spiders (Araneae, Nephilidae): testing morphological and ethological homologies. Cladistics 24:147–217.

Kuntner, M., & I. Agnarsson. 2011. Phylogeography of a successful aerial disperser: the golden orb spider *Nephila* on Indian Ocean islands. BMC Evolutionary Biology 11:119.

Kuntner, M., C.A. Hamilton, R.-C. Cheng, M. Gregorič, N. Lupše, T. Lokovšek et al. 2019. Golden Orbweavers Ignore Biological Rules: Phylogenomic and Comparative Analyses Unravel a Complex Evolution of Sexual Size Dimorphism: Systematic Biology 68:555–572.

Leach, W.E. 1815. Zoological Miscellany; being Descriptions of New and Interesting Animals. London, 2:1–154.

Levi, H.W. & V.R.D. von Eickstedt. 1989. The Nephilinae spiders of the neotropics. Memórias do Instituto Butantan 51:43–56.

Meyer, H.W. 2003. The fossils of Florissant. Smithsonian Books.

Moore, C.W. 1977. The life cycle, habitat and variation in selected web parameters in the spider, *Nephila clavipes* Koch (Araneidae). American Midland Naturalist 98:95–108.

Pan, H.-C., K.-Y. Zhou, D.-X. Song, Y. & Qiu. 2004. Phylogenetic placement of the spider genus *Nephila* (Araneae: Araneoidea) inferred from rRNA and MaSp1 gene sequences: Zoological Science 21:343–351.

Patel, R., R.S. Rana, & P.A. Selden. 2019. An orb-weaver spider (Araneae, Araneidae) from the early Eocene of India: Journal of Paleontology 93:98–104.

Petrunkevitch, A. 1922. Tertiary spiders and opilionids of North America. Transactions of the Connecticut Academy of Arts and Sciences 25:211–279.

Penney, D. & P.A. Selden. 2011. Fossil spiders: the evolutionary history of a mega-diverse order. Siri Scientific Press 1.

Poinar Jr., G.O. & R. Buckley. 2012. Predatory behaviour of the social orb-weaver spider, *Geratonephila burmanica* n. gen., n. sp. (Araneae: Nephilidae) with its wasp prey, *Cascoscelio incassus* n. gen., n. sp. (Hymenoptera: Platygastridae) in Early Cretaceous Burmese amber. Historical Biology 24:519–525.

Robinson, M.H. & H. Mirick. 1971. The predatory behavior of the golden-web spider *Nephila clavipes* (Araneae: Araneidae): Psyche; a Journal of Entomology 78:123–139.

Robinson, M.H. & B. Robinson. 1973. Ecology and behavior of the giant wood spider *Nephila maculata* (Fabricius) in New Guinea. Smithsonian Contributions to Zoology 149.

Scudder, S.H. 1890. The Tertiary insects of North America. United States Government Printing Office 13.

Selden P.A. 2012. A redescription of *Jurararaneus rasnitsyni* Eskov 1984 (Araneae: Jurararaneidae), from the Jurassic of Russia. Bulletin British Arachnological Society 15:315–321.

Selden, P.A., C. Shih, & D. Ren. 2013. A giant spider from the Jurassic of China reveals greater diversity of the orbicularian stem group. Die Naturwissenschaften 100:1171–1181.

Tikader, B.K. 1982. The Fauna of India; Spiders: Araneae Volume II. Part 1 Family Araneidae (= Argiopidae) typical orb-weavers; Part 2 Family Gnaphosidae: Calcutta, Zoological Survey of India, xiv + 536 p.

World Spider Catalog. 2020. World Spider Catalog. Version 20.0. Natural History Museum Bern, online at http://wsc.nmbe.ch

Wunderlich, J. 1982. Die häufigsten Spinnen (Araneae) des Dominikanischen Bernsteins. Neue Entomologische Nachrichten 1:26–45.

Wunderlich, J. 1986. Spinnenfauna Gestern und Heute. Fossile Spinnen in Bernstein und ihre heute lebenden Verwandten. Erich Bauer Verlag bei Quelle und Meyer, Wiesbaden.

Yong-Chao, S., C. Yung-Hau, D. Smith, Z. Ming-Zhu, M. Kuntner & I.M. Tso. 2011. Biogeography and speciation patterns of the golden orb spider genus *Nephila* (Araneae: Nephilidae) in Asia. Zoological Science 28:47–55.

EXPLANATION OF TABLES AND FIGURES

Figure 1.—Fossil *Nephila pennatipes* (submerged in ethanol) and interpretative drawing.

Figure 2.—*Nephila pennatipes* characteristics (WBV). A. Setal brush (gaiter) of Leg1 tibia. Scale bar 0.2 mm; B. Tarsus of pedipalp with palpal claw at 20x magnification. Scale bar = 0.02 mm.

Figure 3.—Femoral macrosetal patterns of *Nephila pennatipes* with macrosetae marked by arrows. A = plain light, B–D = WBV. A. Leg 1; B. Leg 2; C. Leg 3 with single row of macrosetae; D leg 4. Scale bars = 0.2 mm.

Figure 4.—Abdomen and spinnerets of *Nephila pennatipes*. A. Arrows indicate true edges of abdomen and are marked by fine setae. Fine setae also outline the ALS, PLS, and colulus (WBV); B. Close up of terminal abdomen and spinnerets (WUV). Scale bars = 0.2 mm.

Figure 5.— Setal ultrastructure in fossil and modern Araneidae. A. *Trichonephila pennatipes* (WBV); B. *T. clavipes* spine-like macrosetae; C. *T. clavipes* scaly setae on palp; D. Close up of *T. clavipes* macrosetae ultrastructure.

Figure 6.—Femoral macrosetal patterns in fossil and modern *Nephila*. A. *Trichonephila clavipes*; B. *Nephila pilipes*; C. *Nephila pennatipes*.


5mm

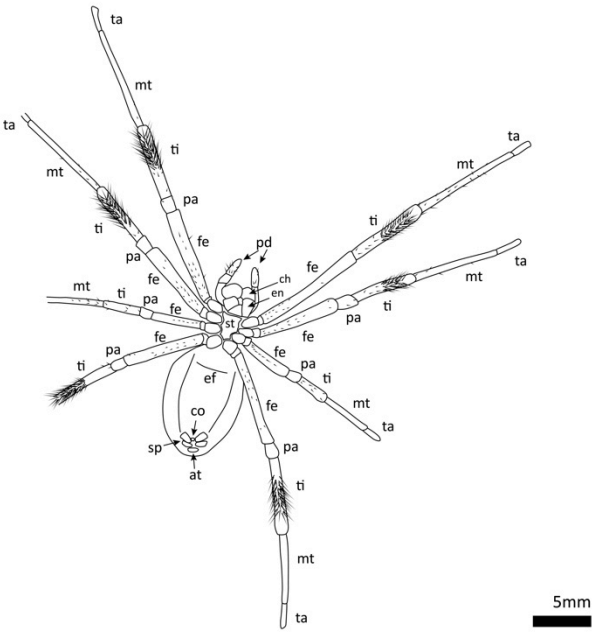
ta
mt
ti
pa
fe
pd
ch
en
st
ef
co
sp
at
5mm

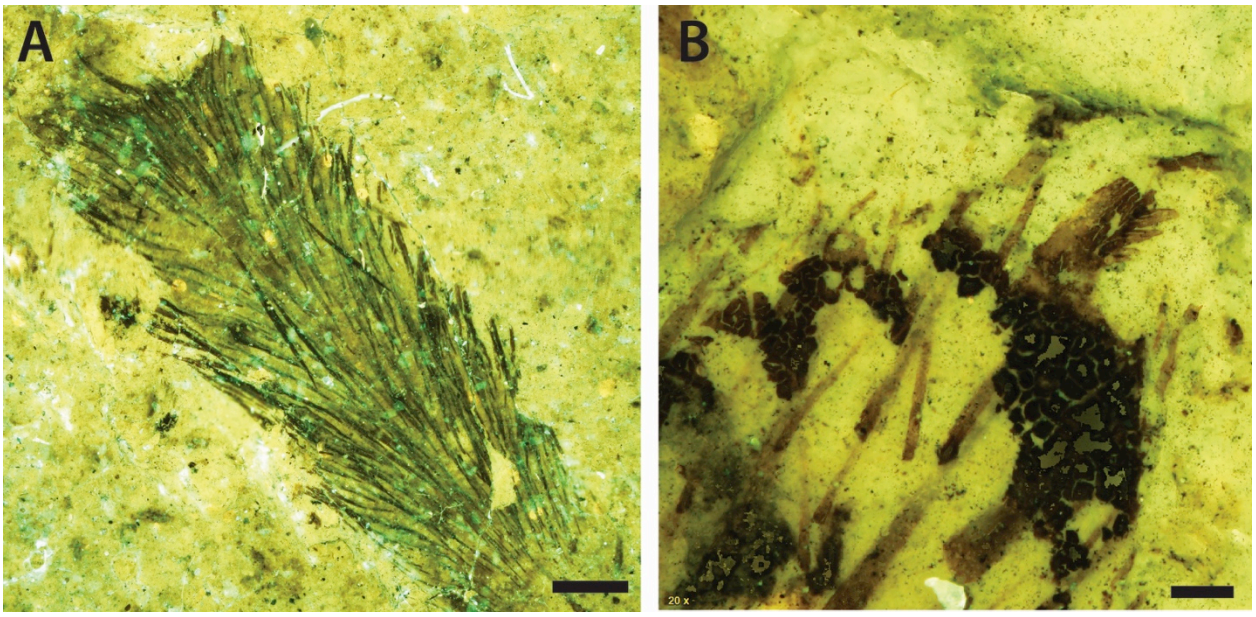
A
B
20 x

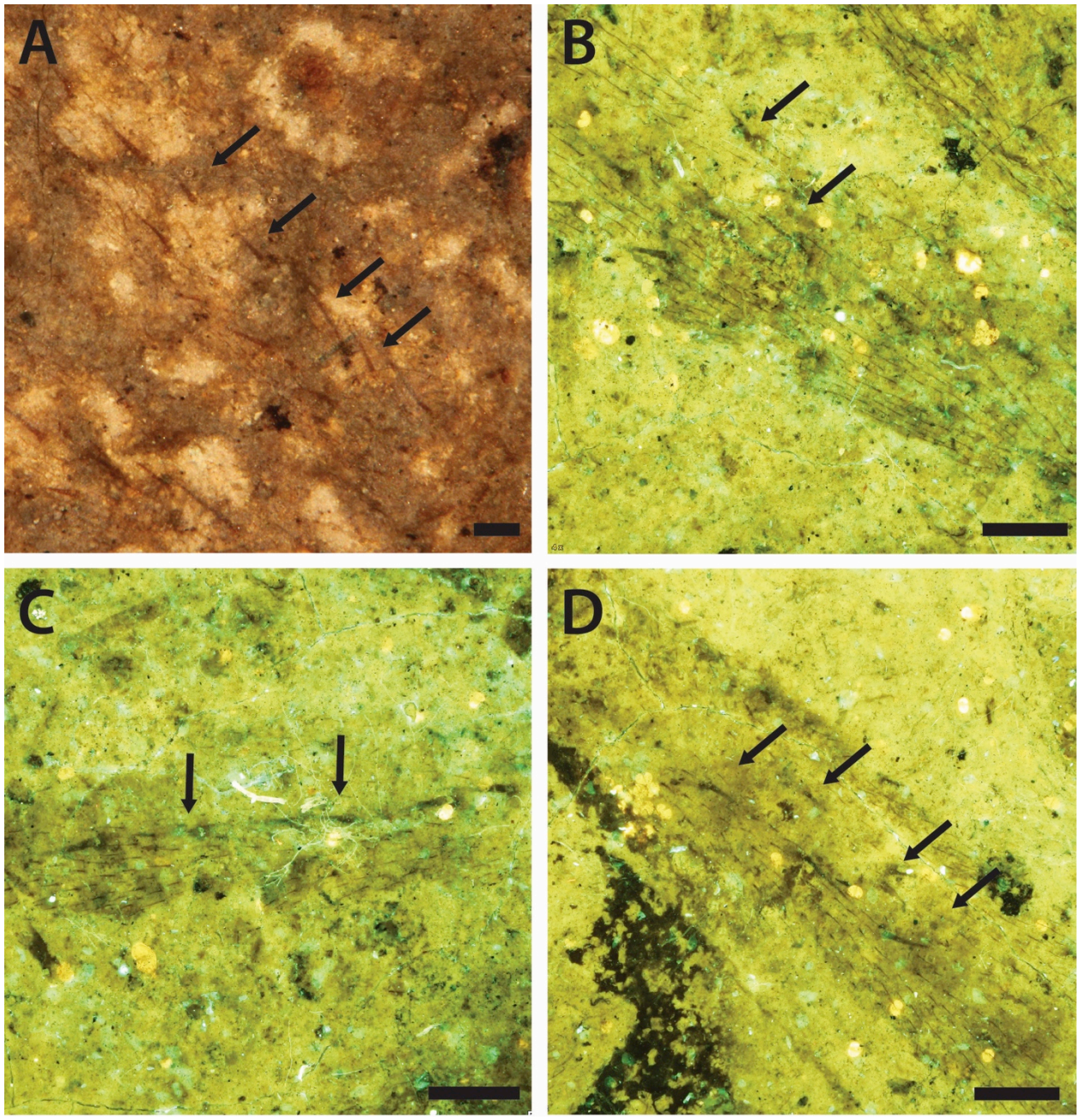
A
B
C
D

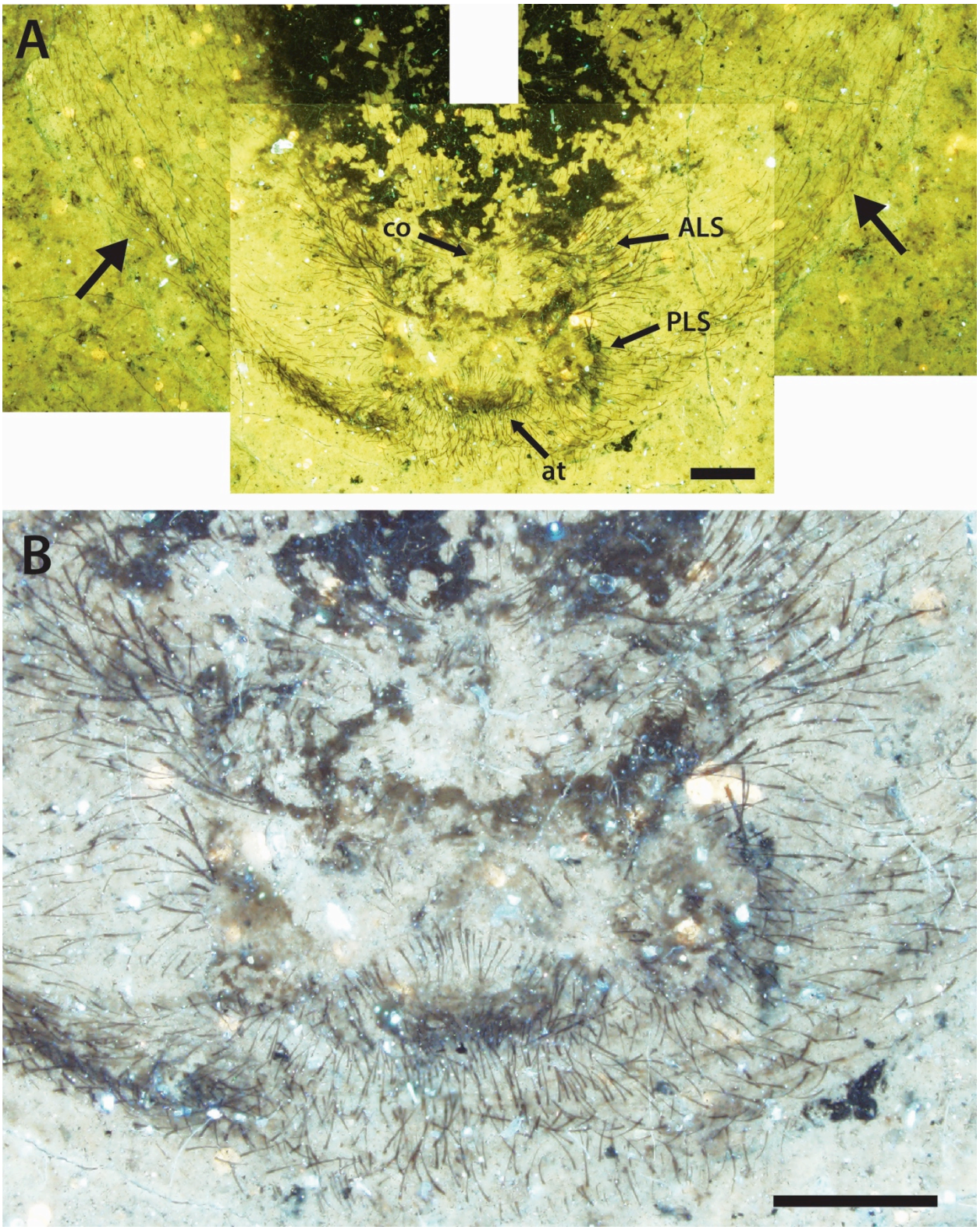
A
co
ALS
PLS
at
B

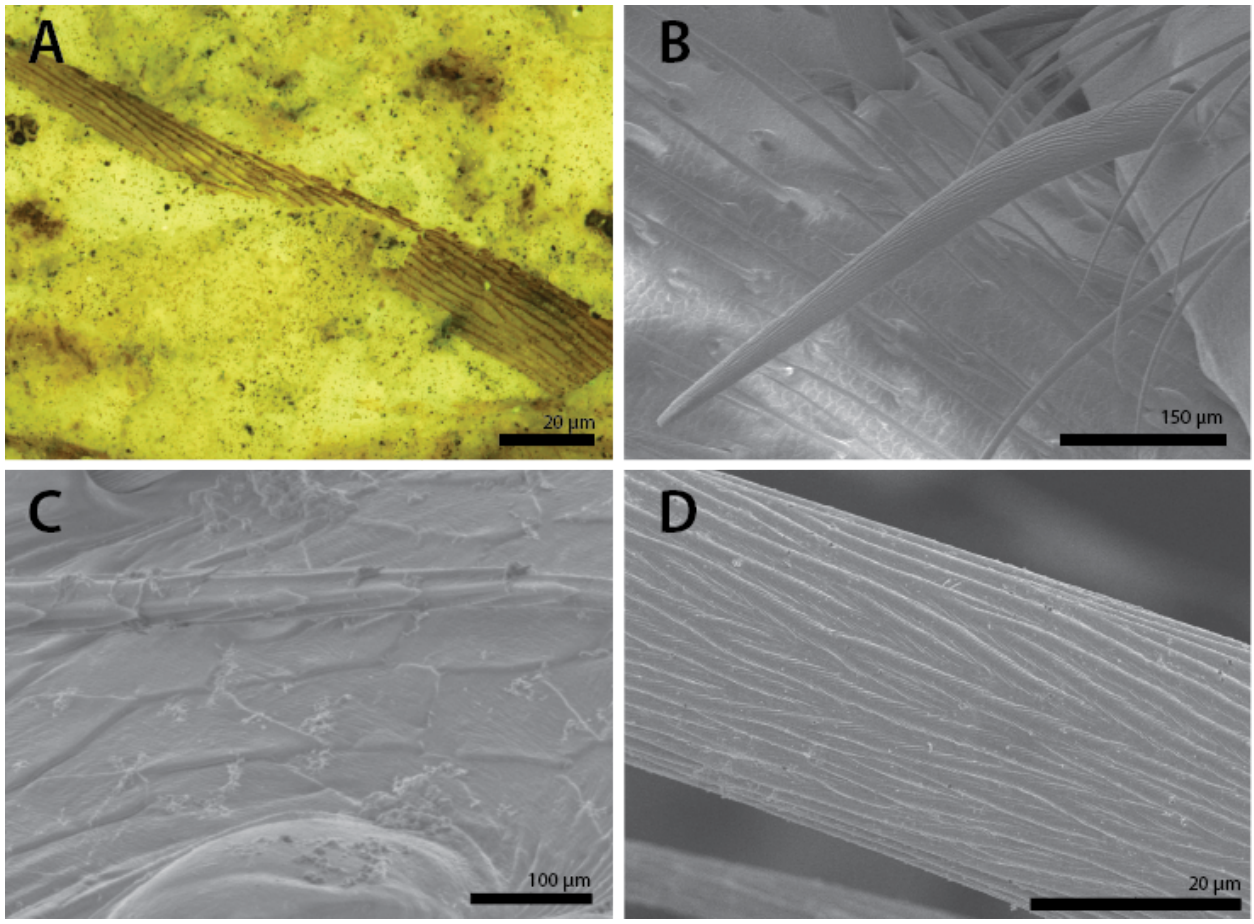
A
20 µm
B
150 µm
C
100 µm
D
20 µm

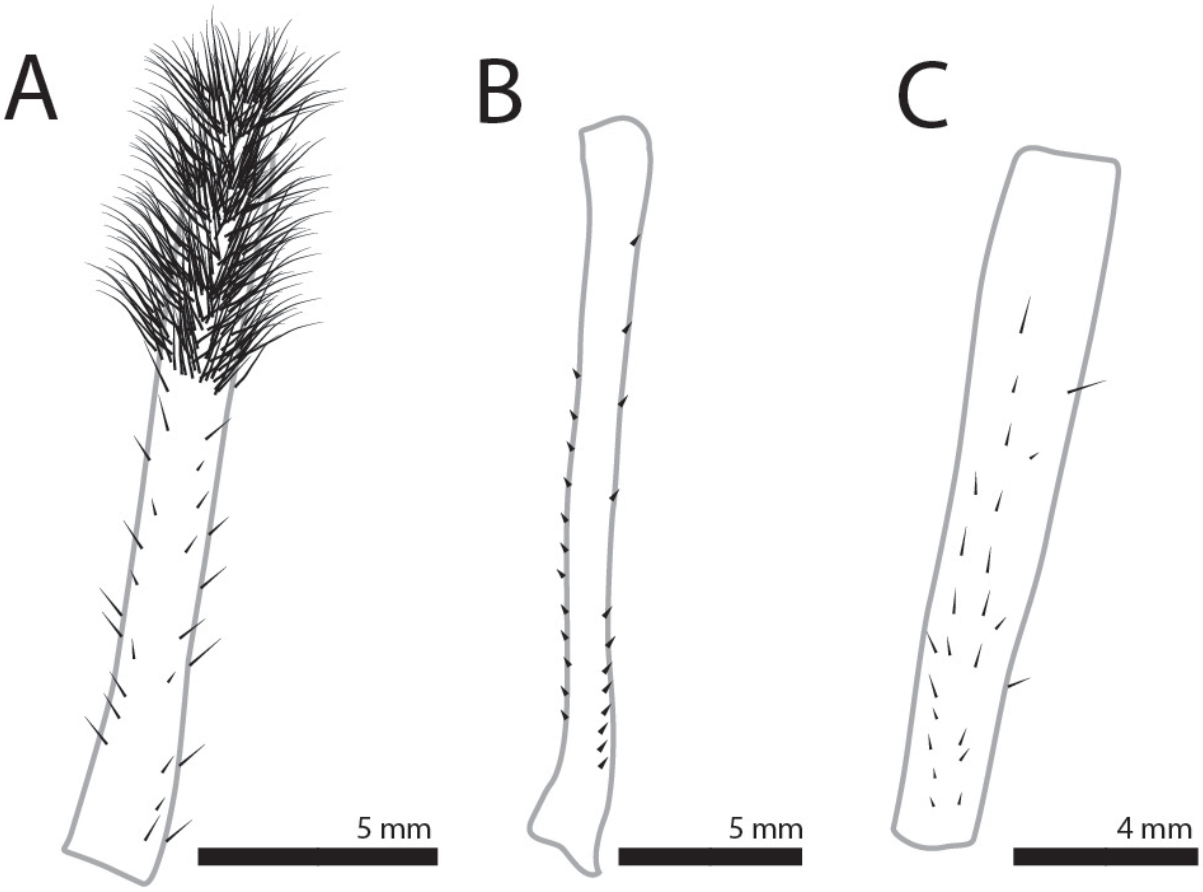
A
5 mm
B
5 mm
C
4 mm

Chapter 5

A unique model of microbially driven fossil preservation in the Oligocene Aix-en-Provence Fossil-Lagerstätte, France

(Formatted for submission to *Geology*)

Matthew R. Downen, Paul A. Selden, and Alison N. Olcott

Department of Geology, University of Kansas, Lawrence, Kansas 66045, USA

Paleontological Institute, 1475 Jayhawk Blvd, Lawrence, KS 66045

ABSTRACT

The Aix-en-Provence Formation is an Oligocene (23 Ma) Fossil-Lagerstätte in southern France that contains an abundance of soft-bodied fossils preserved in exceptional detail. Many taxa have been described from this formation, including insects, spiders, plants, and fish, suggesting a diverse ecosystem in a subtropical, brackish, lacustrine paleoenvironment. While hundreds of fossils have been recovered from this unit, there has been no research explicitly investigating the taphonomic pathway(s) responsible for this assemblage. The presence of microbial mats in the Aix-en-Provence Formation has been suggested in passing, but not explicitly linked to fossil preservation or examined at the microscopic scale. Three main modes of preservation in fossil spiders from these rocks include: (1) carbonized compressions, (2) high relief internal molds and impressions, and (3) flattened casts with organic material. The preservation of fossil spiders and their matrix were investigated using a multitechnique approach

including fluorescence microscopy and scanning electron microscopy. Fluorescence microscopy of fossil spiders revealed the emission of fluorescent light in the red, orange, and blue spectra indicating the presence of aromatic carbon, a product of the alteration of arthropod cuticle. An abundance of evidence for microbial mats is observed in the samples. Three main matrix fabrics are observed: wavy, granular, and finely laminated. Wavy laminae contain tubular and filamentous structures similar to bacterial sheaths and extracellular polymeric substances (EPS). Granular laminae are composed entirely of calcium carbonate mineral grains. Finely laminated specimens contain alternating layers of silica and calcium carbonate with abundant organic masses with a biofilm-like texture. The evidence provided here supports prolific microbial mat communities during deposition of the Aix-en-Provence Formation, and suggests that they likely facilitated the process of fossilization. The taphonomic pathway for the Aix-en-Provence spiders includes a microbial death mask, in which microbes precipitate minerals around the site of a dead organism, resulting in the abundant molds and preservation of altered cuticle.

INTRODUCTION

The Fossil-Lagerstätte of Aix-en-Provence, France is an Oligocene deposit with an abundance of fossil fish, plants, and terrestrial arthropods (Hope, 2009). Study of this fossil biota began in the late 1700s and continues to this day (Nury, 1987; Gaudant et al., 2018). Most of the research is focused on the taxonomy of the fossils, which is important for understanding diversity and paleoenvironments, but little research has focused on the taphonomic processes and pathways responsible for the exceptional preservation of soft-bodied fossils like insects and spiders. Two modes of preservation have been reported previously from this formation: carbonized compression fossils and calcite replacements (Gaudant et al., 2018). Compression fossils and carbonized remains are a common mode of preservation for arthropods in lacustrine deposits,

although it seems to be less common in the Aix-en-Provence Formation (Martínez-Delclòs et al., 2004; Smith, 2012). The most common mode of preservation has been described as organic material being completely replaced with calcite, a conclusion based on visual observation rather than chemical analyses (Gaudant et al., 2018). Some researchers have mentioned the presence of microbial laminations in the Aix-en-Provence Formation, but no other evidence has been published (Peinado, 2002; Gaudant et al., 2018). Here, we investigate the possible taphonomic pathway of the Aix-en-Provence Fossil-Lagerstätte by examining fossil spiders and the relationships between chemistry, fossil preservation, and microbial indicators to test a death-mask model of fossilization.

The death-mask model of preservation was first applied to the Neoproterozoic Ediacaran Biota (635–541 Ma) and describes the preservation of soft tissues by a microbial death mask that develops around carcasses and preserves their three-dimensional form. Ediacaran fossils are preserved in siliciclastic sediments (sandstone) as external molds and casts, with rare instances of internal molds (Narbonne, 2004). In this model, microbial mats containing sulfur-reducing bacteria precipitate iron sulfides that form a mineralized crust around the remains of organisms; as the soft tissues decay, they subsequently are filled in with sediment, leading to the three-dimensional preservation similar to that observed in the Aix-en-Provence Formation (Gehling, 1999; Kenchington and Wilby, 2014; Liu, 2016). A similar model, carbonate casting, a process by which carbonate minerals precipitated by microbes cement the surrounding sediment and create a thin layer of mineralized crust, has been suggested as a possible mechanism in Ediacaran preservation (Serezhnikova, 2011). Taphonomic pathways similar to the death-mask model may be more pervasive in younger deposits like the Aix-en-Provence Formation than previously thought.

Microbial mats and fossil preservation

Microbial mats are complex associations of biofilms, composed of communities of various species of microbes, and often associated with a matrix of extracellular polymeric substances (EPS), that are hypothesized to play a significant role in soft-bodied preservation (Stolz, 2000). Microbial mats may aid in the process of fossilization in several ways: stabilizing sediment and carcasses, directly precipitating minerals on the surface of remains or replacing organic remains, inducing precipitation of minerals by altering the surrounding chemistry of the environment, and/or reducing scavenging and decay (Wilby et al., 1996; Martínez-Delclòs et al., 2004; Iniesto et al., 2016). Actualistic experiments have demonstrated that microbial mats help preserve soft tissues and can fossilize material rapidly, supporting their involvement of exceptional preservation in ancient environments (Briggs and Kear, 1993; Sagemann et al., 1999; Darroch et al., 2012; Iniesto et al., 2016).

The preservation of soft tissues has been linked to microbial mats and microbial processes in several examples of lacustrine deposits and Fossil-Lagerstatten (Gall, 1990; Wilby et al., 1996). Evidence of exceptional preservation via microbial mats has been reported from the Cretaceous Crato Formation of Brazil, which includes finely laminated strata rich in terrestrial arthropods and vertebrates (Martill et al., 2007). The laminations are attributed to microbial mats and supported by microbially induced precipitates and lithified bacterial cells (Warren et al., 2016). In the Green River Formation of Colorado (Eocene), stromatolites are abundant and microbial mats are thought to aid in fossil preservation by binding and/or enveloping carcasses (Schieber, 2007; Miller et al., 2011; Hellawell and Orr, 2012). Fossil insects are found within microbial mat derived laminae of the Kishenehn Formation (Eocene) of Montana including a blood-engorged mosquito with biomolecules derived from hemoglobin (Greenwalt et al., 2013,

2014). The model of the taphonomic pathway of fossils in the Florissant Formation of Colorado (Eocene) includes mucilaginous diatom mats that coated the remains of arthropods and helped them sink, protecting them from scavengers (Harding and Chant, 2000; O'Brien et al., 2002, 2008; Henning et al., 2012). Microbes play many possible roles in the pathway to fossil preservation especially with regard to soft-bodied organisms like insects and other arthropods, and this type of taphonomic pathway occurs throughout geologic time (Wilby et al., 1996; Briggs, 2003).

Fossil spiders

Spiders are considered soft-bodied fauna as they lack mineralized hard parts, and thus, are rare in the fossil record. Non-amber fossil spiders typically are found in rocks of lacustrine origin that were deposited under special conditions like anoxia, rapid burial, and calm waters. Under such conditions, spiders often are preserved as 2D carbonized compression fossils and fully articulated (Penney and Selden, 2011). Usually only external features of a spider are visible due to the structure of the cuticle, or exoskeleton. The cuticle is composed of chitin cross-linked with proteins and is more decay-resistant than other biomolecules like DNA (Briggs, 1999). The chitin in cuticle can persist in younger sediments up to 25 million year old, but degrades over time and is altered to various organic compounds dominated by hydrocarbons (Artur Stankiewicz et al., 1997).

Although fossil spiders are relatively rare, hundreds of specimens have been recovered from the Aix-en-Provence Fossil-Lagerstätte. The spider fauna described by Gourret (1887) includes 16 species of unreliable taxonomic affinity (Gourret, 1887). Many of the fossil spiders preserved in this deposit are lycosids and tetragnathids. Lycosids are commonly known as wolf spiders, and have a carapace, the dorsal side of the cephalothorax, with a raised cephalic area and

large chelicerae, mouthparts that contain the fang (Jocqué and Dippenaar-Schoeman, 2007). Tetragnathids are known as long-jawed orbweavers, and can be recognized by large porrect chelicerae and long slender legs with a distinctly short third pair of legs (Jocqué and Dippenaar-Schoeman, 2007). These features, the carapace and the chelicerae, are more sclerotized (hardened) than other parts of the body making them more resistant to decay, and as a result may influence the mode of preservation of fossil spiders in the Aix-en-Provence (Foelix, 2011).

GEOLOGY, PALEOENVIRONMENT, and PALEOECOLOGY

The Aix-en-Provence Formation is dated to 22.5 Ma, and represented by a 150 m succession of informally named subunits (Nury, 1987; Gaudant et al., 2018). The abundant fossil insects come from the Insect Bed, which, in turn, is part of the Calcaires et marnes à gypse d'Aix; i.e., limestones and gypsum marls. Underlying the Insect Bed are several distinct layers of gypsum and marlstone (Murchison and Lyell, 1829). The Insect Bed is roughly 80 cm in thickness and represented by thinly laminated light grey and light green calcareous marlstone. There are no reported trace fossils or bioturbation, and as a result, the extremely thin laminations are preserved continuous. Overlying the Insect Bed is another fossiliferous layer of light brown marlstones known as La Feuille à Poissons; i.e., the fish layer, that is rich in fossil fishes (Saporta, 1889).

This interpreted paleoenvironment of the Aix-en-Provence Formation is a brackish lacustrine/lagoonal setting with varying salinity with a diverse paleoecosystem (Gaudant et al., 2018). Various types of fish suggest brackish conditions in a lagoonal setting, but episodes of freshwater lacustrine settings are supported by the presence of frogs and turtles in the Insect Bed (Piveteau, 1927; Gaudant, 1978; Fontes et al., 1980). Fluctuating salinity is also supported by mass mortality events. Fossil fish and dragonfly nymphs occur in great numbers and are likely

mass mortality events that may have been the result of changes in salinity (Nury, 1987; Gaudant et al., 2018). The plant and insect assemblages indicate a warm subtropical paleoclimate (Gregor and Knobloch, 2001; Collomb et al., 2008). The flora includes freshwater plants, banana trees, pine trees, and palm leaf trees, many of which resemble modern day species from Africa. Beetles (Coleoptera), flies (Diptera), and wasps (Hymenoptera) are the most abundant insects, but spiders are also relatively abundant and include wolf spiders, crab spiders (Thomisidae), and long-jawed orbweavers (Gourret, 1887).

MATERIALS AND METHODS

Materials

This study uses fossil spiders from the Oligocene Aix-en-Provence, France, Fossil-Lagerstätte. Specimens were loaned to PAS and are deposited in the National Museum of Natural History, Paris, France. The specimens had been glued to small pieces of notecard before this study began because the fossils are extremely thin and delicate. List of specimens: Aix_flat1, Aix_17a,b, Aix_24, Aix_25, Aix_Big1, Aix_NoName2, Aix_PS4, Aix_PNN5, Aix343_soldari.

Methods

Fossils were photographed with a Canon EOS 5D Mark II digital camera attached to a copy stand and the same camera attached to a Leica M650C microscope and viewed in low angle light to enhance details not easily seen. Pieces of matrix material from five fossil specimens were embedded in epoxy to make thin sections: Aix_flat1, Aix_Big1, Aix_25, Aix_32, Aix_PNN5. Thin sections were prepared in the Rock Crushing Laboratory at the University of Kansas (KU). Fluorescence imaging was done with an Olympus BX51 Petrographic Scope with a mercury vapor-arc-discharge lamp, and two exciter filters designed to transmit in the UV (330–385 nm

wavelength) and violet-blue (400–440 nm wavelength) region. Whole fossil specimens were imaged using both wavelengths of light. Stacked and stitched images were created using Stream Essentials software. Scanning electron microscopy (SEM) and energy-dispersive x-ray spectroscopy (EDS) analyses were conducted at the KU Microscopy and Analytical Imaging Laboratory. Each fossil specimen and slide were sputter-coated with iridium and mounted on individual aluminum stubs with copper tape for image acquisition. Images and analyses were acquired on a Cold Field Emission Scanning Electron Microscope, Hitachi High Technologies, SU8230 series, with a YAB backscattered electron (BSE) detector, at accelerating voltages ranging from 1.0 to 2.0 kV. EDS used a Silicon Drift Detector (SDD) to create elemental maps.

RESULTS

Modes of preservation

Three primary modes of preservation are recognized in the Aix-en-Provence Formation fossils examined here: (1) abundant internal and external molds, (2) moderately abundant flattened casts, and (3) rare carbonized compression fossils (Fig. 1). The majority of the fossils are in part and counterpart, a result of the splitting of the fossil into two mirrored halves along the separation of laminations of the matrix. The most abundant mode of preservation is internal and external molds. The external molds are concave impressions in the matrix that show the appearance of the external features like setae. Some internal molds are preserved in high relief and represent a Steinkern-like preservation. The areas of highest relief in the fossils are in the cephalothorax of the spiders (Fig. 1A). Both low and high relief molds appear to possess a mineralized crust that is distinct from the matrix. The second most common mode of preservation is low relief fossils like Aix_flat1 (Fig. 1B). These fossils are relatively flat, and appear as low-relief plateaus on the matrix that roughly outline the body of the spiders, and give

the appearance of a halo. The body of the spider usually possesses dark brown coloration. Apart from the dark brown coloration, the fossils are nearly the same color as the matrix, but appear to have a slightly different texture. To the unaided eye, these fossils appear as typical carbonized compression fossils due to the coloration, but differ in that they lack a distinct carbonized film. In the material examined, only one compression true fossil exists, in part only, with a dark brown carbonized film that preserves the anatomy of the spider in high detail (Figs. 1C, 2).

The matrix of fossils is composed of paper-thin sheet-like laminations, with a variety of textures found on the bedding surfaces as well as within the laminae of the matrix. The bedding surface of most specimens with fossils preserved as molds exhibit a texture that is wrinkled, pustular, or covered in small fragments and chips (Fig. 3). Individual laminations of these wrinkled and pustular samples are approximately 0.1–0.5mm thick. Less common are specimens with a matrix that is smooth and flat composed of even thinner laminations (10–50μm) visible in cross section. Fossils in finely laminated matrix are preserved as flattened casts.

Fluorescence microscopy

Some fossil spiders exhibit autofluorescence (about 30%), typically in the orange and blue range, but specimens exhibit different intensities and patterns of fluorescence. Molds often weakly fluoresce pale orange uniformly throughout the body of the spiders, although some fluoresce blue in UV light (Fig. 4). The mineralized crust of some molds has a variable fluorescence pattern, and different regions of the spider body may fluoresce different colors. In these specimens, the cephalothorax is blue and the abdomen is bright orange. Other fossils appear to have internal structures that fluoresce more strongly than the outline of the body or are a different color. Internal structures are usually restricted to the legs and cephalothorax of the spider. The entire body of the spider in these specimens fluoresces pale orange, but internal

structures in the legs and cephalothorax fluoresce bright blue, while internal structures in the abdomen fluoresce bright orange (Fig. 5). Flattened casts typically have the most intense fluorescence response (Fig. 6). In some specimens, the dark material fluoresces bright orange and usually is confined to the abdomen and cephalothorax of the spiders. The dark material of Aix_25 fluoresces pale orange creating a clear outline of the true body, but is surrounded by a halo that fluoresces light blue in color (Fig. 6E–F). The dark brown material in Specimen Aix_17 fluoresces bright orange in both UV and BV light. In the counterpart (Fig. 6C), most of the cephalothorax and legs lack dark brown material and fluoresce a dark blue color, different from the surrounding matrix. Both Aix_17 and Aix_25 also have internal portions of the legs that are fluorescent.

Three distinct types of internal architecture are visible in thin sections of the matrix of the fossils with fluorescence microscopy: clotted and filamentous, granular, and fine laminae (Fig. 7). Both clotted and granular laminations vibrantly fluoresce bright blue in UV light and bright green in BV. The clotted fabric appears as overlapping tubular slivers interspersed with rounded globular masses (Fig. 7A). A vertical crack approximately 2 mm long is visible in Aix_32 and tapers downward. The fabric bends with this crack (Fig. 7B). The uppermost layer of Aix-32 bends upward, and the internal parts of the matrix bend downward. Granular specimens contain abundant clusters of granules (5–10μm) throughout the laminae that fluoresce pale orange in both UV and BV (Fig. 7C). Granular samples exhibited such intense fluorescence that the exposure has to be reduced to obtain an image.

The finely laminated samples differ in their fluorescence response and composition (Fig. 7D). The laminae are horizontal and slightly wrinkled and wavy. In UV light, the laminations of Aix_flat1 fluoresce varying shades of blue and purple, and in BV light shades of orange and

green (Fig. 7D–G). In Aix_25, the laminations fluoresce shades of blue in UV light and shades of green in BV. In both UV and BV light, there are very thin bright orange horizons and particles in Aix_25 (Fig. 7G). Both samples also possess organic inclusions that range in size from 10–100μm that do not exhibit a fluorescence response (Fig. 7F). Larger inclusions are typically flattened and run parallel with the laminae, although the laminae appear to bend around these inclusions.

Electron Microscopy

SEM/EDS analysis reveals differing composition with respect to mode of preservation and matrix fabric. Aix_24 is preserved as a mold that appears to be a uniform composition throughout the body of the fossil (Fig. 8A–B). The most abundant elements present are O (51.8 wt%), Ca (25.9 wt%), and C (17.4 wt%) and Si (2.7 wt%). The fossil is composed of O, Ca, and C, while Si is mostly absent in the body of the fossil, and instead is abundant in the matrix. Other elements like Al, Mg, Fe, and K are less abundant (<1 wt%), but dispersed evenly through the sample. Phosphorus (0.2 wt%) was present in the cephalothorax, but not in the legs. Centric diatom valves and fragments of girdles are also present in the sample, which are composed of silica (Fig. 8C). These diatoms possess relatively few punctae in the center and smaller more abundant punctae near the distal margins of the valves. Two kinds of microtextures are observed in the body of the fossil: crystals (100μm) with a platy habit, and small (20μm) spherical masses (Fig. 8D–F). The small spherical masses are extremely abundant and appear to be composed of filamentous bacteria.

SEM/EDS analysis of Aix_flat1, a flattened cast in a finely laminated matrix, revealed a texture and composition representing the altered remains of spider cuticle (Fig. 9). The abdomen appears as a flaky and cracked material in back-scattered electron imaging and is darker,

indicating lighter elements. Elemental mapping (EDS) reveals that the dark brown material of the abdomen is almost devoid of Si and O, and is greatly enriched in C (43 wt%) and S (5.3 wt%). In contrast, the matrix immediately surrounding the fossil contains a high Si (15.7 wt%) and O (31.7 wt%) content, and low C and S. The Ca signal is weak and uniformly dispersed through the fossil and matrix.

The finely laminated matrix of Aix_flat1 in thin section has abundant O, Si, C, and Ca and contains two distinct laminae compositions: silica and carbonate (Fig. 9E, Table 1). Silica-rich laminae are enriched in Si and O. Carbonate layers are enriched in Ca, C, S, Fe, K, and Mg compared to silica-rich laminae and appear lighter in color in BSE than silica-rich layers. Oxygen is present in the carbonate layers, but the signal is weaker than the silica-rich layers. Small granules in the carbonate layers are where Al, Fe, Mg, and K are most concentrated. Two crystal morphologies are observed in the carbonate layers and include rhombohedral plate-like crystals and small (approx. 3μm) spherules (Fig. 10). The organic inclusions are most often found within the carbonate layers, but do occur in the silica layers. These inclusions are composed entirely of carbon, with no presence of Ca, Si, or O. The ultrastructure of these carbon-rich inclusions appears as interconnected folds and tubules (Fig. 11).

Aix_25 in thin section is finely laminated like Aix_flat1, but differs somewhat in composition (Fig. 12). There are distinct alternating silica-rich and carbonate-rich layers, but the carbonate layers are much more defined in Aix_25 compared to Aix_flat1. Within the carbonate layers, there are grains heavily enriched in Ca. Silicon is present throughout all of the layers, but is more concentrated in layers not enriched in Ca. Aluminum, Mg, and Fe are present and in higher concentrations in the silica-rich layers. Throughout most of the sample, there is a strong carbon signal. Aix_25 has much more C and much less O , Si , and Ca than Aix_flat1 (Table 1).

The weight percent of C in Aix_25 is over 4x the weight percent of C in Aix_flat1.

Thin section Aix_Big1 has three distinct laminae that all look uniform in composition and texture. The laminae are made of small granules similar to fossil Aix_24. Oxygen, Ca, and C are the most abundant elements, and are distributed uniformly throughout the sample (Table 1). Magnesium and S are also present, although much less abundant (< 1 wt%), and are dispersed throughout the sample.

In BSE imaging, Aix_32 has a strikingly different texture and composition from the other samples of matrix (Figs. 13, 14; Table 1). In thin section, the laminae are composed of structures with a variety of shapes. The most abundant are circular hollow structures (100–200 μm) and elongated structures that are tubular and filamentous and range in size from 200–600 μm. The composition of these structures is C and O, and lacks Ca and Si, and they appear embedded within a C-rich matrix. These circular and elongated structures also have numerous small (20 μm long, 1–3 μm wide) filaments connecting them to each other and to the matrix. The top layer of the sample lacks these structures and contains abundant small (approx. 40 μm) granules that appear bright white in BSE and are composed of Si and O. Elongated grains (200–300 μm), distinct from the elongated tubular and filamentous structures, that appear bright in BSE are scattered throughout the matrix, but not present in the topmost layer. These grains are composed of Si, O, Mg, Al, and Fe. Overall, Aix_32 is enriched in C compared to the other samples. The C and O-rich tubular structures define distinct laminae within the sample, and Cl, though less abundant, appears to be more concentrated in some layers. The Ca signal is extremely weak and does not appear concentrated in any specific areas.

DISCUSSION

Fossil spider preservation

Matrix fabric appears to be linked to the differing modes of preservation and composition of the fossil spiders. Flattened casts are preserved in a matrix that is finely laminated with alternating silic-rich and carbonate-rich layers. Fossil arthropods preserved in finely laminated sediments are typically preserved as compression fossils, but the specimens from Aix-en-Provence lack a carbonized film and, instead, are composed of sediment with cuticle remains. Three-dimensional molds are preserved in matrices of fine carbonate mineral grains with abundant spherules of filamentous bacteria or complex tubular structures.

The fluorescence patterns in the fossils and matrix also likely are related to their composition. Autofluorescence in minerals is attributed to crystal lattice defects, organic material, or the presenence of rare earth elements. Here, EDS analysis did not reveal any traces of rare earth elements. The strong fluorescence and high carbon content of the dark brown colorations on some of the fossils indicates the presence of organic compounds, likely cuticle of the spider that has been altered to some form of aromatic carbon or kerogen instead of actual crystalline material. The strong blue fluorescent internal structures in the legs and prosoma of some of the spiders may represent musculature altered to aliphatic carbon or replaced with calcite. Similar preservation ocurrs in fossil spiders from the Crato Formation, where they are preserved as goethite replacements, but muscles in the legs and void spaces in the prosoma have been replaced and/or filled with calcite (Barling et al., 2015). The pale orange fluorescence exhibited by some of the spiders preserved as molds matches the fluorescence color of the calcite-rich laminations, but is not as bright as the pure carbon masses or cuticle. These fossils may represent small amounts of organic material that are included within the mineral structure, especially where clear and distinct fluorescent outlines of the exoskeleton are visible and

surrounded by a weakly fluorescent shroud. Another possible explanation for the fluorescence of the fossil samples is the naturally occurring fluorophores in spider hemolymph (blood) and cuticle. Guanine is an amino acid, found in the cuticle of the abdomens of some spiders, and as excreta (Oxford, 1997; Kariko et al., 2018). The structural arrangement of guanine crystals in spider cuticle gives them a silvery appearance in life, and is also strongly fluorescent. Original structural components of spider cuticle in the fossils could likely be tested with Raman spectroscopy.

Microbial mat evidence

The texture and composition of the thinly laminated marlstones as well as the ultrastructure of crystal grains and organic inclusions suggests microbial mats were prevalent during the deposition of sediments in the Oligocene Aix-en-Provence basin of France. The wrinkled and pustular textures observed on the bedding surfaces of Aix-en-Provence samples are documented in other fossil and modern microbial mats (Schieber, 1998; Retallack et al., 2012). The small fragments likely are tiny microbial mat chips, where pieces of the microbial mat tear and are ripped up and redeposited (Noffke et al., 2013). Microbial mat chips can form in subaerial and subaqueous environments, but commonly are associated with desiccation (Gerdes, 2007). The uppermost layer of Aix_32 curls upwards at the vertical crack, also consistent with desiccation cracks observed in microbial mats; however the other laminae in the sample bend downward. Vertical cracks in microbial mats are typically the result of desiccation or gas escape structures, and the laminae of the mats bend or curl upward (Schieber et al., 2007). The vertical crack may represent a partially healed desiccation crack or a trace fossil, in which an extremely small organism created a burrow in the microbial mat layers (Schieber et al., 2007; Seckbach and Oren, 2010). At present, the origin of the crack remains ambiguous.

The matrix fabric of specimen Aix_32 resembles a thrombolitic texture in UV light, but the fluorescence response is so strong that it overshadows the distinct layers of tubes and circular structures visible in BSE. Many of the elongated and tubular structures in the matrix closely resemble filamentous microbial sheaths and also contain many small filaments connecting them to each other the surrounding matrix similar to the structure of some EPS (Chafetz and Buczynski, 1992; DeFarge et al., 1996; Chan et al., 2016; Mei et al., 2020). The equally high C and O, but low Ca, composition of this material suggests a lack of calcium carbonate. This composition may represent carbonyl groups, in which O and C are double bonded, which have been found in oil shales (Wang et al., 2019).

The bright white structures in BSE images of Aix_32 are likely clays, and more specifically, illite ($(K,H_3O)(Al,Mg,Fe)_2(Si,Al)_4O_{10}[(OH)_2,(H_2O)]$. The clay masses are scattered throughout the sample, but the tubular structure in Fig. 14C appears to be replaced entirely by illite. Illite has been found in other fossiliferous deposits, and connected to microbial precipitation and influence (Gabbott et al., 2001; Briggs, 2003).

The extremely fine and undisturbed laminations in Aix_25 and Aix_flat1 also support the presence of microbial mats. The fine laminations resemble those of stromatolites and microbial mats reported in other lacustrine deposits like the Green River and Crato formations, although no macroscopic domal structures have been reported from the Aix-en-Provence (Surdam and Wolfbauer, 1975; Schieber, 1999; Warren et al., 2016; Mustoe et al., 2019). The rhombohedral/platy crystals suggest bacterially induced precipitation of calcite, while spherules suggest direct carbonate precipitation by microbes (Dupraz et al., 2009). Rhombs and spherules have been produced by microbes experimentally, but spherules have also been interpreted as coccoidal bacterial cells (Wei et al., 2015; Warren et al., 2016; Meier et al., 2017). The

ultrastructure of the organic inclusions is interpreted as EPS, and commonly is observed in modern and fossil biofilms and microbial mats (Epstein et al., 2011; Iniesto et al., 2016).

The spheroids in the mold fossil of Aix_24 resemble spherules found in carbonate microbialites and filamentous bacteria (Perri and Tucker, 2007; Perri and Spadafora, 2011). Both carbonate rhombs and spherules are interpreted as the result of passive microbially influenced precipitation, yet here, filamentous bacteria are an extremely abundant component of the spherules and appear to be autolithified. The spheroids themselves are extremely abundant in the mold of the body of the spider and likely formed a crust of mineralized material around the spider body.

Arthropod preservation in other deposits

The modes of preservation of fossils in the Aix-en-Provence Formation differ from other well-known spider-bearing Fossil-Lagerstätten. Fossil insects and spiders from most lacustrine deposits are preserved as compression fossils, in which only a thin layer of carbonized material remains and possibly very low relief impressions. This type of preservation is observed in the Eocene Green River (50 Ma) and Florissant (34 Ma) formations of Colorado, and in older deposits like the Jurassic Haifanggou Formation (also known as the Jiulongshan Formation; 162 Ma) and Cretaceous Jinju Formation of Korea (112 Ma). The cuticle of insects and spiders is composed of chitin and other proteins, and after fossilization, is usually altered to aliphatic compounds (Martínez-Delclòs et al., 2004). Aliphatic compounds typically do not exhibit strong fluorescence, explaining why the carbon films of many of the compression fossils from other lacustrine deposits do not fluoresce in UV light (Díaz-García and Badía-Laíño, 2019). In contrast, aromatic compounds often exhibit strong fluorescence. The high sulfur content in the abdomen of the flat spider may represent thiophenes, aromatic compounds that have been found

in other arthropod fossils (Artur Stankiewicz et al., 1997; Briggs et al., 1998). Most of the Aix-en-Provence specimens are not true compression fossils, but the flattened casts may represent an intermediate stage of preservation of organic compounds by compression.

The 3D preservation of the Aix-en-Provence fossils is most similar to arthropod fossils in the Bembridge Marls from the Isle of Wight (Eocene). Isle of Wight arthropods are preserved as mineralized 3D calcified replacements with aliphatic organic material (McCobb et al., 1998). Muscle fibers and cuticle texture are preserved in the Isle of Wight fossils, much greater detail than in Aix-en-Provence, suggesting the rapid mineralization of internal and external remains (Selden, 2002). Cuticle-lined voids were also reported, and may represent the early formation of concretions to keep carcasses from collapsing, and thus preserving their 3D structure. This process is similar to the mineralized crust of the high relief external and internal molds of the spiders described here.

The fossils preserved as internal and external molds from the Aix-en-Provence Fossil-Lagerstätte also resemble those of the Neoproterozoic Ediacaran biota, but differ in composition and likely have a slightly different taphonomic pathway. Framboidal pyrite is found in the mineralized crusts of Ediacaran fossils, and the presence of iron sulfides in fossilization has been demonstrated experimentally, but this was not observed in Aix-en-Provence fossils (Darroch et al., 2012; Liu, 2016). The lack of iron in the Aix-en-Provence samples suggests pyrite formation was not widespread during fossilization, and instead, an abundance of calcium carbonate appears to favor mineralized crusts of calcite with likely incorporated organic matter.

Paleoenvironmental implications

The results from this study provide additional interpretations to the paleoenvironment of the Aix-en-Provence Formation. Pustular microbial mat textures are found in peritidal settings

(Gerdes et al., 2001). Microbial mat chips (and a possible desiccation crack) suggest a shallow paleolake with periods of very shallow water and possibly subaerial conditions (Gerdes et al., 2000). Particularly shallow conditions may correspond to episodes of increasing salinity. The diatoms found in Aix_24 resemble those belonging to Class Coscinodiscophyceae. Specifically, they resemble the diatom families Thalassiosiraceae, Coscinodiscaceae, and Hemidiscaceae, all of which have centric diatoms with abundant punctae (Sims et al., 1989; Lee et al., 2002; Hasle et al., 1996; Tulan and Sachsenhofer, 2020). These families contain marine, brackish, and freshwater species, although the genus *Azpeitia* Peragallo, 1912, which the diatoms here most closely resemble, is marine (Sims et al., 1989). These increases in salinity may also be tied to mass mortality events of fishes and dragonfly nymphs (Gaudant et al., 2018). The finely laminated samples likely represent slightly deeper waters below storm wave base, and possibly anoxic or saline bottom conditions suggested by a lack of bioturbation (Kemp, 1996). One sample, Aix_Big1, likely represents periods of sedimentary mineral deposition suggested by the uniform composition of calcium carbonate granules (Trower et al., 2019). This evidence supports a shallow lacustrine or lagoonal setting, with possible episodes of subaerial exposure and fluctuating salinity.

The Aix-en-Provence taphonomic pathway

The proposed model of the taphonomic pathway of fossils in Aix-en-Provence includes varying sedimentary deposition, microbial mat influence, and the death-mask model (Fig. 15). Fossils that are preserved as external and internal molds follow the wavy mat fossilization pathway. The wavy mat refers to those microbial mats with wrinkled and pustular textures. Fossils that are preserved as the flattened casts follow the fine lamination fossilization pathway. Both pathways have been divided into stages. Stage 1 represents a carcass that is washed into the

paleolake, sinks through the water column, and comes to rest at the sediment water interface where a microbial mat exists. Stage 2 represents microbes colonizing the spider body and enveloping it. Following Stage 2, the pathways are different depending on the type of microbial mat that is present.

Pustular fossilization pathway

In this pathway, after microbes have colonized and enveloped the spider body, the formation of a mineralized crust begins (Stage 3). The mineralized crust is the result of microbial induced precipitation of calcium carbonate on and around the carcass. In this stage, minerals are precipitated on the exoskeleton of the spider and also bind sediment grains and minerals around the spider body forming a death mask. The formation of this crust keeps the three-dimensional form of the spider intact. The spider decays and organic components from the spider are incorporated into the minerals to varying degrees, while some internal tissues are replaced with minerals. The actual organic components of the spider body decay and are lost, and filled in or replaced with mineral precipitates, sediments, and microbial mat material (Stage 4). When laminations are split, the fossils preferentially break along the mineralized crust producing internal and external molds, typically in high relief (Stage 5).

Fine lamination fossilization pathway

In this pathway, the bodies of the spiders collapse and flatten (Stage 3). Here, sediment and mineral grains are cemented together around the flattened body of the spider creating a halo of cohesive mineral and sediment grains. Much of the spider decays, but some organic material from the cuticle of the spider remains, especially in the cephalothorax and abdomen. The cuticle of the spider is altered from its original composition, chitin and other proteins, to aromatic hydrocarbons. In Stage 4, this pathway creates a flattened cast of the spider in convex epirelief

and a counterpart concave mold in hyporelief with organic material from the spider cuticle that is imprinted on the surfaces and/or possibly entombed within the minerals and sediment.

CONCLUSION

Fossil-Lagerstätten provide a window into ancient ecosystems and diversity, especially with regard to soft-bodied fauna, but the mechanisms of exceptional fossil preservation are not always clear. Many taxa have been described from the Aix-en-Provence Fossil-Lagerstätte and improved our understanding of arthropod diversity due to the preservation of tissues that would decay in most circumstances; however, the mode of fossil preservation and the taphonomic pathway was largely understudied. Fossils are identified here as molds, flatttened casts, and compression fossils. The mechanism responsible for the preservation of fossils in the Aix-en-Provence Formation can be attributed to microbial mats. The presence of microbial mats is supported by textural and geochemical observations that include wrinkled textures, fine laminations, and microbial induced mineralization, and abundant organic material. Fluorescence microscopy reveals vivid responses from fossil spiders, and including the presence aromatic carbon, a likely altered product of the spider exoskeleton. The taphonomic pathway proposed here includes a modified death-mask model in which microbial mats create mineralized crusts that preserve the three-dimensional forms of fossils. This type of preservation is widely attributed to soft-tissue preservation in the Neoproterozoic Ediacaran biota, but is likely more pervasive in younger deposits than previously thought.

ACKNOWLEDGEMENTS

The authors thank Dr. André Nel (National Museum of Natural History, France) for loaning the specimens; Pike Hollman (University of Kansas) for making thin sections; Dr. Prem Thapa-

Chetri and the KU Microscopy and Analytical Imaging Laboratory for electron microscopy sample prep and imaging; Evolving Earth Foundation for funding.

LITERATURE CITED

Artur Stankiewicz, B., Briggs, D.E.G., Evershed, R.P., Flannery, M.B., and Wuttke, M., 1997, Preservation of chitin in 25-million-year-old fossils: Science, v. 276, p. 1541–1543.

Barling, N., Martill, D.M., Heads, S.W., and Gallien, F., 2015, High-fidelity preservation of fossil insects from the Crato Formation (Lower Cretaceous) of Brazil: Cretaceous Research, v. 52, p. 605–622.

Briggs, D.E.G., 1999, Molecular taphonomy of animal and plant cuticles: selective preservation and diagenesis: Philosophical Transactions of the Royal Society of London. Series B, Biological Sciences, v. 354, p. 7–17.

Briggs, D.E.G., 2003, The role of decay and mineralization in the preservation of soft-bodied fossils: Annual Review of Earth and Planetary Sciences, v. 31, p. 275–301.

Briggs, D.E.G., Artur Stankiewicz, B., Meischner, D., Bierstedt, A., and Evershed, R.P., 1998, Taphonomy of arthropod cuticles from Pliocene lake sediments, Willershausen, Germany: PALAIOS, v. 13, p. 386–394.

Briggs, D.E., and Kear, A.J., 1993, Fossilization of soft tissue in the laboratory: Science, v. 259, p. 1439–1442.

Chafetz, H.S., and Buczynski, C., 1992, Bacterially Induced Lithification of Microbial Mats: Palaios, v. 7, p. 277–293.

Chan, C.S., McAllister, S.M., Leavitt, A.H., Glazer, B.T., Krepski, S.T., and Emerson, D., 2016, The Architecture of Iron Microbial Mats Reflects the Adaptation of Chemolithotrophic Iron Oxidation in Freshwater and Marine Environments: Frontiers in microbiology, v. 7, p. 796.

Collomb, F.-M., Nel, A., Fleck, G., and Waller, A., 2008, March flies and European Cenozoic palaeoclimates (Diptera: Bibionidae): Annales de la Societe entomologique de France. Societe entomologique de France, v. 44, p. 161–179.

Darroch, S.A.F., Laflamme, M., Schiffbauer, J.D., and Briggs, D.E.G., 2012, Experimental formation of a microbial death maskexperimental microbial death mask: Palaios, v. 27, p. 293–303.

DeFarge, C., Trichet, J., Jaunet, A.-M., Robert, M., Tribble, J., and Sansone, F.J., 1996, Texture of microbial sediments revealed by cryo-scanning electron microscopy: Journal of Sedimentary Research, v. 66, p. 935–947.

Díaz-García, M.E., and Badía-Laíño, R., 2019, Fluorescence| Fluorescence Derivatization:.

Dupraz, C., Reid, R.P., Braissant, O., Decho, A.W., Norman, R.S., and Visscher, P.T., 2009, Processes of carbonate precipitation in modern microbial mats: Earth-Science Reviews, v. 96, p. 141–162.

Epstein, A.K., Pokroy, B., Seminara, A., and Aizenberg, J., 2011, Bacterial biofilm shows persistent resistance to liquid wetting and gas penetration: Proceedings of the National Academy of Sciences of the United States of America, v. 108, p. 995–1000.

Foelix, R., 2011, Biology of Spiders: Oxford University Press, USA, 419 p.

Fontes, J.-C., Gaudant, J., and Truc, G., 1980, Donnees paleoecologiques, teneurs en isotopes lourds et paleohydrologie du bassin gypsifere oligocene d'Aix-en-Provence: Bulletin de la Société géologique de France, v. 7, p. 491–500.

Gabbott, S.E., Norry, M.J., Aldridge, R.J., and Theron, J.N., 2001, Preservation of fossils in clay minerals; a unique example from the Upper Ordovician Soom Shale, South Africa: Proceedings of the Yorkshire Geological Society, v. 53, p. 237–244.

Gall, J.C., 1990, Les voiles microbiens. Leur contribution à la fossilisation des organismes au corps mou. Lethaia, v. 23(1), p. 21-28.

Gaudant, J., 1978, Sur les conditions de gisement de l'ichthyofaune oligocène d'Aix-en-Provence (Bouches-du-Rhône): Essai de définition d'un modèle paléoécologique et paléogéographique: Geobios . Memoire special, v. 11, p. 393–397.

Gaudant, J., Nel, A., Nury, D., Véran, M., and Carnevale, G., 2018, The uppermost Oligocene of Aix-en-Provence (Bouches-du-Rhône, Southern France): A Cenozoic brackish subtropical Konservat-Lagerstätte, with fishes, insects and plants: Comptes rendus. Palevol, v. 17, p. 460–478.

Gehling, J.G., 1999, Microbial mats in terminal Proterozoic siliciclastics; Ediacaran death masks: Palaios, v. 14, p. 40–57.

Gerdes, G., 2007, Structures left by modern microbial mats in their host sediments, *in* Atlas of microbial mat features preserved within the siliciclastic rock record, Elsevier Amsterdam, v. 2, p. 5–38.

Gerdes, G., Klenke, T., and Noffke, N., 2001, Microbial signatures in peritidal siliciclastic

sediments: a catalogue: Sedimentology, v. 47, p. 279–308.

Gerdes, G., Krumbein, W.E., and Noffke, N., 2000, Evaporite Microbial Sediments, *in* Riding, R.E. and Awramik, S.M. eds., Microbial Sediments, Berlin, Heidelberg, Springer Berlin Heidelberg, p. 196–208.

Gourret, P., 1887, Recherches sur les Arachnides tertiaires d'Aix en Provence: Recueil Zoologique Suisse, v. 4, p. 431–496.

Greenwalt, D.E., Goreva, Y.S., Siljeström, S.M., Rose, T., and Harbach, R.E., 2013, Hemoglobin-derived porphyrins preserved in a Middle Eocene blood-engorged mosquito: Proceedings of the National Academy of Sciences of the United States of America, v. 110, p. 18496–18500.

Greenwalt, D.E., Rose, T.R., Siljestrom, S.M., Goreva, Y.S., Constenius, K.N., and Wingerath, J.G., 2014, Taphonomy of the fossil insects of the middle Eocene Kishenehn Formation: Acta palaeontologica Polonica, v. 60, p. 931–948.

Gregor, H.-J. von, and Knobloch, E., 2001, Kritische Bemerkungen zu Saporta's fossilen Floren in Süd-Frankreich, speziell in der Provence: Flora Tertiaria Mediterranea, v. 4, p. 1–57.

Harding, I.C., and Chant, L.S., 2000, Self-sedimented diatom mats as agents of exceptional fossil preservation in the Oligocene Florissant lake beds, Colorado, United States: Geology, v. 28, p. 195–198.

Hasle, G.R., Syvertsen, E.E., Steidinger, K.A., Tangen, K., and Tomas, C.R., 1996, Identifying Marine Diatoms and Dinoflagellates: Elsevier, 598 p.

Hellawell, J., and Orr, P.J., 2012, Deciphering taphonomic processes in the Eocene Green River Formation of Wyoming: Palaeobiodiversity and Palaeoenvironments, v. 92, p. 353–365.

Henning, J.T., Smith, D.M., Nufio, C.R., and Meyer, H.W., 2012, Depositional setting and fossil insect preservation: A study of the late Eocene Florissant Formation, Colorado: Palaios, v. 27, p. 481–488.

Hope, F.W., 2009, XXXIX. Observations on the Fossil Insects of Aix in Provence, with Descriptions and Figures of Three Species: Transactions of the Royal Entomological Society of London, v. 4, p. 250–255.

Iniesto, M., Buscalioni, Á.D., Carmen Guerrero, M., Benzerara, K., Moreira, D., and López-Archilla, A.I., 2016, Involvement of microbial mats in early fossilization by decay delay and formation of impressions and replicas of vertebrates and invertebrates: Scientific reports, v. 6, p. 25716.

Jocqué, R., and Dippenaar-Schoeman, A.S., 2007, Spider Families of the World. Royal Museum for Central Africa, Tervuren:.

Kariko, S., Timonen, J.V.I., Weaver, J.C., Gur, D., Marks, C., Leiserowitz, L., Kolle, M., and Li, L., 2018, Structural origins of coloration in the spider Phoroncidia rubroargentea Berland, 1913 (Araneae: Theridiidae) from Madagascar: Journal of the Royal Society, Interface / the Royal Society, v. 15, doi:10.1098/rsif.2017.0930.

Kemp, A.E.S., 1996, Laminated sediments as palaeo-indicators: Geological Society, London, Special Publications, v. 116, p. vii–xii.

Kenchington, C., and Wilby, P.R., 2014, Of time and taphonomy: preservation in the Ediacaran, *in* Geological Society of America.

Lee J.H., Byun J.S. and Lee E.H., 1992, Taxonomy and Phylogeny of the Marine Diatom Family Hemidiscaceae in the Korean Coastal Waters Algae , v. 7, p. 185–205.

Liu, A.G., 2016, framboidal pyrite shroud confirms the “death mask”model for moldic preservation of ediacaran soft-bodied organisms Ediacaran taphonomy. G. Liu: Palaios, v. 31, p. 259–274.

Martill, D.M., Bechly, G., and Loveridge, R.F., 2007, The Crato Fossil Beds of Brazil: Window into an Ancient World: Cambridge University Press, 572 p.

Martínez-Delclòs, X., Briggs, D.E.G., and Peñalver, E., 2004, Taphonomy of insects in carbonates and amber: Palaeogeography, palaeoclimatology, palaeoecology, v. 203, p. 19–64.

McCobb, L.M.E., Duncan, I.J., Jarzembowski, E.A., Stankiewicz, B.A., Wills, M.A., and Briggs, D.E.G., 1998, Taphonomy of the insects from the insect bed (Bembridge Marls), late Eocene, Isle of Wight, England: Geological magazine, v. 135, p. 553–563.

Meier, A., Kastner, A., Harries, D., Wierzbicka-Wieczorek, M., Majzlan, J., Büchel, G., and Kothe, E., 2017, Calcium carbonates: induced biomineralization with controlled macromorphology: Biogeosciences , v. 14, p. 4867.

Mei, M., Latif, K., Mei, C., Gao, J., and Meng, Q., 2020, Thrombolitic clots dominated by filamentous cyanobacteria and crusts of radio-fibrous calcite in the Furongian Changshan

Formation, North China: Sedimentary geology, v. 395, p. 105540.

Miller, S.E., Bahniuk Rumbelsperger, A.M., Sauvage, J.F., Jarrett, A.J., Petryshyn, V.A., Corsetti, F.A., and Shapiro, R.S., 2011, Microfacies analysis of Green River Formation stromatolites and comparison to microbial mat experiments, *in* adsabs.harvard.edu, v. 2011, https://ui.adsabs.harvard.edu/abs/2011AGUFM.B51I0534M.

Murchison, R.I., and Lyell, C., 1829, On the Tertiary Fresh-water Formations of Aix, in Provence, including the Coal-field of Fuveau, with a Description of Fossil Insects, Shells and Plants, contained therein; by John Curtis, FLS; J. de C. Sowerby, Esq. FLS, and J. Lindley Esq., Professor of Botany in the London University.(Communicated by the Authors): The Edinburgh New Philosophical Journal, v. 7, p. 287–298.

Mustoe, G.E., Viney, M., and Mills, J., 2019, Mineralogy of Eocene Fossil Wood from the "Blue Forest" Locality, Southwestern Wyoming, United States: Geosciences Journal, v. 9, p. 35.

Narbonne, G.M., 2004, Modular construction of early Ediacaran complex life forms: Science, v. 305, p. 1141–1144.

Noffke, N., Christian, D., Wacey, D., and Hazen, R.M., 2013, Microbially induced sedimentary structures recording an ancient ecosystem in the ca. 3.48 billion-year-old Dresser Formation, Pilbara, Western Australia: Astrobiology, v. 13, p. 1103–1124.

Nury, D., 1987, L'Oligocène de Provence méridionale: Stratigraphie, dynamique sédimentaire, reconstitutions paléographiques: Aix-Marseille 1, https://www.theses.fr/1987AIX11124.

O'Brien, N.R., Meyer, H.W., and Harding, I.C., 2008, The role of biofilms in fossil preservation,

Florissant Formation, Colorado: Paleontology of the Upper Eocene Florissant Formation, Colorado, v. 435, p. 19.

O'Brien, N.R., Meyer, H.W., Reilly, K., Ross, A.M., and Maguire, S., 2002, Microbial taphonomic processes in the fossilization of insects and plants in the late Eocene Florissant Formation, Colorado: Rocky Mountain Geology, v. 37, p. 1–11.

Oxford, G.S., 1997, July. Guanine as a colorant in spiders: development, genetics, phylogenetics and ecology. In Proceedings of the 17th European Colloquium of Arachnology, Edinburgh (pp. 121-131).

Peinado, J., 2002, L'Oligocène terminal d'Aix-en-Provence: genèse d'un gisement d'insectes à conservation exceptionnelle:.

Penney, D., and Selden, P., 2011, Fossil Spiders: The Evolutionary History of a Mega-diverse Order: Siri Scientific Press, 127 p.

Perri, E., and Spadafora, A., 2011, Evidence of Microbial Biomineralization in Modern and Ancient Stromatolites, *in* Tewari, V. and Seckbach, J. eds., STROMATOLITES: Interaction of Microbes with Sediments, Dordrecht, Springer Netherlands, p. 631–649.

Perri, E., and Tucker, M., 2007, Bacterial fossils and microbial dolomite in Triassic stromatolites: Geology, v. 35, p. 207–210.

Piveteau, J., 1927, Études sur quelques amphibiens et reptiles fossiles: Masson.

Retallack, G.J., Noffke, N., and Chafetz, H., 2012, Criteria for distinguishing microbial mats and earths: Soc. Econ. Paleont. Mineral. Spec. Pap, v. 101, p. 136–152.

Sagemann, J., Bale, S.J., Briggs, D.E.G., and Parkes, R.J., 1999, Controls on the formation of authigenic minerals in association with decaying organic matter: an experimental approach: Geochimica et cosmochimica acta, v. 63, p. 1083–1095.

Saporta, G. de, 1889, Dernières adjonctions à la flore fossile d'Aix-en-Provence: Ann sci nat Bot, v. 10, p. 1–192.

Schieber, J., 2007, Benthic microbial mats as an oil shale component: Green River Formation (Eocene) of Wyoming and Utah: Atlas of microbial mat features preserved within the clastic rock record. Elsevier, Amsterdam, p. 225–232.

Schieber, J., 1999, Microbial Mats in Terrigenous Clastics: The Challenge of Identification in the Rock Record: Palaios, v. 14, p. 3–12.

Schieber, J., 1998, Possible indicators of microbial mat deposits in shales and sandstones: examples from the Mid-Proterozoic Belt Supergroup, Montana, USA: Sedimentary geology, v. 120, p. 105–124.

Schieber, J., Bose, P.K., Eriksson, P.G., Banerjee, S., Sarkar, S., Altermann, W., and Catuneanu, O., 2007, Atlas of Microbial Mat Features Preserved within the Siliciclastic Rock Record: Elsevier, 324 p.

Seckbach, J., and Oren, A., 2010, Microbial Mats: Modern and Ancient Microorganisms in Stratified Systems: Springer Science & Business Media, 606 p.

Selden, P.A., 2002, First British Mesozoic spider, from Cretaceous amber of the Isle of Wight, southern England. Palaeontology, v. 45(5), p. 973–983.

Serezhnikova, E.A., 2011, Microbial Binding as a Probable Cause of Taphonomic Variability of Vendian Fossils: Carbonate Casting?, *in* Reitner, J., Quéric, N.-V., and Arp, G. eds., Advances in Stromatolite Geobiology, Berlin, Heidelberg, Springer Berlin Heidelberg, p. 525–535.

Sims, P.A., Fryxell, G.A., and Baldauf, J.G., 1989, Critical Examination of the Diatom Genus Azpeitia: Species Useful as Stratigraphic Markers for the Oligocene and Miocene Epochs: Micropaleontology, v. 35, p. 293–307.

Smith, D.M., 2012, Exceptional preservation of insects in lacustrine environments: Palaios, v. 27, p. 346–353.

Stolz, J.F., 2000, Structure of Microbial Mats and Biofilms, *in* Riding, R.E. and Awramik, S.M. eds., Microbial Sediments, Berlin, Heidelberg, Springer Berlin Heidelberg, p. 1–8.

Surdam, R.C., and Wolfbauer, C.A., 1975, Green River Formation, Wyoming: A Playa-Lake Complex: GSA Bulletin, v. 86, p. 335–345.

Trower, E.J., Lamb, M.P., and Fischer, W.W., 2019, The Origin of Carbonate Mud: Geophysical research letters, v. 46, p. 2696–2703.

Tulan, E., Sachsenhofer, R.F., Witkowski, J., Tari, G.A.B.O.R., Ćorić, S. and Bechtel, A., 2020. Microfossil assemblages (diatoms, calcareous nannofossils, and silicoflagellates), paleoenvironment, and hydrocarbon source rock potential of the Oligocene Ruslar Formation at Karadere, Bulgaria: Turkish Journal of Earth Sciences, 29(SI-1), p.154–169.

Wang, Q., Hua, Z., and Guan, J., 2019, Structure of Wangqing oil shale and mechanism of

carbon monoxide release during its pyrolysis: Energy Science & Engineering, v. 7, p. 2398–2409.

Warren, L.V., Varejão, F.G., Quaglio, F., Simões, M.G., Fürsich, F.T., Poiré, D.G., Catto, B., and Assine, M.L., 2016, Stromatolites from the Aptian Crato Formation, a hypersaline lake system in the Araripe Basin, northeastern Brazil: Facies, v. 63, p. 3.

Wei, S., Cui, H., Jiang, Z., Liu, H., He, H., and Fang, N., 2015, Biomineralization processes of calcite induced by bacteria isolated from marine sediments: Brazilian journal of microbiology: [publication of the Brazilian Society for Microbiology], v. 46, p. 455–464.

Wilby, P.R., Briggs, D.E.G., Bernier, P., and Gaillard, C., 1996, Role of microbial mats in the fossilization of soft tissues: Geology, v. 24, p. 787–790.

List of figures and tables

Figure 1. Modes of preservation of fossil spiders in the Aix-en-Provence lagerstätte. A) External and internal mold fossil in part (left) and counterpart (right). This spider has a high cephalix area. B) Flattened cast of a spider with dark colored material in the body and legs. C) True carbonized compression fossil spider. Abreviations: ct = cephalothorax, im = internal mold, mc = mineralized crust.

Figure 2. Compression fossil spider viewed with fluoresence microscopy. A) UV image showing fine setae and spines on the legs. B) Magnified UV image of a spine with ultrastructure details. C) BV image of palps and anterior portion of cephalothorax showing well preserved carbonized film.

Figure 3. Matrix textures of fossil molds. A) Fossil spider preserved as a mold. Upper arrow points to external mold with setae visible and lower arrow indicates internal mold of the ventral parts of the cephalothorax. B) Possible microbial mat chips. C) Wrinkled and pustular texture of the surface of a microbial mat.

Figure 4. Fluorescence images of spiders preserved as molds. A) Spider in UV light with body fluorescing paleo orange. B) Same spider with body fluorescing paleo orange in BV light. C) Brightfield image of fossil spider mold in absence of UV or BV light. D) Same spider in BV light fluorescing bright green. E) Full body of same spider in UV light fluorescing bright blue with halo of less intense blue fluorescence around body.

Figure 5. Mold of a fossil spider with varying fluorescence response. A) Plain-light image of fossil. B) UV image of specimen with internal structures of the cephalothoroax fluorescing bright

blue and the abdomen strongly fluorescing bright orange. The outline of the body autofluoresces pale orange.

Figure 6. Fluorescence responses of flattened cast spiders. A–B) Counterpart (A) and part (B) of fossil spider with dark brown material. C) Counterpart in UV light. Abdomen and parts of cephalothorax fluoresce bright orange, while the legs and parts of the cephalothorax fluoresce blue. D) Part in BV light. The dark brown material intensely fluoresces bright orange and resembles arthropod cuticle. E) Flattened cast of spider with dark brown material. F) Same spider (E) with true outline of body fluorescing pale orange and surrounded by a halo of blue fluorescent matrix.

Figure 7. Matrix fabrics in thin sections under fluorescence microscopy. A) UV image of matrix of Aix_32 showing wavy fabric. B) Vertical crack in lamination with matrix laminae bending along the crack. C) Laminations with a granular texture fluorescing blue and pale orange. D) UV image of fine laminations in sample Aix_flat1. E) Aix_flat1 in BV light fluorescing orange and green. F-–G) Aix_25 in BV light. Some extremely thin laminations fluorescence bright orange while some linear features are extremely bright, and amorphous masses do not have a fluorescence response in Aix_25.

Figure 8. BSE images and EDS of mold fossil spider Aix_24. A) BSE image of anterior portion of the spider—prosoma and legs. B) EDS maps reveal the fossil is mostly made of Ca, C, and O. C) Centric diatom remains. D) Cluster of rhombohedral crystals and spheroids. E) Spheroids magnified and are composed of filamentous bacteria. F) Magnified image of filamentous bacteria on spheroid.

Figure 9. Analysis of flattened cast of fossil spider Aix_flat1. A) Full fossil imaged in BV light with bright orange abdomen. B) Close up of abdomen in UV light. The texture of the fluorescent bright orange material resembles the cuticle found in other fossil arthropods. C) Back-scatter electron micrograph of abdomen. D) Elemental maps reveal the abdomen is rich in carbon and sulfur lacks silica and oxygen. E) Back-scatter electron micrograph and EDS elemental maps of Aix_flat1 reveal alternating silica rich and carbonate rich layers.

Figure 10. Electron micrographs of matrix material in Aix_flat1. A) Dark organic inclusion (om) in carbonate rich later (arrow). B–C) Rhombohedral/platy texture of a carbonate grain. D) Spherules (arrows) are abundant on the surfaces of the carbonate grains.

Figure 11. SEM/EDS analysis of organic inclusions. A) Back-scatter electron micrograph. B) EDS elemental maps of organic inclusion. The masses lack silica, calcium, and oxygen, and are enturely composed of carbon. C) Back-scatter electron micrograph of organic inclusion in a siica-rich layer. D) EDS elemental maps of amorphous mass showing a similar composition. E) High magnification electron micrograph of surface texture of organic inclusion showing a series of interconnected folds and tubes.

Figure 12. Matrix of finely laminated sample Aix_25. A) Laminations are difficult to see in BSE. B) EDS maps reveal C and O are not bound in specific layers, but dispersed throughout the sample. Laminae are mostly defined by Si (although difficult), Ca, Al, and Fe. C) BSE image of laminations and organic inclusions. D) EDS maps showing laminae composition and larger organic inclusions and some Ca-rich and Si-rich grains.

Figure 13. Matrix fabric in thin section of Aix_32. A) BSE image of upper most laminae of sample showing abundant bright white inclusions. B) BSE image of crack in matrix with bent laminae, tubular and circular structures, and bright white linear inclusions. C) Close up of tubular structures and rounded bright white inclusion. D) Magnified view of circular structure. E) Magnified view of tubular structures with abundant filaments.

Figure 14. EDS maps of matrix constituents of Aix_32. A) BSE image of tubular structures. B) EDS maps reveal a composition that is high in C and O, but low in other elements. C) BSE image of bright white tubular structure. C) EDS maps reveal the structure lacks C and is enriched in silica and other metals.

Figure 15. Illustration of possible taphonomic pathways of a fossil spider in the Aix-en-Provence lagerstätte. Wavy mats lead to internal and external molds, and are typically in high relief. Spiders preserved in extremely fine laminations are preserved as flattened casts and possess altered organic material.

Element	Aix_flat1	Aix_25	Aix_32	Aix_Big1
C	15.7	68.1	63.6	13.4
O	48.8	20.5	34.2	48.9
Si	25.1	8.1	1.2	-
Ca	7.9	2.2	0.1	36.6
Mg	0.2	0.1	0.5	0.8
S	0.3	0.1	-	0.3
Al	1.1	0.5	0.2	-
Fe	0.6	0.2	-	-
K	0.3	0.1	-	-
Cl	-	-	0.2	-

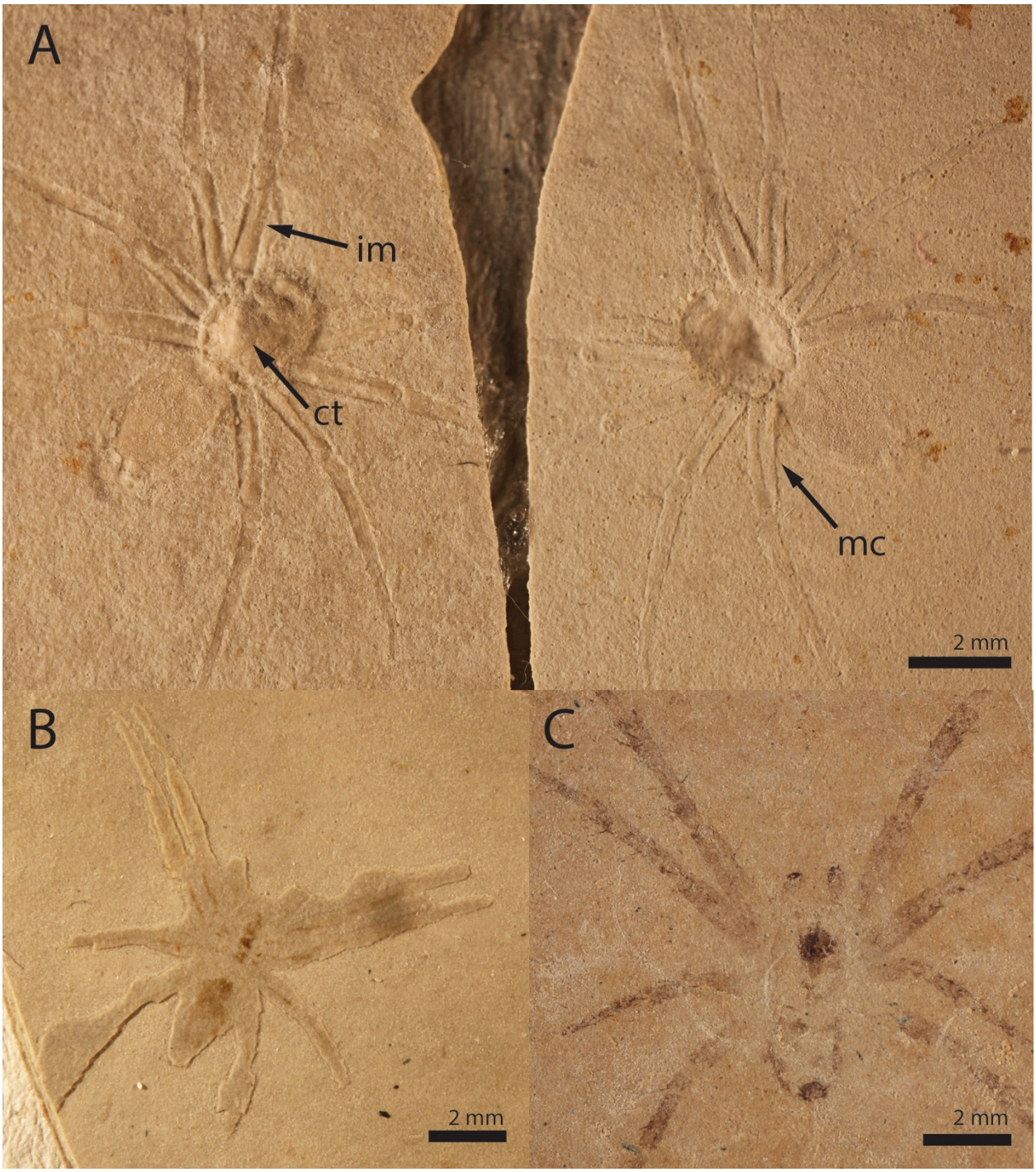
A
im
ct
mc
2 mm
B
2 mm
C
2 mm

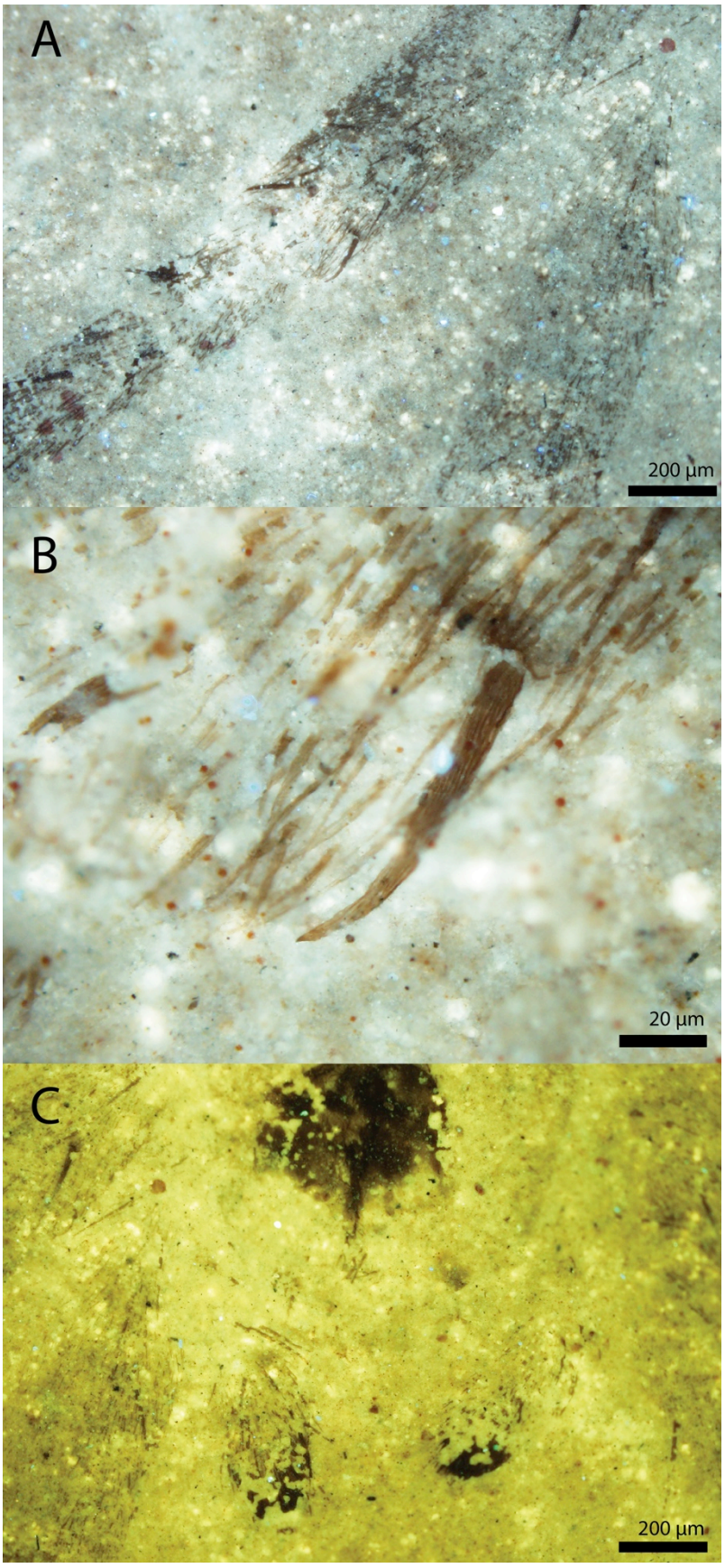
A
200 µm
B
20 µm
C
200 µm

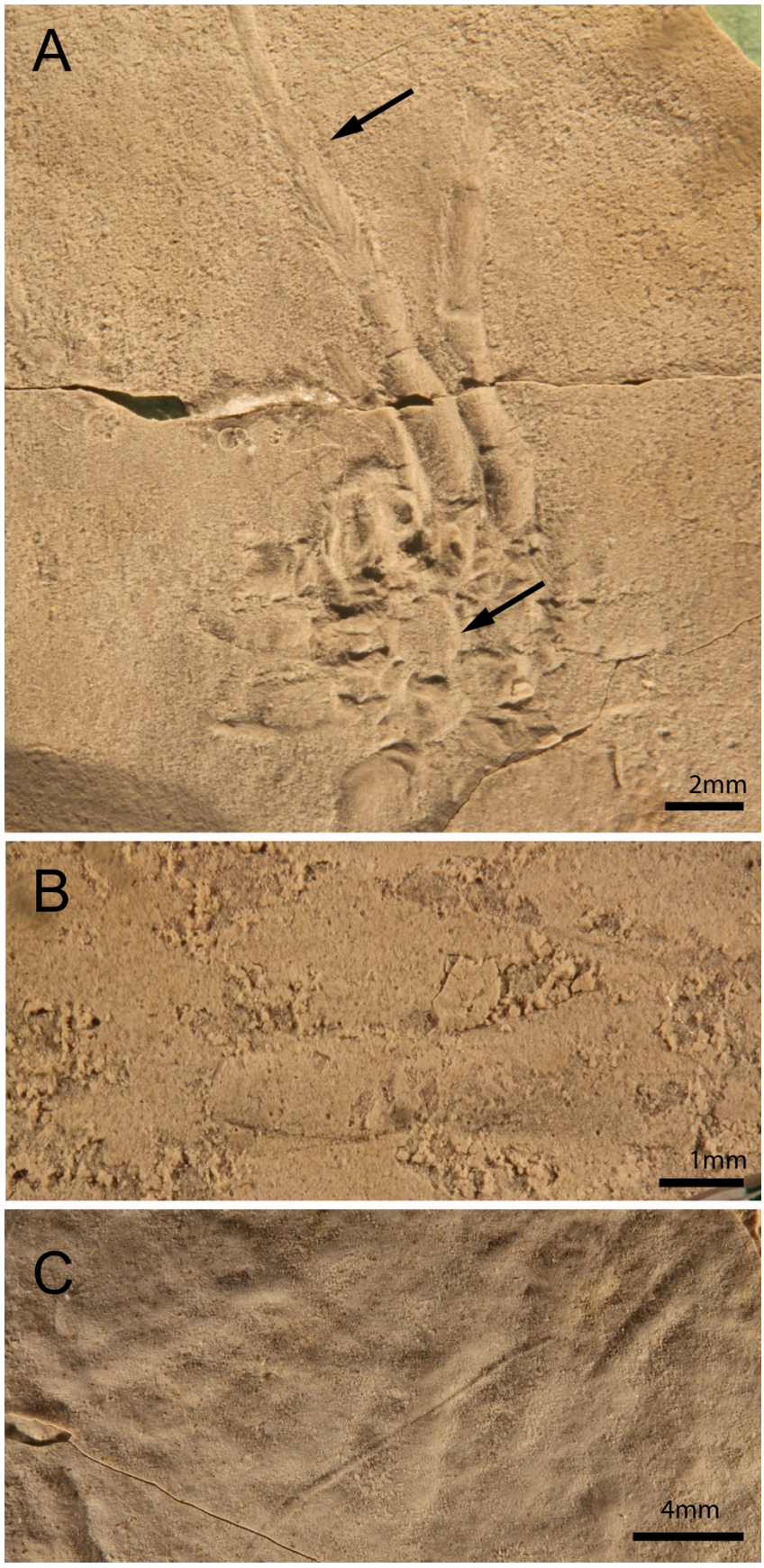
A
2mm
B
1mm
C
4mm

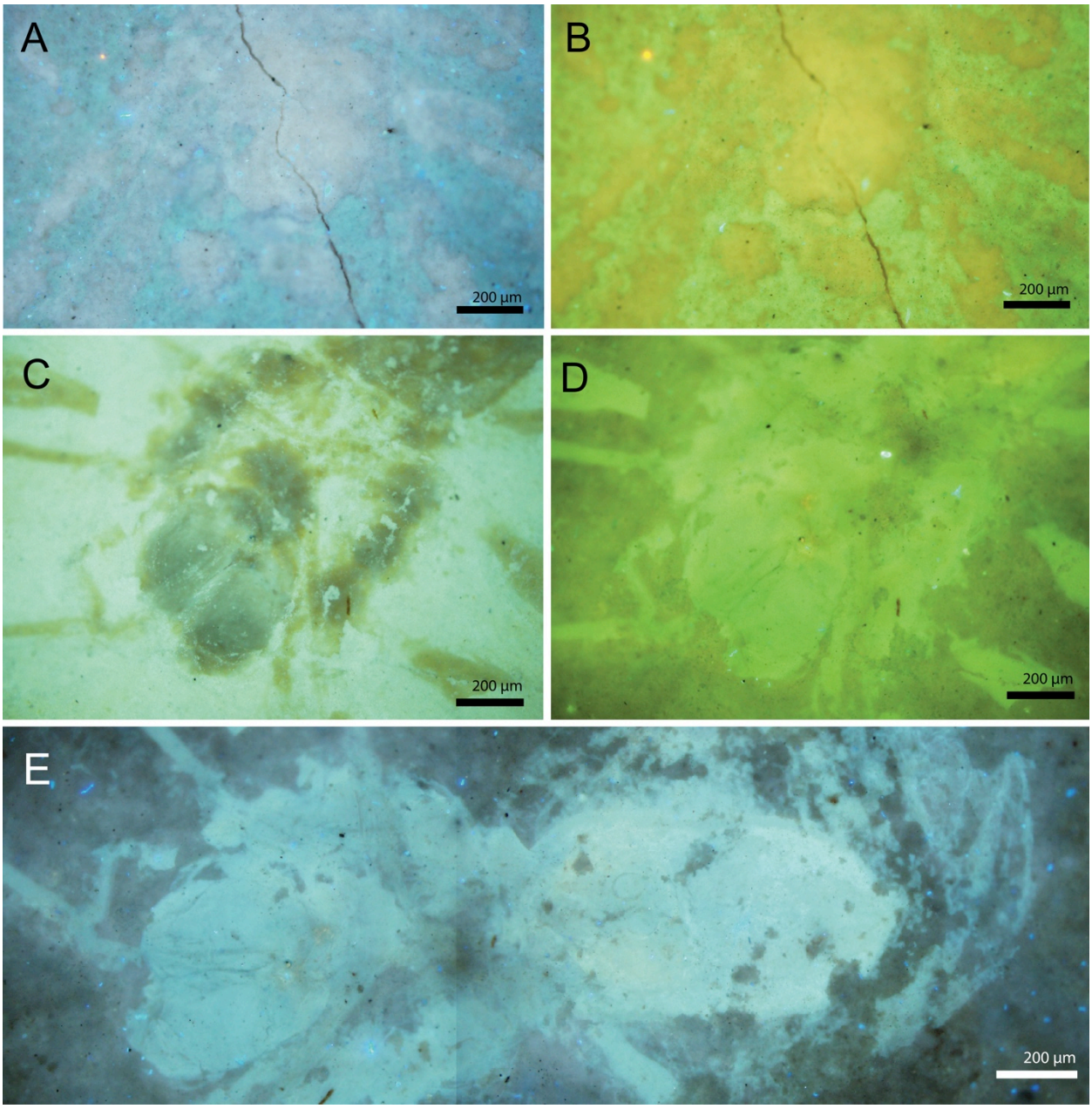
A
200 µm
B
200 µm
C
200 µm
D
200 µm
E
200 µm

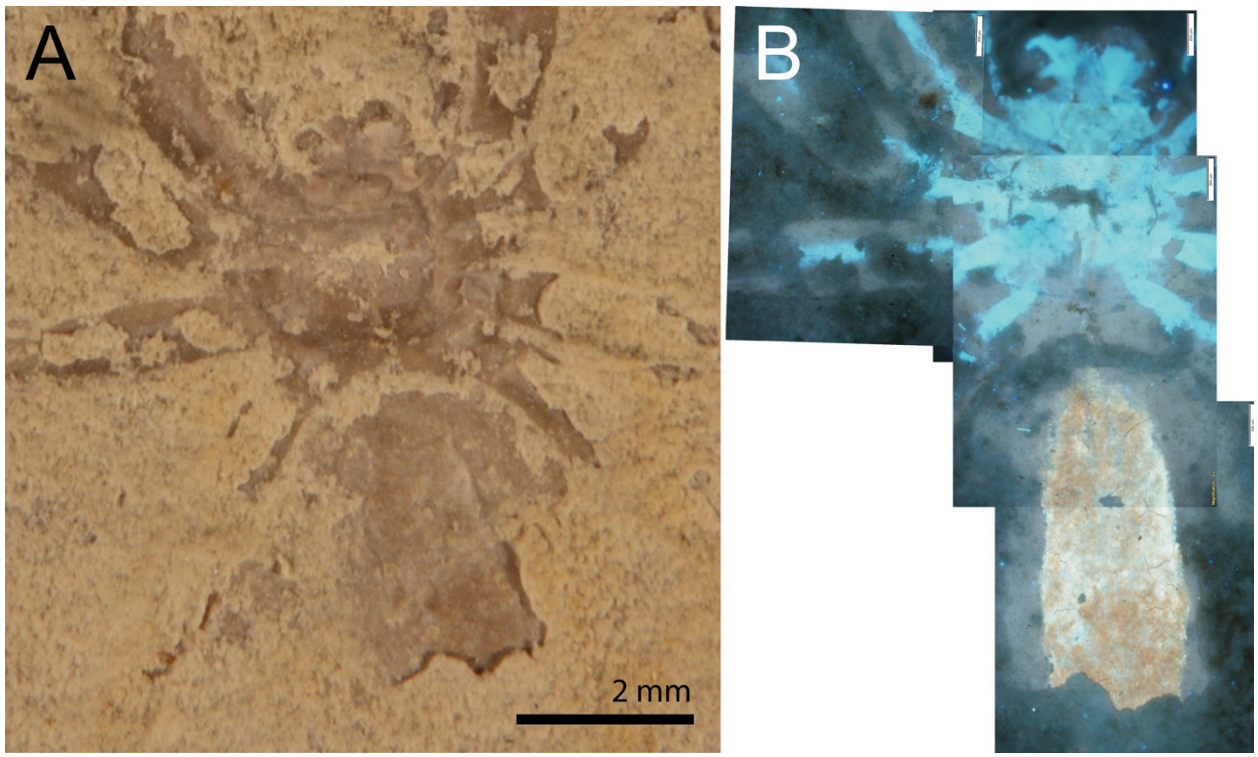
A
2 mm
B

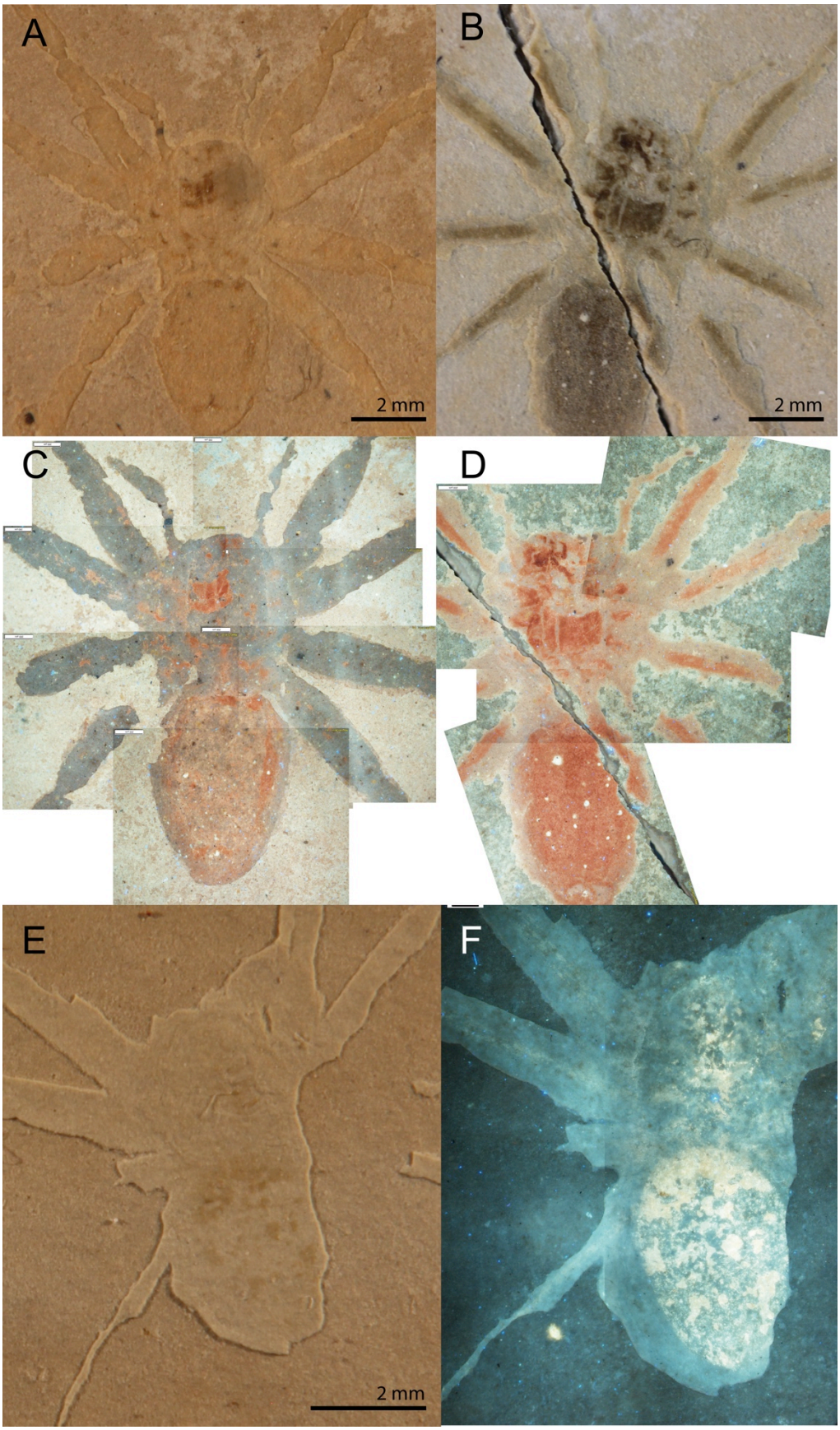
A
2 mm
B
2 mm
C
D
E
2 mm
F

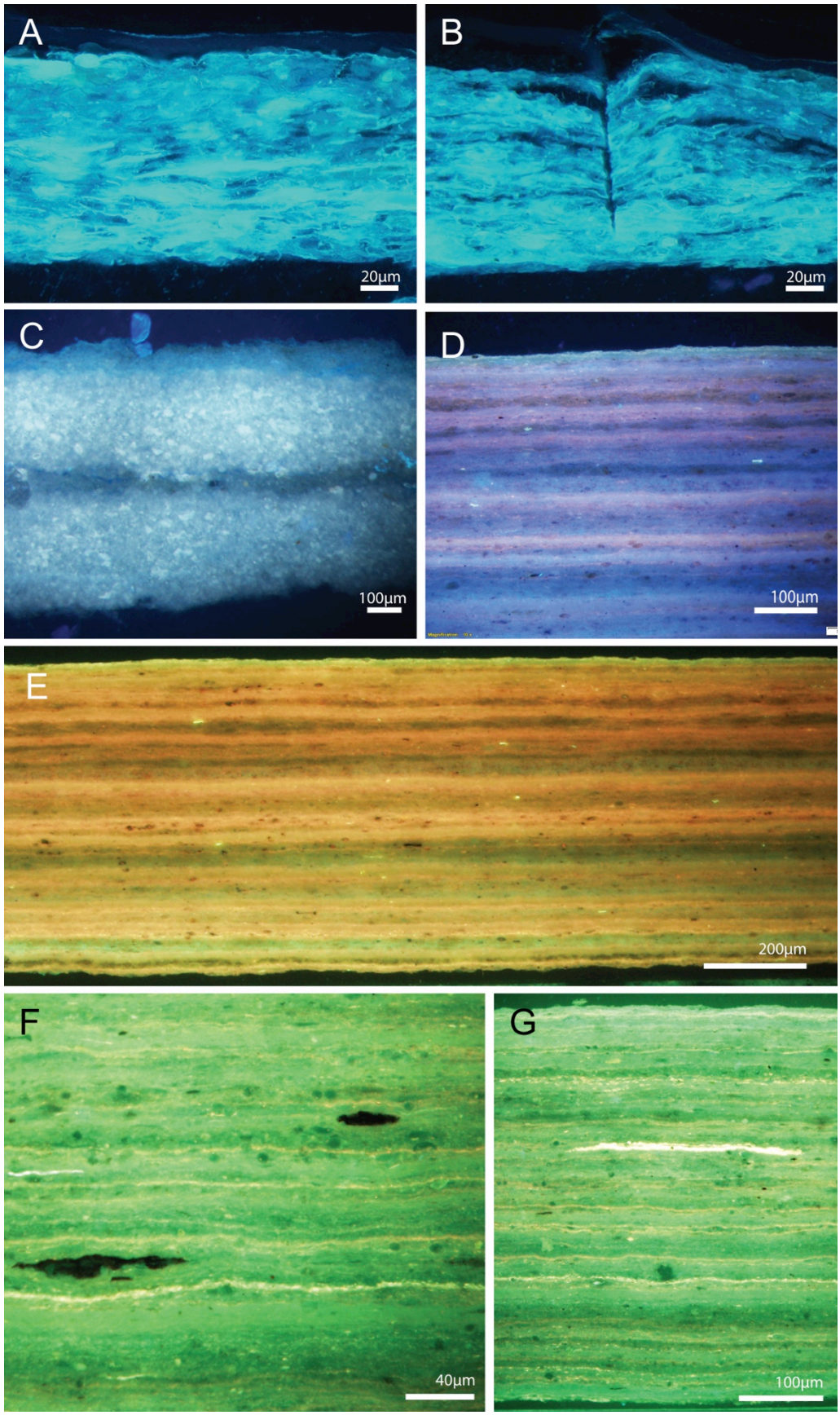
A
20µm
B
20µm
C
100µm
D
100µm
E
200µm
F
40µm
G
100µm

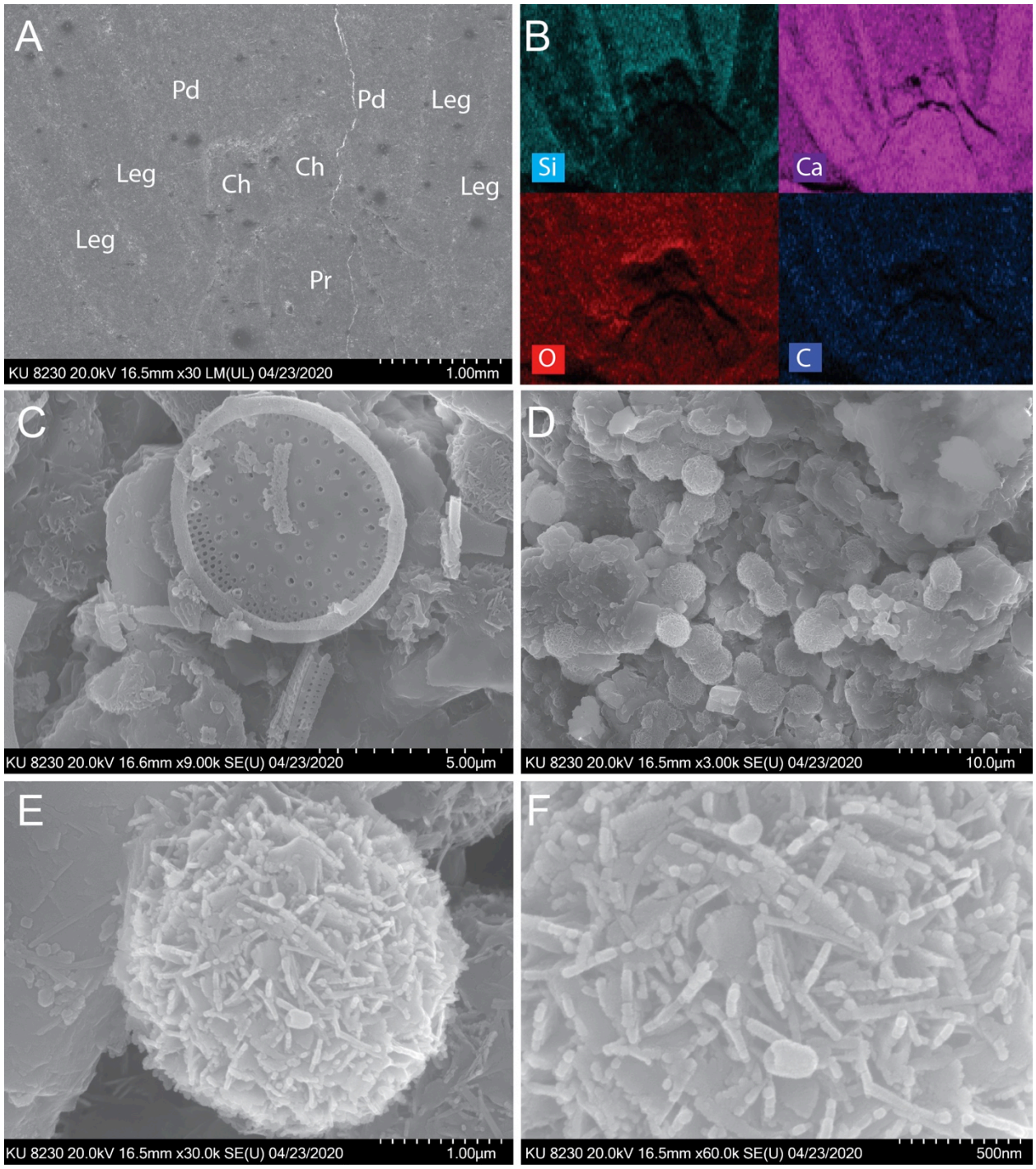
A
Pd
Pd
Leg
Leg
Ch
Ch
Leg
Leg
Pr
KU 8230 20.0kV 16.5mm x30 LM(UL) 04/23/2020
1.00mm
B
Si
Ca
O
C
C
KU 8230 20.0kV 16.6mm x9.00k SE(U) 04/23/2020
5.00µm
D
KU 8230 20.0kV 16.5mm x3.00k SE(U) 04/23/2020
10.0µm
E
KU 8230 20.0kV 16.5mm x30.0k SE(U) 04/23/2020
1.00µm
F
KU 8230 20.0kV 16.5mm x60.0k SE(U) 04/23/2020
500nm

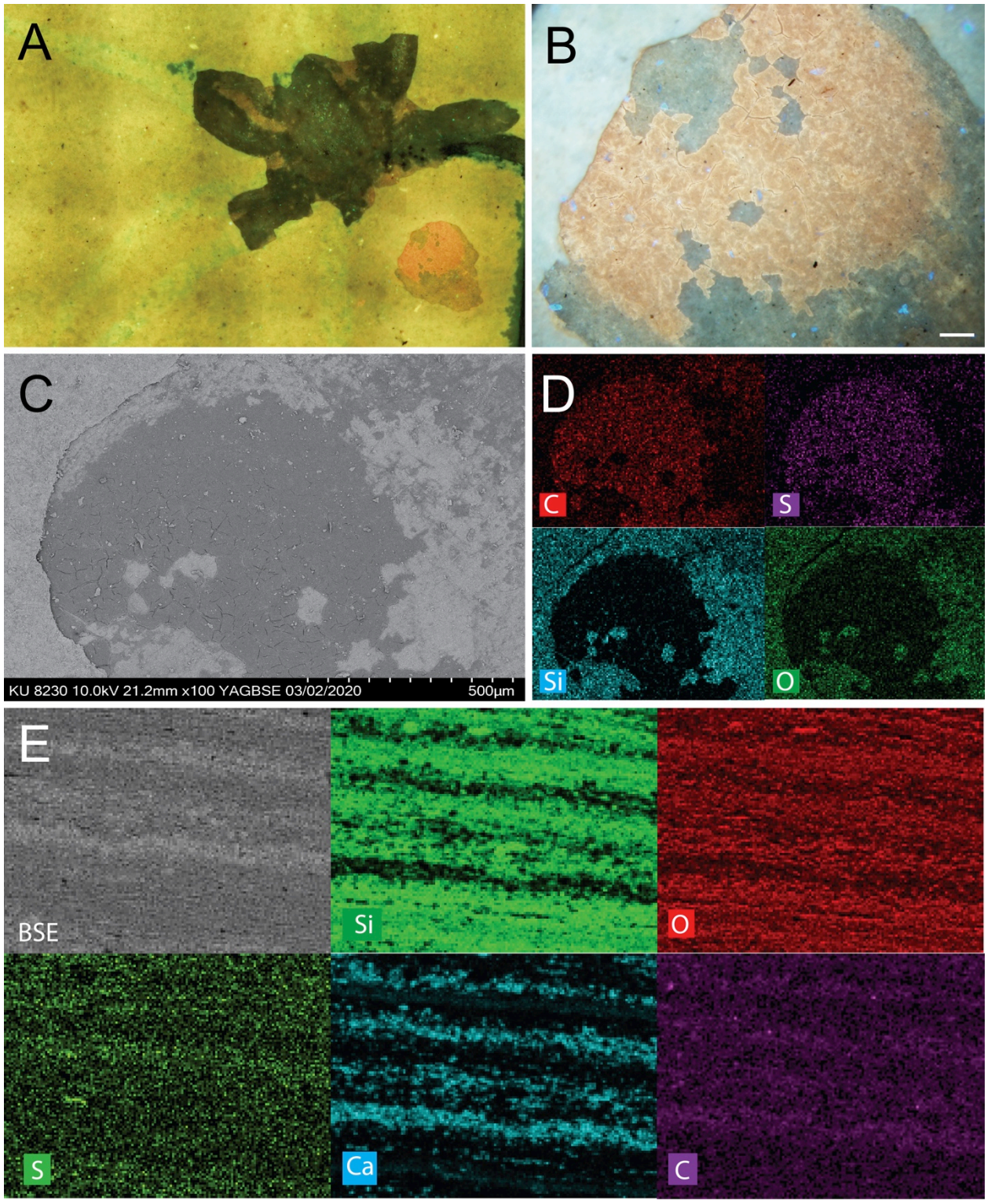
A
B
C
KU 8230 10.0kV 21.2mm x100 YAGBSE 03/02/2020
500µm
D
C
S
Si
O
E
BSE
Si
O
S
Ca
C

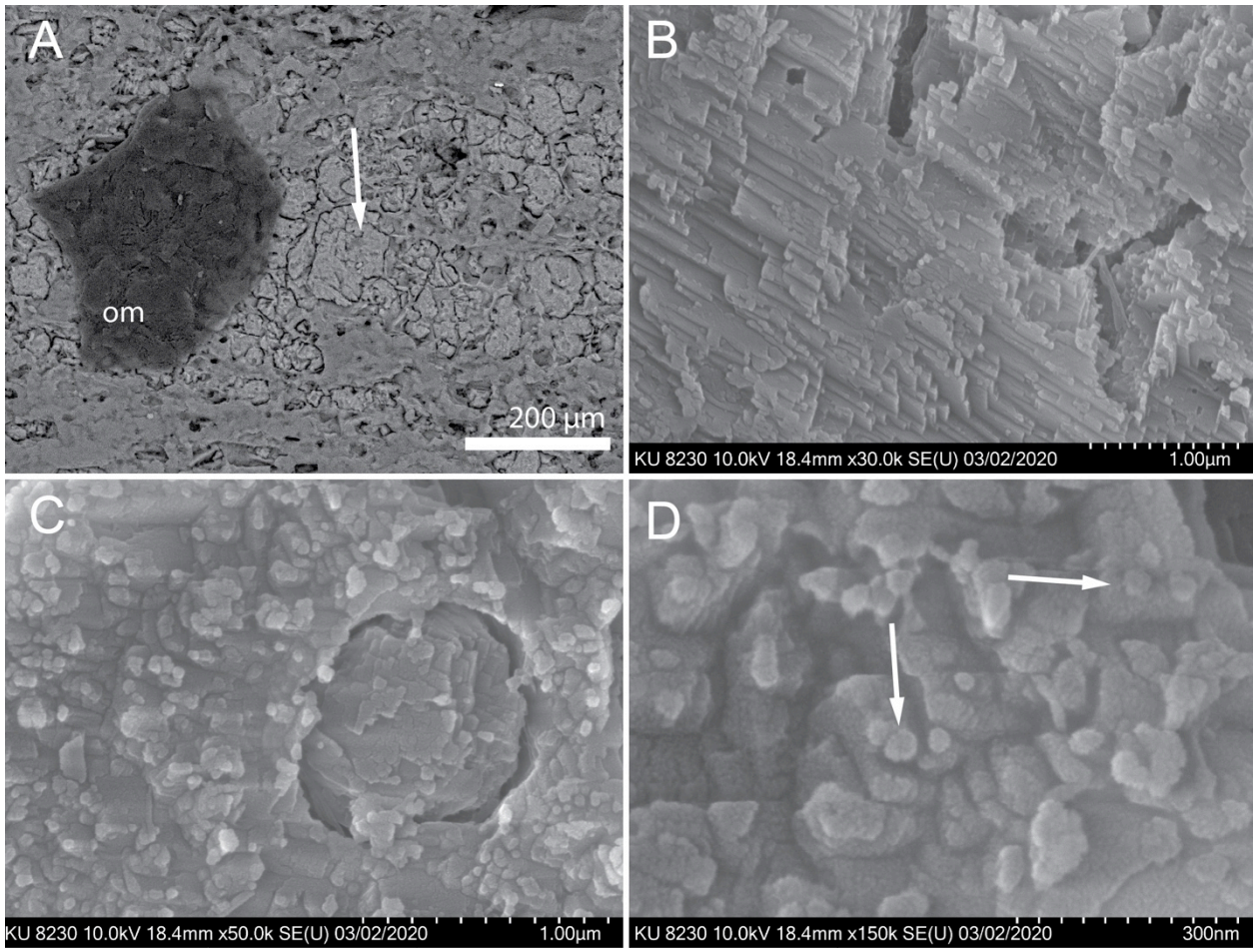
A
om
200 µm
B
KU 8230 10.0kV 18.4mm x30.0k SE(U) 03/02/2020
1.00µm
C
KU 8230 10.0kV 18.4mm x50.0k SE(U) 03/02/2020
1.00µm
D
KU 8230 10.0kV 18.4mm x150k SE(U) 03/02/2020
300nm

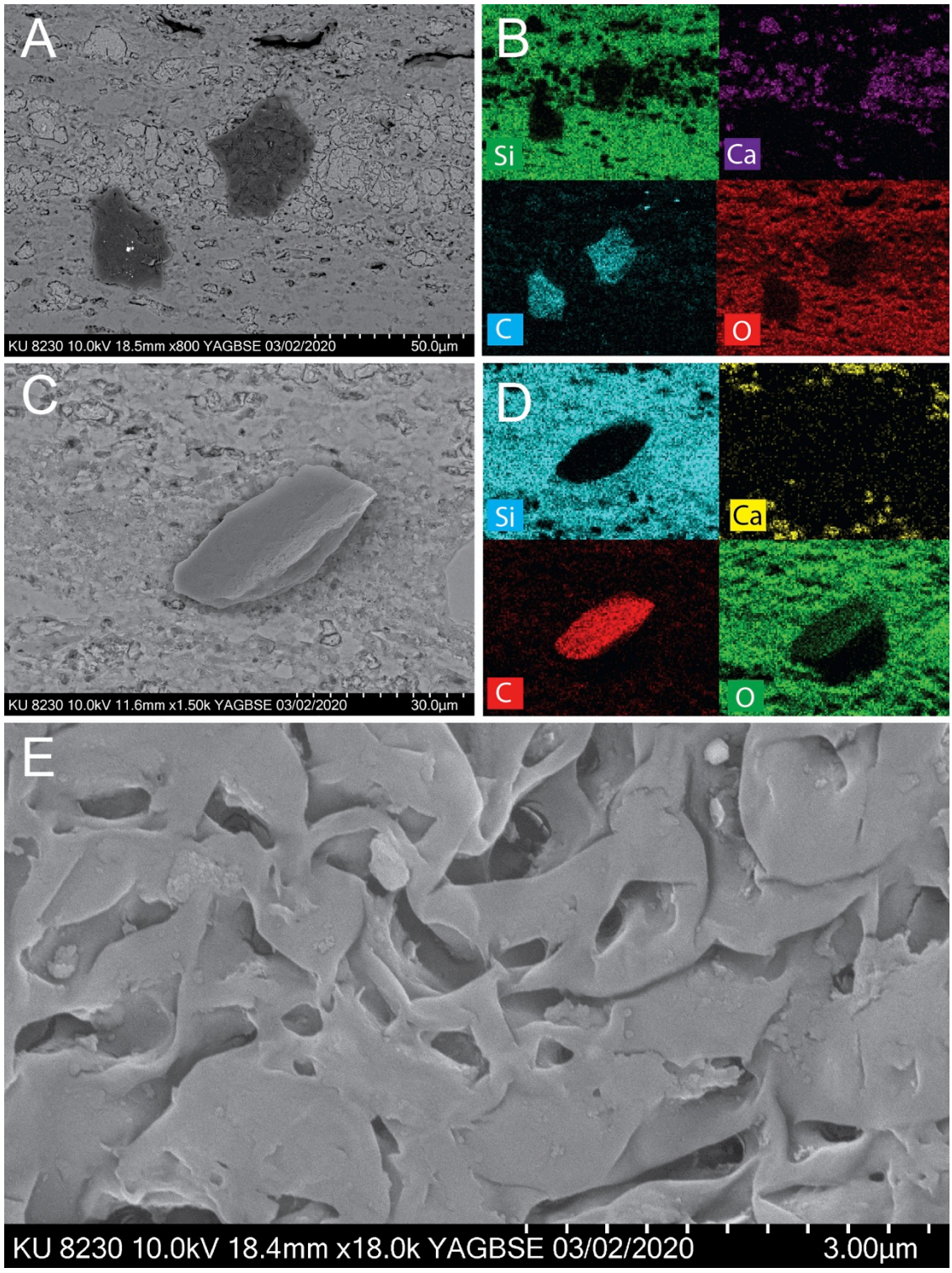
A
KU 8230 10.0kV 18.5mm x800 YAGBSE 03/02/2020
50.0µm
B
Si
Ca
C
O
C
KU 8230 10.0kV 11.6mm x1.50k YAGBSE 03/02/2020
30.0µm
D
Si
Ca
C
O
E
KU 8230 10.0kV 18.4mm x18.0k YAGBSE 03/02/2020
3.00µm

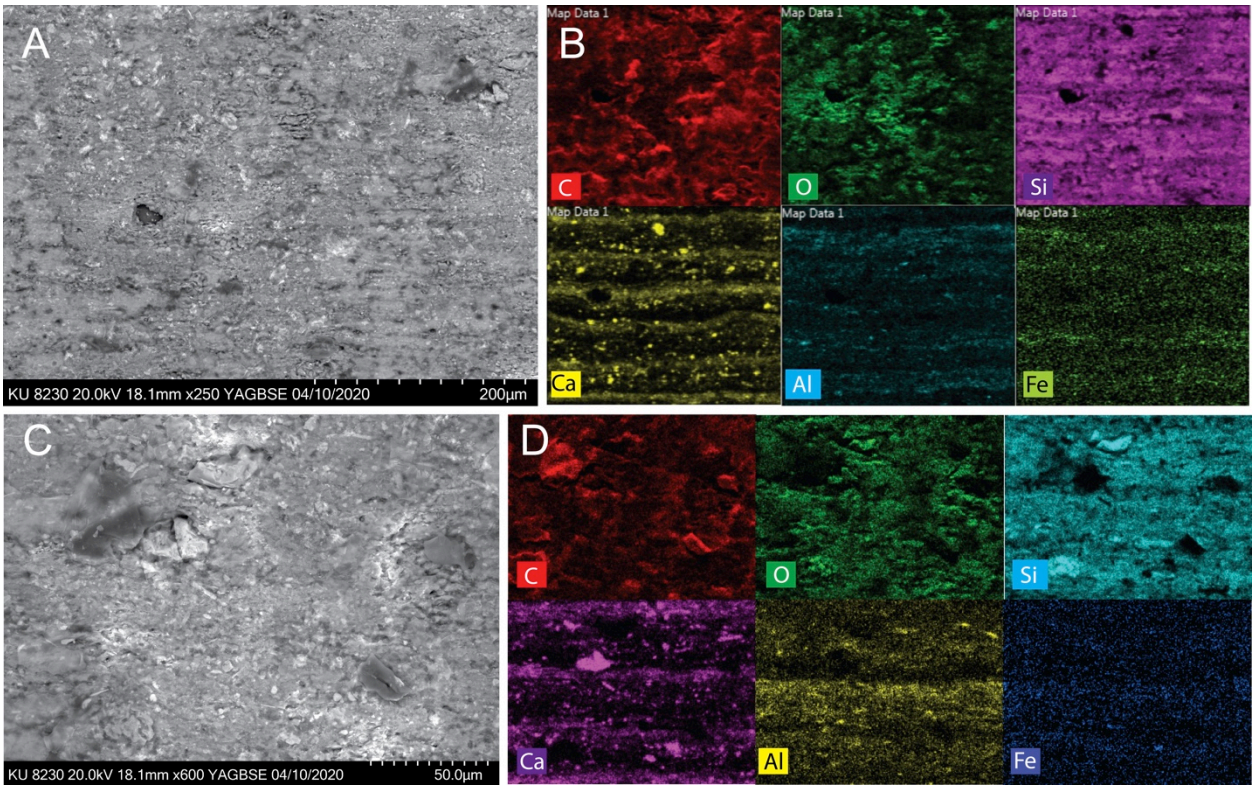
A
KU 8230 20.0kV 18.1mm x250 YAGBSE 04/10/2020
200µm
B
Map Data 1
C
O
Si
Ca
Al
Fe
C
KU 8230 20.0kV 18.1mm x600 YAGBSE 04/10/2020
50.0µm
D

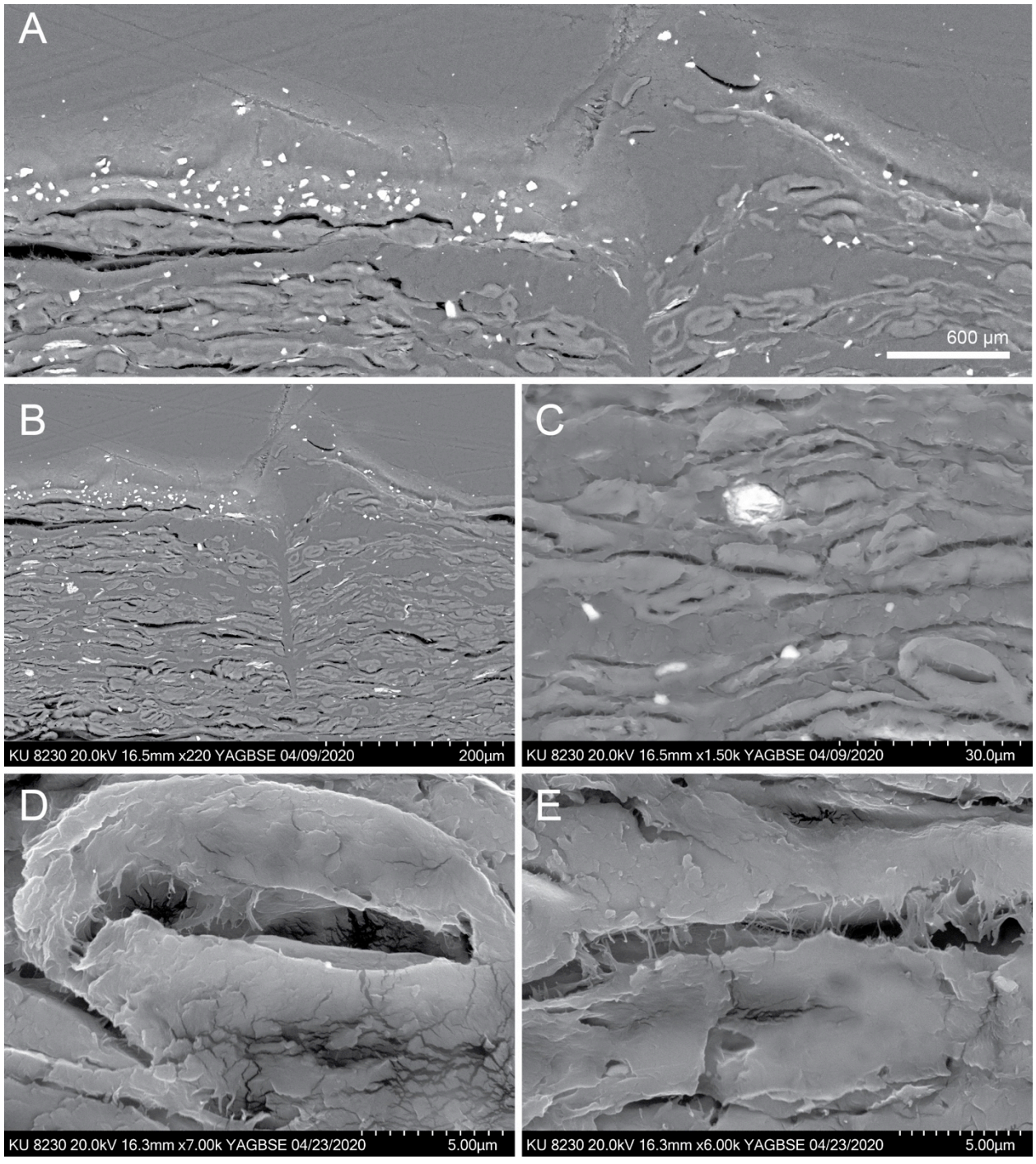
A
600 µm
B
KU 8230 20.0kV 16.5mm x220 YAGBSE 04/09/2020
200µm
C
KU 8230 20.0kV 16.5mm x1.50k YAGBSE 04/09/2020
30.0µm
D
KU 8230 20.0kV 16.3mm x7.00k YAGBSE 04/23/2020
5.00µm
E
KU 8230 20.0kV 16.3mm x6.00k YAGBSE 04/23/2020
5.00µm

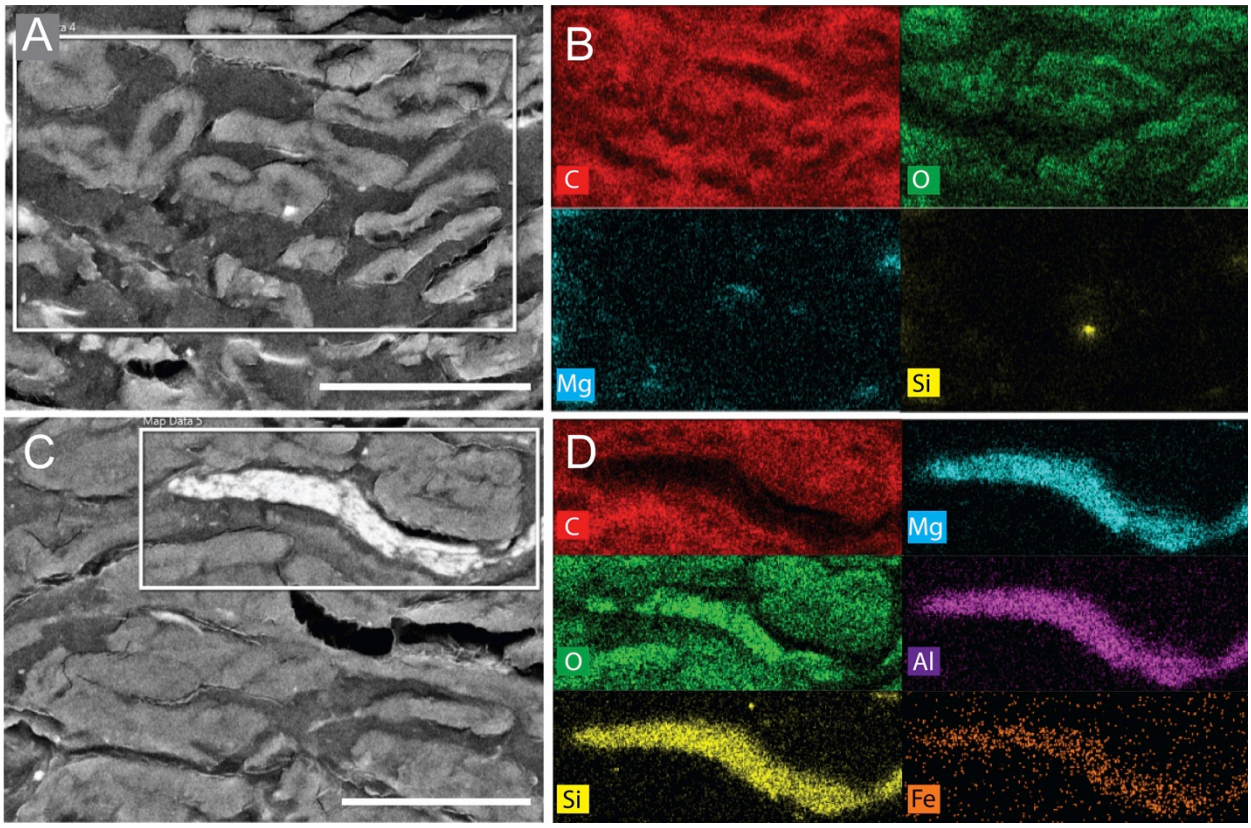
A
B
C
D
C
O
Mg
Si
C
Mg
O
Al
Si
Fe

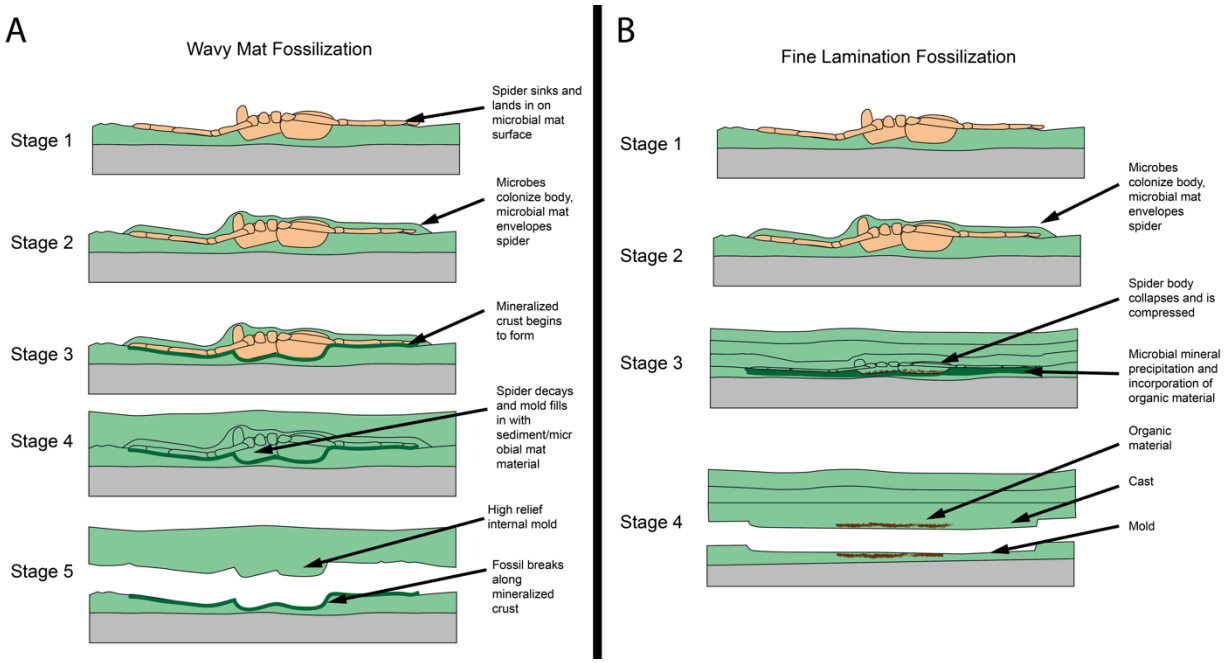
A
Wavy Mat Fossilization
Stage 1
Spider sinks and lands in on microbial mat surface
Stage 2
Microbes colonize body, microbial mat envelopes spider
Stage 3
Mineralized crust begins to form
Stage 4
Spider decays and mold fills in with sediment/microbial mat material
Stage 5
High relief internal mold
Fossil breaks along mineralized crust
B
Fine Lamination Fossilization
Stage 1
Stage 2
Microbes colonize body, microbial mat envelopes spider
Stage 3
Spider body collapses and is compressed
Microbial mineral precipitation and incorporation of organic material
Stage 4
Organic material
Cast
Mold

Chapter 6

TAPHONOMIC BIAS IN THE FOSSIL RECORD OF SPIDERS (ARANEAE) FROM LACUSTRINE DEPOSITS

MATTHEW R. DOWNEN[1] and PAUL A. SELDEN[1,2]

[1]Department of Geology, University of Kansas, Lawrence, Kansas 66045, USA

[2]Natural History Museum, Cromwell Road, London SW7 5BD, UK

email: mattdownen@ku.edu

(Formatted for submission to *PALAIOS*)

ABSTRACT:

The fossil record is heavily influenced by biases as a result of taphonomic filters and controls. These biases control the information gathered from the fossil record, and in turn, influences our perception of the diversity of life. Spiders are an extremely diverse and successful group with an extensive fossil record that is composed mostly of amber and lacustrine deposits. Amber is relatively well studied due to the high level of detail preserved in specimens. In contrast, the lacustrine fossil record of spiders has received little focus examining diversity and taphonomic biases. For the first time, the large-scale trends and biases of the record of fossil spiders preserved in lacustrine deposits are investigated. Fossil spider assemblages from six lacustrine deposits are examined and tested for biases related to diversity, size, life mode, and sex. In

general, lacustrine deposits are found to have relatively low diversity compared to amber. Fossil spiders from the Green River Formation and Kishenehn Formation of North America are smaller than other deposits, which typically have broader size distributions and larger spiders. Webweaving spiders are more abundant in deposits like the Crato Formation of Brazil, whereas ground-dwelling spiders are more common in the Aix-en-Provence Formation of France. Roughly equal proportions of males and females are found in lacustrine deposits, whereas amber is dominated by males. These results suggest that taphonomic biases do not influence the lacustrine record uniformly and provide a more complete view of the fossil record of spiders.

INTRODUCTION

Spiders (Araneae) today are extremely diverse (~48,500 species: World Spider Catalog, 2020), abundant, have a worldwide distribution, and a fossil record extending back nearly 300 million years. Although fossil spiders are relatively rare, over 1300 fossil spider species have been described (Dunlop et al., 2020). Most described fossil spiders are from amber, but there are also examples from lacustrine deposits (Penney and Selden, 2011). The fossil record of spiders in amber extends back to the Cretaceous, and is relatively well studied compared to spiders preserved in rock. Previous studies have examined the amber spider fossil record to investigate taxonomic and taphonomic biases that influence the composition of fossil spider assemblages (Penney, 2002a; Penney and Langan, 2006). Hitherto, no such studies have explicitly examined biases of fossil spiders preserved in rock, which accounts exclusively for the first 175 million years of the spider fossil record. There is likely a difference in the composition of spider assemblages from amber and rock due to differences in taphonomic pathways and controls. Here, the fossil record of spiders preserved in lacustrine deposits is investigated in an attempt to

answer two main questions: how similar are fossil spider assemblages in lacustrine deposits to each other, and how similar are lacustrine deposits assemblages and amber assemblages.

The only studies that have investigated biases in the fossil record of spiders have focused on Baltic and Dominican ambers, due mostly to the abundance of specimens that have been recovered. Spider assemblages in these amber deposits are dominated by active trunk-dwelling fauna and found to have a higher abundance of males (Penney, 2002a; Penney and Langan, 2006). The Dominican amber spider assemblage is also similar to modern Hispanolian spider diversity (Henwood, 1993; Penney, 2005). Whereas lacustrine deposits have considerably less material, they are still a valuable source of information on fossil spiders. Hundreds of fossil spiders have been recovered from some lacustrine deposits, such as the Green River Formation and Aix-en-Provence Formation. This paper seeks to summarize and quantify the diversity of fossil spiders preserved in lacustrine deposits and identify biases in fossil spider assemblages to better understand the history of this group.

Lacustrine taphonomy

The preservation of soft-bodied fossils like terrestrial arthropods typically requires special conditions like anoxia, rapid burial, or rapid mineralization, which are likely to occur in lacustrine environments. The taphonomic pathway for lacustrine deposits includes transportation, breaking the surface tension of the water, sinking, and burial. A number of factors and controls potentially remove material from the fossil record in lacustrine environments including decay, scavenging, and predation. For insects, the taphonomic pathway is relatively well studied, and includes multiple ways in which organic remains can enter the lacustrine environment (Smith, 2012; Tian et al., 2020).

The taphonomic pathway for spiders likely differs from insects, largely due to their lack of wings. The wings of insects allow for the possibility of entering a lake environment by flight. Spiders do not actively fly, but can disperse via ballooning which is a passive mode of aerial transport in which spiders release lines of silk to catch air currents and interact with Earth's electromagnetic field (Greenstone et al., 1987; Bishop, 1990; Morley and Robert, 2018). The wings of insects also assist in trapping insects in the water, but can also hinder them from sinking and making them susceptible to scavenging or predation (Martínez-Delclòs and Martinell, 1993; Smith, 2012). Spiders likely enter lakes most commonly by being washed in during floods and storms. This hypothesis is supported for other fossil arthropod assemblages like the Crato Formation of Brazil, in which fossils of whole plants with roots and attached soil are found, and suggest high-energy episodes.

The fossil record of spiders

The first 175 million years (Carboniferous–Jurassic) of the spider fossil record is preserved in rock, and is mainly represented mainly in fluvial, lagoonal, or lacustrine deposits. The earliest fossil spiders includes Mesothelae-like spiders from the Carboniferous, and the oldest definitive mesothele (suborder Mesothelae), *Palaeothele montceauensis* (Selden, 1996), from the Montceau-les-Mines, France (Carboniferous: 299 Ma) (Petrunkevitch, 1949; Selden, 1996). Mesothele spiders today are represented by a single family (8 genera, 131 species) and possess a segmented abdomen with spinnerets in the middle. In contrast, mygalomorph and araneomorph spiders (suborder Opisthothelae) are the most abundant and diverse spiders today and are characterized by non-segmented abdomens with posterior-positioned spinnerets. Mygalomorph and araneomorph spiders first appear in the Triassic, and are represented by relatively few fossils (Selden and Gall, 1992; Selden et al., 1999, 2009; Dalla Vecchia and

Selden, 2013; Raven et al., 2015). The oldest assemblages of fossil spiders, in terms of abundance, comes from the Jurassic Haifanggou Formation of China. Many of these spiders appear to be palpimanoids or cribellate web-weaving spiders (Selden et al., 2008, 2013, 2019). The most significant spider-bearing lacustrine deposits from the Cretaceous include the Crato Formation of Brazil, the Jinju Formation of Korea, and the Yixian Formation of China (Dunlop et al., 2007; Selden et al., 2016). Spiders from these deposits include many extant families in addition to several extinct families like Lagonomegopidae. The Cretaceous also marks the first appearance of spiders preserved in amber. Notable Cretaceous amber assemblages include the Burmese amber, Canadian amber, and New Jersey amber (Penney, 2002b, 2004a, 2004b, 2006; Selden and Ren, 2017). Many extant families had appeared by this time including, but not limited to, Araneidae, Uloboridae. Some families are exclusive to the Mesozoic. Lagonomegopidae are abundant in some ambers, and may have occupied the same ecospace as salticids do today (Guo et al., 2020). The Cenozoic fossil record of spiders includes several well-known lacustrine and amber deposits including the Green River and Florissant formations (Eocene) of North America and the Baltic (Eocene) and Domincan (Miocene) ambers of Europe and the Dominican Republic, respectively (Surdam and Wolfbauer, 1975; Meyer, 2003; Penney and Langan, 2006).

MATERIALS AND METHODS

The fossil spiders that are the focus of this study come from six lacustrine deposits. The sources of fossil spiders from the Crato Formation are the University of Kansas Biodiversity Institute & Natural History Museum Invertebrate Paleontology (KUMIP), the Natural History Museum Berlin (Berlin Museum für Naturkunde), and the American Museum of Natural History (AMNH). The sources of fossil spiders from the Green River Formation include the University

of Colorado Boulder Natural History Museum (UCM), the Smithsonian Institute National Museum of Natural History database (USNM), AMNH, and the Yale Peabody Museum database (YPM IP). Fossil spiders from the Florissant Formation come from UCM, YPM IP, and KUMIP. Fossil spiders from Aix-en-Provence come from the National Museum of Natural History France (Muséum national d'histoire naturelle; (MNHN). Fossil spiders from the Kishenehn Formation come from the USNM. Data on fossil spiders previously described from these lacustrine deposits and amber assemblages came from the literature.

For each fossil, data collected includes taxonomy, sex, body length, and life mode (Appendix 2). Most fossil spiders in lacustrine deposits are unable to be identified to species. Sex was categorized as male, female, indeterminate. Male spiders are characterized by the inflated distal segment of the pedipalp. Because genitalia are not fully developed in spiders until adulthood, it is difficult to differentiate between male and female spiders in juvenile stages, so spiders withought clear reproductive structures visible were classified as indeterminant. Body length was measured in Adobe Photoshop using the ruler tool. Each fossil was measured from the anterior-most margin of the carapace to the posterior-most margin of the abdomen. Due to the difficulty of taxonomic determination for many specimens, life mode was broken into two broad categories: Aerial web weavers and ground dwellers. Aerial web weavers have a mostly sedentary lifestyle and construct webs to capture prey, and they are typically recognized by long tapering legs with a distinctly shorter third pair of legs. Aerial web weaving spider families include Araneidae, Uloboridae, Tetragnathidae, and Linyphiidae. Ground-dwelling spiders do not weave webs for prey capture, and instead actively hunt or ambush prey on the ground or in foliage. They typically have more robust legs of subequal length. Ground-dwelling families are represented by Lycosidae, Pisauridae, Thomisidae, Palpimanidae, and Clubionidae.

Data visualization and statistical analyses were conducted in RStudio Version 1.2.5019. The Vegan library was installed to compute diversity statistics. Spiders were classified to family level, and because further classification is difficult, specimens were assigned to different morphospecies. To quantify the diversity for each lacustrine deposit the Shannon Index and Simpson Index. Evenness was calculated with Pielou's Evenness Index and Hill's ratio. To identify possible biases present in the fossil assemblages, three hypotheses related to size, life mode, and sex were tested. Body size distributions are hypothesized to be the same among the the different lacustrine deposits. An ANOVA was used to test whether the mean body length of spider assemblages from the formation was significantly different, and coupled with Tukey analysis to determine which means were significantly different. With respect to life mode, ground-dwelling spiders are hypothesixzed to be more abundant than web-spinning spiders, and the proportions of male spiders is hypothesized to be equal to female spiders in each lacsutrine deposit. For each formation, a binomial test was used to test for a significant difference in the counts of web-spinning spiders and ground-dwelling spiders as well as for sex. The testing of these hypotheses will reveal if certain types of spiders (based on size, life mode, and sex) are preferentially preserved in the lacsutrine deposits, a notion known as bias. R code can be found in Appendix 2.

RESULTS

Diversity in the spider fossil record

The fossil spider assemblages vary in their diversity (Table 1). The Green River and Florissant Formations are the most diverse with respect to family richness, and the Green River, Florissant, and Crato formations are the most diverse with respect to morphospecies richness. The Florissant

and Green River formations have the highest Simpson's Diversity Indices indicating higher diversity. With respect to evenness, all of the assemblages analyzed have relatively low values.

Several spider families are common across the deposits, whereas others are unique to the assemblages examined here. Araneidae is found in each of the deposits, Gnaphosidae is found in three, and Tetragnathidae and Thomisidae are found in two. Only three families have been identified from the Crato Formation, and one specimen is clearly a different family, but is unable to be determined thus far. Palpimanidae and Dipluridae are both only found in the Crato Formation. The Green River and Florissant formations overlap the most with respect to families represented, as Araneidae, Tetragnathidae, Gnaphosidae, and Thomisidae are present in both.

Taphonomic biases

The body lengths of fossil spiders vary between and within lacustrine deposits. In some deposits smaller sized spiders dominate, and for others, larger spiders are more abundant (Fig. 2A). The average body size across all deposits is 4.28 mm. The smallest spiders from any formation were less than 1 mm, and the largest were over 20 mm in length. The Green River and Kishenehn formations are dominated by smaller spiders with the Green River Formation being strongly dominated by spider 1–2 mm in length and, in contrast, the Aix-en-Provence, Florissant, and Crato formations generally have larger spiders and broader distributions. The spiders from the Haifanggou Formation have a mean body length of 4.09, and most spiders are 4–5.5 mm in length creating a relatively narrow peak similar to those of the Green River Formation. In addition, the mean body length of spiders is not the same across all lacustrine deposits ($p < 0.05$, Fig. 2B). The Florissant Formation has the largest mean body length (7.18 mm), but the largest individual spiders were from the Crato Formation (maximum body length = 22 mm). All of the

formations are significantly different from each other with respect to mean body length except the Green River and Kishenehn formations (Tukey $p = 0.99$), the Crato and Florissant formations (Tukey $p = 0.43$), and the Haifanggou and Aix-en-Provence formations (Tukey $p = 0.98$), although the Aix-en-Provence Formation has a broader distribution.

With respect to life mode, the proportions of web-weaving spiders and ground-dwelling spiders also differ across the deposits (Fig. 3). In the Aix-en-Provence Formation there are significantly more ground-dwelling spiders ($p = 0.0002$), and in the Green River, Kishenehn, and Crato formations there are more web-weaving spiders (significant at $p < 0.05$). The Florissant Formation has a similar ratio of web-weaving and ground-dwelling spiders.

With respect to sex, the proportions of female, male, and indeterminate sex also varied within and among the fossil assemblages (Fig. 4). A Chi-square Goodness of Fit test reveals there is a significant difference in the proportions of sex for all deposits (significant at $p < 0.05$). An exact binomial test between males and females results in a significant difference in proportions only for the Crato Formation ($p = 0.0066$), and all other lacustrine deposits have similar proportions of male and female. When female and male are binned, and compared to the indeterminate group with an exact binomial test, the Kishenehn ($p = 0.77$) and Haifanggou ($p = 0.28$) formations are the only deposits without a significant difference in the proportions of the two groups. The Aix-en-Provence Formation has only a slight significant difference between the two groups ($p = 0.03$). Across all of the deposits, there are significantly more spiders of indeterminate sex compared to determined sex (male and female) except in the Haifanggou Formation.

DISCUSSION

The differences and similarities in diversity between the lacustrine deposits likely is related to age of the deposits, paleoenvironmental factors, and other taphonomic controls. The orbweaving families (Araneidae, Uloboridae, Tetragnathidae) are diverse and abundant today, and have a fossil record that extends into the Cretaceous. Orbweaving lineages are estimated to have appeared at 213 Ma in the Jurassic (Selden et al., 2016; Garrison et al., 2016). The spider fauna of other Mesozoic lacustrine deposits, like the Haifanggou Formation and the Jinju Formation of Korea (Cretaceous), are composed primarily of cribellate webweaving and palpimanoid spiders, so the presence of a palpimanid in the Crato Formation is not unexpected. Lycosidae and Gnaphosidae are part of the RTA clade, an extremely diverse and abundant group of spiders today, with an origin hypothesized in the Cretaceous (Garrison et al., 2016; Fernández et al., 2018). The lack of any recovered fossils of the major RTA clade families found in rocks predating the K-Pg extinction event is inconsistent with this hypothesis, but may suggest the RTA clade spiders were not as abundant. While many lineages of spiders may have appeared in the Cretaceous, a major faunal turnover from the Mesozoic to the Cenozoic is supported by the fossil record from this study and others (Magalhaes et al., 2019).

The Green River, Kishenehn, and Florissant formations paleoenvironments are interpreted to be relatively similar. These deposits have diverse plant and animal assemblages that reflect a subtropical to tropical lacustrine setting. A well-known trend is an increase in diversity in the tropics compared to higher latitudes (Hillebrand, 2004). In addition, the habitat heterogeneity hypothesis states that a greater complexity in vegetation is correlated with increased species richness, and this true for spiders (Greenstone, 1984; Jiménez-Valverde and Lobo, 2007). The surrounding environment likely supported a diverse community of spiders in close proximity to the paleolakes, and thus, led to a more diverse fossil record in these deposits.

In contrast, the Crato Formation paleoenvironment is interpreted to be a hypersaline lacustrine setting in a semi-arid to arid climate (Heimhofer et al., 2010). The habitat immediately surrounding the Crato paleolake may not have supported a spider community as diverse as the other deposits, although a jigsaw of habitats, including more humid environments, in the hinterland is hypothesized to have existed based on other arachnid fossils like scorpions and amblypygids (Dunlop and Barov, 2005; Menon, 2007).

There is no bias with respect to size shared by all of the examined lacustrine deposits, and instead, spiders of varying body sizes seem to be preferentially preserved in the fossil assemblages. Both the Green River and Kishenehn formations have significantly smaller spiders than the other deposits, which is consistent with the overall size of the terrestrial arthropod assemblage from the Kishenehn Formation. The Kishenehn has an abundance of very small insects including beetles and fairy wasps and a clear size bias influence the fossil assemblage (Greenwalt et al., 2014). Many of the spiders from the Green River Formation are likely juveniles of the same species, which may explain the narrow distribution of small body size. The Green River and Haifanggou formations, while not statistically similar with respect to size, both have tall and narrow density curves, suggesting these deposits are the most influenced by a bias with respect to size in general, and the Green River and Kishenehn formations are biased toward smaller sized spiders.

The large body size in the Crato and Florissant formations is partially related to taxonomy. In both deposits, nephiline spiders are present. Nephilines are the largest aerial web weaving spiders found today and many of these spiders reach a body length of two centimeters. While these deposits contain very large spiders, the largest fossil spiders ever recovered are *Mongolarachne jurassica* Selden, Shih & Ren, 2013 from the Haifanggou Formation. The Aix-

en-Provence Formation, not included in the diversity analysis, contains mostly tetragnathid and lycosid spiders, both of which can be relatively large conspicuous spiders. For most of the lacustrine deposits examined, the bias with respect to body size seems to be influenced by taxonomy.

Ground-dwelling spiders were hypothesied to be more abundant than web-weaving spiders across the lacustrine deposits, yet in the fossil assemblages examined here, ground-dwelling spiders were only more abundant in the Aix-en-Provence and Florissant formations. Based on how spiders are believed to be washed into lake settings, ground-dwelling spiders should be more likely to end up being deposited in lakes. In contrast, web-weaaving spiders are somewhat removed from the ground since many weave aerial webs to capture prey. Most of the web-weaving spiders in these assemblages wove aerial webs to capture prey (Araneidae and Uloboridae) while relatively few (Dipluridae) mostly wove webs on the ground.

The differences in life mode may be the result of morphology and taxonomy. Many ground-dwelling spiders are covered in dense setae, especially on the tarsi of the legs, and are thus more resistant to breaking the surface tension of water. Some ground-dwelling spiders, for example Pisauridae, are even semi-aquatic, and live their lives on bodies of water, yet do not sink because of the dense setae on their legs and abdomens that creates a hydrophobic surface. Many aerial web-spinning spiders have less setal density, and therefore, are more likely to break the surface tension of water. The water-walking ability of spiders was previously investigated, and revealed that some families of spiders are more apt to moving on the water surface (Stratton et al., 2004; Bush and Hu, 2006). Web-weaving families including Araneidae, Tetragnathidae, Linyphiidae, Theridiidae, and Dipluridae exhibited variable hydrophobicity and more limited movement on the surface of water. In contrast, ground-dwelling families including Lycosidae,

Pisauridae, were more hydrophobic and more likely to walk or row on the surface of water. Ground-dwelling spiders, while more likely to get washed into a lake, are also more likely to escape breaking the surface tension and sinking, and thus less likely to be preserved as fossils in lacustrine deposits (Tian et al., 2020).

In both the Aix-en-Provence and Florissant formations, the reason for the higher abundance of ground-dwelling spiders likely is related to the depositional environment and other taphonomic controls. The preservation pathway of terrestrial arthropods in the Florissant Formation has been linked to the presence of mucilaginous diatom mats that trapped arthropods in the water and helped them sink (O'Brien et al., 2008; Thoene, 2011). A similar process may have been active during the deposition of the Aix-en-Provence Formation, which also had significant microbial activity. In these depositional settings, biofilms or other sticky microbial products likely trapped spiders and hindered ground-dwelling spiders that otherwise may have been able to escape.

Equal proportions of males and females were expected in lacustrine deposits, and was true for all lacustrine deposits except the Crato Formation. The significant number of spiders of indeterminate sex are the result of taphonomic controls on preservation and the likely abundance of juveniles, as the sex is difficult to determine in immature spiders. The sex of spiders from the Crato Formation is particularly difficult to determine due to the abundant curled leg orientation, a taphonomic control. The pedipalps, male reproductive appendages, of most spiders are curled and not visible, likely the result of hypersaline conditions in the paleolake (Downen et al., 2016). In other deposits, the preservation state has resulted in unclear preservation of reproductive structures. The Aix-en-Provence spiders are typically preserved as molds and modified palps or epigynes are not often visible. The presence of juveniles also contributes to the abundance of

spiders of indeterminate sex. In the Crato Formation, most of the spiders appear to be of the same species, but vary in size, representing an assemblage of spiders in various stages of maturity. In the Green River Formation, there is a large proportion of very small (~1 mm) spiders that all appear to be juveniles of the same species. This abundance of small juveniles may represent an assemblage of newly hatched spiders that subsequently washed into the paleolake, similar to a mass mortality event, although this cannot be confirmed because it is not known if the fossils all came from the same horizon within the unit.

Fossil spiders in amber

The amber record is much more studied than lacustrine deposits, and the exceptional preservation and high level of detail of fossil spiders in amber allows for more precise classification and study. Amber deposits are much more taxonomically diverse, with many more families and species recognized. Both the Baltic and Dominican ambers have over 40 families represented, and over 30 families have been identified from in Burmese amber (Penney and Langan, 2006); World Spider Catalog, 2020). Because fossil spiders in lacustrine deposits are typically preserved as compression fossils and do not represent the original 3D form of the organism, details important for taxonomic classification often are lost or not visible, and thus, identification to even at the family level can be challenging.

While the lacustrine record seems to contain a mixed assemblage of aerial web-weaving spiders and ground-dwelling spiders, amber has a bias toward tree-dwelling spiders. Dominican amber is dominated by space-web weavers (Theridiidae, Dictynidae, Pholcidae, etc.) and stalkers (Salticidae, Oxyopidae, Mimetidae), and orbweavers (Penney, 2002a). These types of spiders would likely be found on or around trees and more likely to be preserved in amber. Ground hunters (Lycosidae) and ambush predators (Thomisidae) were less abundant as amber inclusions

(Penney, 2002a). A bias toward web weavers and active hunters on trees is clearly present in the amber record and demonstrated in previous studies. This bias is in contrast to what has been observed here in lacustrine assemblages, which seem to capture more ground-dwelling spiders than amber, with the exception of orbweaving spiders.

Previous studies have found that mean body size in assemblages from the Baltic and Dominican ambers is small, 3.03 mm and 2.06 mm, respectively (Penney and Langan, 2006). A bias with respect to body size likely exists in amber due to the nature of the mode of preservation. In general, larger organisms are less likely to be entombed or trapped in amber because they can escape or require a larger volume of resin. In lacustrine deposits, larger spiders are heavier and may be more likely to break the surface tension and sink.

The sex ratios of the lacustrine assemblages differ from those observed in amber, which have been shown to have a bias toward males (Penney, 2002a). Male spiders are more likely to wander in search of mates, and thus, more likely to become trapped in amber, and in particular males of web-weaving families. For lacustrine deposits, which likely capture more ground-dwelling cursorial spiders, or at least spiders that do not weave a web and remain stationary, both males and females have an equal chance of becoming washed into a lake.

A final bias that should be mentioned is collection and description bias, which has a personal or human component, and is particularly manifested in fossil spider taxonomy. Juvenile spiders are typically more difficult to classify because reproduive structures are not fully developed, while adult males are the more conspicuous due to their inflated pedipalps. Because many species and even families of spiders are distinguished by the palp of the male, those fossils may be favored for collection or purchase and may lead to a bias toward describing male or adult spiders, even though juveniles are shown to be a major component of some fossil assemblages in

this study. Previous studies have shown that all specimens of fossil insects, regardless of the state of preservation, are valuable, and this should be considered for spiders with respect to juveniles versus adults (Smith, 2012).

CONCLUSION

Spiders typically are preserved as fossils as amber inclusions and in lacustrine deposits, and both are influenced by different taphonomic biases. The fossil record of spiders preserved in lacustrine deposits is found to vary across deposits with respect to body size, life mode, and sex. The Green River and Kishenehn formations are dominated by smaller spiders, while the largest spiders are found in the Crato and Florissant Formations. Ground-dwelling spiders are found to comprise a larger portion of lacustrine deposits in general when compared to amber, but some lacustrine deposits, like the Crato Formation, are dominated by aerial webweaving spiders. Lacustrine deposits also capture relatively equal proportions of male and female spiders, while some deposits like Crato and Green River have a high abundance of juveniles. Future investigations into the taphonomic biases influencing fossil spider assemblages that include the Burmese amber and the further revision of lacustrine spiders will provide a clearer picture of spider diversity and evolution.

LITERATURE CITED

Bishop, L., 1990, Meteorological Aspects of Spider Ballooning: Environmental entomology, v. 19, p. 1381–1387.

Bush, J.W.M., and Hu, D.L., 2006, Walking On Water: Biolocomotion at the Interface: Annual

review of fluid mechanics, v. 38, p. 339–369.

Dalla Vecchia, F., and Selden, P., 2013, A Triassic spider from Italy: Australasian plant pathology: Acta Palaeontologica Polonica 58, 325–330.

Downen, M.R., Selden, P.A., and Hasiotis, S.T., 2016, Spider leg flexure as an indicator for estimating salinity in lacustrine paleoenvironments: Palaeogeography, palaeoclimatology, palaeoecology, v. 445, p. 115–123.

Dunlop, J.A., and Barov, V., 2005, A new fossil whip spider (Arachnida: Amblypygi) from the Crato Formation of Brazil: Revista Ibérica de Aracnología, v. 12, p. 53–62.

Dunlop, J.A., Menon, F., Selden, P.A., Martill, D.M., Bechly, G., and Loveridge, R.F., 2007, Arachnida: spiders, scorpions and allies: In Martill, D.M. The Crato Fossil Beds of Brazil: Window into an Ancient World: Cambridge University Press, Cambridge, UK, p. 103–134.

Fernández, R., Kallal, R.J., Dimitrov, D., Ballesteros, J.A., Arnedo, M.A., Giribet, G., and Hormiga, G., 2018, Phylogenomics, Diversification Dynamics, and Comparative Transcriptomics across the Spider Tree of Life: Current biology: v. 28, p. 1489–1497.e5.

Garrison, N.L., Rodriguez, J., Agnarsson, I., Coddington, J.A., Griswold, C.E., Hamilton, C.A., Hedin, M., Kocot, K.M., Ledford, J.M., and Bond, J.E., 2016, Spider phylogenomics: untangling the Spider Tree of Life: PeerJ, v. 4, p. e1719.

Greenstone, M.H., 1984, Determinants of web spider species diversity: Vegetation structural diversity vs. prey availability: Oecologia, v. 62, p. 299–304.

Greenstone, M.H., Morgan, C.E., Hultsch, A.-L., Farrow, R.A., and Dowse, J.E., 1987,

Ballooning Spiders in Missouri, USA, and New South Wales, Australia: Family and Mass Distributions: The Journal of arachnology, v. 15, p. 163–170.

Greenwalt, D.E., Rose, T.R., Siljestrom, S.M., Goreva, Y.S., Constenius, K.N., and Wingerath, J.G., 2014, Taphonomy of the fossil insects of the middle Eocene Kishenehn Formation: Acta palaeontologica Polonica, v. 60, p. 931–948.

Guo, X., Selden, P.A., Shih, C., and Ren, D., 2020, Two new lagonomegopid spiders (Arachnida: Araneae) from the mid-Cretaceous of Northern Myanmar, with comments on the superfamilial placement of Lagonomegopidae: Cretaceous Research, v. 106, p. 104257.

Heimhofer, U., Ariztegui, D., Lenniger, M., Hesselbo, S.P., Martill, D.M., and Rios-Netto, A.M., 2010, Deciphering the depositional environment of the laminated Crato fossil beds (Early Cretaceous, Araripe Basin, North-eastern Brazil): Sedimentology, v. 57, p. 677–694.

Henwood, A.A., 1993, Ecology and taphonomy of Dominican Republic amber and its inclusions: Lethaia, v. 26, p. 237–245.

Hillebrand, H., 2004, On the generality of the latitudinal diversity gradient: The American naturalist, v. 163, p. 192–211.

Jiménez-Valverde, A., and Lobo, J.M., 2007, Determinants of local spider (Araneidae and Thomisidae) species richness on a regional scale: climate and altitude vs. habitat structure: Ecological entomology, v. 32, p. 113–122.

Magalhaes, I.L.F., Azevedo, G.H.F., Michalik, P., and Ramírez, M.J., 2019, The fossil record of spiders revisited: implications for calibrating trees and evidence for a major faunal turnover

since the Mesozoic: Biological reviews of the Cambridge Philosophical Society, doi: 10.1111/brv.12559. http://dx.doi.org/10.1111/brv.12559.

Martínez-Delclòs, X., and Martinell, J., 1993, Insect taphonomy experiments. Their application to the Cretaceous outcrops of lithographic limestones from Spain: Kaupia, v. 2, p. 133–144.

Menon, F., 2007, Higher systematics of scorpions from the Crato Formation, Lower Cretaceous of Brazil: Palaeontology, v. 50, p. 185–195.

Meyer, H.W., 2003, The fossils of Florissant: Smithsonian Books Washington, DC.

Morley, E.L., and Robert, D., 2018, Electric Fields Elicit Ballooning in Spiders: Current biology: CB, v. 28, p. 2324–2330.e2.

O'Brien, N.R., Meyer, H.W., and Harding, I.C., 2008, The role of biofilms in fossil preservation, Florissant Formation, Colorado: Paleontology of the Upper Eocene Florissant Formation, Colorado, v. 435, p. 19.

Penney, D., 2004a, Cretaceous Canadian amber spider and the palpimanoidean nature of lagonomegopids: Acta palaeontologica Polonica, v. 49. http://agro.icm.edu.pl/agro/element/bwmeta1.element.agro-article-2a964df3-561b-4b99-89d1-86ac78c1b587/c/app49-579.pdf.

Penney, D., 2006, Fossil Oonopid Spiders in Cretaceous ambers from Canada and Myanmar: Palaeontology, v. 49, p. 229–235.

Penney, D., 2005, Importance of Dominican Republic amber for determining taxonomic bias of fossil resin preservation—A case study of spiders: Palaeogeography, palaeoclimatology,

palaeoecology, v. 223, p. 1–8.

Penney, D., 2004b, New spiders in Upper Cretaceous amber from New Jersey in the American Museum of Natural History (Arthropoda: Araneae): Palaeontology, v. 47, p. 367–375.

Penney, D., 2002a, Paleoecology of Dominican Amber Preservation: Spider (Araneae) Inclusions Demonstrate a Bias for Active, Trunk-Dwelling Faunas: Paleobiology, v. 28, p. 389–398.

Penney, D., 2002b, Spiders in Upper Cretaceous Amber from New Jersey (Arthropoda: Araneae): Palaeontology, v. 45, p. 709–724.

Penney, D., and Langan, A.M., 2006, Comparing amber fossil assemblages across the Cenozoic: Biology letters, v. 2, p. 266–270.

Penney, D., and Selden, P., 2011, Fossil Spiders: The Evolutionary History of a Mega-diverse Order: Siri Scientific Press, 127 p.

Petrunkevitch, A., 1949, A study of Palaeozoic Arachnida: Connecticut Academy of Arts and Sciences.

Raven, R.J., Jell, P.A., and Knezour, R.A., 2015, Edwa maryae gen. et sp. nov. in the Norian Blackstone Formation of the Ipswich Basin—the first Triassic spider (Mygalomorphae) from Australia: Alcheringa: An Australasian Journal of Palaeontology, v. 39, p. 259–263.

Selden, P.A., 1996, First fossil mesothele spider, from the Carboniferous of France: https://kuscholarworks.ku.edu/handle/1808/26571. Checked October 2019.

Selden, P.A., Anderson, H.M., and Anderson, J.M., 2009, A Review of the Fossil Record of

Spiders (Araneae) with Special Reference to Africa, and Description of a New Specimen from the Triassic Molteno Formation of South Africa: African invertebrates, v. 50, p. 105–116.

Selden, P.A., Anderson, J.M., Anderson, H.M., and Fraser, N.C., 1999, Fossil araneomorph spiders from the Triassic of South Africa and Virginia: The Journal of arachnology, v. 27, p. 401–414.

Selden, P.A., Diying, H., and Dong, R., 2008, Palpimanoid spiders from the Jurassic of China: The Journal of arachnology, v. 36, p. 306–321.

Selden, P.A., and Gall, J.-C., 1992, A Triassic mygalomorph spider from the northern Vosges, France: https://kuscholarworks.ku.edu/handle/1808/8350. Checked November 2019.

Selden, P.A., Huang, D., and Garwood, R.J., 2019, New spiders (Araneae: Palpimanoidea) from the Jurassic Yanliao Biota of China: Journal of Systematic Palaeontology, p. 1–49.

Selden, P.A., and Ren, D., 2017, A review of Burmese amber arachnids: The Journal of arachnology, v. 45, p. 324–343.

Selden, P.A., Ren, D., and Shih, C., 2016, Mesozoic cribellate spiders (Araneae: Deinopoidea) from China: Journal of Systematic Palaeontology, v. 14, p. 49–74.

Selden, P.A., Shih, C., and Ren, D., 2013, A giant spider from the Jurassic of China reveals greater diversity of the orbicularian stem group: Die Naturwissenschaften, v. 100, p. 1171–1181.

Smith, D.M., 2012, Exceptional preservation of insects in lacustrine environments: Palaios, v.

27, p. 346–353.

Stratton, G.E., Suter, R.B., and Miller, P.R., 2004, Evolution of water surface locomotion by spiders: a comparative approach: Biological journal of the Linnean Society. Linnean Society of London, v. 81, p. 63–78.

Surdam, R.C., and Wolfbauer, C.A., 1975, Green River Formation, Wyoming: A Playa-Lake Complex: GSA Bulletin, v. 86, p. 335–345.

Thoene, J.J., 2011, Taphonomy of Insects from the Florissant Formation, Colorado:University of Colorado http://files.cfc.umt.edu/cesu/NPS/CU/2008/08Smith_FLFO_%20fossil%20excavation_MSc_thesis.pdf.

Tian, Q., Wang, S., Yang, Z., McNamara, M.E., Benton, M.J. and Jiang, B., 2020. Experimental investigation of insect deposition in lentic environments and implications for formation of Konservat Lagerstätten. Palaeontology, p.1–14.

LIST OF TABLES AND FIGURES

Density plots showing distributions with smaller spiders in the Green River Formation. B) Box plot of body sizes of of lacustrine deposits with means as bold black line and outliers as grey dots.

Figure 3. Plot of life modes of fossil spiders in lacustrine deposits. Web (blue) represents webweaving spiders like Araneidae and Dipluridae. Ground (brown) represents spiders that do not weave webs for prey capture, and instead, live on the ground.

Figure 4. Plot of sex of fossil spiders in lacustrine deposits. Indeterminate consists of juveniles and spiders in which the sex is unable to be determined.

Formation	Family Richness	Morphospecies Richness	Simpson's Index	Pielou Evenness	Hill's Index of Evenness
Florissant	7	10	0.8	0.28	0.38
Kishenehn	2	3	0.61	0.46	0.44
Green River	7	13	0.72	0.26	0.34
Crato	4	10	0.27	0.26	0.17

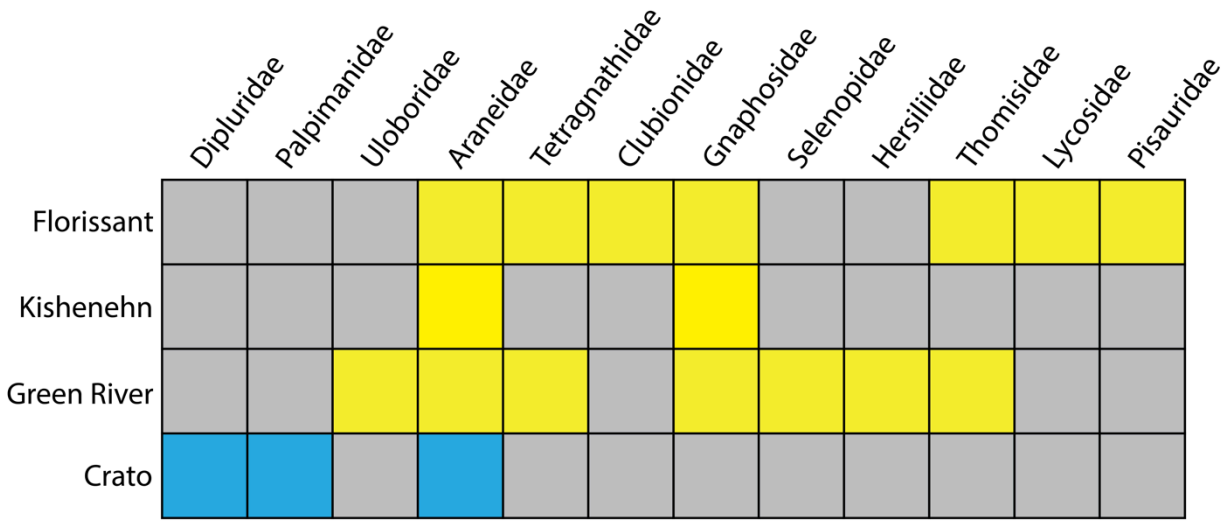
Dipluridae
Palpimanidae
Uloboridae
Araneidae
Tetragnathidae
Clubionidae
Gnaphosidae
Selenopidae
Hersiliidae
Thomisidae
Lycosidae
Pisauridae
Florissant
Kishenehn
Green River
Crato

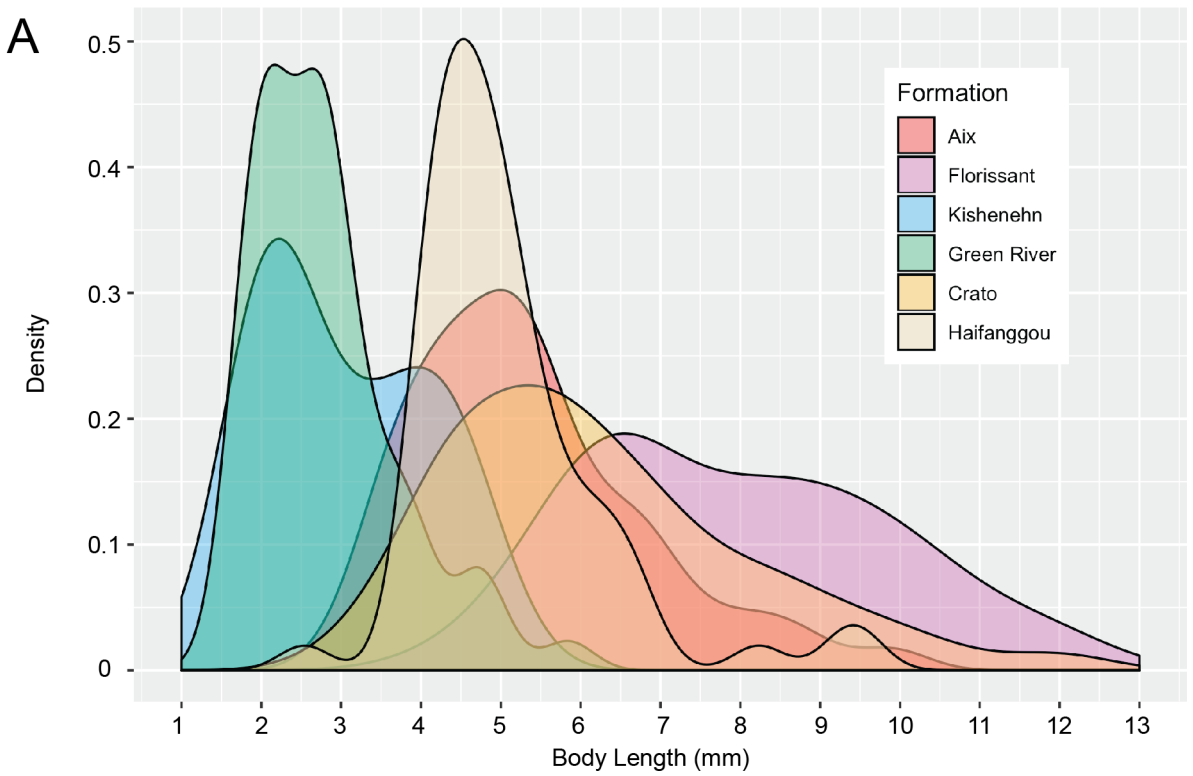
A
Density
0.5
0.4
0.3
0.2
0.1
0
1
2
3
4
5
6
7
8
9
10
11
12
13
Body Length (mm)
Formation
Aix
Florissant
Kishenehn
Green River
Crato
Haifanggou

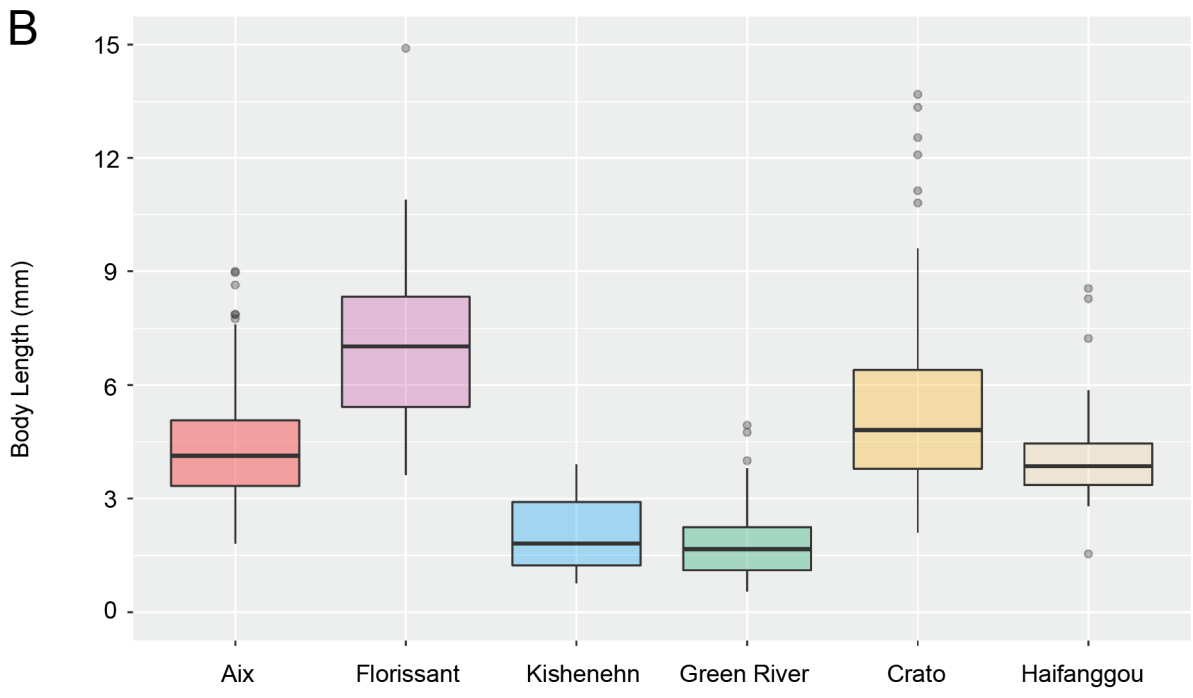
B
Body Length (mm)
15
12
9
6
3
0
Aix
Florissant
Kishenehn
Green River
Crato
Haifanggou

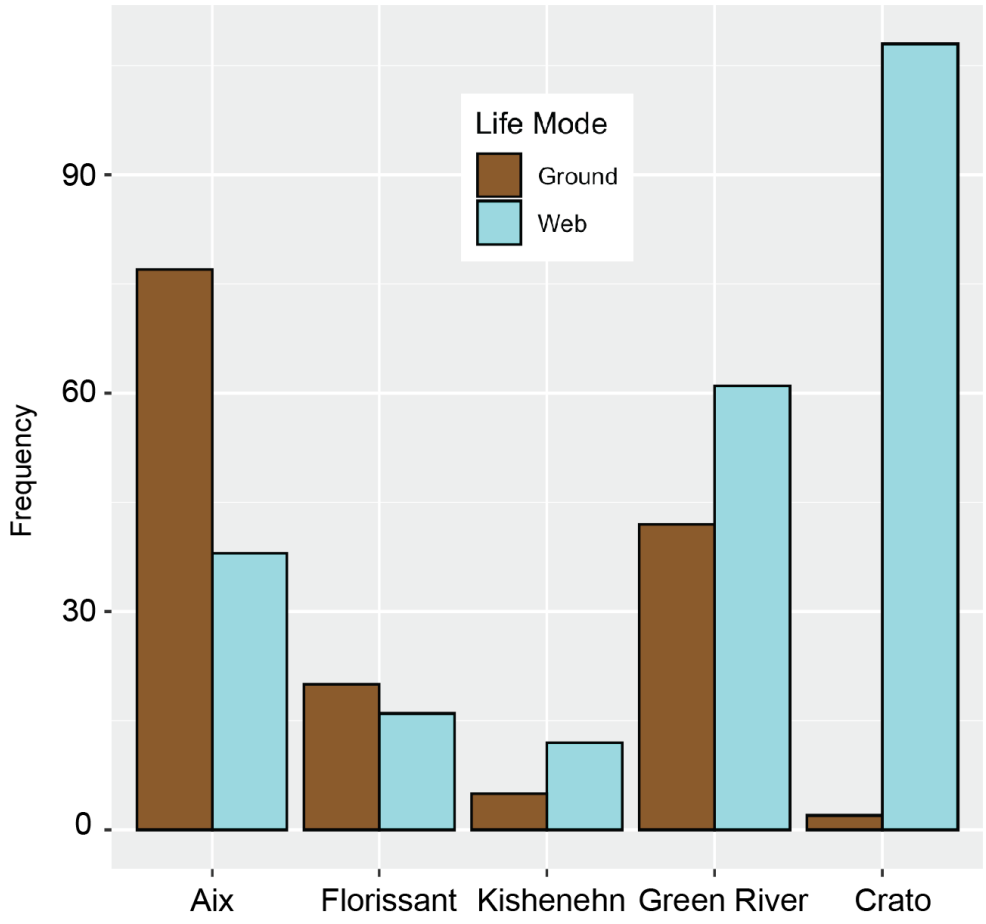
Life Mode
Ground
Web
Frequency
90
60
30
0
Aix
Florissant
Kishenehn
Green River
Crato

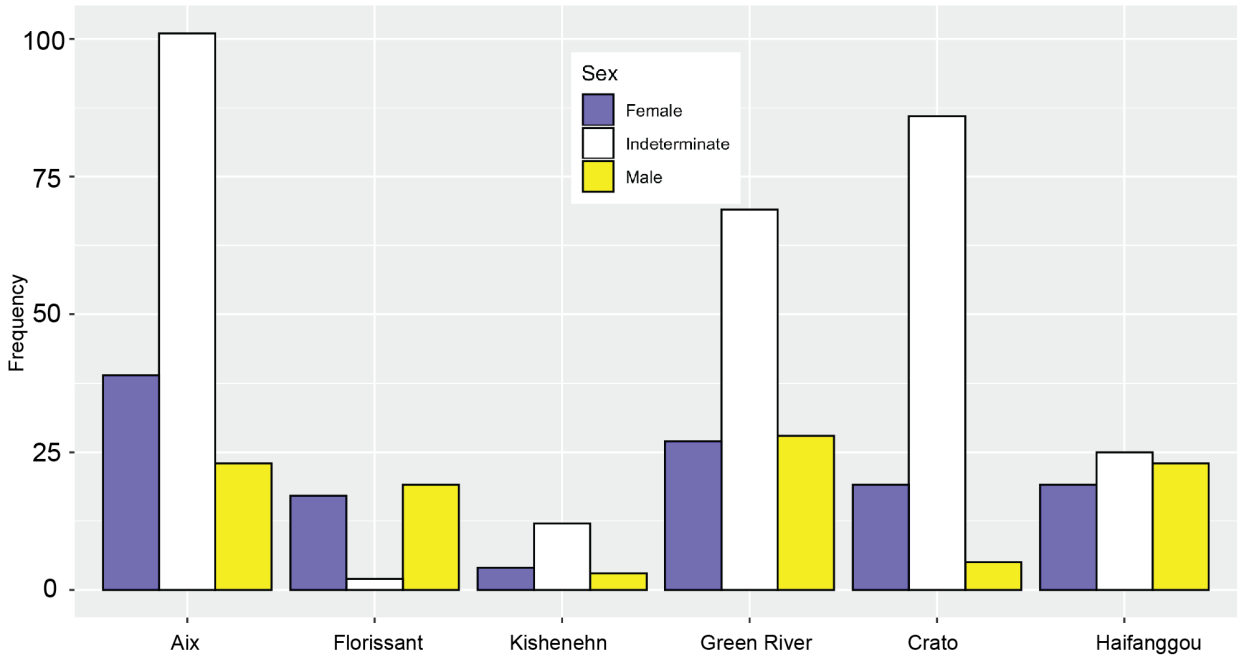
Sex
Female
Indeterminate
Male
Frequency
100
75
50
25
0
Aix
Florissant
Kishenehn
Green River
Crato
Haifanggou

Conclusion

The lacustrine deposits in this study are sites of exceptional preservation that are facilitated by microbes. They serve as important sources of information regarding the completeness of the spider fossil record. The previously poorly defined taphonomic pathway of the Aix-en-Provence Formation has an abundance of evidence supporting the presence of microbial mats that are directly linked to the preservation of fossil spiders. This taphonomic pathway is consistent with other spider-bearing Fossil-Lagerstätten that have previously been shown to include microbially influenced preservation. However, the taphonomic pathway of the Aix-en-Provence appears to be somewhat unique in possessing variable microbial fabrics that lead to 3D and organic preservation with fossil spiders that have strong and variable fluorescence responses.

With respect to taphonomic bias, fossil spider assemblages in lacustrine deposits are found to be influenced by biases in differing ways revealing that biases are not uniform across deposits. Smaller spiders dominate some deposits, like the Green River and Kishenehn formations, while the spiders in the Florissant and Crato formations are lager. Life mode also seems to vary across the deposits, with the Crato Formation being dominated by webweaving spiders and the Aix-en-Provence Formation containing more ground-dwelling spiders. Sex seemed to be the most consistent across the deposits, in which the abundance of males and females were relatively equal in some deposits, but juveniles and spiders of indeterminate sex often made up the largest portion of the fossil spider assemblages. These differences in biases are likely the result of paleoenvironmental conditions for the respective deposits and may be related to factors like the surrounding ecosystems, climate, and the nature of the paleolakes themselves.

Future work includes the continuing revision of the taxonomy of notable lacustrine deposits including the Green River and Florissant formations, as well as describing fossil spiders

from new lacustrine deposits that are discovered. Undescribed fossil spiders remain from the Huitrera Formation in Argentina, the Mühldorf Formation of Austria, and others, and these will likely provide important biogeographical information and may be able to be included in statistical analyses related to taphonomic biases. A significant goal is the merging of fossil spider datasets from both amber and lacustrine assemblages in order to develop a comprehensive picture of the spider fossil record. Additionally, the taphonomic pathways of some Fossil-Lagerstätten are still poorly understood or in need of further investigation, such as in the Wellington Formation of Kansas and the Barstow Formation of California. It is likely that microbial influence, while pervasive in the preservation of spider-bearing Fossil-Lagerstätten, is responsible for the differing modes of preservation in these deposits.

Appendices

Appendix 1

Chapter 1: The earliest palpimanid spider (Araneae: Palpimanidae), from the Crato Fossil-Lagerstätte (Cretaceous, Brazil)

Micro-CT Parameters

BeginSection Sample

project_name	Matt
sample_name	Sample1
date_received	
obtained_by	
organisation	
origin_place	
material_type	fossil
dimensions	
shape	rectangular_prism
sample_notes	__start_multi_string__
sample_notes	__end_multi_string__

EndSection

BeginSection Acquisition

operator_name	
notification_email	
sample_filter_notes	Matt_1st_iter
exposure_time	.52
trajectory	helix

```
BeginSection Helix
  num_projections_per_revolution          1800
  z_start_position                        20
  z_end_position                          75
  iterative_trajectory                    true

  BeginSection Winding
    n                                     119
    Stride                                15.0479
  EndSection
  pitch                                   39.1919
  total_num_projections                   2527
EndSection
camera_x_start_position                   -1
skip_accums                               1
num_accumulations                         5
specify_clearfield_exp_time               false
specify_live_imaging_exp_time             false
rotate_during_focus                       true

BeginSection FocusRotationSection
  rotation_speed                          15
EndSection
warmup_time                               5
use_num_accums_for_snap                   false
```

num_wedge_accumulations 1

do_auto_clearfields true

BeginSection ClearFieldSection

  z_clearfield_position 1

  clearfield_type both

EndSection

num_clear_fields 10

num_dark_fields 5

key_field_spacing 180

reverse_direction_of_keyfields false

test_spacing 80

experiment cone-helical-attenuation-003

rotation_start_position 0

do_camera_x_shift true

BeginSection Sideways

  camera_x_shift_columns 9

EndSection

beam_off_after 1

do_multi_pass false

experiment_date 2018-09-18 18:53:30

image_datatype ushort

BeginSection Geometry

specimen_distance 38.5

camera_length 357.295

voxel_size 15.1355

num_voxels <2640><2640><1080>

field_of_view <39.9577><39.9577><16.3463>

rotation_x 0

rotation_phi 0

rotation_psi 0

camera_psi 0

camera_theta 0

angle_range 360000

EndSection

BeginSection Info

acq_duration 02:39:11

acq_finish_time 2018-09-19 12:45:32

free_disk_space 4.71TB

EndSection

BeginSection Detector

camera_type Varian Flat Panel

system_id 5555 57d7 5575

image_width 3040

image_height 3040

subsample false

camera_binning 1

subsample_factor 1

pixel_size_x 0.139

pixel_size_y 0.139

EndSection

EndSection

BeginSection Source

x_ray_energy 0

x_ray_current 0

x_ray_focus_mode M

x_ray_object_focus 11158

x_ray_initial_target_current 50.3

x_ray_end_target_current 51.3

EndSection

BeginSection MetaData

qrumba_version 1.1.2.231

flip_image_y true

flip_image_x false

EndSection

Phylogenetic Analysis Nexus File

#NEXUS

[written Mon Dec 09 20:36:13 CST 2019 by Mesquite version 3.51 (build 898) at MacBookPro15s-MacBook-Pro.local/10.106.193.11]

BEGIN TAXA;

TITLE Taxa;

DIMENSIONS NTAX=33;

TAXLABELS

Hypochilus Hickmania Lycosidae Araneus Pararchaeinae Stegodyphus Uroctea Gnaphosidae Palpimanus Colopea Huttonia Aotearo Mesarchaea Chilarchaea_quellon Zearchaea Eriauchenius_lavatenda Eriauchenius_jeanneli Eriauchenius_legendrei Eriauchenius_workmani Eriauchenius_bourgini Afrarchaea Afrarchaea_woodae Austrarchaea_nodosa Austrarchaea_daviesae Austrarchaea_mainae Archaea_paradoxa Burmesarchaea_grimaldii Myrmecarchaea Baltarchaea_conica Patarchaea_muralis Caestaranea_jurassica Sinaranea_brevicrus Sinaranea_metaxyostraca

;

END;

BEGIN CHARACTERS;

TITLE Character_Matrix;

DIMENSIONS NCHAR=129;

FORMAT DATATYPE = STANDARD GAP = - MISSING = ? SYMBOLS = " 0 1 2 3 4 5 6 7 8 9 A B C D E F G H J K M N P Q R S T U V W X Y Z a b c d e f g h j k m n p q r s";

MATRIX

Hypochilus 0000000000--10000000000--000-000000--0001000-0000110--00-0--00-0--0000000-0101020-0000-010100--0--00111??10000-0001000-01000-0???

Hickmania 0000000000--10000010200--000-000000--0001000-0100100--00-0--1130--0000000-0101000-0000-010100--101000-0??0-000-000100110100101???

Lycosidae 0000002030--10010000000--000-01-000--000101112001100--00-0--10-0--0010000-200?000-0000-010110--0--00101??0-000-0000-----001101???

Araneus 0000011010--11010000000--000-01-000--0101010-0111000--00-0--00-0--0010000-2001010-0100-010110--0--011010012000-0010-----110111???

Pararchaeinae 0000001011210000400000010-000-01-000--0001000-0111110--01010000-0100000010-200101120000-010110--0--00111??12000-0000-----011121???

Stegodyphus 0000003000--00003010000--000-21-000--0101000-0020210--00-0--00-0--0010000-2001010-0000-010110--0--00110??0-000-0001100-0100101???

Uroctea 0001000000--10000000000--000-01-000--0101000-0020100--00-0--00-0--0000000-2001010-0000-010110--0--00101000-000-0000-----000121???

Gnaphosidae 0000021000--10025010000--000-01-0012101000012020100--00-0--00-0--0010000-20110a0-0000-010110--0--000-1??0-00100000-----101101???

Palpimanus 0001001021301310000l110--011211-00100012aa00-0000210--00-10001000-1000010-200011120101110-000--111?0???110-000-0010-----001121???

Colopea 000100112120101000010l0--001010000101012a000-0000210--00-0--0100--1000010-200010130101110-200--11000100??0-000-0010-----001121???

Huttonia 0001001010--00100000000--001031-0012101b1000-00a0210--00-1110110101000010-2000010-01011110000--11100101??0-000-0010-----001121???

Aotearo 120000101111011010ll?010-0011101000--01b1000-0??0?1100111110010011000010-200?1?0-0?00-111?00--11100101??0-00111010-----??1??????

Mesarchaea 121---10b1110110101100111011101000--01b1000-0??0?1100111110011011000010-20011?0-0?00-1???0??????0010???0-00121010-----??1??????

Chilarchaea_quellon 001---1011110110101100l0-0011101000--01b1000-00a0111011111100120b-1000010-2001100-0100-11-200--101000-0??1100111010-----001121???

Zearchaea sp?2200001011110110b0110010-0011101000--01b1000-00a0211001111000100001000010-2001100-0100-111200--11100101??0-10111010-----011121

Eriauchenius_lavatenda 2101111021010211211110111011111-111211111000-01a02110010-11101011011000l0-210000111111010-101100--00101??0-010-0110-----011101???

Eriauchenius_jeanneli 2101111021010211210110110011111-111211111000-0????110010-1110101101100010-21000?111?11000-101100--00101??0-010-0110-----??1??????

Eriauchenius_legendrei 2101111021010211210110111011111-1112?1111000-0????110010-1110101101100010-21000?111?11000-101000--00101??0-110-0110-----??1??????

Eriauchenius_workmani 1001111021010211211110111011111-111211111000-01a02110010-11101011011000111210000111111000-101100--00101??0-000-0110-----011101???

Eriauchenius_bourgini 1101111021010211210110110011111-111211111000-0????110010-1110101101100010-21000?111?11000-101100--00101??0-000-0010-----??1??????

Afrarchaea 1101111021010211210110111011111-111111111000-0????110010-1110101101100010-21000?111?11000-101110--00101??0-000-0110-----??1??????

Afrarchaea_woodae 1101111021010211210110111011111-111101111000-01a02110010-1110101101100010-210000111111000-101110--00101??0-000-0110-----011121???

Austrarchaea_nodosa 1001101021010211210110110011111-111201111000-01a02111110-11101011011000110211100111111000-100--10000101??0-000-0110-----011101???

Austrarchaea_daviesae 1001101021010211210110110011111-111211111000-0????111110-11101011011000110211?0?111?11000-100--10000101??0-000-0110-----??1??????

Austrarchaea_mainae 0001101021010211210110110011111-111201111000-0????111110-11101011011000110211?0?111?11000-100--10000101??0-000-0010-----??1??????

Archaea_paradoxa 000110?0210100l?21011?1111011l??111??11?1000-0????10--10-111?100111100010-??1?0?111?10-10-?0??????00101??0-000-0010-----?????????

Burmesarchaea_grimaldii 000110?0210100l???011?11110?????1????11?1000-0????10--10-11??1?010??00010-????0???1?10-???????????0010???0-000-01?0-----?????????

Myrmecarchaea 000110?011?100????01??11110?????011??11???0???????10--?0-1?????011??00010-????0???1?1????????????????????????????0-----?????????

Baltarchaea_conica 100110?0211100??2?011?11110?????01???11???0???????10--10-1???1001???00011a????0???1?1??????0?????????????????????0-----?????????

Patarchaea_muralis ?????????1?????????????11?1??????0?11??1?10????????10--10-11??1101?1?0001?????????????0-?10????????0??????0-??11???0-----?????????

Caestaranea_jurassica 000?0?????--??1??????010-0???0??0011001110???????10--011111010010?0000?0-??1???0-0000-?10?????????0???????000-???0-----?????????

Sinaranea_brevicrus 000?0?????--?????????010-0???0??0012101110???????00--011111010010?0000?0-??1???0-0000-?10?????????0???????000-???0-----?????????

Sinaranea_metaxyostraca 000?0?????--?????????010-0???0??0012101?100???????00--0??111010010?0000?0-??1???0-0000-?10?????????0???????000-???0-----?????????

;

END;

BEGIN ASSUMPTIONS;

TYPESET * UNTITLED = unord: 1- 129;

END;

BEGIN MESQUITECHARMODELS;

ProbModelSet * UNTITLED = 'Mk1 (est.)': 1- 129;

END;

Begin MESQUITE;

MESQUITESCRIPTVERSION 2;

TITLE AUTO;

tell ProjectCoordinator;

timeSaved 1575945373834;

getEmployee #mesquite.minimal.ManageTaxa.ManageTaxa;

tell It;

setID 0 5451365825857416023;

endTell;

getEmployee #mesquite.charMatrices.ManageCharacters.ManageCharacters;

tell It;

setID 0 2969045789998741118;

mqVersion 351;

checksumv 0 3 2855925409 null getNumChars 129 numChars 129 getNumTaxa 33 numTaxa 33 short false bits 316685118603327 states 316685118603327 sumSquaresStatesOnly 10077.0 sumSquares 10077.0 longCompressibleToShort false usingShortMatrix false NumFiles 1 NumMatrices 1 errorReportedDuringRun;

mqVersion;

endTell;

getWindow;

tell It;

suppress;

setResourcesState false false 185;

setPopoutState 300;

setExplanationSize 0;

setAnnotationSize 0;

setFontIncAnnot 0;

setFontIncExp 0;

setSize 1390 604;

setLocation 8 23;

```
                setFont SanSerif;
                setFontSize 10;
                getToolPalette;
                tell It;
                endTell;
                desuppress;
        endTell;
        getEmployee
#mesquite.charMatrices.BasicDataWindowCoord.BasicDataWindowCoord;
        tell It;
                showDataWindow #2960457899987411 18
#mesquite.charMatrices.BasicDataWindowMaker.BasicDataWindowMaker;
                tell It;
                        getWindow;
                        tell It;
                                setExplanationSize 30;
                                setAnnotationSize 20;
                                setFontIncAnnot 0;
                                setFontIncExp 0;
                                setSize 1205 532;
                                setLocation 8 23;
                                setFont SanSerif;
                                setFontSize 10;
                                getToolPalette;
                                tell It;
                                endTell;
```

setActive;

setTool
mesquite.charMatrices.BasicDataWindowMaker.BasicDataWindow.arrow;

colorCells #mesquite.charMatrices.NoColor.NoColor;

colorRowNames
#mesquite.charMatrices.TaxonGroupColor.TaxonGroupColor;

colorColumnNames
#mesquite.charMatrices.CharGroupColor.CharGroupColor;

colorText #mesquite.charMatrices.NoColor.NoColor;

setBackground White;

toggleShowNames on;

toggleShowTaxonNames on;

toggleTight off;

toggleThinRows off;

toggleShowChanges on;

toggleSeparateLines off;

toggleShowStates on;

toggleAutoWCharNames on;

toggleAutoTaxonNames off;

toggleShowDefaultCharNames off;

toggleConstrainCW on;

toggleBirdsEye off;

toggleShowPaleGrid off;

toggleShowPaleCellColors off;

toggleShowPaleExcluded off;

togglePaleInapplicable on;

```
        toggleShowBoldCellText off;
        toggleAllowAutosize on;
        toggleColorsPanel off;
        toggleDiagonal on;
        setDiagonalHeight 80;
        toggleLinkedScrolling on;
        toggleScrollLinkedTables off;
endTell;
showWindow;
getWindow;
tell It;
        forceAutosize;
endTell;
getEmployee #mesquite.charMatrices.AlterData.AlterData;
tell It;
        toggleBySubmenus off;
endTell;
getEmployee #mesquite.charMatrices.ColorByState.ColorByState;
tell It;
        setStateLimit 9;
        toggleUniformMaximum on;
endTell;
getEmployee #mesquite.charMatrices.ColorCells.ColorCells;
tell It;
        setColor Red;
```

```
            removeColor off;
        endTell;
        getEmployee #mesquite.categ.StateNamesStrip.StateNamesStrip;
        tell It;
            showStrip off;
        endTell;
        getEmployee #mesquite.charMatrices.AnnotPanel.AnnotPanel;
        tell It;
            togglePanel off;
        endTell;
        getEmployee
#mesquite.charMatrices.CharReferenceStrip.CharReferenceStrip;
        tell It;
            showStrip off;
        endTell;
        getEmployee
#mesquite.charMatrices.QuickKeySelector.QuickKeySelector;
        tell It;
            autotabOff;
        endTell;
        getEmployee
#mesquite.charMatrices.SelSummaryStrip.SelSummaryStrip;
        tell It;
            showStrip off;
        endTell;
        getEmployee
#mesquite.categ.SmallStateNamesEditor.SmallStateNamesEditor;
```

```
                    tell It;
                        panelOpen true;
                    endTell;
                endTell;
            endTell;
            endTell;
end;
```

Appendix 2

Chapter 6: TAPHONOMIC BIAS IN THE FOSSIL RECORD OF SPIDERS (ARANEAE) FROM LACUSTRINE DEPOSITS

Fossil Spider Data Set for bias analyses (CSV file for R)

Formation	Family	Morphospecies	Sex	Body_Length	Guild
Crato	Dipluridae	8	I	13.35	ground
Crato	Araneidae	1	I	3.1	web
Crato	Araneidae	1	I	3.22	web
Crato	Araneidae	1	I	4.73	web
Crato	Araneidae	1	I	9.3	web
Crato	Araneidae	1	I		web
Crato	Ind	10	I	13.69	ground
Crato	Palpimanidae	6	I		web
Crato	Araneidae	1	I	6.31	web
Crato	Araneidae	1	I	3.7	web
Crato	Araneidae	1	I	7.73	web
Crato	Araneidae	1	I	4.79	web
Crato	Araneidae	1	I	3.36	web
Crato	Araneidae	1	I	5.48	web
Crato	Araneidae	1	I	5.23	web
Crato	Araneidae	1	F	4.52	web
Crato	Ind	2	I	6.2	web
Crato	Araneidae	1	F		web
Crato	Araneidae	1	I	5.35	web
Crato	Araneidae	1	M	3.26	web
Crato	Araneidae	1	I	8.18	web
Crato	Ind	2	F	6.67	web
Crato	Araneidae	1	I	5.62	web
Crato	Dipluridae	3	I	8.32	web
Crato	Araneidae	1	I	4.34	web
Crato	Araneidae	1	F	5.21	web
Crato	Nephilidae	5	M		web
Crato	Araneidae	1	F	7.88	web
Crato	Araneidae	1	I	4.02	web
Crato	Araneidae	1	I	4.17	web
Crato	Araneidae	1	I	6.67	web
Crato	Araneidae	1	I	4.48	web
Crato	Araneidae	1	I	7.52	web

Crato	Araneidae	1	I	6.04	web
Crato	Araneidae	1	I	4.25	web
Crato	Araneidae	1	I	2.98	web
Crato	Araneidae	1	I	5.95	web
Crato	Araneidae	1	I	2.19	web
Crato	Araneidae	1	F	4.77	web
Crato	Araneidae	1	I	5.85	web
Crato	Araneidae	1	I	3.78	web
Crato	Araneidae	1	I	5.38	web
Crato	Araneidae	1	I	6.98	web
Crato	Araneidae	1	I	8.72	web
Crato	Araneidae	1	F	3.54	web
Crato	Araneidae	1	I	6.39	web
Crato	Araneidae	1	I	4.34	web
Crato	Araneidae	1	I	5.57	web
Crato	Araneidae	1	I	4.89	web
Crato	Araneidae	1	I	4.46	web
Crato	Araneidae	1	I	3.65	web
Crato	Araneidae	1	I	3.96	web
Crato	Araneidae	1	I	4.71	web
Crato	Ind	4	F	5.99	web
Crato	Araneidae	1	I	6.09	web
Crato	Araneidae	1	I	7.09	web
Crato	Araneidae	1	I	3.15	web
Crato	Araneidae	1	I	2.59	web
Crato	Araneidae	1	I	9.62	web
Crato	Araneidae	1	I	7.4	web
Crato	Araneidae	1	I	4.83	web
Crato	Dipluridae	3	I	12.08	web
Crato	Araneidae	1	I	4.62	web
Crato	Araneidae	1	I	11.13	web
Crato	Araneidae	1	I	4.44	web
Crato	Araneidae	1	I	5.88	web
Crato	Araneidae	1	I	3.46	web
Crato	Araneidae	1	I	3.03	web
Crato	Araneidae	1	F	8.99	web
Crato	Araneidae	1	I	4.71	web
Crato	Araneidae	1	I	7.26	web
Crato	Araneidae	1	I	5.62	web
Crato	Araneidae	1	I	5.49	web
Crato	Araneidae	1	I	2.43	web
Crato	Araneidae	1	I	4.22	web
Crato	Araneidae	1	I	3.19	web

Crato	Araneidae	1	I	3.71	web
Crato	Araneidae	1	F	4.9	web
Crato	Araneidae	1	I		web
Crato	Araneidae	1	F	6.4	web
Crato	Araneidae	1	I	4.07	web
Crato	Araneidae	1	M	4.67	web
Crato	Araneidae	1	F	8.4	web
Crato	Araneidae	1	I	3.79	web
Crato	Araneidae	1	I	3.06	web
Crato	Araneidae	1	I	3.8	web
Crato	Dipluridae	8	I	23.32	web
Crato	Nephilidae	5	F		web
Crato	Nephilidae	5	F	23.6	web
Crato	Araneidae	1	I	3.88	web
Crato	Araneidae	1	I	7.36	web
Crato	Araneidae	1	I	3.3	web
Crato	Araneidae	1	I	4.46	web
Crato	Araneidae	1	I	3.48	web
Crato	Araneidae	1	F	12.55	web
Crato	Araneidae	1	I	5.4	web
Crato	Araneidae	1	I	5.45	web
Crato	Araneidae	1	I	3.19	web
Crato	Araneidae	1	I	3.28	web
Crato	Araneidae	1	I	3.41	web
Crato	Araneidae	1	I	4.63	web
Crato	Araneidae	1	I	5.29	web
Crato	Araneidae	1	I	4.62	web
Crato	Nephilidae	5	F	16.62	web
Crato	Nephilidae	5	F		web
Crato	Dipluridae	7	F	10.81	web
Crato	Dipluridae	7	M	7.25	web
Crato	Dipluridae	8	F	26.15	web
Crato	Dipluridae	9	M	22.56	web
Crato	Araneidae	1	I	2.1	web
GreenRiver	Ind	8	I	0.79	ground
GreenRiver	Ind		I	0.76	ground
GreenRiver	Ind		M	2.25	ground
GreenRiver	Gnaphosidae	9	F	2.26	ground
GreenRiver	Ind		I	1.86	ground
GreenRiver	Thomisidae	6	F	1.8	ground
GreenRiver	Salticidae?		F	1.74	ground
GreenRiver	Araneidae	3	M		ground
GreenRiver	Ind		I	2.76	ground

GreenRiver	Ind		I	1.86	ground
GreenRiver	Ind		I	1.24	ground
GreenRiver	Ind		I	0.62	ground
GreenRiver	Hersiliidae	5	M	1.94	ground
GreenRiver	Ind		M	1.96	ground
GreenRiver	Ind		I	1.52	ground
GreenRiver	Ind		M	1.64	ground
GreenRiver	Ind		M	1.77	ground
GreenRiver	Ind		I	1.83	ground
GreenRiver	Hersiliidae	5	M	1.85	ground
GreenRiver	Ind	13	I	1.7	ground
GreenRiver	Selenopidae	7	F	2.03	ground
GreenRiver	Ind		I	2.29	ground
GreenRiver	Ind	12	I	1.63	ground
GreenRiver	Thomisidae	6	I	1.68	ground
GreenRiver	Ind		F	1.61	ground
GreenRiver	Thomisidae	6	I	1.41	ground
GreenRiver	Ind		I		ground
GreenRiver	Hersiliidae	5	M		ground
GreenRiver	Selenopidae	7	F		ground
GreenRiver	Ind		I		ground
GreenRiver	Ind		F	2.31	ground
GreenRiver	Ind	9	F	2.98	ground
GreenRiver	Ind	11	M	2.99	ground
GreenRiver	Ind		F	1.2	ground
GreenRiver	Ind	11	M		ground
GreenRiver	Thomisidae	6	F	2.94	ground
GreenRiver	Ind	1	F	1.17	web
GreenRiver	Ind		M	2.52	web
GreenRiver	Uloboridae	2	F	3.11	web
GreenRiver	Uloboridae	2	I	1.97	web
GreenRiver	Uloboridae	2	I	1.81	web
GreenRiver	Ind	1	I	1.67	web
GreenRiver	Uloboridae	4	F	3.67	web
GreenRiver	Uloboridae	2	F	2.66	web
GreenRiver	Ind		I	1.73	web
GreenRiver	Uloboridae	2	I	1.21	web
GreenRiver	Ind		F	1	web
GreenRiver	Ind	1	I	0.74	web
GreenRiver	Uloboridae	2	I	1.71	web
GreenRiver	Ind	1	F	0.82	web
GreenRiver	Uloboridae	4	I	1.17	web
GreenRiver	Uloboridae	4	F	1.49	web

GreenRiver	Ind	1	I	0.76	web
GreenRiver	Ind		I	1.63	web
GreenRiver	Ind		M	1.73	web
GreenRiver	Ind		F	1.11	web
GreenRiver	Ind		F	1.1	web
GreenRiver	Ind	1	M	1.39	web
GreenRiver	Ind	1	I	1.01	web
GreenRiver	Ind		I	1.72	web
GreenRiver	Ind	1	F	0.94	web
GreenRiver	Uloboridae	2	F	2.6	web
GreenRiver	Ind	1	I	1.03	web
GreenRiver	Ind	1	I	0.89	web
GreenRiver	Ind	1	I	1.3	web
GreenRiver	Ind		I	1.2	web
GreenRiver	Uloboridae	4	I	1.3	web
GreenRiver	Ind	1	I	0.95	web
GreenRiver	Uloboridae	4	I	3	web
GreenRiver	Ind		F	0.76	web
GreenRiver	Araneidae	3	M	2.08	web
GreenRiver	Ind	1	I	0.8	web
GreenRiver	Ind	1	I	0.83	web
GreenRiver	Uloboridae	4	M	2.91	web
GreenRiver	Ind	1	I	0.54	web
GreenRiver	Ind	1	I	1.19	web
GreenRiver	Ind	1	I	1.67	web
GreenRiver	Ind	1	I	1.25	web
GreenRiver	Ind	1	I	0.92	web
GreenRiver	Ind	1	I	1.11	web
GreenRiver	Ind	1	I	0.84	web
GreenRiver	Ind	1	I	1.04	web
GreenRiver	Ind	1	I	0.97	web
GreenRiver	Ind	1	I	2.59	web
GreenRiver	Ind	1	I	0.82	web
GreenRiver	Araneidae	3	M	2.25	web
GreenRiver	Ind		I		web
GreenRiver	Uloboridae	4	I		web
GreenRiver	Ind	10	M	2.58	web
GreenRiver	Ind		I	1.88	web
GreenRiver	Ind	1	I	0.92	web
GreenRiver	Araneidae	3	M		web
GreenRiver	Ind		I	1.53	NA
GreenRiver	Ind		I	1.56	NA
GreenRiver	Ind		I	4	NA

GreenRiver	Ind		I	1.66	NA
GreenRiver	Ind		M	3.6	NA
GreenRiver	Ind		I	1.34	NA
GreenRiver	Ind		I	1.97	NA
GreenRiver	Ind		I	1.12	NA
GreenRiver	Ind		I	0.84	NA
GreenRiver	Ind		I		NA
GreenRiver	Araneidae	3	M	1.95	web
GreenRiver	Ind		I	0.85	NA
GreenRiver	Ind		M		NA
GreenRiver	Ind		I	1.26	NA
GreenRiver	Ind		I		NA
GreenRiver	Ind		I	1.91	NA
GreenRiver	Ind	3	F	1.2	NA
GreenRiver	Ind		I	2.28	NA
GreenRiver	Ind		F	2.09	NA
GreenRiver	Ind		I	1.02	NA
GreenRiver	Ind		I	1.8	NA
GreenRiver	Ind		F	1.07	NA
GreenRiver	Hersiliidae	5	I	2.24	ground
GreenRiver	Uloboridae	4	M	3.81	web
GreenRiver	Uloboridae	2	F	4.75	web
GreenRiver	Uloboridae	2	M	3.8	web
GreenRiver	Uloboridae	2	M	4.94	web
GreenRiver	Hersiliidae	5	M	3.76	ground
GreenRiver	Hersiliidae	5	M	2.72	ground
GreenRiver	Selenopidae	7	F	3.64	ground
GreenRiver	Thomisidae	6	M	1.9	ground
GreenRiver	Thomisidae	6	M		ground
Kishenehn	Ind		I		ground
Kishenehn	Ind		M	1.31	ground
Kishenehn	Clubionidae	3	I	2.12	ground
Kishenehn	Ind		I	1	ground
Kishenehn	Ind		I	0.76	ground
Kishenehn	Ind		I	1.33	web
Kishenehn	Ind		F		web
Kishenehn	Araneidae	1	M	3.29	web
Kishenehn	Araneidae		M	2.28	web
Kishenehn	Ind		I	0.87	web
Kishenehn	Araneidae		F	3.4	web
Kishenehn	Ind		I	1.41	web
Kishenehn	Araneidae	1	F	3.91	web
Kishenehn	Araneidae	1	I		web

Kishenehn	Araneidae		I	2.68	web
Kishenehn	Ind		I	2.79	web
Kishenehn	Araneidae	2	F	1.51	web
Kishenehn	Ind		I	0.89	NA
Kishenehn	Ind		I	3.3	NA
Florissant	Ind	8	F	10.8	NA
Florissant	Ind		I	5.26	NA
Florissant	Lycosidae	3	M	7.82	ground
Florissant	Lycosidae	5	F	4.45	ground
Florissant	Lycosidae	3	M	6.64	ground
Florissant	Lycosidae	3	M	5.57	ground
Florissant	Clubionidae	2	F	7.24	ground
Florissant	Lycosidae	5	F	8.02	ground
Florissant	Clubionidae	2	F	7.09	ground
Florissant	Clubionidae	9	F	8.08	ground
Florissant	Lycosidae		F	5.54	ground
Florissant	Pisaurid	10	F	5.34	ground
Florissant	Ind		F	8.97	ground
Florissant	Clubionidae	6	F	5.25	ground
Florissant	Clubionidae	2	F	7.98	ground
Florissant	Lycosidae	3	F	5.16	ground
Florissant	Clubionidae	2	F	5.7	ground
Florissant	Clubionidae	6	F	6.07	ground
Florissant	Pisauridae	7	F	8.27	ground
Florissant	Lycosidae	3	F	6.96	ground
Florissant	Clubionidae	2	M	5.5	ground
Florissant	Clubionidae	2	M		ground
Florissant	Tetragnathidae	1	M	9.25	web
Florissant	Tetragnathidae	1	M	9.38	web
Florissant	Tetragnathidae	1	M	9.08	web
Florissant	Ind	4	M	4.77	web
Florissant	Ind		M	4.46	web
Florissant	Tetragnathidae	1	M	8.4	web
Florissant	Ind	4	M	5.23	web
Florissant	Tetragnathidae	1	M	7.02	web
Florissant	Tetragnathidae	1	M	7.04	web
Florissant	Tetragnathidae	1	M	10.9	web
Florissant	Tetragnathidae	2	M	5.85	web
Florissant	Tetragnathidae	1	M	9.77	web
Florissant	Tetragnathidae	1	M	3.62	web
Florissant	Ind		I		web
Florissant	Araneidae	7	F	14.91	web
Florissant	Araneidae	4	M		web

Aix	Lycosidae	F	5.6	ground
Aix		I	5.52	ground
Aix	Pisauridae	F	3.9	ground
Aix	Thomisidae	I	2.11	ground
Aix	Thomisidae	F	3.74	ground
Aix	Lycosidae	F	3.95	ground
Aix	Lycosidae	F	5.24	ground
Aix	Thomisidae	M	3.39	ground
Aix		F	4.26	ground
Aix	Thomisidae	I	5.83	ground
Aix	Thomisidae	M	4.23	ground
Aix	Thomisidae	M	3.4	ground
Aix		I	4.06	ground
Aix	Thomisidae	I	2.56	ground
Aix		F	5.31	ground
Aix		F	4.47	ground
Aix		F	5.29	ground
Aix		I	3.83	ground
Aix		M	4.22	ground
Aix		I	3.91	ground
Aix		I	5.82	ground
Aix		F	5.08	ground
Aix		I	4.79	ground
Aix		I	4.46	ground
Aix		M	3.51	ground
Aix		M	3.46	ground
Aix		F	5.06	ground
Aix		I	7.02	ground
Aix		I	2.54	ground
Aix		F	2.94	ground
Aix		M	4.58	ground
Aix		I	2.85	ground
Aix		I	2.42	ground
Aix		F	4.22	ground
Aix		I	7.17	ground
Aix		F	5.03	ground
Aix		F	4.9	ground
Aix		I	3.57	ground
Aix		F	5.75	ground
Aix		I	4.47	ground
Aix		I	7.86	ground
Aix		I	4.62	ground
Aix		M	3.19	ground

Aix		F	9	ground
Aix		I	3.51	ground
Aix		I	2.55	ground
Aix		I	2.99	ground
Aix		I	4.43	ground
Aix		F	2.96	ground
Aix		I	5.61	ground
Aix		I	2.82	ground
Aix		F	5.46	ground
Aix		I	2.71	ground
Aix		F	4.29	ground
Aix		I	3.29	ground
Aix		M	2.47	ground
Aix		I	2.96	ground
Aix		I	4.17	ground
Aix		F	4.13	ground
Aix		I	4.71	ground
Aix		M	3.42	ground
Aix		F	4.34	ground
Aix		I	4.63	ground
Aix		I	7.1	ground
Aix		I	7.6	ground
Aix		I	5.02	ground
Aix		I	3.31	ground
Aix		I	8.97	ground
Aix		I	3.81	ground
Aix		I	4.66	ground
Aix		I	3.42	ground
Aix		I	4.63	ground
Aix		I		ground
Aix		I	3.77	ground
Aix		M	7.32	ground
Aix		I	6.16	ground
Aix		I	8.64	ground
Aix		F	6.53	web
Aix	Tetragnathid	F	6.42	web
Aix	Tetragnathid	M	4.38	web
Aix	Tetragnathid	F	7.75	web
Aix	Tetragnathid	F	4.2	web
Aix		F	3.63	web
Aix		M	7.18	web
Aix		I	5.77	web
Aix		I	3.37	web

Aix	M	2.81	web
Aix	M	2.84	web
Aix	M	6.52	web
Aix	M	2.64	web
Aix	M	3.25	web
Aix	F	4.68	web
Aix	F	4.42	web
Aix	F	3.331	web
Aix	I	2.2	web
Aix	F	3.43	web
Aix	F	5.18	web
Aix	F	6.31	web
Aix	I	5.91	web
Aix	I	2.78	web
Aix	F	3.95	web
Aix	I	3.33	web
Aix	I	2.52	web
Aix	I	4.81	web
Aix	F	4.53	web
Aix	M	3.94	web
Aix	I	3.94	web
Aix	I	3.94	web
Aix	I	3.03	web
Aix	I	1.8	web
Aix	I	4.4	web
Aix	I	3.98	web
Aix	I	5.93	web
Aix	I	4.42	web
Aix	I		web
Aix	F	5.8	NA
Aix	I	5.9	NA
Aix	I	3.43	NA
Aix	I	2.99	NA
Aix	I		NA
Aix	I	7.87	NA
Aix	F	3.72	NA
Aix	M		NA
Aix	M	3.4	NA
Aix	M	4.21	NA
Aix	F	3.19	NA
Aix	I	3.69	NA
Aix	I		NA
Aix	I	2.89	NA

Aix	I	2.54	NA
Aix	I	2.66	NA
Aix	F	3.16	NA
Aix	I		NA
Aix	I		NA
Aix	I	3.69	NA
Aix	I	3.67	NA
Aix	I		NA
Aix	I	2.63	NA
Aix	I	4.18	NA
Aix	I	4.23	NA
Aix	I	4.07	NA
Aix	I	3.95	NA
Aix	I	4.06	NA
Aix	I	6.56	NA
Aix	I	2.3	NA
Aix	I	5.8	NA
Aix	I	2.26	NA
Aix	I	3.39	NA
Aix	I	4.46	NA
Aix	I	4.95	NA
Aix	I	4.28	NA
Aix	I	2.87	NA
Aix	I	2.32	NA
Aix	I	2.85	NA
Aix	I	4.07	NA
Aix	I	4.89	NA
Aix	I	3.42	NA
Aix	I	5.59	NA
Aix	I	5.82	NA
Aix	M	3.32	NA
Aix	I	4.09	NA
Aix	I	5.15	NA
Aix	I	4.82	NA
Haifanggou	F	5.58	NA
Haifanggou	F	2.93	NA
Haifanggou	M	2.8	NA
Haifanggou	F	8.55	NA
Haifanggou	I	3	NA
Haifanggou	M	4	NA
Haifanggou	M	4.58	NA
Haifanggou	I	4.91	NA
Haifanggou	I	4.01	NA

Haifanggou	I	5.19	NA
Haifanggou	I	3.86	NA
Haifanggou	I	4.23	NA
Haifanggou	I	3.5	NA
Haifanggou	M	3.89	NA
Haifanggou	I	3.5	NA
Haifanggou	I	5.48	NA
Haifanggou	I	4.73	NA
Haifanggou	I	2.97	NA
Haifanggou	I	3.39	NA
Haifanggou	M	3.28	NA
Haifanggou	M	4.05	NA
Haifanggou	M	5.12	NA
Haifanggou	I	3.22	NA
Haifanggou	F	4.33	NA
Haifanggou	F	4.65	NA
Haifanggou	M	3.16	NA
Haifanggou	F	8.28	NA
Haifanggou	M	3.15	NA
Haifanggou	M	3.13	NA
Haifanggou	M	3.8	NA
Haifanggou	M	3.61	NA
Haifanggou	F	4.23	NA
Haifanggou	F	4.33	NA
Haifanggou	M	7.23	NA
Haifanggou	I	3.89	NA
Haifanggou	I	4.01	NA
Haifanggou	I	3.1	NA
Haifanggou	I	3.64	NA
Haifanggou	I	1.54	NA
Haifanggou	F	4.98	NA
Haifanggou	I	3.39	NA
Haifanggou	I	3.57	NA
Haifanggou	I	3.34	NA
Haifanggou	F	3.69	NA
Haifanggou	F	5.87	NA
Haifanggou	F	4.43	NA
Haifanggou	F	3.6	NA
Haifanggou	M	4.01	NA
Haifanggou	M	4.52	NA
Haifanggou	F	5.63	NA
Haifanggou	M	3.62	NA
Haifanggou	I	3.45	NA

Haifanggou	M	3.85	NA
Haifanggou	M		NA
Haifanggou	F		NA
Haifanggou	M	3.09	NA
Haifanggou	I	3.37	NA
Haifanggou	F	3.64	NA
Haifanggou	I	3.91	NA
Haifanggou	F	3.06	NA
Haifanggou	M	5.29	NA
Haifanggou	M	3.17	NA
Haifanggou	F	3.25	NA
Haifanggou	M		NA
Haifanggou	F	4.3	NA
Haifanggou	M	3.52	NA
Haifanggou	I	4.04	NA

R markdown document. Code for bias analyses in R.

Lacustrine_Code.R

matt

2020-05-19

```
library(ggplot2)

SpiderDf <- read.csv("SpiderDatabaseR.csv", header = T)
str(SpiderDf)

## 'data.frame':    521 obs. of  6 variables:
##  $ Formation    : Factor w/ 6 levels "Aix","Crato",..: 2 2 2 2 2 2 2 2 2 2
...
##  $ Family       : Factor w/ 18 levels "","Araneidae",..: 4 2 2 2 2 2 7 10
2 2 ...
##  $ Morphospecies: int  8 1 1 1 1 1 10 6 1 1 ...
##  $ Sex          : Factor w/ 3 levels "F","I","M": 2 2 2 2 2 2 2 2 2 2 ...
##  $ Body_Length  : num  13.35 3.1 3.22 4.73 9.3 ...
##  $ Guild        : Factor w/ 2 levels "ground","web": 1 2 2 2 2 2 1 2 2 2 .
..

head(SpiderDf)

##   Formation     Family Morphospecies Sex Body_Length  Guild
## 1     Crato Dipluridae             8   I       13.35 ground
## 2     Crato  Araneidae             1   I        3.10    web
## 3     Crato  Araneidae             1   I        3.22    web
## 4     Crato  Araneidae             1   I        4.73    web
## 5     Crato  Araneidae             1   I        9.30    web
## 6     Crato  Araneidae             1   I          NA    web

SpiderDf$Formation <- factor(SpiderDf$Formation, levels=c("Aix", "Florissant"
, "Kishenehn", "GreenRiver", "Crato", "Haifanggou"),
                             labels=c("Aix", "Florissant", "Kishenehn", "Gree
n River", "Crato", "Haifanggou"))


Size <- SpiderDf$Body_Length
Size

##   [1] 13.350  3.100  3.220  4.730  9.300     NA 13.690     NA  6.310  3.70
0
##  [11]  7.730  4.790  3.360  5.480  5.230  4.520  6.200     NA  5.350  3.26
0
##  [21]  8.180  6.670  5.620  8.320  4.340  5.210     NA  7.880  4.020  4.17
0
```

```
##  [31]  6.670  4.480  7.520  6.040  4.250  2.980  5.950  2.190  4.770  5.85
0
##  [41]  3.780  5.380  6.980  8.720  3.540  6.390  4.340  5.570  4.890  4.46
0
##  [51]  3.650  3.960  4.710  5.990  6.090  7.090  3.150  2.590  9.620  7.40
0
##  [61]  4.830 12.080  4.620 11.130  4.440  5.880  3.460  3.030  8.990  4.71
0
##  [71]  7.260  5.620  5.490  2.430  4.220  3.190  3.710  4.900     NA  6.40
0
##  [81]  4.070  4.670  8.400  3.790  3.060  3.800 23.320     NA 23.600  3.88
0
##  [91]  7.360  3.300  4.460  3.480 12.550  5.400  5.450  3.190  3.280  3.41
0
## [101]  4.630  5.290  4.620 16.620     NA 10.810  7.250 26.150 22.560  2.10
0
## [111]  0.790  0.760  2.250  2.260  1.860  1.800  1.740     NA  2.760  1.86
0
## [121]  1.240  0.620  1.940  1.960  1.520  1.640  1.770  1.830  1.850  1.70
0
## [131]  2.030  2.290  1.630  1.680  1.610  1.410     NA     NA     NA     N
A
## [141]  2.310  2.980  2.990  1.200     NA  2.940  1.170  2.520  3.110  1.97
0
## [151]  1.810  1.670  3.670  2.660  1.730  1.210  1.000  0.740  1.710  0.82
0
## [161]  1.170  1.490  0.760  1.630  1.730  1.110  1.100  1.390  1.010  1.72
0
## [171]  0.940  2.600  1.030  0.890  1.300  1.200  1.300  0.950  3.000  0.76
0
## [181]  2.080  0.800  0.830  2.910  0.540  1.190  1.670  1.250  0.920  1.11
0
## [191]  0.840  1.040  0.970  2.590  0.820  2.250     NA     NA  2.580  1.88
0
## [201]  0.920     NA  1.530  1.560  4.000  1.660  3.600  1.340  1.970  1.12
0
## [211]  0.840     NA  1.950  0.850     NA  1.260     NA  1.910  1.200  2.28
0
## [221]  2.090  1.020  1.800  1.070  2.240  3.810  4.750  3.800  4.940  3.76
0
## [231]  2.720  3.640  1.900     NA     NA  1.310  2.120  1.000  0.760  1.33
0
## [241]     NA  3.290  2.280  0.870  3.400  1.410  3.910     NA  2.680  2.79
0
## [251]  1.510  0.890  3.300 10.800  5.260  7.820  4.450  6.640  5.570  7.24
0
## [261]  8.020  7.090  8.080  5.540  5.340  8.970  5.250  7.980  5.160  5.70
0
## [271]  6.070  8.270  6.960  5.500     NA  9.250  9.380  9.080  4.770  4.46
0
```

```
## [281]  8.400  5.230  7.020  7.040 10.900  5.850  9.770  3.620     NA 14.91
0
## [291]     NA  5.600  5.520  3.900  2.110  3.740  3.950  5.240  3.390  4.26
0
## [301]  5.830  4.230  3.400  4.060  2.560  5.310  4.470  5.290  3.830  4.22
0
## [311]  3.910  5.820  5.080  4.790  4.460  3.510  3.460  5.060  7.020  2.54
0
## [321]  2.940  4.580  2.850  2.420  4.220  7.170  5.030  4.900  3.570  5.75
0
## [331]  4.470  7.860  4.620  3.190  9.000  3.510  2.550  2.990  4.430  2.96
0
## [341]  5.610  2.820  5.460  2.710  4.290  3.290  2.470  2.960  4.170  4.13
0
## [351]  4.710  3.420  4.340  4.630  7.100  7.600  5.020  3.310  8.970  3.81
0
## [361]  4.660  3.420  4.630     NA  3.770  7.320  6.160  8.640  6.530  6.42
0
## [371]  4.380  7.750  4.200  3.630  7.180  5.770  3.370  2.810  2.840  6.52
0
## [381]  2.640  3.250  4.680  4.420  3.331  2.200  3.430  5.180  6.310  5.91
0
## [391]  2.780  3.950  3.330  2.520  4.810  4.530  3.940  3.940  3.940  3.03
0
## [401]  1.800  4.400  3.980  5.930  4.420     NA  5.800  5.900  3.430  2.99
0
## [411]     NA  7.870  3.720     NA  3.400  4.210  3.190  3.690     NA  2.89
0
## [421]  2.540  2.660  3.160     NA     NA  3.690  3.670     NA  2.630  4.18
0
## [431]  4.230  4.070  3.950  4.060  6.560  2.300  5.800  2.260  3.390  4.46
0
## [441]  4.950  4.280  2.870  2.320  2.850  4.070  4.890  3.420  5.590  5.82
0
## [451]  3.320  4.090  5.150  4.820  5.580  2.930  2.800  8.550  3.000  4.00
0
## [461]  4.580  4.910  4.010  5.190  3.860  4.230  3.500  3.890  3.500  5.48
0
## [471]  4.730  2.970  3.390  3.280  4.050  5.120  3.220  4.330  4.650  3.16
0
## [481]  8.280  3.150  3.130  3.800  3.610  4.230  4.330  7.230  3.890  4.01
0
## [491]  3.100  3.640  1.540  4.980  3.390  3.570  3.340  3.690  5.870  4.43
0
## [501]  3.600  4.010  4.520  5.630  3.620  3.450  3.850     NA     NA  3.09
0
## [511]  3.370  3.640  3.910  3.060  5.290  3.170  3.250     NA  4.300  3.52
0
## [521]  4.040
```

```r
# Plotting the density curves
# Individual curves
tiff(file="Density_Sep.tiff", units="in", width=7, height=5, res=300)
ggplot(SpiderDf, aes(x= Body_Length, fill = Formation)) +
  geom_density(alpha = 0.4) + ggtitle("Body Lengths Fossil Spiders in Lacustr
ine Deposits") +
  theme(plot.title = element_text(hjust = 0.5)) + theme(legend.position = "no
ne") +
  xlab("Body Length") + ylab("Density") +
  scale_fill_manual(values=c("red", "#E76BF3", "#00B0F6", "#00BF7D", "goldenr
od1", "wheat2")) +
  scale_x_continuous(breaks = seq(0, 15, by = 3), limits = c(0, 15)) +
  scale_y_continuous(breaks = seq(0, 0.5, by = 0.1)) +
  facet_wrap( ~ Formation, ncol=3) + theme(strip.text.x = element_text(size=1
2))

## Warning: Removed 42 rows containing non-finite values (stat_density).

dev.off()

## quartz_off_screen
##                 2

# Grouped density curve
tiff(file="Density_All.tiff", units="in", width=7, height=5, res=300)
ggplot(SpiderDf, aes(x= Body_Length, fill = Formation)) +
  geom_density(alpha = 0.4) + ggtitle("Body Lengths Fossil Spiders in Lacustr
ine Deposits") +
  theme(plot.title = element_text(hjust = 0.5)) +
  xlab("Body Length") + ylab("Density") + theme(legend.position = c(0.8, 0.7)
) +
  scale_fill_manual(values=c("red", "#E76BF3", "#00B0F6", "#00BF7D", "goldenr
od1", "wheat2")) +
  scale_x_continuous(breaks = seq(0, 15, by = 1), limits = c(0, 12)) +
  scale_y_continuous(breaks = seq(0, 0.5, by = 0.1))

## Warning: Removed 47 rows containing non-finite values (stat_density).

dev.off()

## quartz_off_screen
##                 2

# Making box plots

tiff(file="Spider_Box.tiff", units="in", width=8, height=5, res=300)
ggplot(SpiderDf, aes(x = Formation, y = Body_Length, fill = Formation)) +
  geom_boxplot(alpha = 0.4) + theme(legend.position = "none") +
  ggtitle("Mean Body Lengths Fossil Spiders in Lacustrine Deposits") +
  theme(plot.title = element_text(hjust = 0.5)) + ylab("Body Length") +
  theme(axis.title.x = element_blank()) +
  stat_summary(fun.y= mean, geom = "errorbar", width = 0.25, position = posit
```

```
ion_dodge(width = .25)) +
  scale_fill_manual(values = c("red", "#E76BF3", "#00B0F6", "#00BF7D", "golde
nrod1", "wheat2")) +
  scale_y_continuous(breaks = seq(0, 15, by = 3), limits = c(0, 15)) +
  theme(axis.text.x = element_text(size=12),
        axis.text.y = element_text(size=12))
```

```
## Warning: Removed 42 rows containing non-finite values (stat_boxplot).
```

```
## Warning: Removed 42 rows containing non-finite values (stat_summary).
```

```
## Warning: Removed 6 rows containing missing values (geom_errorbar).
```

```
dev.off()
```

```
## quartz_off_screen
##                 2
```

```
# Testing means
# Start writing to an output file
sink("Spider_Stats.txt")

# ANOVA to test difference in means
cat("-----------------------------------\n")
```

```
## -----------------------------------
```

```
cat("Anova for body length means\n")
```

```
## Anova for body length means
```

```
cat("-----------------------------------\n")
```

```
## -----------------------------------
```

```
SpiderAnova <- aov(SpiderDf$Body_Length ~ SpiderDf$Formation)

cat("Anova Summary\n")
```

```
## Anova Summary
```

```
summary.aov(SpiderAnova)
```

```
##                      Df Sum Sq Mean Sq F value Pr(>F)
## SpiderDf$Formation   5   1499  299.84   53.26 <2e-16 ***
## Residuals          478   2691    5.63
## ---
## Signif. codes:  0 '***' 0.001 '**' 0.01 '*' 0.05 '.' 0.1 ' ' 1
## 37 observations deleted due to missingness
```

```
cat("-----------------------------------------------------------------\n")
```

```
## -----------------------------------------------------------------
```

```
cat("Tukey Analysis to see which means are not significantly different\n")

## Tukey Analysis to see which means are not significantly different

cat("-----------------------------------------------------------------\n")

## -----------------------------------------------------------------

TukeySpider <- TukeyHSD(SpiderAnova)
TukeySpider

##   Tukey multiple comparisons of means
##     95% family-wise confidence level
##
## Fit: aov(formula = SpiderDf$Body_Length ~ SpiderDf$Formation)
##
## $`SpiderDf$Formation`
##                               diff        lwr        upr     p adj
## Florissant-Aix           2.8330166  1.5625156  4.1035176 0.0000000
## Kishenehn-Aix           -2.2964298 -4.0790971 -0.5137626 0.0034449
## Green River-Aix         -2.5487440 -3.3928783 -1.7046097 0.0000000
## Crato-Aix                1.9962704  1.1332452  2.8592956 0.0000000
## Haifanggou-Aix          -0.2645548 -1.2732601  0.7441504 0.9753570
## Kishenehn-Florissant    -5.1294464 -7.1781973 -3.0806956 0.0000000
## Green River-Florissant  -5.3817606 -6.6978306 -4.0656906 0.0000000
## Crato-Florissant        -0.8367462 -2.1650119  0.4915196 0.4650752
## Haifanggou-Florissant   -3.0975714 -4.5247938 -1.6703490 0.0000000
## Green River-Kishenehn   -0.2523142 -2.0677398  1.5631114 0.9987150
## Crato-Kishenehn          4.2927002  2.4684142  6.1169863 0.0000000
## Haifanggou-Kishenehn     2.0318750  0.1343256  3.9294244 0.0277971
## Crato-Green River        4.5450144  3.6162088  5.4738201 0.0000000
## Haifanggou-Green River   2.2841892  1.2186593  3.3497190 0.0000000
## Haifanggou-Crato        -2.2608252 -3.3413823 -1.1802682 0.0000001

cat("\n")

cat("Diversity stats to follow...\n")

## Diversity stats to follow...

cat("\n")

cat("\n")

# stop output to file
sink()

tiff(file="TukeySpiders.tiff")
par(mar= c(4, 10, 2, 2), oma = c(1, 1, 1, 1))
plot(TukeySpider, las=1)
dev.off()
```

```
## quartz_off_screen
##                 2
```

```
# Violin plot to see density and means
tiff(file="Spider_Violin.tiff", units="in", width=9, height=5, res=300)
ggplot(SpiderDf, aes(x = Formation, y = Body_Length, fill = Formation)) +
  geom_violin(trim=FALSE, alpha = 0.4) +
  geom_crossbar(stat="summary", fun.y=mean, fun.ymax=mean, fun.ymin=mean, fat
ten=2, width=.5) +
  scale_fill_manual(values = c("red", "#E76BF3", "#00B0F6", "#00BF7D", "golde
nrod1", "wheat2")) +
  scale_y_continuous(breaks = seq(0, 15, by = 3), limits = c(0, 15)) +
  theme(axis.text.x = element_text(size=12), axis.text.y = element_text(size=
12)) +
  theme(axis.title.x = element_blank()) + ylab("Body Length") +
  ggtitle("Mean Body Lengths Fossil Spiders in Lacustrine Deposits") +
  theme(plot.title = element_text(hjust = 0.5)) +
  theme(legend.position = "none")
```

```
## Warning: Removed 42 rows containing non-finite values (stat_ydensity).
```

```
## Warning: Removed 42 rows containing non-finite values (stat_summary).
```

```
## Warning: Removed 210 rows containing missing values (geom_violin).
```

```
dev.off()
```

```
## quartz_off_screen
##                 2
```

```
# Sex and formation -- Binomial test and grouped bar plot

library(reshape2)

Formation <- factor(SpiderDf$Formation, levels=c("Aix", "Florissant", "Kishen
ehn", "Green River", "Crato", "Haifanggou"))
str(Formation)
```

```
##  Factor w/ 6 levels "Aix","Florissant",..: 5 5 5 5 5 5 5 5 5 5 ...
```

```
Formation
```

```
##   [1] Crato       Crato       Crato       Crato       Crato       Crato
##   [7] Crato       Crato       Crato       Crato       Crato       Crato
##  [13] Crato       Crato       Crato       Crato       Crato       Crato
##  [19] Crato       Crato       Crato       Crato       Crato       Crato
##  [25] Crato       Crato       Crato       Crato       Crato       Crato
##  [31] Crato       Crato       Crato       Crato       Crato       Crato
##  [37] Crato       Crato       Crato       Crato       Crato       Crato
##  [43] Crato       Crato       Crato       Crato       Crato       Crato
##  [49] Crato       Crato       Crato       Crato       Crato       Crato
##  [55] Crato       Crato       Crato       Crato       Crato       Crato
```

```
##  [61] Crato       Crato       Crato       Crato       Crato       Crato
##  [67] Crato       Crato       Crato       Crato       Crato       Crato
##  [73] Crato       Crato       Crato       Crato       Crato       Crato
##  [79] Crato       Crato       Crato       Crato       Crato       Crato
##  [85] Crato       Crato       Crato       Crato       Crato       Crato
##  [91] Crato       Crato       Crato       Crato       Crato       Crato
##  [97] Crato       Crato       Crato       Crato       Crato       Crato
## [103] Crato       Crato       Crato       Crato       Crato       Crato
## [109] Crato       Crato       Green River Green River Green River Green Ri
ver
## [115] Green River Green River Green River Green River Green River Green Ri
ver
## [121] Green River Green River Green River Green River Green River Green Ri
ver
## [127] Green River Green River Green River Green River Green River Green Ri
ver
## [133] Green River Green River Green River Green River Green River Green Ri
ver
## [139] Green River Green River Green River Green River Green River Green Ri
ver
## [145] Green River Green River Green River Green River Green River Green Ri
ver
## [151] Green River Green River Green River Green River Green River Green Ri
ver
## [157] Green River Green River Green River Green River Green River Green Ri
ver
## [163] Green River Green River Green River Green River Green River Green Ri
ver
## [169] Green River Green River Green River Green River Green River Green Ri
ver
## [175] Green River Green River Green River Green River Green River Green Ri
ver
## [181] Green River Green River Green River Green River Green River Green Ri
ver
## [187] Green River Green River Green River Green River Green River Green Ri
ver
## [193] Green River Green River Green River Green River Green River Green Ri
ver
## [199] Green River Green River Green River Green River Green River Green Ri
ver
## [205] Green River Green River Green River Green River Green River Green Ri
ver
## [211] Green River Green River Green River Green River Green River Green Ri
ver
## [217] Green River Green River Green River Green River Green River Green Ri
ver
## [223] Green River Green River Green River Green River Green River Green Ri
ver
## [229] Green River Green River Green River Green River Green River Green Ri
ver
```

```
## [235] Kishenehn   Kishenehn   Kishenehn   Kishenehn   Kishenehn   Kisheneh
n
## [241] Kishenehn   Kishenehn   Kishenehn   Kishenehn   Kishenehn   Kisheneh
n
## [247] Kishenehn   Kishenehn   Kishenehn   Kishenehn   Kishenehn   Kisheneh
n
## [253] Kishenehn   Florissant  Florissant  Florissant  Florissant  Florissa
nt
## [259] Florissant  Florissant  Florissant  Florissant  Florissant  Florissa
nt
## [265] Florissant  Florissant  Florissant  Florissant  Florissant  Florissa
nt
## [271] Florissant  Florissant  Florissant  Florissant  Florissant  Florissa
nt
## [277] Florissant  Florissant  Florissant  Florissant  Florissant  Florissa
nt
## [283] Florissant  Florissant  Florissant  Florissant  Florissant  Florissa
nt
## [289] Florissant  Florissant  Florissant  Aix         Aix         Aix
## [295] Aix         Aix         Aix         Aix         Aix         Aix
## [301] Aix         Aix         Aix         Aix         Aix         Aix
## [307] Aix         Aix         Aix         Aix         Aix         Aix
## [313] Aix         Aix         Aix         Aix         Aix         Aix
## [319] Aix         Aix         Aix         Aix         Aix         Aix
## [325] Aix         Aix         Aix         Aix         Aix         Aix
## [331] Aix         Aix         Aix         Aix         Aix         Aix
## [337] Aix         Aix         Aix         Aix         Aix         Aix
## [343] Aix         Aix         Aix         Aix         Aix         Aix
## [349] Aix         Aix         Aix         Aix         Aix         Aix
## [355] Aix         Aix         Aix         Aix         Aix         Aix
## [361] Aix         Aix         Aix         Aix         Aix         Aix
## [367] Aix         Aix         Aix         Aix         Aix         Aix
## [373] Aix         Aix         Aix         Aix         Aix         Aix
## [379] Aix         Aix         Aix         Aix         Aix         Aix
## [385] Aix         Aix         Aix         Aix         Aix         Aix
## [391] Aix         Aix         Aix         Aix         Aix         Aix
## [397] Aix         Aix         Aix         Aix         Aix         Aix
## [403] Aix         Aix         Aix         Aix         Aix         Aix
## [409] Aix         Aix         Aix         Aix         Aix         Aix
## [415] Aix         Aix         Aix         Aix         Aix         Aix
## [421] Aix         Aix         Aix         Aix         Aix         Aix
## [427] Aix         Aix         Aix         Aix         Aix         Aix
## [433] Aix         Aix         Aix         Aix         Aix         Aix
## [439] Aix         Aix         Aix         Aix         Aix         Aix
## [445] Aix         Aix         Aix         Aix         Aix         Aix
## [451] Aix         Aix         Aix         Aix         Haifanggou  Haifangg
ou
## [457] Haifanggou  Haifanggou  Haifanggou  Haifanggou  Haifanggou  Haifangg
ou
## [463] Haifanggou  Haifanggou  Haifanggou  Haifanggou  Haifanggou  Haifangg
```

```
ou
## [469] Haifanggou  Haifanggou  Haifanggou  Haifanggou  Haifanggou  Haifangg
ou
## [475] Haifanggou  Haifanggou  Haifanggou  Haifanggou  Haifanggou  Haifangg
ou
## [481] Haifanggou  Haifanggou  Haifanggou  Haifanggou  Haifanggou  Haifangg
ou
## [487] Haifanggou  Haifanggou  Haifanggou  Haifanggou  Haifanggou  Haifangg
ou
## [493] Haifanggou  Haifanggou  Haifanggou  Haifanggou  Haifanggou  Haifangg
ou
## [499] Haifanggou  Haifanggou  Haifanggou  Haifanggou  Haifanggou  Haifangg
ou
## [505] Haifanggou  Haifanggou  Haifanggou  Haifanggou  Haifanggou  Haifangg
ou
## [511] Haifanggou  Haifanggou  Haifanggou  Haifanggou  Haifanggou  Haifangg
ou
## [517] Haifanggou  Haifanggou  Haifanggou  Haifanggou  Haifanggou
## Levels: Aix Florissant Kishenehn Green River Crato Haifanggou

SpiderSex <- factor(SpiderDf$Sex, levels=c("F", "I", "M"))


SexCounts <- data.frame(table(SpiderDf$Sex, Formation))
SexCounts

##    Var1   Formation Freq
## 1     F         Aix   39
## 2     I         Aix  101
## 3     M         Aix   23
## 4     F  Florissant   17
## 5     I  Florissant    2
## 6     M  Florissant   19
## 7     F   Kishenehn    4
## 8     I   Kishenehn   12
## 9     M   Kishenehn    3
## 10    F Green River   27
## 11    I Green River   69
## 12    M Green River   28
## 13    F       Crato   19
## 14    I       Crato   86
## 15    M       Crato    5
## 16    F  Haifanggou   19
## 17    I  Haifanggou   25
## 18    M  Haifanggou   23

tiff(file="Sex.tiff", units="in", width=9, height=5, res=300)
ggplot(SexCounts, aes(fill=Var1, y=Freq, x=Formation)) +
  geom_bar(position="dodge", colour="black", stat="identity") +
  ggtitle("Sex of Fossil Spiders in Lacustrine Deposits") +
```

```
  theme(plot.title = element_text(hjust = 0.5)) +
  scale_fill_manual(values = c("slateblue1", "white", "yellow"), labels = c("
Female", "Indeterminate", "Male")) +
  theme(legend.position="top") + labs(fill = "Sex") +
  theme(legend.position = c(0.5, 0.8)) + xlab("Formation") + ylab("Frequency"
) +
  theme(axis.text.x = element_text(size=12), axis.text.y = element_text(size=
12)) +
  theme(axis.title.x = element_blank())
dev.off()

## quartz_off_screen
##                 2

sink("Spider_Stats.txt", append=TRUE)

cat("------------------------------------------------------------------\n")

## ------------------------------------------------------------------

cat("Chi-square Goodness of Fit test for Sex\n")

## Chi-square Goodness of Fit test for Sex

cat("Female, Indeterminate, Male\n")

## Female, Indeterminate, Male

cat("------------------------------------------------------------------\n")

## ------------------------------------------------------------------

cat("\n")

AixSex <- c(39, 101, 23)
FlorissantSex <- c(17, 2, 19)
KishenehnSex <- c(4, 12, 3)
GreenRiverSex <- c(27, 69, 28)
CratoSex <- c(19, 86, 5)
HaifanggouSex <- c(19, 25, 23)

cat("\n")

cat("Aix\n")

## Aix

AixSexTest <- chisq.test(AixSex, p = c(1/3, 1/3, 1/3))
cat(AixSexTest$p.value)

## 2.709943e-14

cat("\n")
```

```r
cat("Florissant\n")

## Florissant

FlorissantSexTest <- chisq.test(FlorissantSex, p = c(1/3, 1/3, 1/3))
cat(FlorissantSexTest$p.value)

## 0.001096327

cat("\n")

cat("Kishnehn\n")

## Kishnehn

KishenehnSexTest <- chisq.test(KishenehnSex, p = c(1/3, 1/3, 1/3))
cat(KishenehnSexTest$p.value)

## 0.0214484

cat("\n")

cat("Green River\n")

## Green River

GreenRiverSexTest <- chisq.test(GreenRiverSex, p = c(1/3, 1/3, 1/3))
cat(GreenRiverSexTest$p.value)

## 9.234388e-07

cat("\n")

cat("Crato\n")

## Crato

CratoSexTest <- chisq.test(CratoSex, p = c(1/3, 1/3, 1/3))
cat(CratoSexTest$p.value)

## 6.304573e-23

cat("\n")

cat("Haifanggou\n")

## Haifanggou

HaifanggouSexTest <- chisq.test(HaifanggouSex, p = c(1/3, 1/3, 1/3))
cat(HaifanggouSexTest$p.value)

## 0.6584212

cat("\n")
```

```r
sink()



AixMvF <- c(39, 23)
FlorissantMvF <- c(17, 19)
KFMvF <- c(4, 3)
GRFMvF <- c(27, 28)
CratoMvF <- c(19, 5)
HaifanggouMvF <- c(19, 23)

sink("Spider_Stats.txt", append=TRUE)
cat("------------------------------------------------------------------\n")

## ------------------------------------------------------------------

cat("Males vs Females\n")

## Males vs Females

cat("------------------------------------------------------------------\n")

## ------------------------------------------------------------------

cat("\n")

#Males vs females
cat("\n")

cat("Aix\n")

## Aix

cat(binom.test(AixMvF, p = 0.5)$p.value)

## 0.05589723

cat("\n")

cat("Florissant\n")

## Florissant

cat(binom.test(FlorissantMvF, p = 0.5)$p.value)

## 0.8679394

cat("\n")

cat("Kishnehn\n")

## Kishnehn

cat(binom.test(KFMvF, p = 0.5)$p.value)
```

```
## 1

cat("\n")

cat("Green River\n")

## Green River

cat(binom.test(GRFMvF, p = 0.5)$p.value)

## 1

cat("\n")

cat("Crato\n")

## Crato

cat(binom.test(CratoMvF, p = 0.5)$p.value)

## 0.006610751

cat("\n")

cat("Haifanggou\n")

## Haifanggou

cat(binom.test(HaifanggouMvF, p = 0.5)$p.value)

## 0.643969

cat("\n")

sink()




sink("Spider_Stats.txt", append=TRUE)
cat("\n")

cat("------------------------------------------------------------------\n")

## ------------------------------------------------------------------

cat("Binomial test for age\n")

## Binomial test for age

cat("Adult, Indeterminate/Juvenile\n")

## Adult, Indeterminate/Juvenile
```

```r
cat("-----------------------------------------------------------------\n")
```

```
## -----------------------------------------------------------------
```

```r
cat("\n")
```

```r
#Adult vs Juvenile
AixAge <- c(62, 101)
FlorissantAge <- c(36, 2)
KishenehnAge <- c(7, 12)
GreenRiverAge <- c(55, 69)
CratoAge <- c(24, 86)
HaifanggouAge <- c(42, 25)


(binom.test(184, 270, p = 0.5)$p.value)
```

```
## [1] 2.402064e-09
```

```r
cat("\n")

cat("Aix\n")
```

```
## Aix
```

```r
cat(binom.test(62, 101, p = 0.5)$p.value)
```

```
## 0.02808947
```

```r
cat("\n")

cat("Florissant\n")
```

```
## Florissant
```

```r
cat(binom.test(FlorissantAge, p = 0.5)$p.value)
```

```
## 5.398761e-09
```

```r
cat("\n")

cat("Kishnehn\n")
```

```
## Kishnehn
```

```r
cat(binom.test(7, 12, p = 0.5)$p.value)
```

```
## 0.7744141
```

```r
cat("\n")

cat("Green River\n")
```

```
## Green River
```

```r
cat(binom.test(55, 69, p = 0.5)$p.value)
```

```
## 6.921917e-07
```

```r
cat("\n")
cat("Crato\n")
```

```
## Crato
```

```r
cat(binom.test(24, 86, p = 0.5)$p.value)
```

```
## 5.083654e-05
```

```r
cat("\n")
cat("Haifanggou\n")
```

```
## Haifanggou
```

```r
cat(binom.test(25, 42, p = 0.5)$p.value)
```

```
## 0.2799562
```

```r
cat("\n")
sink()

# Life modes and formation -- Binomial test and grouped bar plot

library(reshape2)

Formation <- factor(SpiderDf$Formation, levels=c("Aix", "Florissant", "Kishen
ehn", "Green River", "Crato"))
str(Formation)
```

```
##  Factor w/ 5 levels "Aix","Florissant",..: 5 5 5 5 5 5 5 5 5 5 ...
```

```r
Formation
```

```
##   [1] Crato       Crato       Crato       Crato       Crato       Crato
##   [7] Crato       Crato       Crato       Crato       Crato       Crato
##  [13] Crato       Crato       Crato       Crato       Crato       Crato
##  [19] Crato       Crato       Crato       Crato       Crato       Crato
##  [25] Crato       Crato       Crato       Crato       Crato       Crato
##  [31] Crato       Crato       Crato       Crato       Crato       Crato
##  [37] Crato       Crato       Crato       Crato       Crato       Crato
##  [43] Crato       Crato       Crato       Crato       Crato       Crato
##  [49] Crato       Crato       Crato       Crato       Crato       Crato
##  [55] Crato       Crato       Crato       Crato       Crato       Crato
##  [61] Crato       Crato       Crato       Crato       Crato       Crato
##  [67] Crato       Crato       Crato       Crato       Crato       Crato
##  [73] Crato       Crato       Crato       Crato       Crato       Crato
##  [79] Crato       Crato       Crato       Crato       Crato       Crato
```

```
##  [85] Crato       Crato       Crato       Crato       Crato       Crato
##  [91] Crato       Crato       Crato       Crato       Crato       Crato
##  [97] Crato       Crato       Crato       Crato       Crato       Crato
## [103] Crato       Crato       Crato       Crato       Crato       Crato
## [109] Crato       Crato       Green River Green River Green River Green Ri
ver
## [115] Green River Green River Green River Green River Green River Green Ri
ver
## [121] Green River Green River Green River Green River Green River Green Ri
ver
## [127] Green River Green River Green River Green River Green River Green Ri
ver
## [133] Green River Green River Green River Green River Green River Green Ri
ver
## [139] Green River Green River Green River Green River Green River Green Ri
ver
## [145] Green River Green River Green River Green River Green River Green Ri
ver
## [151] Green River Green River Green River Green River Green River Green Ri
ver
## [157] Green River Green River Green River Green River Green River Green Ri
ver
## [163] Green River Green River Green River Green River Green River Green Ri
ver
## [169] Green River Green River Green River Green River Green River Green Ri
ver
## [175] Green River Green River Green River Green River Green River Green Ri
ver
## [181] Green River Green River Green River Green River Green River Green Ri
ver
## [187] Green River Green River Green River Green River Green River Green Ri
ver
## [193] Green River Green River Green River Green River Green River Green Ri
ver
## [199] Green River Green River Green River Green River Green River Green Ri
ver
## [205] Green River Green River Green River Green River Green River Green Ri
ver
## [211] Green River Green River Green River Green River Green River Green Ri
ver
## [217] Green River Green River Green River Green River Green River Green Ri
ver
## [223] Green River Green River Green River Green River Green River Green Ri
ver
## [229] Green River Green River Green River Green River Green River Green Ri
ver
## [235] Kishenehn   Kishenehn   Kishenehn   Kishenehn   Kishenehn   Kisheneh
n
## [241] Kishenehn   Kishenehn   Kishenehn   Kishenehn   Kishenehn   Kisheneh
n
```

```
## [247] Kishenehn   Kishenehn   Kishenehn   Kishenehn   Kishenehn   Kisheneh
n
## [253] Kishenehn   Florissant  Florissant  Florissant  Florissant  Florissa
nt
## [259] Florissant  Florissant  Florissant  Florissant  Florissant  Florissa
nt
## [265] Florissant  Florissant  Florissant  Florissant  Florissant  Florissa
nt
## [271] Florissant  Florissant  Florissant  Florissant  Florissant  Florissa
nt
## [277] Florissant  Florissant  Florissant  Florissant  Florissant  Florissa
nt
## [283] Florissant  Florissant  Florissant  Florissant  Florissant  Florissa
nt
## [289] Florissant  Florissant  Florissant  Aix         Aix         Aix
## [295] Aix         Aix         Aix         Aix         Aix         Aix
## [301] Aix         Aix         Aix         Aix         Aix         Aix
## [307] Aix         Aix         Aix         Aix         Aix         Aix
## [313] Aix         Aix         Aix         Aix         Aix         Aix
## [319] Aix         Aix         Aix         Aix         Aix         Aix
## [325] Aix         Aix         Aix         Aix         Aix         Aix
## [331] Aix         Aix         Aix         Aix         Aix         Aix
## [337] Aix         Aix         Aix         Aix         Aix         Aix
## [343] Aix         Aix         Aix         Aix         Aix         Aix
## [349] Aix         Aix         Aix         Aix         Aix         Aix
## [355] Aix         Aix         Aix         Aix         Aix         Aix
## [361] Aix         Aix         Aix         Aix         Aix         Aix
## [367] Aix         Aix         Aix         Aix         Aix         Aix
## [373] Aix         Aix         Aix         Aix         Aix         Aix
## [379] Aix         Aix         Aix         Aix         Aix         Aix
## [385] Aix         Aix         Aix         Aix         Aix         Aix
## [391] Aix         Aix         Aix         Aix         Aix         Aix
## [397] Aix         Aix         Aix         Aix         Aix         Aix
## [403] Aix         Aix         Aix         Aix         Aix         Aix
## [409] Aix         Aix         Aix         Aix         Aix         Aix
## [415] Aix         Aix         Aix         Aix         Aix         Aix
## [421] Aix         Aix         Aix         Aix         Aix         Aix
## [427] Aix         Aix         Aix         Aix         Aix         Aix
## [433] Aix         Aix         Aix         Aix         Aix         Aix
## [439] Aix         Aix         Aix         Aix         Aix         Aix
## [445] Aix         Aix         Aix         Aix         Aix         Aix
## [451] Aix         Aix         Aix         Aix         <NA>        <NA>
## [457] <NA>        <NA>        <NA>        <NA>        <NA>        <NA>
## [463] <NA>        <NA>        <NA>        <NA>        <NA>        <NA>
## [469] <NA>        <NA>        <NA>        <NA>        <NA>        <NA>
## [475] <NA>        <NA>        <NA>        <NA>        <NA>        <NA>
## [481] <NA>        <NA>        <NA>        <NA>        <NA>        <NA>
## [487] <NA>        <NA>        <NA>        <NA>        <NA>        <NA>
## [493] <NA>        <NA>        <NA>        <NA>        <NA>        <NA>
## [499] <NA>        <NA>        <NA>        <NA>        <NA>        <NA>
```

```
## [505] <NA>        <NA>        <NA>        <NA>        <NA>        <NA>
## [511] <NA>        <NA>        <NA>        <NA>        <NA>        <NA>
## [517] <NA>        <NA>        <NA>        <NA>        <NA>
## Levels: Aix Florissant Kishenehn Green River Crato

LifeCounts <- data.frame(table(SpiderDf$Guild, Formation))

sink("Spider_Stats.txt", append=TRUE)

cat("-----------------------------------------------------------------\n")

## -----------------------------------------------------------------

cat("Binomial Tests for Life Mode\n")

## Binomial Tests for Life Mode

cat("Ground vs web spinning spiders\n")

## Ground vs web spinning spiders

cat("-----------------------------------------------------------------\n")

## -----------------------------------------------------------------

cat("\n")

cat("Aix\n")

## Aix

cat(binom.test(76, 112, p = 0.5)$p.value)

## 0.000198237

cat("\n")

cat("Florissant\n")

## Florissant

cat(binom.test(18, 30, p = 0.5)$p.value)

## 0.3615946

cat("\n")

cat("Kishnehn\n")

## Kishnehn

cat(binom.test(6, 6, p = 0.5)$p.value)

## 0.03125
```

```r
cat("\n")

cat("Green River\n")

## Green River

cat(binom.test(18, 70, p = 0.5)$p.value)

## 5.849547e-05

cat("\n")

cat("Crato\n")

## Crato

cat(binom.test(8, 63, p = 0.5)$p.value)

## 9.761673e-10

cat("\n")

sink()

tiff(file="LifeMode.tiff", units="in", width=6, height=5, res=300)
ggplot(LifeCounts, aes(fill=Var1, y=Freq, x=Formation)) +
  geom_bar(position="dodge", colour="black", stat="identity") +
  ggtitle("Life Modes of Fossil Spiders in Lacustrine Deposits") +
  theme(plot.title = element_text(hjust = 0.5)) +
  scale_fill_manual(values = c("tan4", "darkslategray2"), labels = c("Ground"
, "Web")) +
  theme(legend.position="top") + labs(fill = "Life Mode") +
  theme(legend.position = c(0.5, 0.8)) + xlab("Formation") + ylab("Frequency"
) +
  theme(axis.text.x = element_text(size=12), axis.text.y = element_text(size=
12)) +
  theme(axis.title.x = element_blank())
dev.off()

## quartz_off_screen
##                 2

str(LifeCounts)

## 'data.frame':    10 obs. of  3 variables:
##  $ Var1     : Factor w/ 2 levels "ground","web": 1 2 1 2 1 2 1 2 1 2
##  $ Formation: Factor w/ 5 levels "Aix","Florissant",..: 1 1 2 2 3 3 4 4 5
5
##  $ Freq     : int  77 38 20 16 5 12 42 61 2 108

# Species rank abundance curve for each deposit (not ggplot)

LakeSpeciesCount <- SpiderDf$Morphospecies
```

```
LacustrineSpecies <- as.character(LakeSpeciesCount)
LakeSpeciesCount
```

```
##   [1]  8  1  1  1  1  1 10  6  1  1  1  1  1  1  1  1  2  1  1  1  1  2  1
3  1
##  [26]  1  5  1  1  1  1  1  1  1  1  1  1  1  1  1  1  1  1  1  1  1  1  1
1  1
##  [51]  1  1  1  4  1  1  1  1  1  1  1  3  1  1  1  1  1  1  1  1  1  1  1
1  1
##  [76]  1  1  1  1  1  1  1  1  1  1  1  8  5  5  1  1  1  1  1  1  1  1  1
1  1
## [101]  1  1  1  5  5  7  7  8  9  1  8 NA NA  9 NA  6 NA  3 NA NA NA NA  5
NA NA
## [126] NA NA NA  5 13  7 NA 12  6 NA  6 NA  5  7 NA NA  9 11 NA 11  6  1 NA
2  2
## [151]  2  1  4  2 NA  2 NA  1  2  1  4  4  1 NA NA NA NA  1  1 NA  1  2  1
1  1
## [176] NA  4  1  4 NA  3  1  1  4  1  1  1  1  1  1  1  1  1  1  1  3 NA  4
10 NA
## [201]  1  3 NA NA NA NA NA NA NA NA NA NA  3 NA NA NA NA NA  3 NA NA NA NA
NA  5
## [226]  4  2  2  2  5  5  7  6  6 NA NA  3 NA NA NA NA  1 NA NA NA NA  1  1
NA NA
## [251]  2 NA NA  8 NA  3  5  3  3  2  5  2  9 NA 10 NA  6  2  3  2  6  7  3
2  2
## [276]  1  1  1  4 NA  1  4  1  1  1  2  1  1 NA  7  4 NA NA NA NA NA NA NA
NA NA
## [301] NA NA NA NA NA NA NA NA NA NA NA NA NA NA NA NA NA NA NA NA NA NA NA
NA NA
## [326] NA NA NA NA NA NA NA NA NA NA NA NA NA NA NA NA NA NA NA NA NA NA NA
NA NA
## [351] NA NA NA NA NA NA NA NA NA NA NA NA NA NA NA NA NA NA NA NA NA NA NA
NA NA
## [376] NA NA NA NA NA NA NA NA NA NA NA NA NA NA NA NA NA NA NA NA NA NA NA
NA NA
## [401] NA NA NA NA NA NA NA NA NA NA NA NA NA NA NA NA NA NA NA NA NA NA NA
NA NA
## [426] NA NA NA NA NA NA NA NA NA NA NA NA NA NA NA NA NA NA NA NA NA NA NA
NA NA
## [451] NA NA NA NA NA NA NA NA NA NA NA NA NA NA NA NA NA NA NA NA NA NA NA
NA NA
## [476] NA NA NA NA NA NA NA NA NA NA NA NA NA NA NA NA NA NA NA NA NA NA NA
NA NA
## [501] NA NA NA NA NA NA NA NA NA NA NA NA NA NA NA NA NA NA NA NA NA
```

```
LacustrineSpecies
```

```
##   [1] "8"  "1"  "1"  "1"  "1"  "1"  "10" "6"  "1"  "1"  "1"  "1"  "1"  "1"
"1"
##  [16] "1"  "2"  "1"  "1"  "1"  "1"  "2"  "1"  "3"  "1"  "1"  "5"  "1"  "1"
```

```
"1"
##  [31] "1"  "1"  "1"  "1"  "1"  "1"  "1"  "1"  "1"  "1"  "1"  "1"  "1"  "1"
"1"
##  [46] "1"  "1"  "1"  "1"  "1"  "1"  "1"  "1"  "4"  "1"  "1"  "1"  "1"  "1"
"1"
##  [61] "1"  "3"  "1"  "1"  "1"  "1"  "1"  "1"  "1"  "1"  "1"  "1"  "1"  "1"
"1"
##  [76] "1"  "1"  "1"  "1"  "1"  "1"  "1"  "1"  "1"  "1"  "1"  "8"  "5"  "5"
"1"
##  [91] "1"  "1"  "1"  "1"  "1"  "1"  "1"  "1"  "1"  "1"  "1"  "1"  "1"  "5"
"5"
## [106] "7"  "7"  "8"  "9"  "1"  "8"  NA   NA   "9"  NA   "6"  NA   "3"  NA
NA
## [121] NA   NA   "5"  NA   NA   NA   NA   NA   "5"  "13" "7"  NA   "12" "6"
NA
## [136] "6"  NA   "5"  "7"  NA   NA   "9"  "11" NA   "11" "6"  "1"  NA   "2"
"2"
## [151] "2"  "1"  "4"  "2"  NA   "2"  NA   "1"  "2"  "1"  "4"  "4"  "1"  NA
NA
## [166] NA   NA   "1"  "1"  NA   "1"  "2"  "1"  "1"  "1"  NA   "4"  "1"  "4"
NA
## [181] "3"  "1"  "1"  "4"  "1"  "1"  "1"  "1"  "1"  "1"  "1"  "1"  "1"  "1"
"1"
## [196] "3"  NA   "4"  "10" NA   "1"  "3"  NA   NA   NA   NA   NA   NA   NA
NA
## [211] NA   NA   "3"  NA   NA   NA   NA   NA   "3"  NA   NA   NA   NA   NA
"5"
## [226] "4"  "2"  "2"  "2"  "5"  "5"  "7"  "6"  "6"  NA   NA   "3"  NA   NA
NA
## [241] NA   "1"  NA   NA   NA   NA   "1"  "1"  NA   NA   "2"  NA   NA   "8"
NA
## [256] "3"  "5"  "3"  "3"  "2"  "5"  "2"  "9"  NA   "10" NA   "6"  "2"  "3"
"2"
## [271] "6"  "7"  "3"  "2"  "2"  "1"  "1"  "1"  "4"  NA   "1"  "4"  "1"  "1"
"1"
## [286] "2"  "1"  "1"  NA   "7"  "4"  NA   NA   NA   NA   NA   NA   NA   NA
NA
## [301] NA   NA   NA   NA   NA   NA   NA   NA   NA   NA   NA   NA   NA   NA
NA
## [316] NA   NA   NA   NA   NA   NA   NA   NA   NA   NA   NA   NA   NA   NA
NA
## [331] NA   NA   NA   NA   NA   NA   NA   NA   NA   NA   NA   NA   NA   NA
NA
## [346] NA   NA   NA   NA   NA   NA   NA   NA   NA   NA   NA   NA   NA   NA
NA
## [361] NA   NA   NA   NA   NA   NA   NA   NA   NA   NA   NA   NA   NA   NA
NA
## [376] NA   NA   NA   NA   NA   NA   NA   NA   NA   NA   NA   NA   NA   NA
NA
## [391] NA   NA   NA   NA   NA   NA   NA   NA   NA   NA   NA   NA   NA   NA
```

```
NA
## [406] NA   NA   NA   NA   NA   NA   NA   NA   NA   NA   NA   NA   NA   NA
NA
## [421] NA   NA   NA   NA   NA   NA   NA   NA   NA   NA   NA   NA   NA   NA
NA
## [436] NA   NA   NA   NA   NA   NA   NA   NA   NA   NA   NA   NA   NA   NA
NA
## [451] NA   NA   NA   NA   NA   NA   NA   NA   NA   NA   NA   NA   NA   NA
NA
## [466] NA   NA   NA   NA   NA   NA   NA   NA   NA   NA   NA   NA   NA   NA
NA
## [481] NA   NA   NA   NA   NA   NA   NA   NA   NA   NA   NA   NA   NA   NA
NA
## [496] NA   NA   NA   NA   NA   NA   NA   NA   NA   NA   NA   NA   NA   NA
NA
## [511] NA   NA   NA   NA   NA   NA   NA   NA   NA   NA   NA

Spiderdf2 <- cbind(SpiderDf, LacustrineSpecies, stringsAsFactors = FALSE )
str(Spiderdf2)

## 'data.frame':    521 obs. of  7 variables:
##  $ Formation        : Factor w/ 6 levels "Aix","Florissant",..: 5 5 5 5 5
5 5 5 5 5 ...
##  $ Family           : Factor w/ 18 levels "","Araneidae",..: 4 2 2 2 2 2 7
10 2 2 ...
##  $ Morphospecies    : int  8 1 1 1 1 1 10 6 1 1 ...
##  $ Sex              : Factor w/ 3 levels "F","I","M": 2 2 2 2 2 2 2 2 2 2
...
##  $ Body_Length      : num  13.35 3.1 3.22 4.73 9.3 ...
##  $ Guild            : Factor w/ 2 levels "ground","web": 1 2 2 2 2 2 1 2 2
2 ...
##  $ LacustrineSpecies: chr  "8" "1" "1" "1" ...

CFspecies <- Spiderdf2$LacustrineSpecies[Spiderdf2$Formation=="Crato"]
GRFspecies <- Spiderdf2$LacustrineSpecies[Spiderdf2$Formation=="Green River"]
KFspecies <- Spiderdf2$LacustrineSpecies[Spiderdf2$Formation=="Kishenehn"]
FFspecies <- Spiderdf2$LacustrineSpecies[Spiderdf2$Formation=="Florissant"]
AFspecies <- Spiderdf2$LacustrineSpecies[Spiderdf2$Formation=="Aix"]

CFspCount <- table(CFspecies)
GRFspCount <- table(GRFspecies)
KFspCount <- table(KFspecies)
FFspCount <- table(FFspecies)
AFspCount <- table(AFspecies)

RankedCratoAbund <- sort(CFspCount, decreasing = TRUE)
RankedGRFAbund <- sort(GRFspCount, decreasing = TRUE)
RankedKFAbund <- sort(KFspCount, decreasing = TRUE)
RankedFFAbund <- sort(FFspCount, decreasing = TRUE)
RankedAFAbund <- sort(AFspCount, decreasing = TRUE)
```

```
RankedCratoAbund

## CFspecies
##  1  5  8  2  3  7 10  4  6  9
## 92  5  3  2  2  2  1  1  1  1

RankedGRFAbund

## GRFspecies
##  1  2  4  3  5  6  7 11  9 10 12 13  8
## 26 10  8  6  6  6  3  2  2  1  1  1  1

RankedKFAbund

## KFspecies
## 1 2 3
## 3 1 1

RankedFFAbund

## FFspecies
##  1  2  3  4  5  6  7 10  8  9
##  9  7  5  3  2  2  2  1  1  1

RankedAFAbund

## integer(0)

cf <- as.numeric(RankedCratoAbund)
grf <- as.numeric(RankedGRFAbund)
kf <- as.numeric(RankedKFAbund)
ff <- as.numeric(RankedFFAbund)
af <- as.numeric(RankedAFAbund)

tiff(file="SpiderAbundance.tiff", units="in", width=5, height=5, res=300)
plot(cf, col = "goldenrod1", main = "Species rank abundance curve", ylab = "N
umber of species", xlab = "Rank",
     xlim = c(1, 13), ylim = c(0,30), pch = 16, cex.axis = 0.75)
axis(1, seq(1, 13, 1), cex.axis =0.75)
points(grf, col = "darkolivegreen", pch = 16)
points(kf, col = "blue", pch = 16)
points(ff, col = "purple", pch = 16)
points(af, col = "red", pch = 16)

lines(cf, col = "goldenrod1", lwd = 1)
lines(grf, col = "darkolivegreen", lwd = 1)
lines(kf, col = "blue", lwd = 1)
lines(ff, col = "purple", lwd = 1)
lines(af, col = "red", lwd = 1)

legend("topright",col=c("red", "purple", "blue", "darkolivegreen", "goldenrod
```

```
1"),lty=c(1,1),
       legend=c("Aix", "Florissant", "Kishenehn", "Green River", "Crato"))

legend("topright",col=c("purple", "blue", "darkolivegreen", "goldenrod1"),lty
=c(1,1),
       legend=c("Florissant", "Kishenehn", "Green River", "Crato"))
dev.off()

## quartz_off_screen
##                 2

# Diversity Stats

library(vegan)

## Loading required package: permute

## Loading required package: lattice

## This is vegan 2.5-6

LakeSpecies <- read.csv("LacustrineSpiderFamily.csv", header=T)

## Warning in read.table(file = file, header = header, sep = sep, quote = quo
te, :
## incomplete final line found by readTableHeader on 'LacustrineSpiderFamily.
csv'

LakeSpecies

##     Formation Araneoidea_Ind Araneidae Tetragnathidae Uloboridae Lycosoide
a_Ind
## 1      Crato               2        92              0          0
0
## 2 Green River              38         5              0         18
6
## 3   Kishenehn               5         7              0          0
1
## 4  Florissant               5         1             10          0
1
##   Selenopidae Hersiliidae Lycosidae Pisauridae Thomisidae Palpimanidae
## 1           0           0         0          0          0            1
## 2           3           6         0          0          6            0
## 3           0           0         0          0          0            0
## 4           0           0         8          2          0            0
##   Nephilidae Clubionidae Gnaphosidae Dipluridae
## 1          5           0           0          8
## 2          0           0           1          0
## 3          0           1           0          0
## 4          1           9           0          0
```

```r
# Append to the file
sink("Spider_Stats.txt", append=TRUE)

# Simpson's Diversity Index
cat("-------------------------------------------------\n")

## -------------------------------------------------

cat("Simpson's Diversity Index\n")

## Simpson's Diversity Index

cat("-------------------------------------------------\n")

## -------------------------------------------------

cat("Simpson's Diversity Index is between 0 and 1\n")

## Simpson's Diversity Index is between 0 and 1

cat("Higher values indicate higher diversity\n")

## Higher values indicate higher diversity

cat("\n")

SimpsonSpider <- diversity(LakeSpecies[-1], index="simpson")
names(SimpsonSpider) <- c("Crato", "Green River", "Kishenehn", "Florissant")
cat(names(SimpsonSpider))

## Crato Green River Kishenehn Florissant

cat("\n")

cat(SimpsonSpider)

## 0.2662894 0.7226012 0.6122449 0.7976625

cat("\n")

# Pielou Evenness
cat("-------------------------------------------------\n")

## -------------------------------------------------

cat("Pielou Evenness\n")

## Pielou Evenness

cat("-------------------------------------------------\n")

## -------------------------------------------------

cat("Lower vales indicate less evenness\n")
```

```r
## Lower vales indicate less evenness

cat("\n")

S <- apply(LakeSpecies[,-1] > 0, 1, sum)
cat(names(SimpsonSpider))

## Crato Green River Kishenehn Florissant

cat("\n")

cat(exp(diversity(LakeSpecies[-1], index = "simpson"))/S)

## 0.2610226 0.257473 0.4611419 0.2775431

cat("\n")

# Hill's ratios for evenness
cat("-------------------------------------------------\n")

## -------------------------------------------------

cat("Hill's Raqtio for Evenness\n")

## Hill's Raqtio for Evenness

cat("-------------------------------------------------\n")

## -------------------------------------------------

cat("Lower vales indicate less evenness\n")

## Lower vales indicate less evenness

cat("\n")

cat(names(SimpsonSpider))

## Crato Green River Kishenehn Florissant

cat("\n")

cat(diversity(LakeSpecies[-1], index = "simpson")/log(S))

## 0.1654549 0.3474977 0.4416413 0.3835946

sink()
```